Spring 2017

Behavior and Strength of Non-Prestressed and Prestressed Hillman Composite Beam Including CFRP Retrofitting

Wajid Khan
Old Dominion University

BEHAVIOR AND STRENGTH OF NON-PRESTRESSED AND PRESTRESSED HILLMAN COMPOSITE BEAM INCLUDING CFRP RETROFITTING

By

Wajid Khan
MSc Structural Engineering, 2010
UET Peshawar, Pakistan.

A dissertation submitted to the faculty of
Old Dominion University in partial fulfillment of the requirement for the degree of

DOCTOR OF PHILOSOPHY

CIVIL ENGINEERING

OLD DOMINION UNIVERSITY

May, 2017

Approved by:

Zia Razzaq (Director)

Duc T. Nguyen (Member)

Julie. Hao (Member)

Sirjani Mojtaba (Member)

ABSTRACT

BEHAVIOR AND STRENGTH OF NON-PRESTRESSED AND PRESTRESSED HILLMAN COMPOSITE BEAM INCLUDING CFRP RETROFITTING

Wajid Khan
Old Dominion University, 2017
Director: Dr. Zia Razzaq

The Hillman Composite Beam (HCB) is a recent innovation used for the first time in 2008 for a bridge construction in USA. It essentially consists of an FRP outer shell, concrete arch inside the shell and steel strands used to tie the two ends of the arch. Being new in the field, the behavior of HCB has not been thoroughly studied. This dissertation presents a study of the flexural behavior and strength of HCB up to the collapse as well as explores the influence of using carbon reinforced polymer (CFRP) retrofitting and prestressed steel for a further increase in HCB stiffness and strength. Materially nonlinear computational algorithms are formulated and programmed to develop moment-curvature relations which are then combined with a finite-difference scheme to predict HCB behavior and strength using Bernoulli beam approach. The nonlinear analysis is performed for various cross sectional configuration of the HCB. A tied arch-and-beam model for predicting the elastic response of HCB is also developed. This model as well as that based on Bernoulli beam approach provided results which are in good agreement with HC Bridge company experiment. A new method involving the combined use of CFRP and steel prestressing resulting in increasing HCB strength by a factor of more than two-and-a-half times is also presented.

My thesis is dedicated to my parents, brothers, my wife and my sons Mustafa and Majid born during the time I was working on this dissertation.

ACKNOWLEDGEMENTS

My principal and utmost thanks and gratitude go to Allah for the successful completion of my PhD dissertation. All the other supports and capabilities I got throughout the course of my PhD are due to His blessings.

Secondly, I would like to express my deepest appreciation for my advisor, Dr. Zia Razzaq, for his kind supervision of my research and valuable guidance at every point. Without him, this dissertation would not have been possible.

The HC Bridge Company and its owner John Hillman deserves special mention for the kind provision of the full scale test data and permission to use it.

I also feel highly indebted to the committee members, my friends and family for their time, encouragement and support.

TABLE OF CONTENTS

Content **Page**

LIST OF FIGURES

LIST OF TABLES

1. INTRODUCTION

1.1 Prelude

This dissertation presents a study of the load-deflection behavior of Hillman Composite Beam (HCB) with an overlying concrete slab as used in a bridge system under four-point loading conditions with and without prestressing and CFRP retrofitting. The HCB is a recent innovation used first time in a bridge construction in 2008. The idea of HCB was originally conceived by John Hillman [1] in 1996 with the aim of enhancing the performance of the conventional bridge beams by intelligently using different materials therein. The HCB consists of three main components, namely, an outer beam shell made of glass fiber reinforced polymer referred to as FRP, a concealed arch made of Portland cement grout or self-consolidating concrete, steel strands embedded into the compression concrete at the ends and polyurethane foam. A 19 ft. long prototype beam was fabricated and tested up to the collapse under gradually increasing static loading at the University of Delaware. The ultimate load for the beam was found to be 180% of the factored design load.

In 2003 Hillman performed a product demonstration of HCB that included fabrication, erection and monitoring of a 30 ft. span full size prototype railroad bridge. The project came to its successful conclusion in 2007 with his demonstration of the desired performance of a HCB bridge at the Facility for Accelerated System Testing (FAST) at Pueblo, Colorado. Since then, HCB has been used in the construction of 18 railway and highway bridges in North America ranging from 52 ft. long single span Tide Mill Bridge, Virginia to 540 ft. long 8 spans Knickerbocker Bridge in Maine. The apparent reasons for the preference of HCB over conventional steel and reinforced concrete bridges are reduced transportation weight, increased corrosion resistance and easy and rapid bridge constructability. However, being a recent development, HCB behavior has not yet been thoroughly studied. Consequently, the current design procedures tend to be simplistic and over conservative. Furthermore, the behavior prediction models do no account for the material nonlinearities.

This research focuses on the behavior of HCB under increasing static vertical loading up to the collapse conditions. Theoretical models for predicting the flexural behavior of HCB are developed and their accuracy is checked by comparing the results with the available

experimental data. The study of the nonlinear flexural behavior of prestressed and CFRP retrofitted HCB is also presented. .

The expected outcome of the research is accurate as well as practical design recommendations for HCB against flexure and deflection control demands.

1.2 Literature review

The Hillman composite beam is a recent innovation in the field of bridge engineering which was introduced in 1996 [2], patented in 2002 [3] and practically used (in bridge construction) in 2008 in Illinois, USA [4]. Being a new development, not much research has been conducted so far on HCB and the literature on this topic is limited to a few research papers and project reports. The summary of the research on HCB is given herein:

For the validation of the concept of HCB, Hillman started his experimental work in 1999 with a grant from the Transportation Research Board-IDEA [2]. Hillman investigated different aspect of HCB for bridge application, namely, cost comparison with equivalent pre-stress concrete and steel girder bridges, manufacturing of Hillman composite beam and tooling for the manufacture, design and analysis and limit states governing the process etc. A prototype HCB was actually produced and tested to verify the validity of the predicted performance. Hillman submitted his final report in 2003 [2]. The important conclusions and suggestions for further investigation were:

1. The behavior of the beam under loading was very close to the predicted behavior.
2. The economic advantages of HCB were related to the span length. For short span, HCB appeared to be cheaper than steel beam and for longer spans, it proved to be superior to even prestressed concrete beam due to its light weight advantages.
3. The serviceability limit state of beam deflection appeared to consistently govern the design.
4. Shear in the beam is mostly carried by the FRP webs but the arching action of the compression reinforcement offered a redundant path that is exploited as the applied forces exceed the factored demand.

5 Relative economic difference between carbon fiber and steel tension fin forcing.

6 Fine tuning the tooling and lay-up using the recyclable mandrel material to facilitate lighter weight for shipping and erection.

7 Refinement in the analysis and design methodologies.

8 Additional load testing to better quantify shear strength, crushing/buckling of the webs and fatigue stress limit states

9 Testing of multiple beam systems to ascertain distribution of loads to the plurality of beams in bridge cross section.

The investigation proved that HCB was a workable concept; thus creating a demand for checking the viability of HCB by constructing a serviceable bridge using HCB girders.

During the period between the submission of Final Report of Type 1 project in 2003 and initiation of the Type 2 Project fatigue testing of the prototype HCB was carried out wherein the beam was subjected to 2,000,000 cycles of fatigue loading and tested to failure [5]. The results confirmed that the structural response was in compliance with AREMA recommended practices. After the successful extermination on the prototype HCB during Type 1 Idea Project, work on Type 2 Idea Project started in 2003 with the aim of performing a product demonstration that included fabrication, erection and monitoring of a full size 30-foot prototype railroad bridge constructed using HCB technology [5]. Before the construction of the actual 30 ft. span bridge, two 30-foot prototype HCB girders were prepared and tested in the laboratory. Before the fabrication of the prototype beams, manufacturing experiments were conducted on smaller scale beams of 8-foot length to determine tooling, lay-up and infusion techniques that could be scaled up for the fabrication of larger beams. Both successful laboratory tests yielded similar results and demonstrated that the prototype beams met all performance requirements in accordance with AREMA recommended practices. Then came the stage of manufacturing eight 30 ft. hybrid composite beams for using in the bridge. The process took more time than had been anticipated as the manufacturing techniques evolved during the process of manufacturing. During next stage of the project, issues related to maintenance, durability, fire resistance, preparation of the beam for deployment in the prototype installation and other constructability and performance related issues were addressed. The last stage of project was the field testing of HCB Bridge that was done at the Transportation Technology Center on November 7, 2007.

A 30 ft. prototype test HCB Bridge was constructed at TTCI in Pueblo in 2007. The bridge comprised of eight beams, grouped in two of four beams each. All beam shells were

manufactured individually without the compression concrete then four teams were tied together to form a single unit, thus giving two units of 4 beams each. The self-consolidating concrete was then poured into the cavity provided in the top flange at mid span to form compression reinforcement. The placement of the shear connectors was done before pouring of concrete. Once concrete was placed in all of the beams, forms were placed around the perimeter to cast the composite deck on the two, four-beam assemblies. The two bridge units were then transported to the site of bridge construction.

The flexural behavior of HCB with and without the concrete deck to investigate load distribution between the sub-components of HCB for both non-composite and composite conditions was studied by [6]. Three prototype HCBs of 43 ft. span were constructed at Virginia Tech for testing. First, only FRP shell (without arch concrete in place) was tested; then, complete HCBs (having concrete arch inside the shell) without the concrete deck and finally, the three HCB Bridge with concrete deck was tested. The research investigated the hypothesis that the beam could be broken down into two separate systems for analysis, namely, the tied arch and the beam shell. Two loading configurations i.e., 15 k load at the mid-span and two identical loads (12.5 kips) at quarter points were used for the individual beam testing. The tests showed that strain compatibility existed between steel strands and FRP shell and the neutral axis prediction based on transformed section strain compatibility was accurate. However, the observed arch concrete strains differed considerably from the predicted ones showing that transformed section strain compatibility could not be used to predict concrete arch strains. The contribution of the tied arch and the shell to resist loads calculated from two different methods namely, curvature method and stress integration method, showed that the tied arch system was responsible for slightly less than 80% of resistance and the shell took approximately 20% of the load.

Tests on HCB composite with concrete deck in the three beam system led to the following findings:

1. Transformed section method is acceptable for predicting the system behavior.
2. The concrete arch is in tension so its strain is not plotted nor is it considered effective in resisting load but even with this arrangement the HCB (shell and tension reinforcement) provided almost 80% of the load resistance. Moreover, the assumption that the arch is cracked leads to simple design procedures as we then have a constant cross section beam throughout the span.

3. FRP has linear strain profiles for both mid and quarter point tests.
4. Compressive strains in concrete deck are consistent with FRP strain trends and strain compatibility exists between the FRP and steel strands.

The accuracy of linear FE analysis in predicting static behavior of the HCB under service loads was examined by [7]. One of the HCB bridges constructed in Missouri named Bridge 0439 was analyzed using SAP 2000 an ANSYS. The deflections obtained from analysis were then compared with the field deflections at mid-span and quarter points. The deflections at the specified points were calculated by using the currently in use simple analytic procedure based on transformed area method. The comparison of the calculated and measured values showed that FEA could predict HCB bridge behavior with acceptable accuracy whereas the simple analytical method gave pretty higher values for deflections than the measured ones.

To the best of the author's knowledge and in view of the literature review conducted, the influence of the CFRP retrofitting and prestressing on the performance of HCB has not been studied. Furthermore, no materially nonlinear analysis procedure for HCB has been published in the past.

1.3 Problem statement

An isometric view of Hillman Composite Beam is shown in Figure 1. The beam consists of three main components, namely, (1) the beam outer shell, made of fiber reinforced polymers, that encapsulates the other two components; (2) the concrete arch, called compression reinforcement, made of self-consolidating concrete or cement grout; (3) the tension reinforcement, consisting of carbon, glass or steel fibers that is used to tie two ends of the arch.

The beam shell is constructed of a vinyl resin reinforced with glass fibers optimally oriented to resist the anticipated forces in the beam. The shell includes a top flange, bottom flange, two vertical webs and a continuous conduit to receive concrete for compression reinforcement. All the components of the shell are fabricated monolithically using Vacuum Assisted Resin Transfer Method (VARTM). The top flange can also be fabricated separately and connected to the remaining shell later on.

The compression reinforcement typically consists of self-consolidating concrete (SCC) or cement grout pumped into the conduit through the ports located typically at the ends and

centerline of the beam but they may also be located at intermediate points depending on length of the beam. The profile of compression reinforcement is parabolic that starts at the bottom corners of the beam ends and reaches an apex at the mid-span where arch and the top flange are tangent.

The tension reinforcement consists of layers of unidirectional steel reinforcing fibers with high tensile strength and high elastic modulus. The tension reinforcement is fabricated monolithically into the composite beam the same time the beam shell is constructed. Consequently, the strands are completely encapsulated in the same resin matrix as the glass fibers.

This research dissertation comprises of two main parts. In the first part, a study is conducted into the linear and nonlinear behavior of HCB under flexure. The experimental data, provided by the HC Bridge Company [9], will be used for the validation of the theory. The load-deflection response of HCB under four-point loading as shown in Figure 2 is theoretically predicted up to the collapse condition. The nonlinear moment-curvature analysis in combination with on the finite-difference method is used for the nonlinear analysis. An alternative approach to the analysis which considers HCB as combination of a beam and concealed arch is also presented for the prediction of the load-deflection behavior in the elastic range only.

In the second part, the nonlinear behavior of HCB up to the collapse is theoretically investigated for prestressing and CFRP retrofitting.

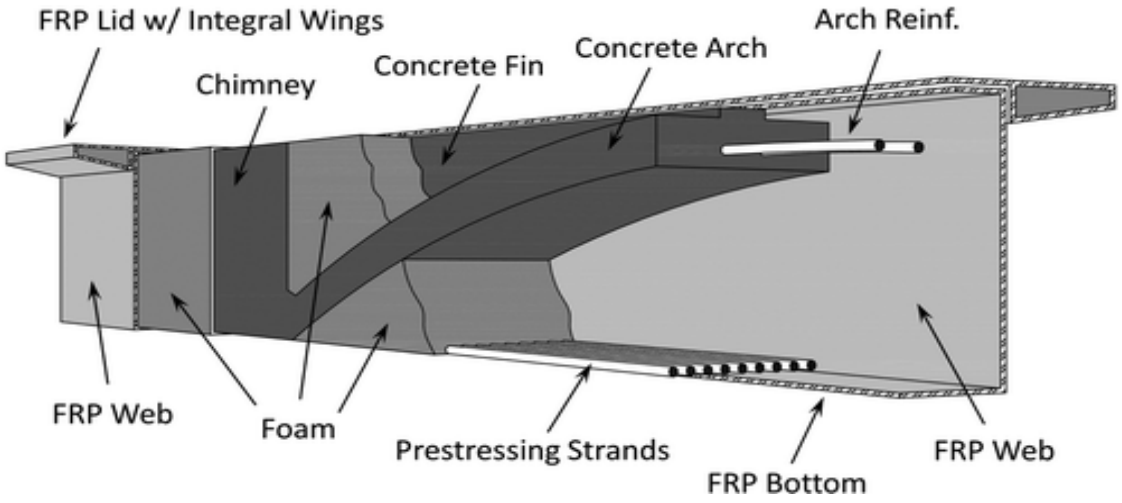

Figure 1. Isometric view of Hillman Composite Beam [9]

1.4 Objectives and Scope

The main objectives of the study are summarized as under:

1. Development of practical theoretical models for predicting the load-deflection response up to the collapse condition for HCB
2. Theoretical assessment of the performance of prestressed HCB
3. Theoretical assessment of the performance of HCB retrofitted with CFRP

The data provided by the HC Bridge Company is used of the validation of first objective. Four- points loading as used by in the experiment [10] is used for the theoretical analysis. The second and third objectives are only a theoretical analyses and no experimental data is available for validation. Other main points defining the scope of the study are as under:

1. High strength self-consolidating concrete as actually used in the construction of the compression reinforcement [10] is used in the theoretical analysis.
2. Yield strength of 250 ksi is used for the tension reinforcement.
3. The webs and top and bottom flanges of the beam outer box are monolithic
4. The tension steel is monolithic with the bottom flange

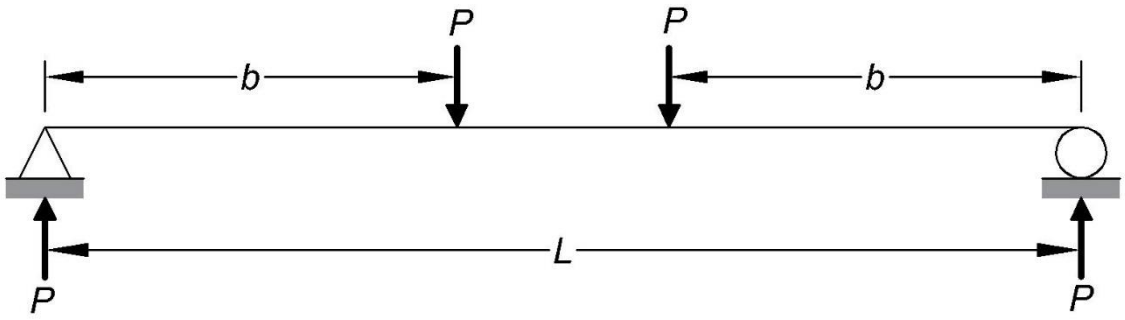

Figure 2. Loading pattern used for analysis of HCB

1.5 Assumptions and Conditions

Assumptions and conditions adopted in this investigation are as follows:

1. All mechanical loads are concentrated loads.
2. Small deflection theory is assumed.
3. Linear strain profile occurs along the depth of the beam and strain compatibility exists between the bottom FRP flange and tension reinforcement and between top flange and concrete deck.
4. No initial imperfections are considered.
5. The beam is a simple supported beam.
6. The steel follows the elastic-perfectly plastic stress-strain relationship as shown in Figures 3 and 4 and its stress-strain relationship is the same for compression and tension.
7. The stress-strain relationship for concrete is simplified to tri-linear curve as shown in Figure 5 and is same for compression and tension.
8. The stress-strain relation for FRP is linear up to the point of failure as shown in Figures 6 and 7.
9. Concrete and steel are assumed to be isotropic materials.
10. FRP is assumed to be orthotropic transversely isotropic material.

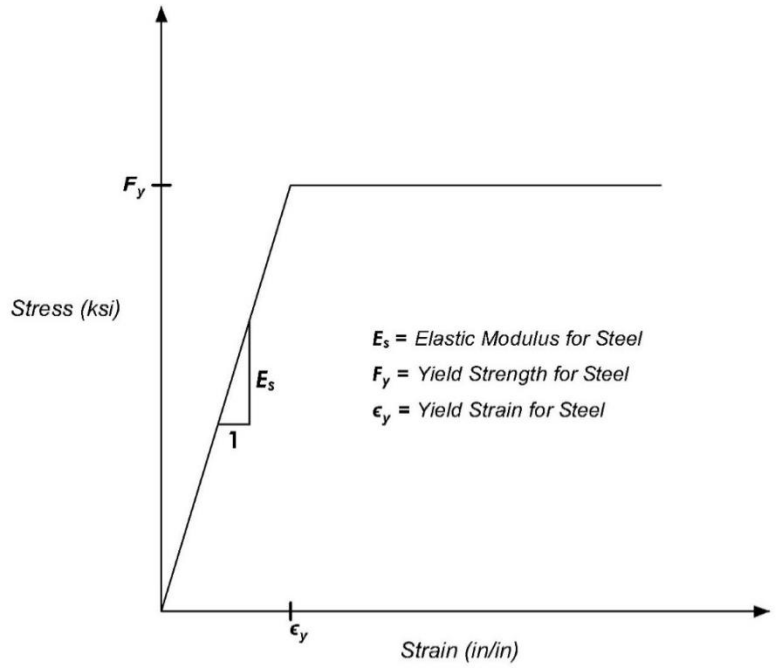

Figure 3. Stress-strain relation for steel rebars

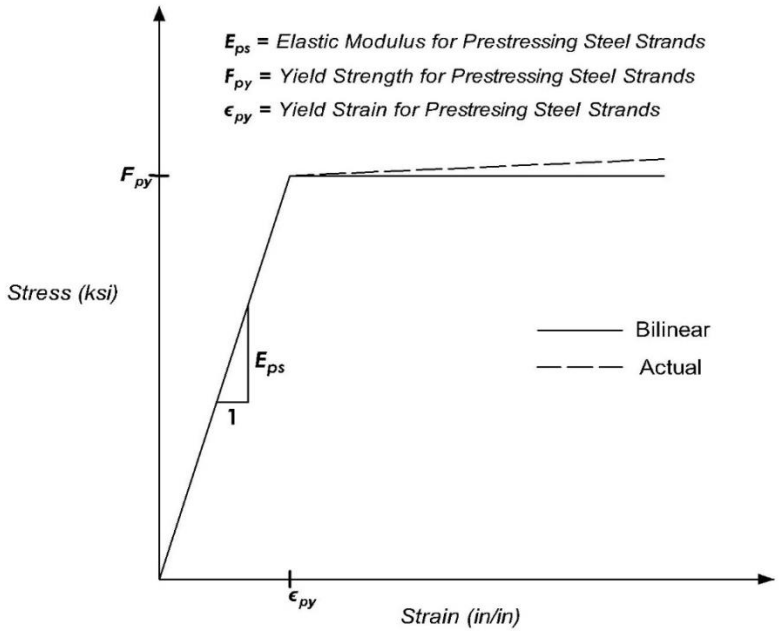

Figure 4. Stress-strain relation for steel strand

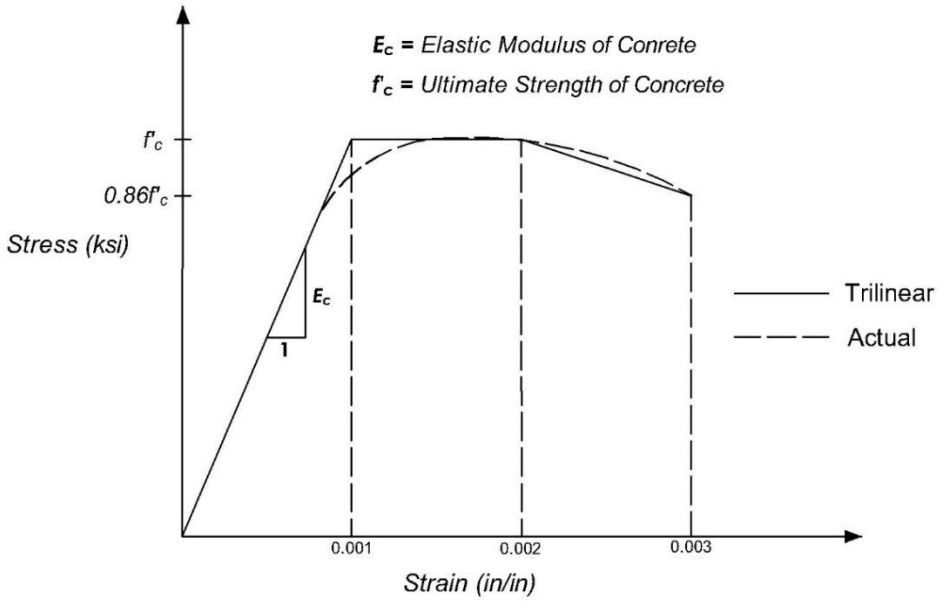

Figure 5. Stress-strain curve for concrete

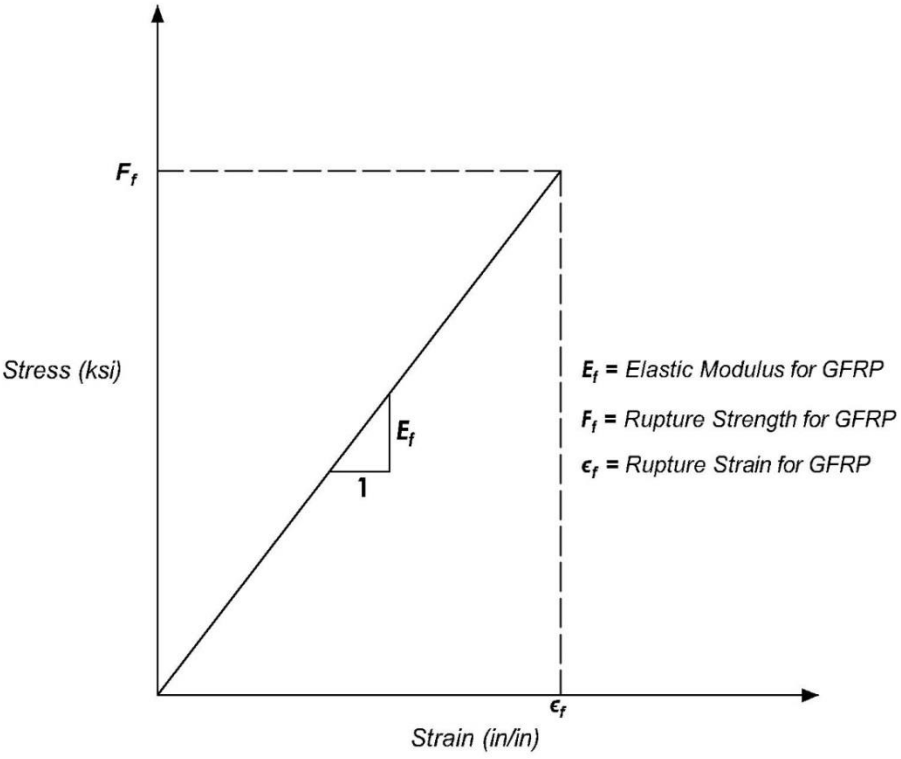

Figure 6. Stress-strain curve for GFRP

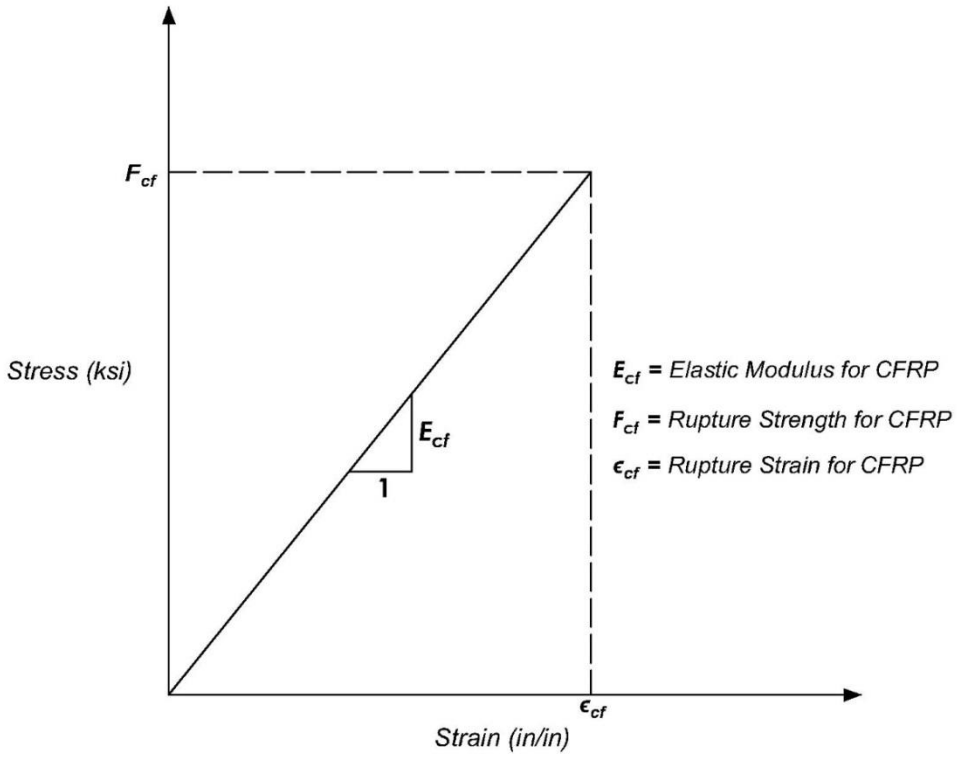

Figure 7. Stress-strain curve for CFRP

2. THEORETICAL FORMULATION

This chapter presents theoretical formulation for the study of the linear and nonlinear behavior of non-prestressed and prestressed HCB under bending loading. Two approaches to HCB analysis are presented herein. In the first approach, the analysis of HCB is performed to predict the load-deflection relation up to the collapse condition by considering the HCB as a Bernoulli beam. In the second approach, HCB is considered as a composite of two elements, namely, a box beam and a concealed arch. The second method is used to determine the load-deflection behavior of HCB in the elastic range only. The theoretical formulation for both approaches of analysis is presented as under:

2.1 HCB analyzed as Bernoulli beam

In this approach HCB is considered as a single beam and analyzed by following the Bernoulli's beam theory [11] to predict the load-deflection response and ultimate load carrying capacity under bending loads. In order to investigate the impact of different cross-sectional elements of HCB on the behavior and find simple practical method of predicting the deflection response and strength, the analysis is performed for the following four cross sections for HCB:

1. .Regular HCB cross section
2. Cross section without concrete arch and fin
3. Cross section without concrete arch and FRP box
4. Cross section with average fin depth

2.1.1 HCB with regular cross section

The cross section of a typical HCB is shown in Figure 8. The FRP wings and foam used as filler, due to their anticipated negligible contribution in shaping the response of HCB, are not considered in the analysis. The cross section of HCB used for the analysis is shown in Figure 9. The analysis includes theoretical prediction of the load-midspan deflection relations for HCB and comparing it with the available experimental data. The components of the analysis procedure and mythologies used therein are given in the following sections.

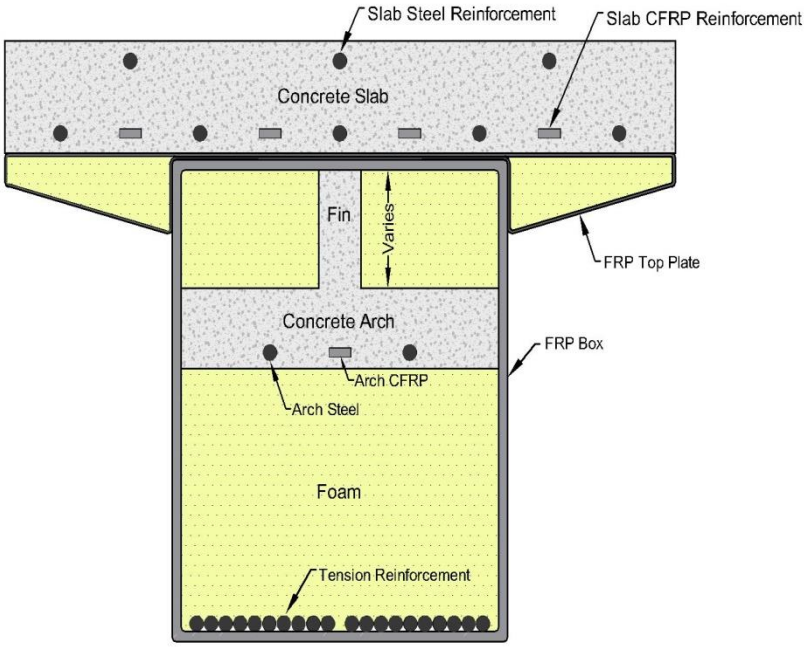

Figure 8. Typical cross section of HCB

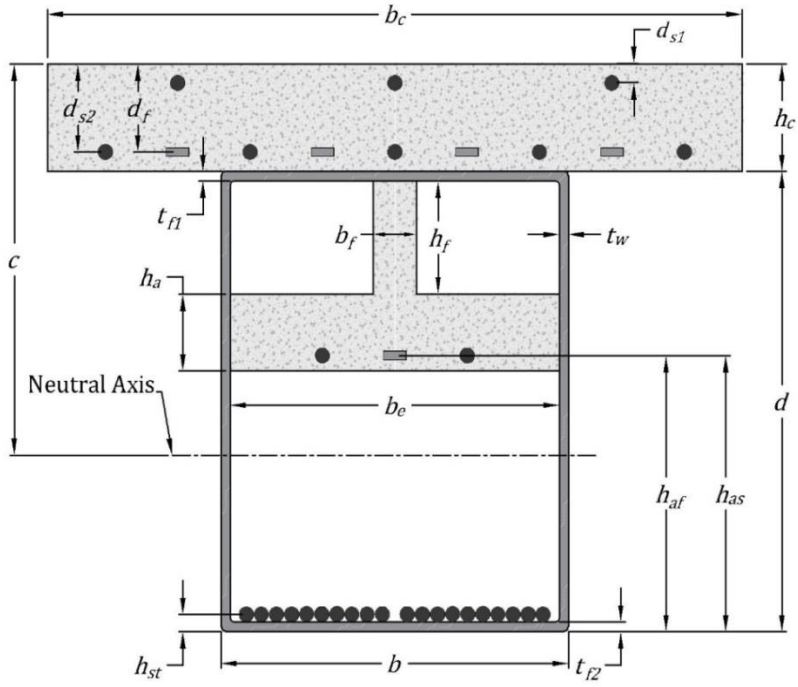

Figure 9. Cross section of HCB used for analysis

2.1.2 Neutral axis of HCB

The first step of the analysis is the determination of the location of the neural axis which is done by using the following fundamental equation:

Moment of cross section = Sum of moments of cross-sectional components

$$(\sum_{i=1}^{n} A_i)\bar{y} = \sum_{i=1}^{n} A_i \bar{y}_i \quad (1)$$

Where

A_i = Area of i-th cross-sectional component

$\bar{y}_i$ = Centroidal distance of area A_i from the top of cross section

$\bar{y}$ = Centroidal distance of cross section from the top of the cross section

Referring to Figure 9, we get:

$$\sum(A\bar{y}) = A_c\,(h_c/2)\,/(E_e/E_c) + A_{s1}\,d_{s1}/(E_e/E_s) + A_{s2}\,d_{s2}/(E_e/E_s) + A_f\,d_f/(E_e/E_f) + 2t_w(d - t_{f1} - t_{f2})(h_c + t_{f1} + (d - t_{f1} - t_{f2})/2) + bt_{f1}\left(h_c + t_{f1}/2\right)/(E_e/E_{ef}) + bt_{f2}\left(h_c + d - t_{f2}/2\right)/(E_e/E_{ef}) + b_f h_f (h_c + t_{f1} + h_f/2)\,/(E_e/E_{ac}) + b_e h_a(h_c + t_{f1} + h_f + h_a/2)/(E_e/E_{ac}) + A_{as}(h_c + d - h_{as})/(E_e/E_{st}) + A_{af}(h_c + d - h_{af})/(E_e/E_f) + A_{st}(h_c + d - h_{st})/(E_e/E_{st}) \quad (2)$$

And

$$\sum A = A_c/(^{E_e}/_{E_c}) + A_{s1}/(^{E_e}/_{E_s}) + A_{s2}/(^{E_e}/_{E_s}) + A_f/(^{E_e}/_{E_f}) + 2t_w(d - t_{f1} - t_{f2}) +$$
$$bt_{f1}/(^{E_e}/_{E_{ef}}) + bt_{f2}/(^{E_e}/_{E_{ef}}) + b_f h_f/(^{E_e}/_{E_{ac}}) + b_e h_a/(^{E_e}/_{E_{ac}}) +$$
$$A_{as}/(^{E_e}/_{E_{st}}) + A_{af}/(^{E_e}/_{E_f}) + A_{st}/(^{E_e}/_{E_{st}}) \quad (3)$$

where

t_w = Thickness of web

t_{f1} = Thickness of top flange

t_{f2} = Thickness of bottom flange

h_c = Thickness of slab

A_c = Area of slab concrete

d = Depth of HCB

b = Width of HCB

A_s = Area of slab steel

d_{s1} = Top slab rebars centroidal distance from the top of slab

d_{s2} = Bottom slab rebars centroidal distance from the top of slab

b_f = Thickness of concrete fin

h_f = Height of concrete fin

A_f = Area of slab CFRP reinforcement

d_f = Centroidal distance of slab CFRP reinforcement form the top of slab

b_e = Width of concrete arch

h_a = Height of concrete arch

A_{as} = Area of arch steel

A_{af} = Area of arch CFRP reinforcement

A_{st} = Area of tension reinforcement

h_{as} = Centroidal distance of arch steel from the bottom of beam

h_{af} = Centroidal distance of arch CFRP from the bottom of beam

h_s = Centroidal distance of tension reinforcement from the bottom of beam

E_e = Modulus of elasticity for FRP used in webs

E_{ef} = Modulus of elasticity for FRP used in flanges

E_c = Modulus of elasticity for slab concrete

E_{ac} = Modulus of elasticity for arch concrete

E_s = Modulus of elasticity for steel rebars

E_{st} = Modulus of elasticity for pre-stress steel strands

The depth of the neutral axis from top of the slab is, then, given by:

$$\bar{y} = {\sum Ay}\Big/{\sum A} \tag{4}$$

Substituting equations 2 and 3, in equation 4 gives an expression for the elastic neutral axis of HCB.

2.1.3 Internal resisting moment in HCB section

The equation for the internal resisting moment at any section of HCB depends upon the strain condition across the depth of beam and location of the neutral axis of the section. Due to the complex geometry of HCB and variety of materials used therein, equation for the internal moment for the same HCB section takes different shapes as the location of the neutral axis and strain level in different materials changes. Here are given equations for individual contributions of the HCB cross-sectional components to the internal resisting moment produced in response to the given strains one situation when neutral axis of the section is below the concrete arch as shown in Figure 9 and stress in slab and arch concrete are within the elastic range. The stress and strain diagrams for the HCB section under the above mentioned conditions are shown in Figure 10.

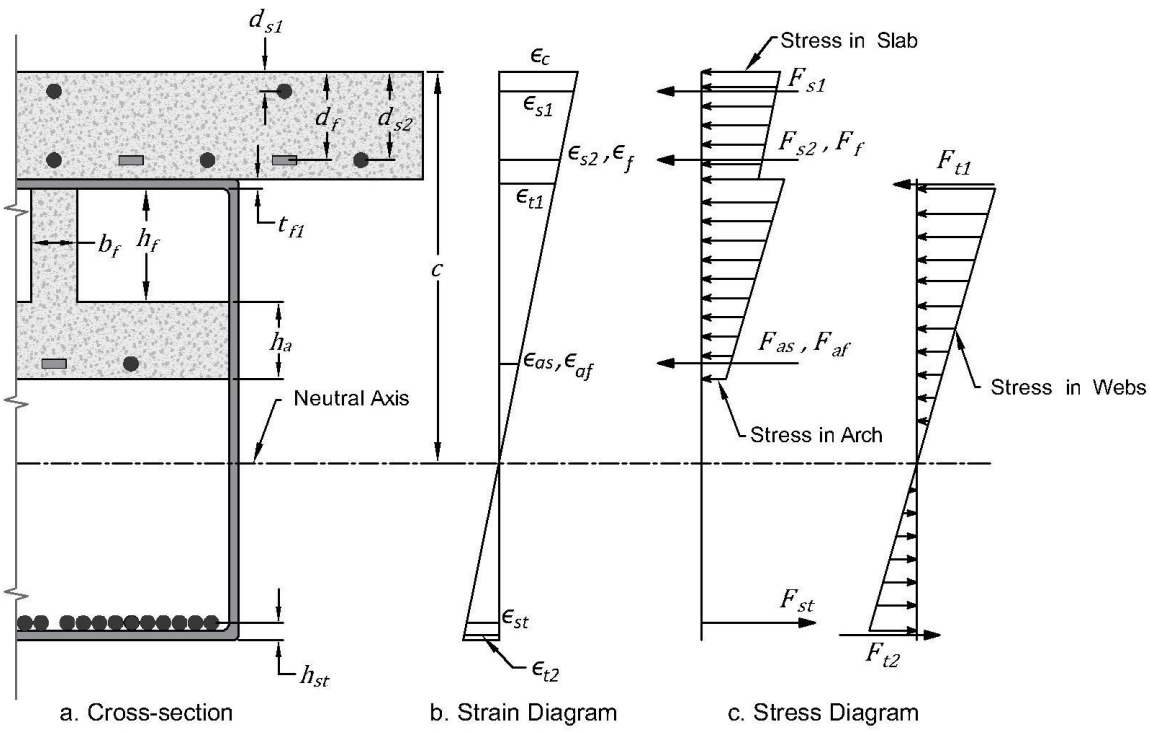

Figure 10. Stress-strain diagram for HCB for neutral axis below concrete arch and stresses elastic

The contribution of slab concrete to the resisting moment under such conditions will be:

$$M_{cs} = \frac{1}{2}\left(\epsilon_c + \frac{\epsilon_c}{c} h_c\right) E_c A_c \left(c - \frac{h_c}{3} \frac{\left(\epsilon_c + 2\frac{\epsilon_c}{c} h_c\right)}{\left(\epsilon_c + \frac{\epsilon_c}{c} h_c\right)}\right) \quad (5)$$

where

ϵ_c= Strain in top fibers of concrete slab

c = Distance of neutral axis from the top of slab

The contribution of the top steel reinforcement in the concrete slab is:

$$M_{s1} = F_{s1}(\mathrm{c} - d_{s1}) \tag{6}$$

where

F_{s1} = Force in top slab steel

$F_{s1} = \in_{s1} E_s A_{s1}$ when $\in_{s1} = \frac{\in_c}{c}(c - d_{s1}) < \in_y$

$F_{s1} = F_y A_{s1}$ when $\in_{s1} \geq \in_y$

$\in_{s1}$ = Strain in top slab steel

$\in_y$ = Yield Strain of top steel rebars

F_y = Yield strength of top steel rebars

The contribution of the bottom steel reinforcement in the concrete slab is:

$$M_{s2} = F_{s2}(\mathrm{c} - d_{s2}) \tag{7}$$

where

F_{s2} = Force in bottom slab steel

$F_{s2} = \in_{s2} E_s A_{s2}$ when $\in_{s2} = \frac{\in_c}{c}(c - d_{s2}) < \in_y$

$F_{s2} = F_y A_{s2}$ when $\in_{s2} \geq \in_y$

$\in_{s2}$ = Strain in bottom slab steel

$\in_y$ = Yield Strain of bottom steel rebars

F_y = Yield strength of bottom steel rebars

The contribution of CFRP slab reinforcement will be:

$$M_f = F_f(\mathrm{c} - d_f) \tag{8}$$

where

F_f = Force in CFRP slab reinforcement

$F_f = \in_f E_f A_f$ when $\in_f = \frac{\in_c}{c}(c - d_f) < \in_{uf}$

$F_f = 0$ when $\in_f \geq \in_{uf}$

$\in_f$ = Strain in CFRP slab reinforcement

$\in_{uf}$ = Ultimate strain of CFRP

The contribution of concrete fin to the internal resisting moment will be:

$$M_{cf} = \frac{\in_c}{c}(c - h_c - t_{f1} - \frac{h_f}{2})E_{ac}b_f h_f y_{cf} \tag{9}$$

where

y_{cf} = Distance of center of the fin force from the top of fin

$$= c - h_c - t_{f1} - \frac{h_f}{3}\frac{\left(\frac{\in_c}{c}((c - h_c - t_{f1}) + 2\frac{\in_c}{c}(c - h_c - t_{f1} - h_f)\right)}{\left(\left(\frac{\in_c}{c}((c - h_c - t_{f1}) + \frac{\in_c}{c}(c - h_c - t_{f1} - h_f)\right)\right)}$$

The contribution of concrete arch to the internal resisting moment will be:

$$M_{ca} = \frac{\in_c}{c}(c - h_c - t_{f1} - h_f - \frac{h_a}{2})E_{ac}b_e h_a y_{ca} \tag{10}$$

where

y_{ca} = Distance of the center of arch force from the top of arch

$$= c - h_c - t_{f1} - h_f - \frac{h_a}{3}\frac{\frac{\epsilon_c}{c}\left(\left(c - h_c - t_{f1} - h_f\right) + 2\left(c - h_c - t_{f1} - h_f - h_a\right)\right)}{\frac{\epsilon_c}{c}\left(\left(c - h_c - t_{f1} - h_f\right) + \left(c - h_c - t_{f1} - h_f - h_a\right)\right)}$$

The contribution of arch steel reinforcement is:

$$M_{as} = F_{as}(c - (h_c + d - h_{as})) \tag{11}$$

where

F_{as} = Force in arch steel

$F_{as} = \epsilon_{as}\, E_{st}\, A_{as}$ when $\epsilon_{as} = \frac{\epsilon_c}{c}(c - (h_c + d - h_{as})) < \epsilon_{ys}$

$F_{as} = F_{ys}\, A_{as}$ when $\epsilon_{as} \geq \epsilon_{ys}$

ϵ_{as} = Strain in arch steel

ϵ_{ys} = Yield strain of arch steel strands

F_{ys} = Yield strength of arch steel strands

The contribution by arch CFRP reinforcement is:

$$M_{af} = F_{af}\left(c - (h_c + d - h_{af})\right) \tag{12}$$

where

F_{af} = Force in arch CFRP

$F_{af} = \epsilon_{af}\, E_f\, A_{af}$ when $\epsilon_{af} = \frac{\epsilon_c}{c}\left(c - (h_c + d - h_{af})\right) < \epsilon_{uf}$

$F_{af} = 0$ when $\epsilon_{af} \geq \epsilon_{uf}$

ϵ_{af} = Strain in arch CFRP

ϵ_{uf} = Rupture strain of arch CFRP

The contribution of the top flange is:

$$M_{t1} = F_{t1}(c - h_c - {}^{t_{f1}}/_{2}) \quad (13)$$

where

F_{t1} = Force in top flange

$F_{t1} = \in_{t1} E_{ef}\, bt_{f1}$ when $\in_{t1} = \frac{\in_c}{c}(c - h_c - {}^{t_{f1}}/_{2}) < \in_{ef}$

$F_{t1} = 0$ when $\in_{t1} \geq \in_{ef}$

$\in_{t1}$ = Strain at the middle of top HCB flange

$\in_{ef}$ = Ultimate strain of FRP used in flanges

Similarly, the moment contribution of the bottom flange is:

$$M_{t2} = F_{t2}(h_c + d - c - {}^{t_{f2}}/_{2}) \quad (14)$$

where

F_{t2} = Force in top flange

$F_{t2} = \in_{t2} E_{ef}\, bt_{f2}$ when $\in_{t2} = \frac{\in_c}{c}(h_c + d - c - {}^{t_{f2}}/_{2}) < \in_{ef}$

$F_{t2} = 0$ when $\in_{t2} \geq \in_{ef}$

$\in_{t1}$ = Strain at the middle of bottom HCB flange

$\in_{ef}$ = Ultimate strain of FRP used in flanges

The moment contribution of the part of the webs in compression will be:

For $\in_{tw} = \frac{\in_c}{c}(c - h_c - t_{f1}) < \in_e$:

$$M_{wc} = \frac{\in_c}{c}(c - h_c - t_{f1}) E_e t_w (c - h_c - t_{f1}) \frac{2}{3}(c - h_c - t_{f1}) \quad (15)$$

For $\in_{tw} \geq \in_e$:

$$M_{wc} = 0 \quad (16)$$

where

$\in_{tw}$ = Strain at the top of HCB webs

$\in_e$ = Ultimate strain of FRP used in webs

The moment contribution of the part of the webs in tension will be:

For $\in_{bw} = \frac{\in_c}{c}(h_c + d - c - t_{f2}) < \in_e$:

$$M_{wt} = \frac{\in_c}{c}(h_c + d - c - t_{f2})\, E_e t_w (h_c + d - c - t_{f2})\, \frac{2}{3}(h_c + d - c - t_{f2}) \quad (17)$$

For $\in_{bw} \geq \in_e$:

$$M_{wt} = 0 \quad (18)$$

where $\in_{bw}$ = Strain at the bottom of HCB webs

The internal moment contribution due to the tension reinforcement will be:

$$M_{st} = F_{st}(h_c + d - c - h_{st}) \quad (19)$$

where

F_{st} = Force in tension reinforcement

$F_{st} = \in_{st} E_{st} A_{st}$ when $\in_{st} = \frac{\in_c}{c}(h_c + d - c - h_{st}) < \in_{ys}$

$F_{st} = F_{ys} A_{s1}$ when $\in_{st} \geq \in_{ys}$

$\in_{st}$ = Strain in tension reinforcement

$\in_{ys}$ = Yield strain of tension reinforcement

F_{ys} = Yield strength of tension reinforcement

The nominal resisting moment of the beam cross section M_n will be equal to the sum of the individual resisting moment contributions of all the components of the HCB cros-section i.e.,

$$M_n = \sum M_i$$
$$= M_{cs} + M_{s1} + M_{s2} + M_f + M_{cf} + M_{ca} + M_{as} + M_{af} + M_{t1} + M_{t2} + M_{wc} + M_{wt} + M_{st} \quad (20)$$

The above equation will be used for calculating the nominal moment at different sections of the beam for getting M-Φ curves.

2.1.4 Equation for flexural equilibrium of HCB

Due to the complicated geometry of HCB cross section and a variety of materials used therein, various moment equilibrium equations are possible for different locations of the neutral axis and stress levels. For the case shown in Figure 10, wherein stress in all components is elastic and neutral axis is located below the concrete arch, the internal resisting moment produced by the cross section for the linear strain distribution is:

$$M_e = M_i = \frac{1}{2}\left(\in_c + \frac{\in_c}{c} h_c\right) E_c A_c \left(c - \frac{h_c}{3}\frac{\left(\in_c + 2\frac{\in_c}{c}h_c\right)}{\left(\in_c + \frac{\in_c}{c}h_c\right)}\right) + \frac{\in_c}{c}(c - d_{s1}) E_s A_{s1}(c - d_{s1}) + \frac{\in_c}{c}(c - d_{s2}) E_s A_{s2}(c - d_{s2}) + \frac{\in_c}{c}(c - d_f) E_s A_f (c - d_f) + \frac{\in_c}{c}(c - h_c - t_{f1} - \frac{h_f}{2}) E_{ac} b_f h_f (c - h_c - t_{f1} - \frac{h_f}{3}\left(\frac{\frac{\in_c}{c}\left((c - h_c - t_{f1}) + 2(c - h_c - t_{f1} - h_f)\right)}{\frac{\in_c}{c}\left((c - h_c - t_{f1}) + (c - h_c - t_{f1} - h_f)\right)}\right)) + \frac{\in_c}{c}(c - h_c - t_{f1} - h_f - \frac{h_a}{2}) E_{ac} b_e h_a \left(c - h_c - t_{f1} - h_f - \frac{h_a}{3}\left(\frac{\frac{\in_c}{c}\left((c - h_c - t_{f1} - h_f) + 2(c - h_c - t_{f1} - h_f - h_a)\right)}{\frac{\in_c}{c}\left((c - h_c - t_{f1} - h_f) + (c - h_c - t_{f1} - h_f - h_a)\right)}\right)\right) + \frac{\in_c}{c}(c - (h_c + d - h_{as})) E_s A_{as} (c - (h_c + d - h_{as})) + \frac{\in_c}{c}\left(c - (h_c + d - h_{af})\right) E_f A_{af} \left(c - (h_c + d - h_{af})\right) + \frac{\in_c}{c}(c - h_c - \frac{t_{f1}}{2}) E_{ef} b t_{f1} (c - h_c - \frac{t_{f1}}{2}) + \frac{\in_c}{c}(h_c + d - c - \frac{t_{f2}}{2}) E_{ef} b t_{f2} (h_c + d - c - \frac{t_{f2}}{2}) + \frac{\in_c}{c}(c - h_c - t_{f1}) E_{ew} t_w (c - h_c - t_{f1}) \frac{2}{3}(c - h_c - t_{f1}) + \frac{\in_c}{c}(h_c + d - c - t_{f2}) E_{ew} t_w (h_c + d - c - t_{f2}) \frac{2}{3}(h_c + d - c - t_{f2}) + \frac{\in_c}{c}(h_c + d - c - h_{st}) E_{st} A_{st} (h_c + d - c - h_{st}) \quad (21)$$

In a different scenario where stresses in all components are elastic and neutral axis is within the concrete fin as shown in Figure 11, the following flexural equilibrium equation for the HCB section holds:

$$M_e = M_i = \frac{1}{2}\left(\epsilon_c + \frac{\epsilon_c}{c}h_c\right)E_cA_c\left(c - \frac{h_c}{3}\frac{\left(\epsilon_c + 2\frac{\epsilon_c}{c}h_c\right)}{\left(\epsilon_c + \frac{\epsilon_c}{c}h_c\right)}\right) + \frac{\epsilon_c}{c}(c - d_{s1})E_sA_{s1}(c - d_{s1}) + \frac{\epsilon_c}{c}(c - d_{s2})E_sA_{s2}(c - d_{s2}) + \frac{\epsilon_c}{c}(c - d_f)E_sA_f(c - d_f) + \frac{\epsilon_c}{c}(c - h_c - t_{f1} - \frac{h_f}{2})E_{ac}b_fh_f(c - h_c - t_{f1} - \frac{h_f}{3}(\frac{\frac{\epsilon_c}{c}\left((c-h_c-t_{f1})+2(c-h_c-t_{f1}-h_f)\right)}{\frac{\epsilon_c}{c}\left((c-h_c-t_{f1})+(c-h_c-t_{f1}-h_f)\right)})) + \frac{\epsilon_c}{c}(c - h_c - \frac{t_{f1}}{2})E_{ef}bt_{f1}(c - h_c - \frac{t_{f1}}{2}) + \frac{\epsilon_c}{c}(h_c + d - c - \frac{t_{f2}}{2})E_{ef}bt_{f2}(h_c + d - c - \frac{t_{f2}}{2}) + \frac{\epsilon_c}{c}(c - h_c - t_{f1})E_{ew}t_w(c - h_c - t_{f1})\frac{2}{3}(c - h_c - t_{f1}) + \frac{\epsilon_c}{c}(h_c + d - c - t_{f2})E_{ew}t_w(h_c + d - c - t_{f2})\frac{2}{3}(h_c + d - c - t_{f2}) + \frac{\epsilon_c}{c}(h_c + d - c - h_{st})E_{st}A_{st}(h_c + d - c - h_{st}) \quad (22)$$

Equations 21 and 22 represent only two different situations of stress distribution across the complex cross section of HCB. Numerous such complex equations are possible for different stress levels and locations of neutral axis.

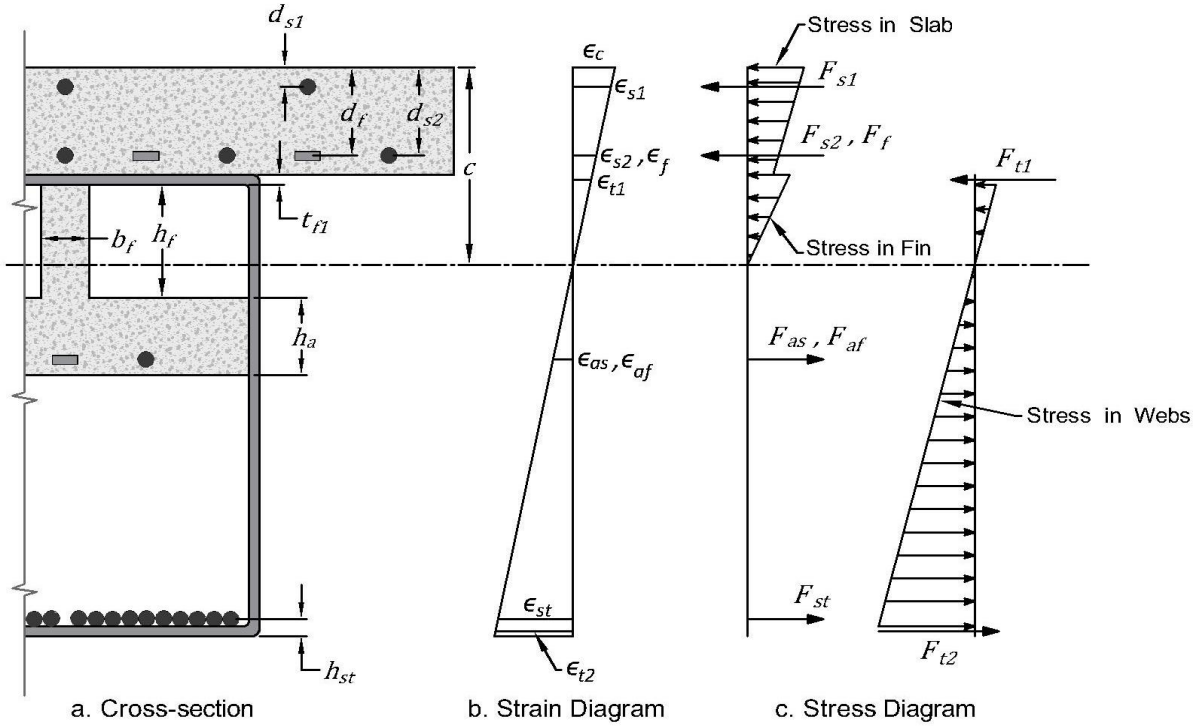

Figure 11. Stress-strain diagram for HCB cross section for neutral axis within

concrete fin and stresses elastic

2.1.5 Load-deflection Relation for HCB

The method followed for predicting the deflection response of HCB under bending loading consists of degenerating load-deflection relation by using theoretical M-ϕ curves equally distant sections along the span of HCB and moment diagram for the actual loading. The description of the method is given as follows:

In order to generate load vs midspan-deflection relation for a simple beam, the span of the beam is divided into *'2n'* number of elements of small equal length *'h'* as shown in Figure 12. Then, at each node is generated theoretical M-ϕ curve using the cross-sectional dimensions at that point. The author have used MATLAB for generating M-ϕ curves. The program written for the purpose is given in Appendix-A. The program takes dimensions of the beam and material properties from user and gives M-ϕ curve as output. The algorithm of the program is structured in a way that strain of concrete at the topmost fiber is varied from 0 to its maximum possible value i.e., 0.003 and for each value of concrete strain the position of the neutral axis is changed until the condition of force equilibrium for the section i.e., $\sum F = 0$ is satisfied. Then the internal moment and curvature is calculated for the equilibrium location of the neutral axis and recorded as a point for plotting M-ϕ graph. In the next step, a new value is assigned to the topmost concrete fiber strain and the above mentioned process repeated for getting next point on the M-ϕ graph.

After M-ϕ curves for the beam at the desired locations are obtained, we can use finite difference method to calculate deflections at the nodes. The scheme followed for finding the midspan deflection is described as follows:

Let $v_{o,} v_{1,}\ v_{2,} \ldots\ldots, v_{n,}$ be the deflection of beam at nodes 0, 1, 2, 3, . . . , *n* , respectively as shown in the Figure 12. The relationship between curvature and deflection is [12]:

$$\phi = \frac{d^2v}{dx^2} \tag{23}$$

The approximate value of ϕ can be calculated by using finite-difference method. The central-difference equation gives [13]:

$$\frac{d^2v_i}{dx^2} = \frac{v_{i-1} - 2v_i + v_{i+1}}{h^2} \quad (24)$$

$$\phi_i h^2 = v_{i-1} - 2v_i + v_{i+1} \quad (25)$$

where i = 1, 2, 3,….., n

The boundary conditions and symmetry of loading gives:

$$v_0 = 0 \quad (26)$$

$$v_{n-1} = v_{n+1} \quad (27)$$

Using the above conditions, the system of linear equations can be written as:

$$h^2\{\emptyset_i\} = [C_{ij}]\{v_i\} \quad (28)$$

where i = 1, 2, 3, … , n and j = 1, 2, 3, … , n. The square matrix C_{ij} is given in Appendix B.

The beam deflections at the chosen sections will be given by:

$$\{v_i\} = h^2[C_{ij}]^{-1}\{\emptyset_i\} \quad (29)$$

Equation 37 can be solved for deflections at the nodes by simply substituting curvature values corresponding to the moments and the interval *'h'*. The system of equation for i =1, 2, 3, … , n and j = 1, 2, 3, … , n is given in Appendix C.

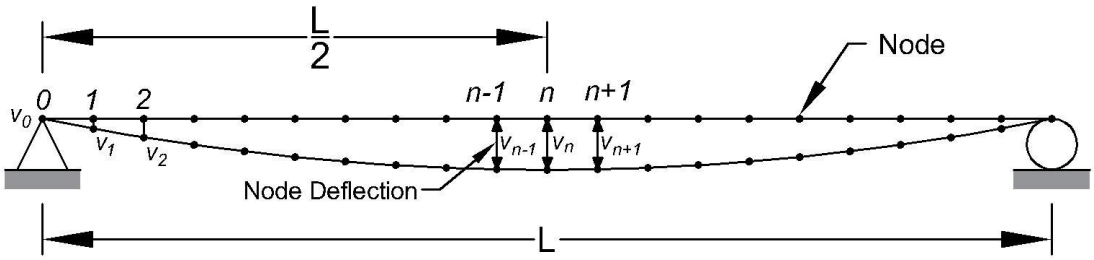

Figure 12. Meshing of HCB for applying finite-difference method

2.1.6 HCB analyzed for cross section without concrete arch and fin

In order to investigate the contribution of concrete arch and fin to the strength and stiffness of HCB, the deflection-response of HCB under bending loading is determined by ignoring the presence of concrete arch and fin and using the cross section with concrete slab over FRP box as shown in Figure 13. The concrete slab and steel reinforcement, under such assumption, are expected to be the major contributors to the structural performance of the beam with FRB outer box and foam contributing only marginally but playing important role of helping HCB maintain its shape to achieve the desired performance.

The load deflection relation for HCB without the concrete arch and fin can be theoretically predicted by using the same finite-difference approach as followed for the regular HCB in section 2.1 except all the nodes in the current case, due to uniform cross section throughout the span of HCB, will have same moment-curvature curve and equation for the internal moment will not have terms for the fin and arch. Referring to the stress and strain diagrams shown in Figure 13, the equation for the internal moment with neutral axis of the section below the slab concrete will be:

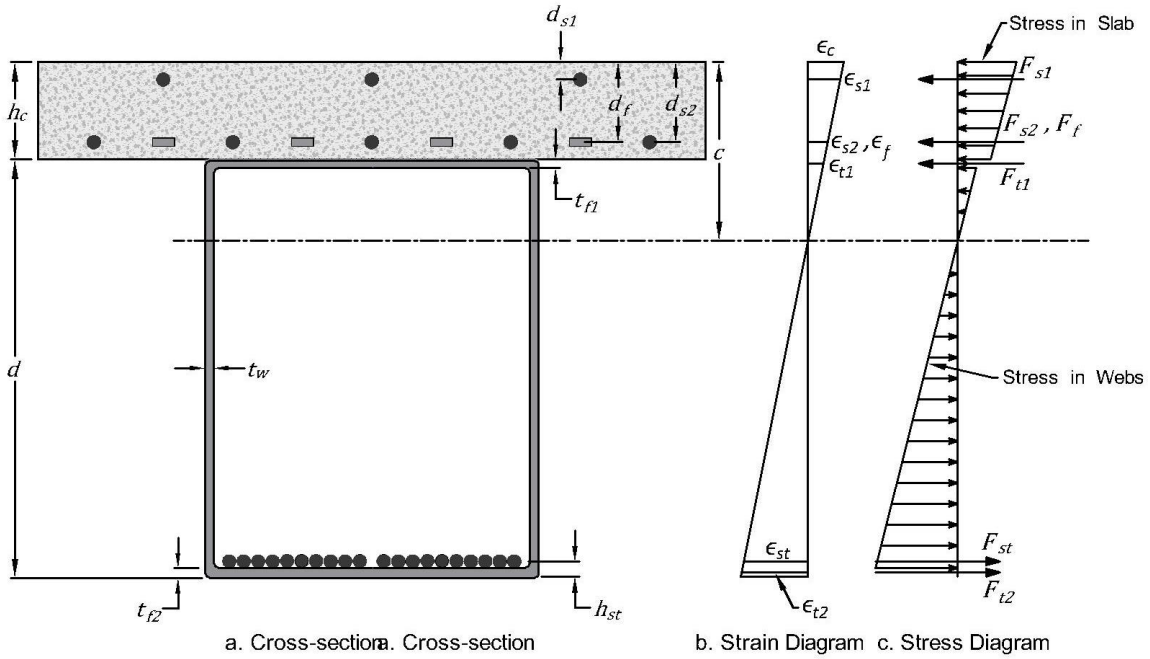

Figure 13. Stress-strain diagram for HCB without concrete arch for neutral axis below concrete slab

$$M_e = M_i = \frac{1}{2}\left(\epsilon_c + \frac{\epsilon_c}{c}h_c\right)E_cA_c\left(c - \frac{h_c}{3}\frac{\left(\epsilon_c + 2\frac{\epsilon_c}{c}h_c\right)}{\left(\epsilon_c + \frac{\epsilon_c}{c}h_c\right)}\right) + \frac{\epsilon_c}{c}(c - d_{s1})E_sA_{s1}(c - d_{s1}) + \frac{\epsilon_c}{c}(c - d_{s2})E_sA_{s2}(c - d_{s2}) + \frac{\epsilon_c}{c}(c - d_f)E_sA_f(c - d_f) + \frac{\epsilon_c}{c}(c - h_c - \frac{t_{f1}}{2})E_{ef}bt_{f1}(c - h_c - \frac{t_{f1}}{2}) + \frac{\epsilon_c}{c}(h_c + d - c - \frac{t_{f2}}{2})E_{ef}bt_{f2}(h_c + d - c - \frac{t_{f2}}{2}) + \frac{\epsilon_c}{c}(c - h_c - t_{f1})E_{ew}t_w(c - h_c - t_{f1})\frac{2}{3}(c - h_c - t_{f1}) + \frac{\epsilon_c}{c}(h_c + d - c - t_{f2})E_{ew}t_w(h_c + d - c - t_{f2})\frac{2}{3}(h_c + d - c - t_{f2}) + \frac{\epsilon_c}{c}(h_c + d - c - h_{st})E_{st}A_{st}(h_c + d - c - h_{st}) \quad (30)$$

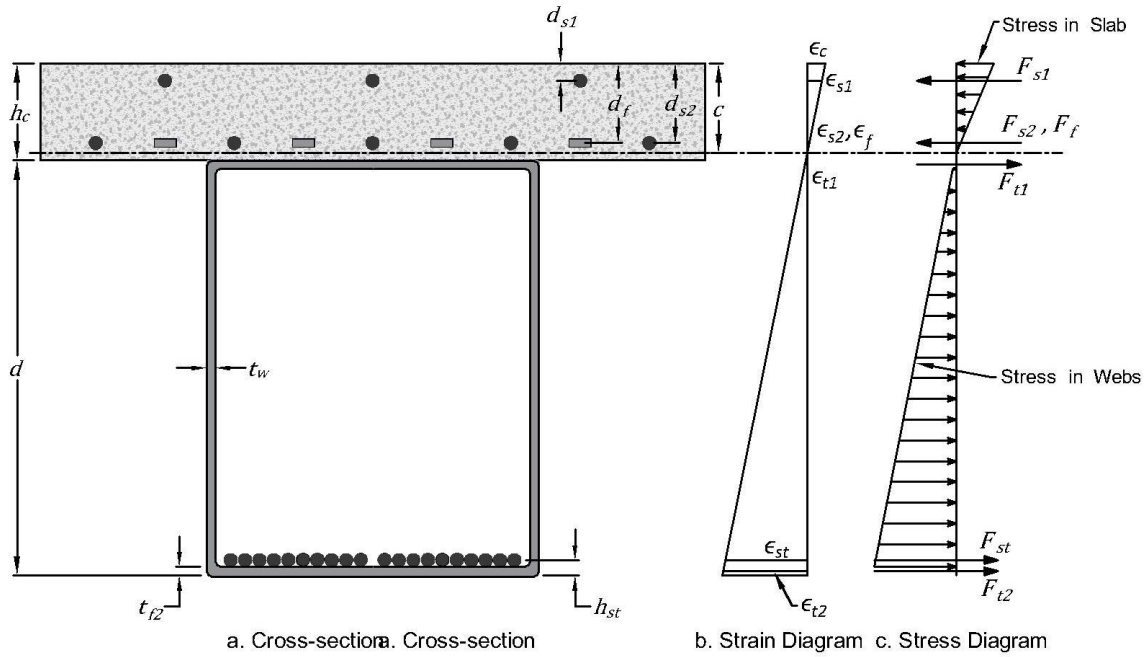

Figure 14. Stress-strain diagram for HCB without concrete arch for neutral axis within concrete slab

Likewise, the equation for the internal moment of the cross section when neutral axis is within the concrete slab, as shown in Figure 14 is given by:

$$M_e = M_i = \frac{1}{2} \in_c E_c A_c \frac{2}{3} c + \frac{\in_c}{c}(c - d_{s1}) E_s A_{s1}(c - d_{s1}) + \frac{\in_c}{c}(c - d_{s2}) E_s A_{s2}(c - d_{s2}) + \frac{\in_c}{c}(c - d_f) E_s A_f (c - d_f) + \frac{\in_c}{c}(h_c + \frac{t_{f1}}{2} - c) E_{ef} b t_{f1}(h_c + \frac{t_{f1}}{2} - c) + \frac{\in_c}{c}(h_c + d - c - \frac{t_{f2}}{2}) E_{ef} b t_{f2}(h_c + d - c - \frac{t_{f2}}{2}) + \frac{\in_c}{c}(h_c + d - c - t_{f1} - \frac{1}{2}(d - t_{f1} - t_{f2})) E_{ew} t_w (d - t_{f1} - t_{f2})(h_c + d - c - t_{f2} - \frac{d - t_{f1} - t_{f2}}{3}(\frac{\frac{\in_c}{c}((h_c + d - c - t_{f2}) - 2(h_c + t_{f1} - c)}{\frac{\in_c}{c}((h_c + d - c - t_{f2}) - (h_c + t_{f1} - c)}) + \frac{\in_c}{c}(h_c + d - c - h_{st}) E_{st} A_{st}(h_c + d - c - h_{st}) \quad (31)$$

Equations 30 and 31 are two of many possible equations to be employed for generating M-ϕ curve fo HCB section. The scheme described in section 2.1 is then used to find the nodal deflections.

2.1.7 HCB analyzed for cross section without concrete arch, fin and FRP box

The equation for the internal moment of HCB without arch and box can be obtained from the equations given in section 2.1.1 by simply omitting the terms f\

the moment contribution of box components. Referring to Figure 15, the equation for the internal moment of HCB section for neutral axis below the concrete slab will be:

$$M_e = M_i = \frac{1}{2}\left(\in_c + \frac{\in_c}{c} h_c\right) E_c A_c \left(c - \frac{h_c}{3}\frac{\left(\in_c + 2\frac{\in_c}{c}h_c\right)}{\left(\in_c + \frac{\in_c}{c}h_c\right)}\right) + \frac{\in_c}{c}(c - d_{s1}) E_s A_{s1}(c - d_{s1}) + \frac{\in_c}{c}(c - d_{s2}) E_s A_{s2}(c - d_{s2}) + \frac{\in_c}{c}(c - d_f) E_s A_f (c - d_f) + \frac{\in_c}{c}(h_c + d - c - h_{st}) E_{st} A_{st}(h_c + d - c - h_{st}) \quad (32)$$

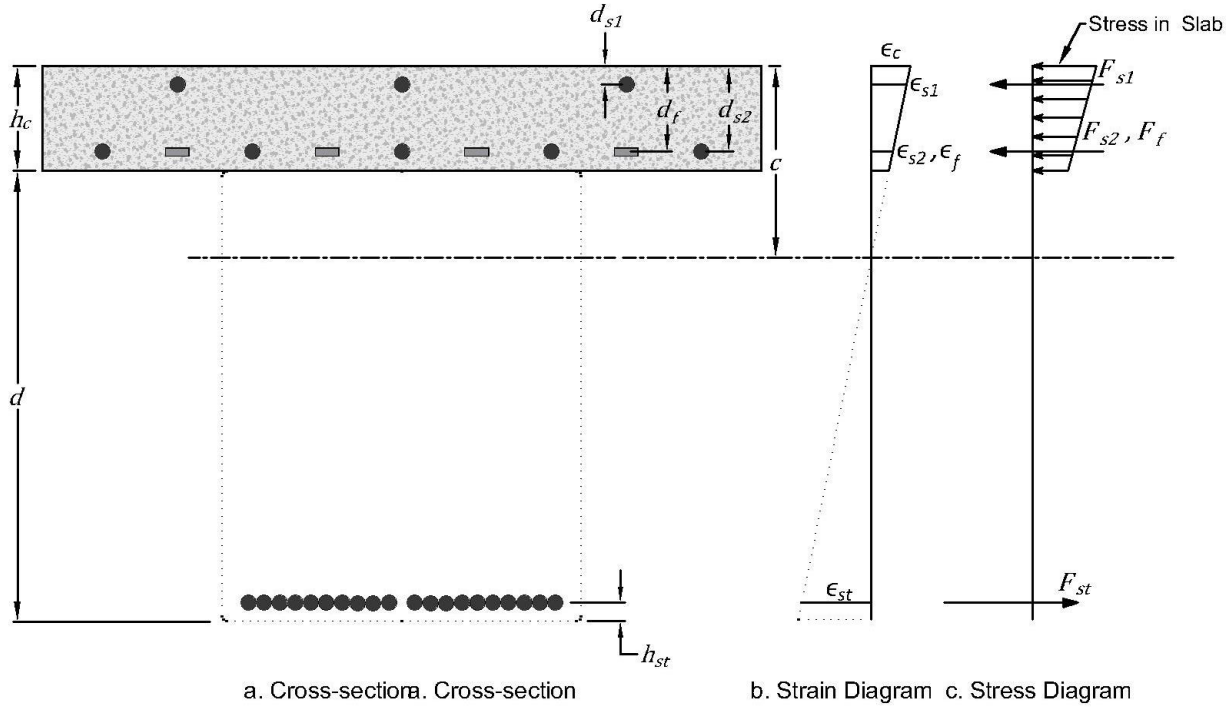

Figure 15. Stress-strain diagram for HCB without concrete arch and FRP box for neutral axis below concrete slab

Similarly, the equation for the internal moment for neutral axis located within the concrete slab, as shown in Figure 16, is given:

$$M_e = M_i = \frac{1}{2} \in_c E_c A_c \frac{2}{3} c + \frac{\in_c}{c}(c - d_{s1}) E_s A_{s1}(c - d_{s1}) + \frac{\in_c}{c}(c - d_{s2}) E_s A_{s2}(c - d_{s2}) + \frac{\in_c}{c}(c - d_f) E_s A_f (c - d_f) + + \frac{\in_c}{c}(h_c + d - c - h_{st}) E_{st} A_{st}(h_c + d - c - h_{st}) \quad (33)$$

Equations 32 and 33 represent moment equilibrium equations for stresses with in the elastic ranges for only two locations of the neutral axis. Several such equations can be generated by changing stress levels and neutral axis locations.

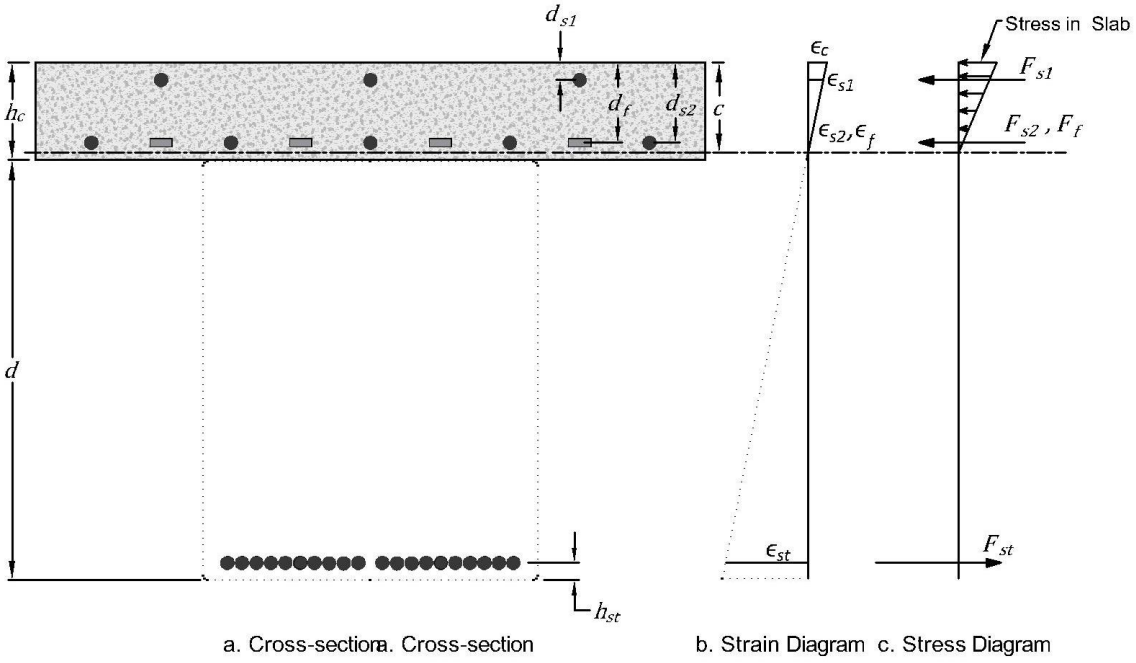

Figure 16. Stress-strain diagram for HCB without concrete arch, fin and FRP box for neutral axis within concrete slab

2.1.8 HCB with average cross section

The depth of concrete fin in HCB does not remain constant across the beam span due to the profile of arch, making the analysis complex because the equations for prismatic beam are no longer valid. To avoid this complexity and get a simple solution for HCB problem, a modification that assumes an inverted T-shaped concrete element in place of concrete arch is studied. Since, this model also assumes constant cross section across the span, therefore, equation for the elastic deflection of prismatic beams can be used within the elastic range. The finite-difference approach is still used to predict the load-deflection behavior in nonlinear range.

2.2 HCB analyzed as combination of arch and box beam

An alternative approach to HCB analysis is presented in this dissertation by treating it as structure composed of concealed concrete arch inside FRP box beam, jointly resisting the applied load and satisfy the compatibility conditions of deflection at the midspan. This is referred to as arch-and-beam model of HCB. To further explore the behavior of the concealed arch the analysis is carried by treating it as a tied arch as well as two-hinged arch.

2.2.1 Tied arch-and-beam model

This tied arch-and-beam model of analysis for HCB is shown in Figure 17. The strain compatibility at a given section along the depth of the beam is not supposed for this model; nor is this approved by the past study [6] that has found that strains at the top and bottom of the concrete arch are different than those at the corresponding points in the FRP outer shell. The reason for this difference is attributed to the local bending of the arch which is the consequence of arch action.

The compatibility condition for finding the forces transmitted by the tied arch and the outer beam is:

$$\Delta_A = \Delta_B \tag{34}$$

where

Δ_A = Tied arch defection at the crown

Δ_B = Beam box deflection at the midspan

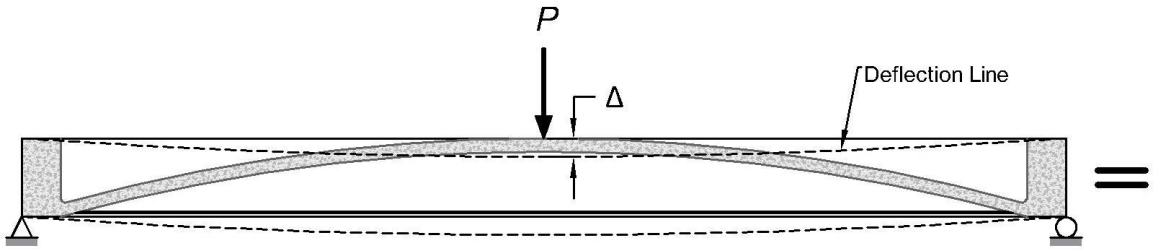

a. Load jointly resisted by tied arch and box beam

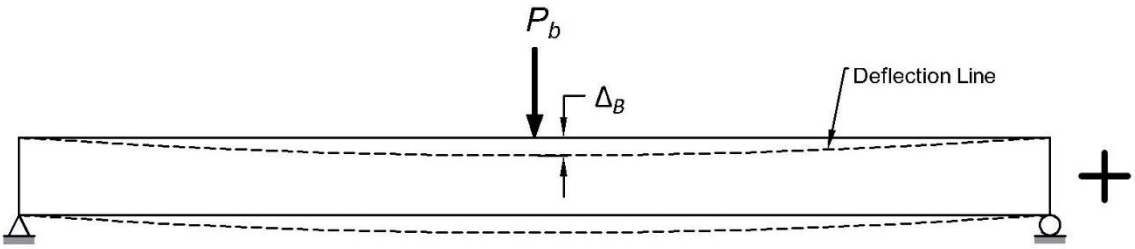

b. Load individually resisted by box beam

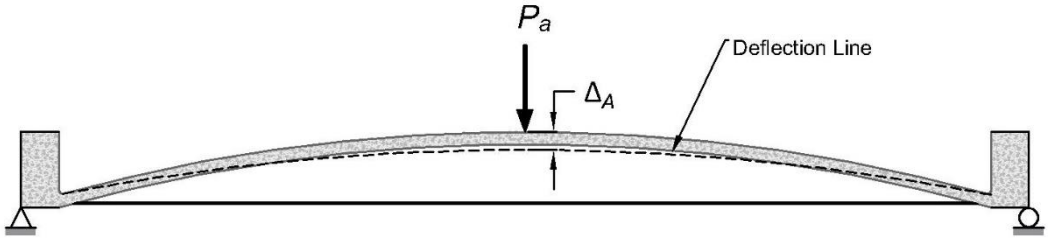

c. Load individually resisted by tied arch

Figure 17. Arch-and-beam model of analysis for HCB

2.2.2 Deflection in Tied Arch

The tied parabolic arch in the HCB can be modeled as shown in Figure 18. The arch has a hinged support at one end and a roller support with a spring of stiffness k attached at the other end. The spring is introduced to represent the collective resistance to change in the relative distance between the arch ends offered by all beam components. Since it is not known if only the steel strands contribute to the stiffness or the FRP outer box has some contribution as well; therefore, response of HCB is determined for different possible values of stiffness of the spring and compared with the experimental values for confirmation. The displacement at the roller end of the arch due to the application of vertical loads is [14]:

$$\Delta_r = \frac{H}{k} \tag{35}$$

where

Δ_r = Displacement at the roller support B

H = Horizontal reaction at each support of the arch

k = Stiffness of spring introduced to represent the resistance of tie

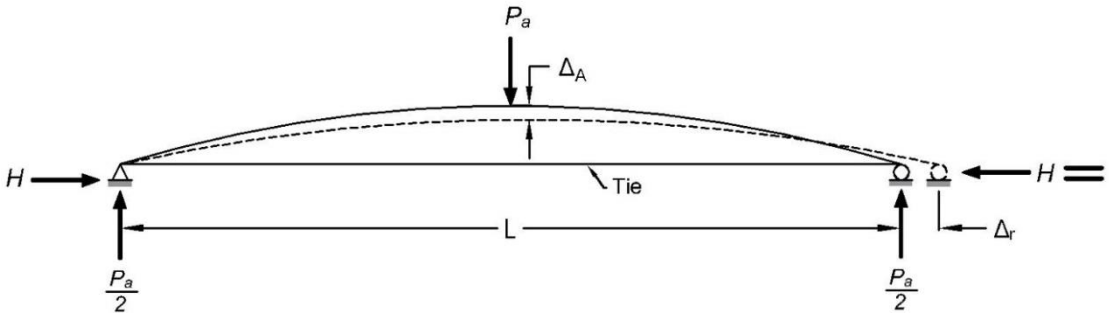

(a) Arch with a tie

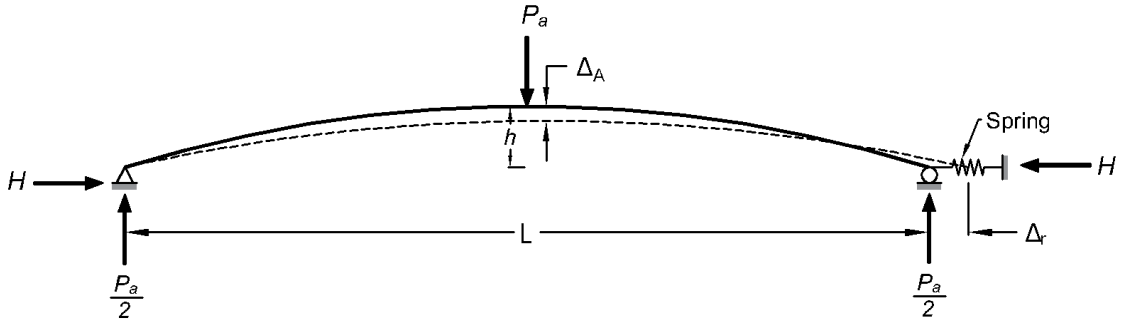

(b). Arch with a spring to account for the tie resistance

Figure 18. Modeling of tied arch

The unknown H is calculated by using Castigliano's Theorem [15]. The total strain energy in the arch is equal to the sum of strain energies due to all actions. The strain energy due to bending moment is given by [16]:

$$U_b = \int_0^S \frac{M^2}{2EI} ds \tag{36}$$

where

M = Bending moment acting at an arbitrary section of arch

E = Modulus of Elasticity for arch

I = Moment of inertial of arch

Strain energy due to the axial force is [17]:

$$U_a = \int_0^S \frac{N^2}{2EA} ds \tag{37}$$

where

N = Axial thrust at any arbitrary section of the arch

A = Cross section area of the arch at the section

Strain energy U_s due to spring force is [17]:

$$U_s = \frac{1}{2} k \Delta_r^2 \tag{38}$$

$$U_s = \frac{1}{2} k (\frac{H}{k})^2 \tag{39}$$

$$U_s = \frac{H}{2k}^2 \tag{40}$$

The strain energy due to shear force is negligible and is, therefore, ignored. So the total strain energy of the arch is given by [17]:

$$U = U_b + U_a + U_s \tag{41}$$

$$U = \int_0^s \frac{M^2}{2EI} ds + \int_0^s \frac{N^2}{2EA} ds + \frac{H}{2k}^2 \tag{42}$$

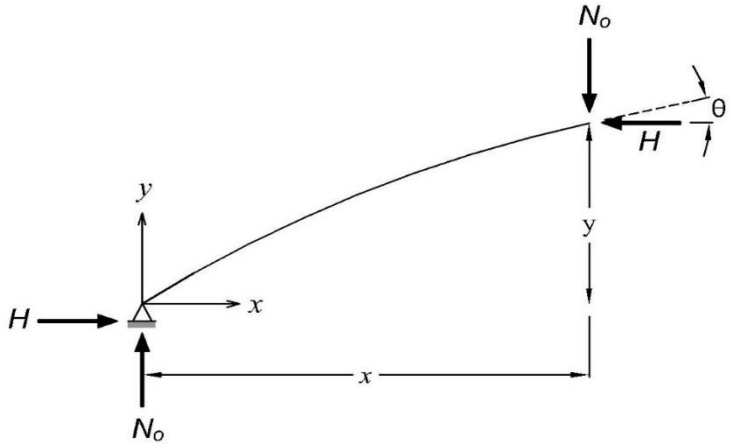

Figure 19. Forces at an arbitrary section of arch at distance x from the origin

Referring to the Figure 19, the moment M is given by:

$$M = M_o - Hy \tag{43}$$

where

M_o = Equivalent beam moment at any chosen section

y = Height of arch at the chosen section

Referring to Figure 20, the normal thrust N at any cross section of the arch is:

$$N = N_o sin\theta + Hcos\theta \tag{44}$$

where

N_o = Vertical force at the section

θ = Inclination of arch at the location of cross section with x-axis

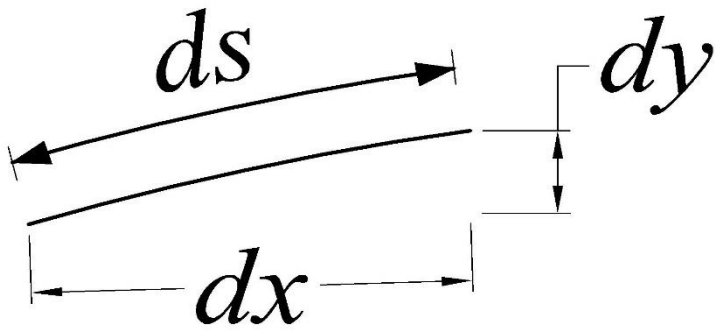

Figure 20. Relationship between *ds, dx* and *dy*

From the principle of virtual work [17], we have:

$$\frac{\partial}{\partial H}(\ U_b + U_a) = \ \Delta_r \tag{45}$$

$$\frac{\partial}{\partial H}\left(\int_0^S \frac{M^2}{2EI} ds + \int_0^S \frac{N^2}{2EA} ds\right) = \frac{-H}{k} \tag{46}$$

$$\int_0^S \frac{M}{EI}\frac{\partial M}{\partial H} ds + \int_0^S \frac{N}{EA}\frac{\partial N}{\partial H} ds = -\frac{H}{k} \tag{47}$$

Where:

$$\int_0^s \frac{M}{EI}\frac{\partial M}{\partial H} ds = -\int_0^s \frac{M_o - Hy}{EI} y\, ds \tag{48}$$

$$\int_0^s \frac{N}{EA}\frac{\partial N}{\partial H} ds = \int_0^s \frac{N_o sin\theta + Hcos\theta}{EA} cos\theta ds \tag{49}$$

Substituting equations 48 and 49 in equation 47, we get:

$$-\int_0^s \frac{M_o - Hy}{EI} y ds + \int_0^s \frac{N_o sin\theta + Hcos\theta}{EA} cos\theta ds = -\frac{H}{k} \tag{50}$$

$$H = \frac{\int_0^s \frac{M_o y}{EI} ds - \int_0^s \frac{N_o sin\theta cos\theta}{EA} ds}{\frac{1}{k} + \int_0^s \frac{y^2}{EI} ds + \int_0^s \frac{cos^2\theta}{EA} ds} \tag{51}$$

Since the second term in the numerator is very small compared with the rest, therefore, we can simplify the equation by simply omitting it to get the following:

$$H = \frac{\int_0^s \frac{M_o y}{EI} ds}{\frac{1}{k} + \int_0^s \frac{y^2}{EI} ds + \int_0^s \frac{cos^2\theta}{EA} ds} \tag{52}$$

Also, for low arches $\cos\theta \approx 1$ and we can further simplify the equation as:

$$H = \frac{\int_0^s \frac{M_o y}{EI} ds}{\frac{1}{k} + \int_0^s \frac{y^2}{EI} ds + \int_0^s \frac{1}{EA} ds} \tag{53}$$

The deflection of arch at the point where load P_a is acting will be [17]:

$$\Delta_A = \frac{\partial U}{\partial P_a} \tag{54}$$

$$\Delta_A = \frac{\partial}{\partial P_a}\left(\int_0^s \frac{M^2}{2EI} ds + \int_0^s \frac{N^2}{2EA} ds + \frac{H}{2k}^2\right) \tag{55}$$

$$\Delta_A = \frac{\partial}{\partial P_a}\left(\int_0^s \frac{(\frac{P_a}{2}x - Hy)^2}{2EI} ds + \int_0^s \frac{(\frac{P_a}{2}sin\theta + Hcos\theta)^2}{2EA} ds + \frac{H}{2k}^2\right) \tag{56}$$

Force resisted by the arch and outer beam can then be calculate by using the compatibility of deflections of arch at the crown and outer box at the midspan and force equilibrium equation for the HCB:

The compatibility condition for arch and outer beam box deflection at the midspan is:

$$\Delta_A = \Delta_B \tag{57}$$

Force equilibrium equation for the composite structure:

$$P = P_a + P_b \tag{58}$$

where

P = Applied load at the mid span

P_a = Load resisted by the concrete arch

P_b = Load resisted by the beam box

2.2.3 Two-hinged arch-and-beam model

The concrete arch inside the beam box may also behave very close to two hinged parabolic arch. To investigate such possibility HCB will also be modeled as consisting of an FRP beam box and two-hinged concrete arch jointly resisting the upcoming load. The concrete arch modeled as two-hinged is shown in Figure 21. The analysis part for the outer box will exactly be same as the previous section where as equations for the analysis of the arch can be easily obtained from those given in the previous section by simply putting the value of stiffness of the spring equal to infinity.

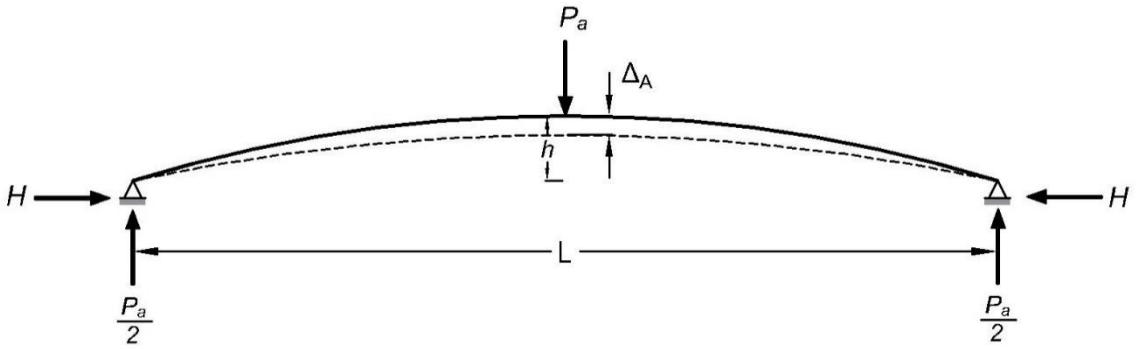

Figure 21. Concrete arch as two hinged arch

The modified equations to be used for the analysis of hinged arch are given as follows:
Horizontal reaction at the arch ends will be:

$$H = \frac{\int_0^s \frac{M_o y}{EI} ds - \int_0^s \frac{N_o \sin\theta \cos\theta}{EA} ds}{\int_0^s \frac{y^2}{EI} ds + \int_0^s \frac{\cos^2\theta}{EA} ds} \quad (59)$$

Ignoring the second term in the numerator, we get:

$$H = \frac{\int_0^s \frac{M_o y}{EI} ds}{\int_0^s \frac{y^2}{EI} ds + \int_0^s \frac{\cos^2\theta}{EA} ds} \quad (60)$$

For low arches i.e., θ very small, $\cos\theta \approx 1$

$$H = \frac{\int_0^s \frac{M_o y}{EI} ds}{\int_0^s \frac{y^2}{EI} ds + \int_0^s \frac{1}{EA} ds} \quad (61)$$

The deflection at the mid-span will be:

$$\Delta_A = \frac{\partial}{\partial P_a}\left(\int_0^s \frac{(\frac{P_a}{2}x - Hy)^2}{2EI} ds + \int_0^s \frac{(\frac{P_a}{2}\sin\theta + H\cos\theta)^2}{2EA} ds \right) \quad (62)$$

The computability and equilibrium equations used for the solution for this case are same as the previous one.

2.3 Load-deflection response of prestressed HCB

The prestressing of tension reinforcement has never been practically used nor theoretically investigated for HCB since its inception in 2008. This research also focuses on the theoretical evaluation of the performance of HCB for prestressing of the tension reinforcement. The load-deflection relation for HCB under prestressed conditions is theoretically predicted using M-Φ curves generated by finite difference method.

2.3.1 Maximum Prestressing Force for HCB

The maximum prestressing force for HCB can be found by using the condition that the stress anywhere must not exceed the limiting stress for the material. For the HCB in question for the transformed section with cracking moment for concrete as the limiting stress, the maximum prestressing force is given by:

$$F \leq \frac{f_r}{(\frac{1}{A}+\frac{ec}{I})} \tag{63}$$

where

F = Maximum prestressing force

f_r = Cracking moment for concrete = $7.5\sqrt{f_c'}$

e = Eccentricity of the prestressing force

A = Cross-sectional area of the transformed cross section

I = Moment of inertial of the transformed cross section

2.3.2 Force equilibrium and strains for prestressed HCB with no external moment

When only prestressing force is applied to the beam at a certain eccentricity from the neutral axis in a manner that it does not cause cracking in concrete at the extreme fibers; then, the load condition can be broken down to two components, namely, stress caused by the axial

prestressing force F and stress caused by the prestressing moment $M_p = Fe$. Under the condition, total stress and total strain at any location will be equal to the sum of the stresses and strains caused by the axial and bending effects of the prestressing force. Total strain at any location is given by:

$$\in_t = \in_o + \in_{pm} + \in_a \quad (64)$$

where

$\in_t =$ Total strain

$\in_o =$ Strain caused by centriod force F

$\in_{pm} =$ Strain caused by prestreseing moment $M_p = Fe$

$\in_a =$ Strain caused by self load

The equilibrium condition for the section requires that net force on the section from both sources i.e., axial and bending be equal to the externally prestressing force F:

$$\sum F_i = F \quad (65)$$

$$F_o + F_{pm} + F_a = F \quad (66)$$

Where

$F_o =$ Net axial force on the section $=$ F

$F_{pm} =$ Net force on the section cuased by prestressing moment $= 0$

$F_a =$ Net axial force on the section due to self load $= 0$

2.3.3 Moment and Curvature for Prestressed HCB without External Moment

The curvature of HCB for full prestressing without external applied load is given by:

$$\emptyset = \frac{\in_c}{c} \quad (67)$$

The above equation is the same as used for finding curvature for non prestressed beam but here it gives a non-zero curvature for zero bending moment.

2.3.4 Force Equilibrium and Strains for Prestressed HCB with Applied Moment

When an external moment is also acting on the prestressed beam then the stain contribution by this load needs to be added to get the total strain at any point in the section. The equation for the net section in this case will be:

$$\in_t = \in_o + \in_{pm} + \in_a + \in_{am} \tag{68}$$

where

$\in_t$ = Total strain

$\in_o$ = Strain caused by centriod force F

$\in_{pm}$ = Strain caused by prestreseing moment $M_p = Fe$

$\in_a$ = Strain caused by self load

$\in_{am}$ = Strain component due to applied moment

Likewise, the equation for the force equilibrium of the cross section will also contain a term for the contribution forces caused by applied moment:

$$\sum F_i = F \tag{69}$$

$$F_o + F_{pm} + F_a + F_{am} = F \tag{70}$$

where

F_o = Net axial force on the section = F

F_{pm} = Net force on the section cuased by prestressing moment = 0

$F_a = Net\ axial\ force\ on\ the\ section\ due\ to\ self\ load = 0$

F_{am} = Net force on the section cuased by prestressing moment = 0

2.3.5 Moment and Curvature for Prestressed HCB with Applied Moment

The equation for the internal resisting moment of HCB produced in response to the external applied moment can be obtained from the flexural equilibrium equation given earlier in the text by simply adding terms for the prestressing force. Since there are numerous forms of exact such equations possible for of strains levels, therefore, only general form of flexural equilibrium equation will be given here for the prestressed HCB i.e.,

$$M_{int} = M_o + M_p + M_a + M_{np} \tag{71}$$

where

M_{int} = Total internal resisting moment in prestressed HCB

M_o = Internal moment component due to axial force F = 0

M_p = Internal moment component due to prestressing of HCB $= Fe$

M_a = Internal moment component due to self-weight of HCB

M_{np} $=$ Internal resisting moment in HCB produced in response to external moment

2.3.6 Load-deflection Relation for HCB

The process and method of finding load-deflection relation for the prestressed HCB will be exactly same as followed for the non-prestressed HCB. The detail of the solution scheme is given chapter 2 and Appendix A and B.

2.3.7 CFRP Retrofitting of HCB

The use of CFRP retrofitting for the enhanced performance HCB is studied for different positions of usage. The equations and method of analysis for this part remain exactly the same as given for non-retrofitted HCB except some terms for the new materials are added.

3. LOAD-DEFLECTION BEHAVIOR AND STRENTH OF NON-PRESTRESSED HCB UNDER BENDING LOADS

The prediction of the linear and nonlinear load-deflection behavior of HCB up to the collapse is presented herein. The methodology and steps of the analysis are given in Chapter 2. The nonlinear analysis is performed by using Bernoulli beam theory and finite-difference method of nonlinear moment-curvature relations. The elastic analysis of HCB using beam and concealed arch approach as explain in chapter two is applied.

The nonlinear analysis of HCB as Bernoulli beam for four variations for the cross-sectional configurations as explained in the previous chapter and the elastic analysis of HCB by using arch and beam approach is presented hereunder:

3.1 HCB analyzed as Bernoulli beam using regular cross section

The cross section of the HCB used for the perdition of the deflection-response is shown in Figure 22. The analysis consists of finding the theoretical load-deflection relation for HCB till collapse condition using methodology described in chapter 2 and make a comparison with the experimental load-deflection relation to draw conclusions.

The process of generating load-deflection curve for the HCB involves following steps:

1. Getting moment-curvature curves for the HCB cross sections at all nodes
2. Generating set of linear equations involving curvature and deflection as variables by using finite-difference method
3. Solving the system of equations to find deflections at nodes by using values of curvature given by the respective moment-curvature curves corresponding to the moment value at nodes

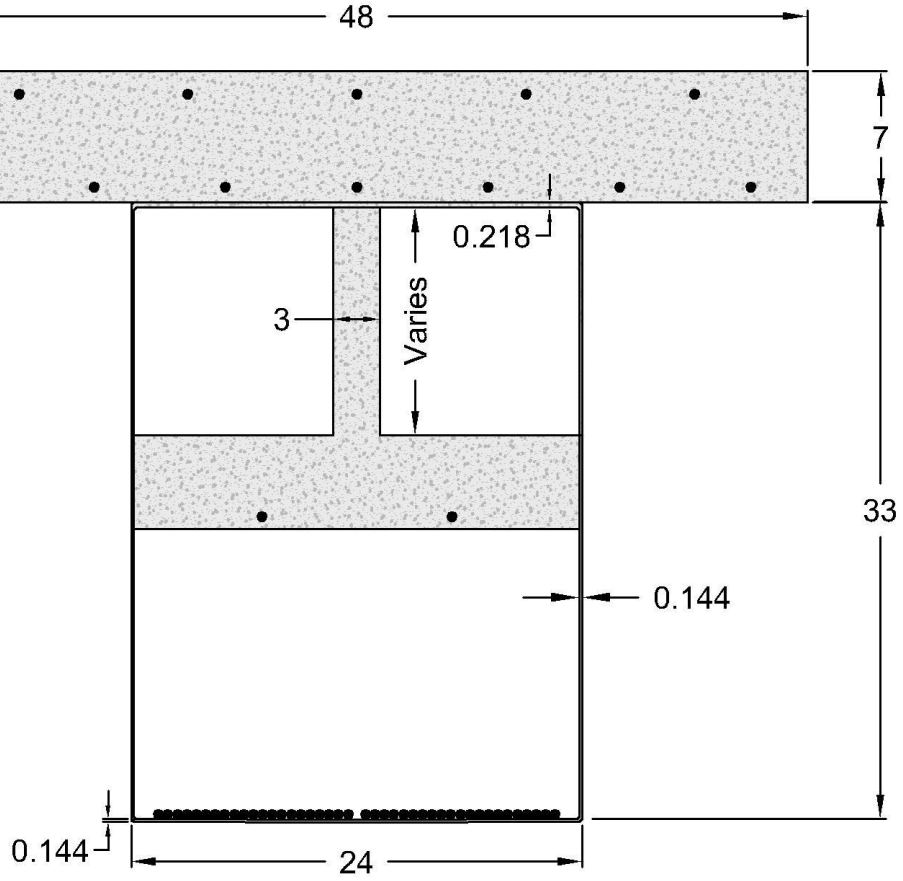

Figure 22. Cross section of HCB used for analysis (Dimensions in inches)

3.1.1 M-ϕ curves for HCB

The M-ϕ curves for the HCB sections at nodes are generated by running a computer program in MATLAB. The algorithm consists of inputting dimensions of the beam cross-sectional elements at the given section and material properties; then varying the location of neutral axis for a chosen value of strain in the top most concrete fiber until equilibrium of forces for the section is reached. The location of the neutral axis is then used to calculate the internal resisting moment and curvature at the section. This pair of curvature and moment constitutes one point on the moment-deflection curve for the section in question. Then next value of strain at the top most concrete fiber is assigned and the same process is repeated to get another pair of curvature and

moment till the top fiber strain reaches 0.003, the ultimate strain for concrete. The meshing of the HCB for applying finite-difference method for nodal interval of 41 in is shown in Figure 23. The M-ϕ curves generated for HCB cross sections at nodes are given in Appendix D.

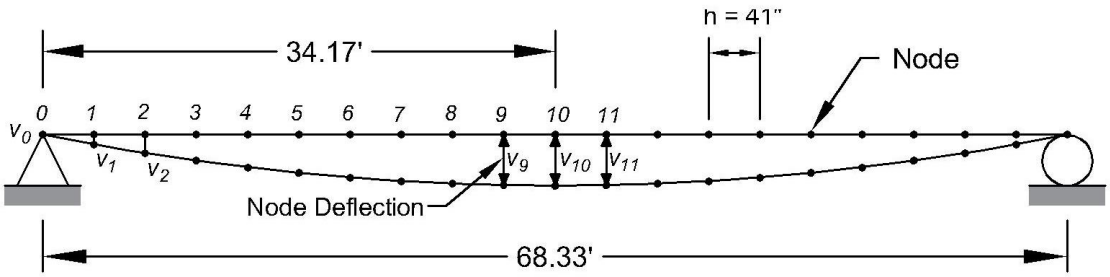

Figure 23. Meshing of HCB for finite-difference formulation

3.1.2 Deflections at nodal points of HCB

The scheme for the determination of the nodal deflections of HCB using finite-difference methods has been explained in chapter 2. The process involves solving a set of linear equations generated by the finite difference formulation of the problem. The number of equations depends on the length of interval length *'h'* between the consecutive nodes. To understand the influence of the interval *'h'* on the precision of the outcome, deflections for the current problem are calculated for two different values of '*h*' namely 41" and 82" and compared with the experimentally obtained values. The finite difference formulation of the problem for h = 41" (n = 10) and h = 82" (n = 82) is given in Appendix E.

The externally applied load values used for calculating load vs midspan deflection are 65k, 133k, 175k, 200k, 240k, 280k, 310k, 340k, 370, 410k and 424k. The calculated values are shown in Table 1 through 24.

Table 1. Results for P=65 k and h=41 in

Node	Moment (K-in)	ϕ (radian)	Deflection (in.)
1	0	0	0
2	1332.5	0.00000548	0.45
3	2665	0.00001110	0.90
4	3997.5	0.00001679	1.33
5	5330	0.00002251	1.73
6	6662.5	0.00002825	2.09
7	7995	0.00003397	2.40
8	9327.5	0.00003969	2.66
9	10596.3	0.00004511	2.85
10	10596.3	0.00004512	2.96
11	10596.3	0.00004511	3.00

Table 2. Results for P=65 k and h=82 in.

Node	Moment (K-in)	ϕ (radian)	Deflection (in.)
1	0	0	0
3	2665	0.000011097	0.91
5	5330	0.000022512	1.74
7	7995	0.000033972	2.43
9	10596.3	0.000045113	2.88
11	10596.3	0.000045113	3.03

Table 3. Results for P=133 Kips and h=41 in.

Node	Moment (K-in)	ϕ (radian)	Deflection (in.)
1	0	0	0
2	2726.5	0.000011220	0.93
3	5453	0.000022707	1.84
4	8179.5	0.000034349	2.72
5	10906	0.000046064	3.53
6	13632.5	0.000057796	4.27
7	16359	0.000069513	4.91
8	19085.5	0.000081202	5.44
9	21681.66	0.000092308	5.82
10	21681.66	0.000092316	6.06
11	21681.66	0.000092307	6.13

Table 4. Results for P=133 Kips and h=82 in.

Node	Moment (K-in)	ϕ (radian)	Deflection (in.)
1	0	0	0
3	5453	0.000022707	1.86
5	10906	0.000046064	3.57
7	16359	0.000069513	4.97
9	21681.66	0.000092308	5.90
11	21681.66	0.000092307	6.21

Table 5. Results for P=175 k and h=41 in.

Node	Moment (K-in)	ϕ (radian)	Deflection (in.)
1	0	0	0
2	3587.5	0.000014764	1.22
3	7175	0.000029878	2.42
4	10762.5	0.000045196	3.56
5	14350	0.000060610	4.63
6	17937.5	0.000076047	5.60
7	21525	0.000091464	6.44
8	25112.5	0.000106845	7.12
9	28528.5	0.000120402	7.63
10	28528.5	0.000120481	7.93
11	28528.5	0.000120509	8.03

Table 6. Results for P=175 k and h=82 in.

Node	Moment (K-in)	ϕ (radian)	Deflection (in.)
1	0	0	0
3	7175	0.000029878	2.44
5	14350	0.000060610	4.68
7	21525	0.000091464	6.51
9	28528.5	0.000120402	7.72
11	28528.5	0.000120509	8.13

Table 7. Results for P=200 k and h=41 in.

Node	Moment (K-in)	ϕ (radian)	Deflection (in.)
1	0	0	0
2	4100	0.000016873	1.38
3	8200	0.000034146	2.74
4	12300	0.000051653	4.04
5	16400	0.000069269	5.25
6	20500	0.000086911	6.34
7	24600	0.000104531	7.29
8	28700	0.000120935	8.06
9	32604	0.000135328	8.63
10	32604	0.000135400	8.97
11	32604	0.000135423	9.08

Table 8. Results for P=200 k and h=82 in.

Node	Moment (K-in)	ϕ (radian)	Deflection (in.)
1	0	0	0
3	8200	0.000034146	2.76
5	16400	0.000069269	5.30
7	24600	0.000104531	7.37
9	32604	0.000135328	8.73
11	32604	0.000135423	9.19

Table 9. Results for P=240 k and h=41 in.

Node	Moment (K-in)	ϕ (radian)	Deflection (in.)
1	0	0	0
2	4920	0.000020247	1.64
3	9840	0.000040975	3.24
4	14760	0.000061983	4.78
5	19680	0.000083123	6.21
6	24600	0.000104293	7.50
7	29520	0.000123767	8.61
8	34440	0.000141944	9.52
9	39120	0.000159193	10.19
10	39120	0.000159251	10.59
11	39120	0.000159268	10.73

Table 10. Results for P=240 k and h=82 in.

Node	Moment (K-in)	ϕ (radian)	Deflection (in.)
1	0	0	0
3	9840	0.000040975	3.27
5	19680	0.000083123	6.27
7	29520	0.000123767	8.71
9	39120	0.000159193	10.31
11	39120	0.000159268	10.85

Table 11. Results for P=280 k and h=41 in.

Node	Moment (K-in)	ϕ (radian)	Deflection (in.)
1	0	0	0
2	4920	0.000023622	1.89
3	9840	0.000047805	3.73
4	14760	0.000072314	5.50
5	19680	0.000096976	7.15
6	24600	0.000120493	8.63
7	29520	0.000141749	9.91
8	34440	0.000162812	10.95
9	39120	0.000182645	11.72
10	39120	0.000182715	12.18
11	39120	0.000182736	12.33

Table 12. Results for P=280 k and h=82 in.

Node	Moment (K-in)	ϕ (radian)	Deflection (in.)
1	0	0	0
3	9840	0.000047805	3.77
5	19680	0.000096976	7.22
7	29520	0.000141749	10.01
9	39120	0.000182645	11.85
11	39120	0.000182736	12.47

Table 13. Results for P=310 k and h=41 in.

Node	Moment (K-in)	ϕ (radian)	Deflection (in.)
1	0	0	0
2	6355	0.000026153	2.08
3	12710	0.000052926	4.11
4	19065	0.000080062	6.06
5	25420	0.000107367	7.87
6	31775	0.000131705	9.49
7	38130	0.000155235	10.90
8	44485	0.000178160	12.05
9	50530	0.000201637	12.90
10	50530	0.000201712	13.41
11	50530	0.000201734	13.58

Table 14. Results for P=310 k and h=82 in.

Node	Moment (K-in)	ϕ (radian)	Deflection (in.)
1	0	0	0
3	12710	0.000052926	4.16
5	25420	0.000107367	7.96
7	38130	0.000155235	11.03
9	50530	0.000201637	13.07
11	50530	0.000201734	13.75

Table 15. Results for P=340 k and h=41 in.

Node	Moment (K-in)	ϕ (radian)	Deflection (in.)
1	0	0	0
2	6970	0.000028684	2.27
3	13940	0.000058048	4.50
4	20910	0.000087810	6.63
5	27880	0.000117095	8.61
6	34850	0.000142917	10.39
7	41820	0.000168344	11.94
8	48790	0.000194593	13.20
9	55420	0.000222077	14.13
10	55420	0.000222153	14.69
11	55420	0.000222175	14.88

Table 16. Results for P=340 k and h=82 in.

Node	Moment (K-in)	ϕ (radian)	Deflection (in.)
1	0	0	0
3	13940	0.000058048	4.55
5	27880	0.000117095	8.71
7	41820	0.000168344	12.08
9	55420	0.000222077	14.32
11	55420	0.000222175	15.07

Table 17. Results for P=370 k and h=41 in.

Node	Moment (K-in)	ϕ (radian)	Deflection (in.)
1	0	0	0
2	7585	0.000031215	2.50
3	15170	0.000063170	4.94
4	22755	0.000095558	7.28
5	30340	0.000126070	9.46
6	37925	0.000154129	11.42
7	45510	0.000181747	13.13
8	53095	0.000212032	14.53
9	60310	0.000243866	15.57
10	60310	0.000243940	16.21
11	60310	0.000266924	16.43

Table 18. Results for P=370 k and h=82 in.

Node	Moment (K-in)	ϕ (radian)	Deflection (in.)
1	0	0	0
3	15170	0.000063170	5.03
5	30340	0.000126070	9.64
7	45510	0.000181747	13.40
9	60310	0.000243866	15.93
11	60310	0.000266924	16.83

Table 19. Results for P=400 k and h=41 in.

Node	Moment (K-in)	ϕ (radian)	Deflection (in.)
1	0	0	0
2	8200	0.000033746	2.69
3	16400	0.000068292	5.33
4	24600	0.000103306	7.85
5	32800	0.000135044	10.20
6	41000	0.000165073	12.32
7	49200	0.000195932	14.17
8	57400	0.000230562	15.68
9	65200	0.000268238	16.81
10	65200	0.000268303	17.49
11	65200	0.000268242	17.71

Table 20. Results for P=400 k and h=82 in.

Node	Moment (K-in)	ϕ (radian)	Deflection (in.)
1	0	0	0
3	16400	0.000068292	5.39
5	32800	0.000135044	10.32
7	49200	0.000195932	14.34
9	65200	0.000268238	17.05
11	65200	0.000268242	17.95

Table 21. Results for P=410 k and h=41 in.

Node	Moment (K-in)	ϕ (radian)	Deflection (in.)
1	0	0	0
2	8405	0.000034589	2.88
3	16810	0.000070000	5.71
4	25215	0.000105888	8.41
5	33620	0.000138036	10.94
6	42025	0.000168664	13.24
7	50430	0.000200790	15.25
8	58835	0.000236940	16.93
9	66830	0.000303078	18.21
10	66830	0.000304388	18.97
11	66830	0.000304787	19.23

Table 22. Results for P=410 k and h=82 in.

Node	Moment (K-in)	ϕ (radian)	Deflection (in.)
1	0	0	0
3	16810	0.000070000	5.81
5	33620	0.000138036	11.15
7	50430	0.000200790	15.57
9	66830	0.000303078	18.63
11	66830	0.000304787	19.65

Table 23. Results for P=424 k and h=41 in.

Node	Moment (K-in)	ϕ (radian)	Deflection (in.)
1	0	0	0
2	8692	0.000035770	3.37
3	17384	0.000072390	6.69
4	26076	0.000109504	9.88
5	34768	0.000142224	12.88
6	43460	0.000173690	15.65
7	52152	0.000207836	18.13
8	60844	0.000246142	20.25
9	69112	0.000406377	21.97
10	69112	0.000408220	23.00
11	69112	0.000408745	23.34

Table 24. Results for P=424 k and h=82 in.

Node	Moment (K-in)	ϕ (radian)	Deflection (in.)
1	0	0	0
3	17384	0.000072390	6.95
5	34768	0.000142224	13.41
7	52152	0.000207836	18.91
9	69112	0.000406377	23.02
11	69112	0.000408745	24.39

3.1.3 Load-deflection relation and strength for HCB with regular cross section

The predicted and the experimental [10] load-deflection curves for the HCB are shown in Figure 24. It can be seen from the figure that the predicted values of deflections are in close agreement with the experimental ones in the initial portion of the curve where deflection are small but later on the predicted curve starts deviating from the experimental and the gap between them increases as the load increases until HCB fails at 210k which is only 50 % of the theoretically predicted ultimate strength of HCB. The reasons for the difference between the theoretical and experimental deflections at higher loads and the smaller experimental strength of HCB than the predicted are mainly due to the premature failure of HCB caused by the detachment of the tensions steel from the concrete abutment at one of the support as shown in Figure 24. Other possible reasons stiffness degradation at higher loads could be the local buckling of the thin parts of the HCB at higher loads. The load-deflection relations produced for interval length of 41 in and 82 in almost same which shows that the interval length of L/20 for the use of finite difference method is appropriate.

Figure 24. Premature failure of HCB due to detachment of tension reinforcement [10]

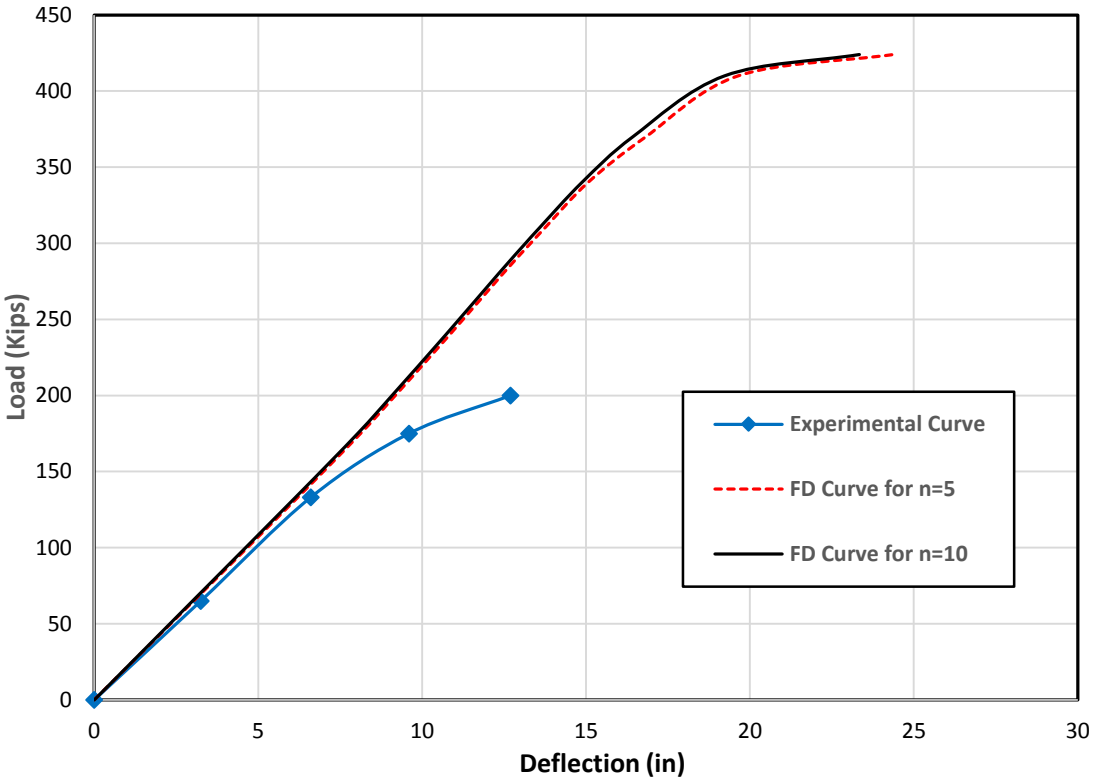

Figure 25. Theoretical and experimental [10] load-deflection relations for HCB with concrete arch and fin included

3.2 HCB analyzed as Bernoulli beam without concrete arch and fin

This model of the HCB assumes that the concrete arch does not contribute to the structural performance of HCB and therefore, presents a modification in the HCB by omitting the concrete arch and fin. The modified cross section of the HCB is shown in Figure 26. Since, the omission of concrete arch makes HCB as having constant cross section across the span, therefore, the equation for the elastic deformation for simply supported prismatic beam can be applied for generating the load-deflection curve during the elastic range. The equation used for generating the elastic curve for four point loading and calculations are shown as under:

$$\Delta = \frac{Pb(3L^2 - 4b^2)}{48EI} \quad (72)$$

where

P = Point load

L = Beam span length

B = Point load distance from the near support

E = Modulus of Elasticity of beam

I = Moment of inertial of beam cross section about the elastic neutral axis

The FRP is treated as reference material for the calculations, therefore, modulus of elasticity value for FRP is used for E in the above equation and moduli of elasticity of all other materials that appear in the cross section are represented in terms of the elastic modulus of FRP when calculating neutral axis location and moment of inertia of the cross section. The neutral axis distance from the bottom of the beam and moment of inertia of the beam are 31.60 in and 92555.64 in^4 , respectively. The calculated values of loads and corresponding deflections are listed in Table 25.

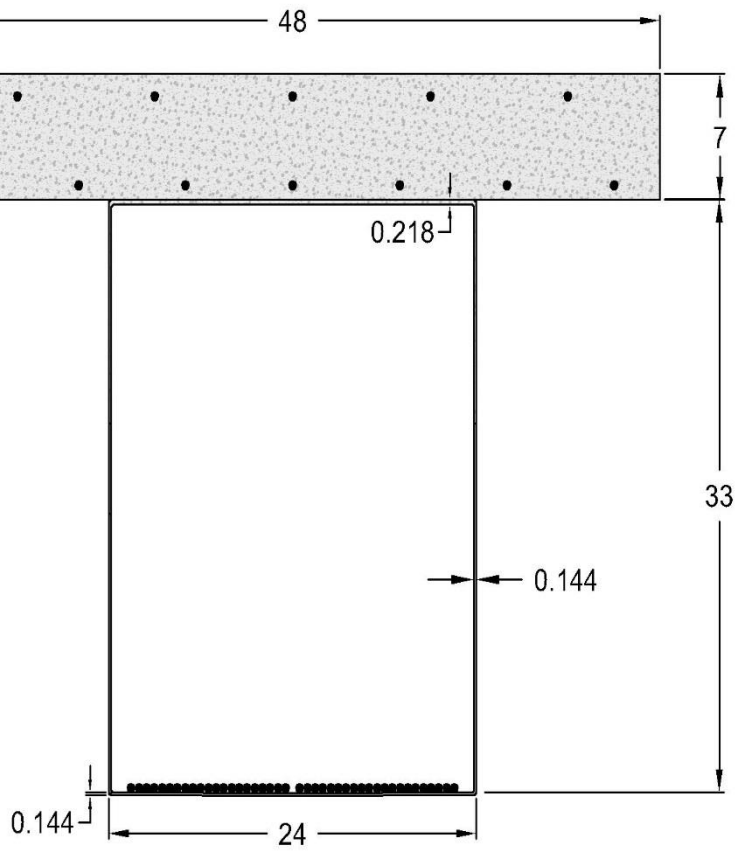

Figure 26. Cross section of HCB without concrete arch (Dimensions in inches)

Since, the goal of current study is to model the nonlinear behavior up to failure, therefore, the finite-difference approach is also used to find the load-deflection curve. The explanation of the analysis under finite-difference scheme and equation of flexural equilibrium for this HCB model are given in Section 2.3. Due to the constant cross section of the beam, same moment-curvature curve is used for all nodal points during the finite-difference analysis. The moment-curvature curve for the HCB used in the FD analysis is given in Figure 27.

Table 25: Midspan deflections under four-point loading given by elastic analysis for HCB without concrete arch and fin

Total Load, 2P, (Kips)	Midspan Deflection (in.)
0	0.00
65	2.99
133	6.12
175	8.05
200	9.20
240	11.04
280	12.88
300	13.80
310	14.26
340	15.64
370	17.02
400	18.40
410	18.86
424	19.50

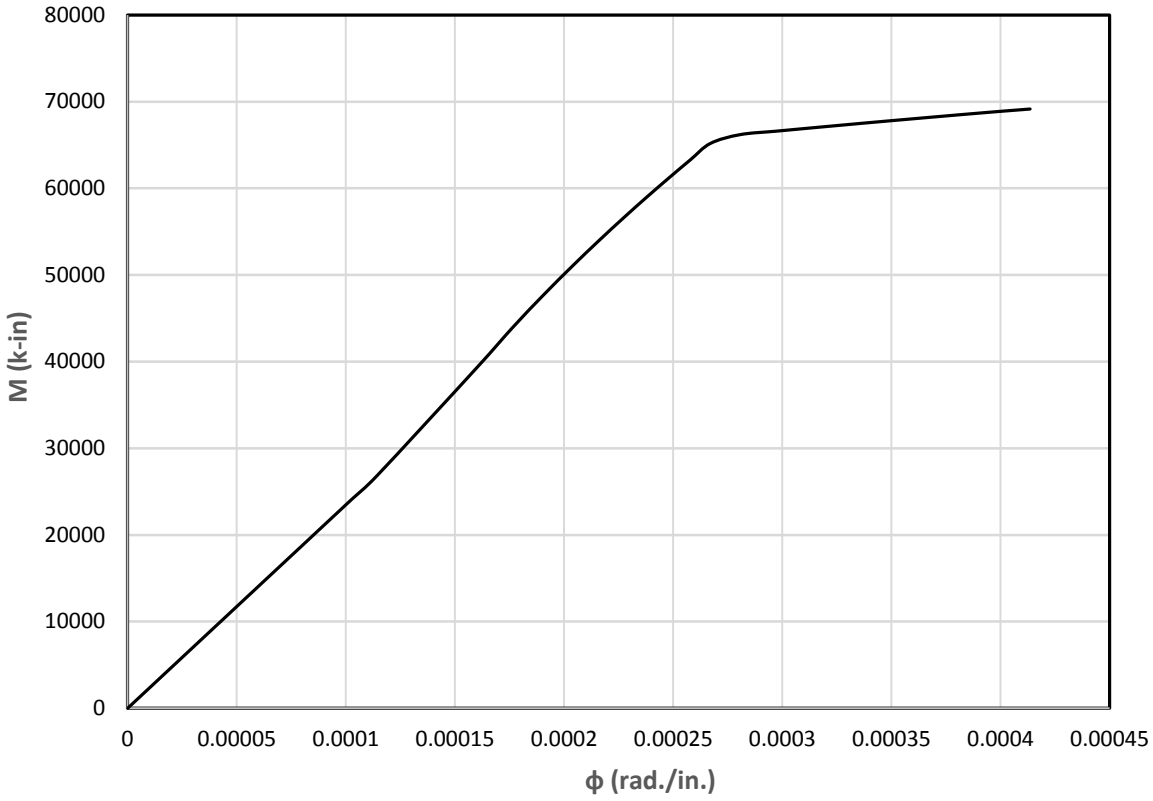

Figure 27. Moment-curvature curve for HCB without concrete arch and fin

The load vs deflection values at midspan generated by the finite-difference analysis are given in Table 26 whereas the theoretical and experimental load-deflection relations for HCB without concrete arch are shown in Figure 28.

3.2.1 Load-deflection relation and strength for HCB without concrete arch and fin

Figure 28 shows load-deflection relations produced theoretically by following elastic analysis and finite-difference method and the experimental curve [10]. The figure shows that all curves are in closed agreement upto150 kips load. Near 150 kips the experimental curve starts deviating from the theoretical ones. The two theoretical curves also start parting at about 220 kips and the gap goes on increasing till the point when the finite difference curve becomes nonlinear and cuts

the elastic curve. The comparison of the theoretical curves with the experimental shows that the deflection response of HCB without considering the concrete arch and fin closely agrees with the experimental load-deflection relation which proves the role of concrete arch and fin in the deflection response of HCB is negligible.

Table 26: Load versus midspan deflection under four-point loading given by finite-difference method for HCB without concrete arch and fin

Total Load, 2P, (Kips)	Midspan Deflection (in.)
0	0.00
65	3.01
133	6.15
200	9.11
310	13.62
340	14.92
370	16.28
400	17.72
410	19.40
424	23.54

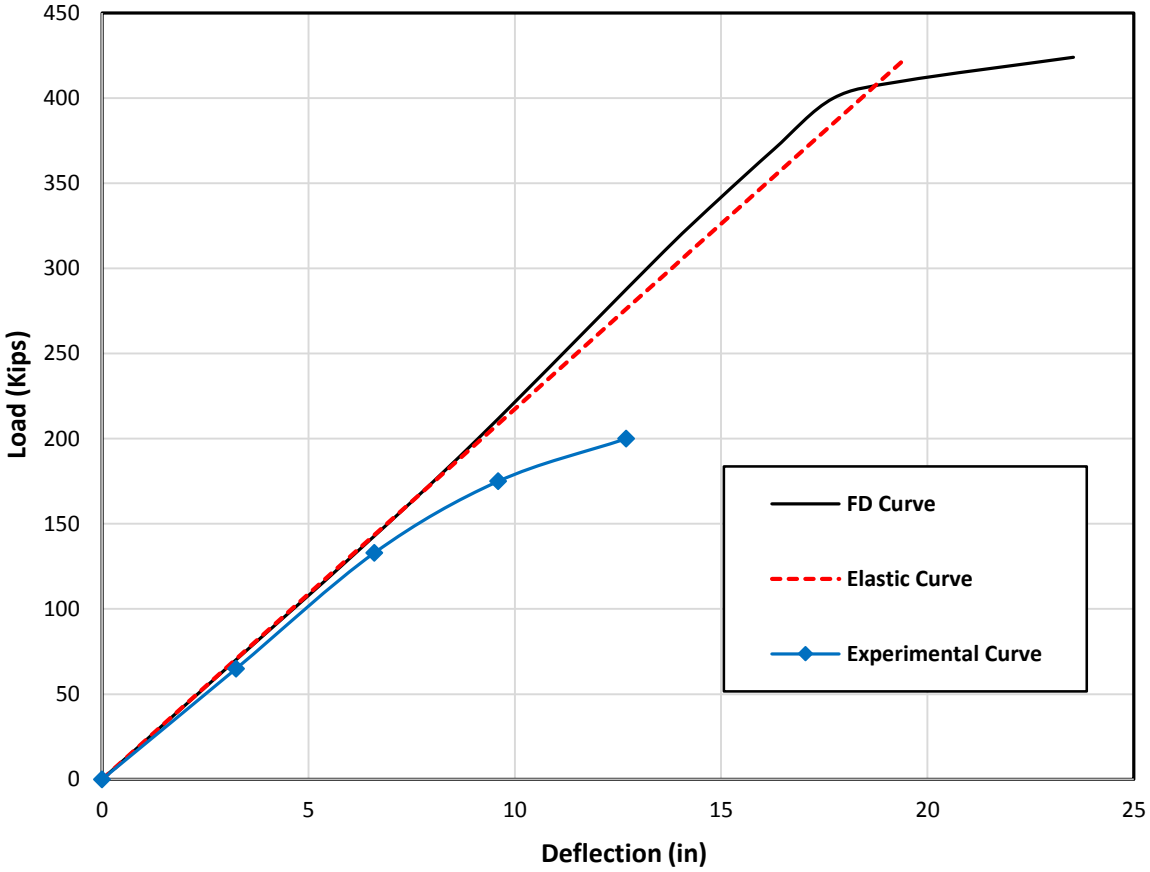

Figure 28. Theoretical and experimental [10] load-deflection curves for HCB without concrete arch and fin

3.3 HCB analyzed as Bernoulli beam without concrete arch, fin and FRP box

This model of HCB assumes that both the concrete arch and the FRP outer box do not contribute to the deflection response and flexural strength of HCB and thus they can be ignored in the analysis. The modified cross section of the HCB for this assumption is shown in Figure 29.

Since, HCB for this model has a constant cross section along the span, therefore, the equation for the elastic deformation of prismatic simply supported beam for four point loading is used to calculate beam deformation for elastic equations.

The neutral axis distance from the bottom of the beam and moment of inertia of the beam are 32.07 in. and 83905.65 in^4, respectively. The calculated values of loads and corresponding deflections are listed in Table 23.

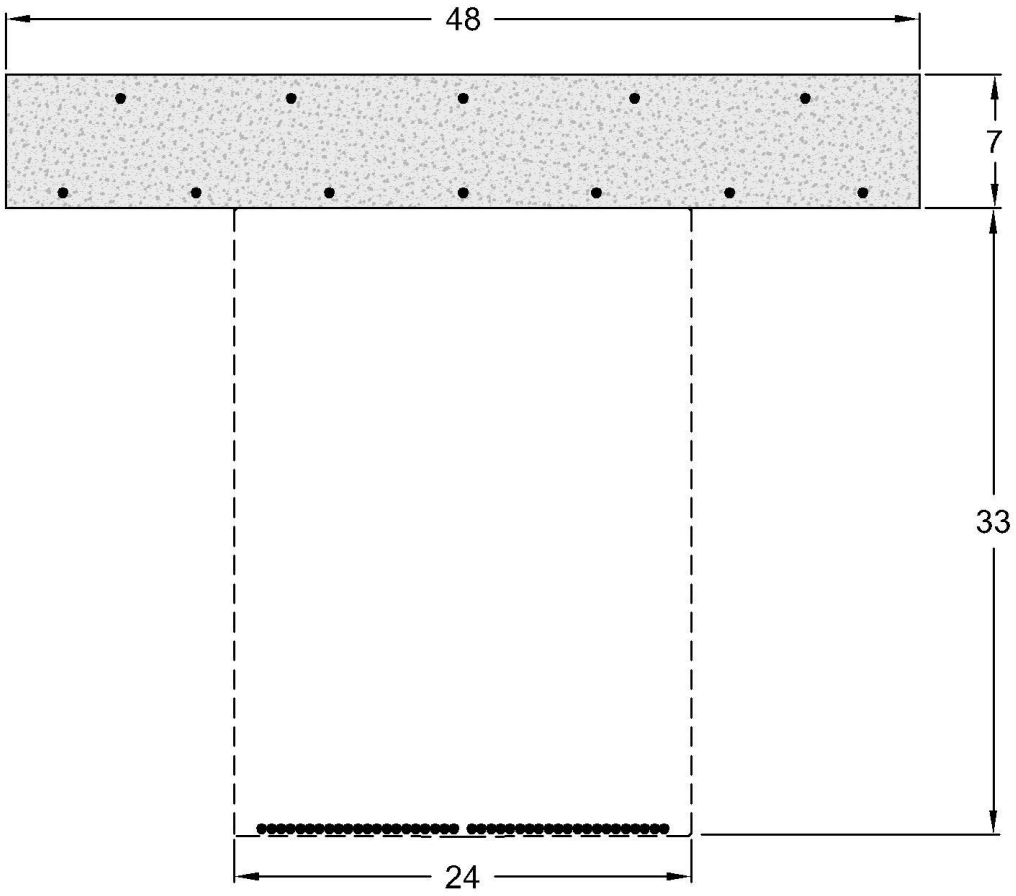

Figure 29. Cross section of HCB without concrete arch and FRP box

Table 27: Load vs midspan deflections under four-point loading given by elastic analysis for HCB without concrete arch and FRP box

Total Load, 2P, (Kips)	Midspan Deflection (in.)
0	0.00
65	3.25
133	6.66
175	8.76
200	10.01
240	12.01
280	14.02
300	15.02
310	15.52
340	17.02
370	18.52
400	20.02

Like the previous model, the finite-difference approach is also used to find the nonlinear load-deflection behavior of the beam. The explanation of the analysis under finite-difference scheme and equation of flexural equilibrium for this HCB model are given in Section 2.4. Due to the constant cross section of the beam, same moment-curvature curve is used for all nodal points during the finite-difference analysis. The moment-curvature curve for the HCB used in the FD analysis is given in Figure 30.

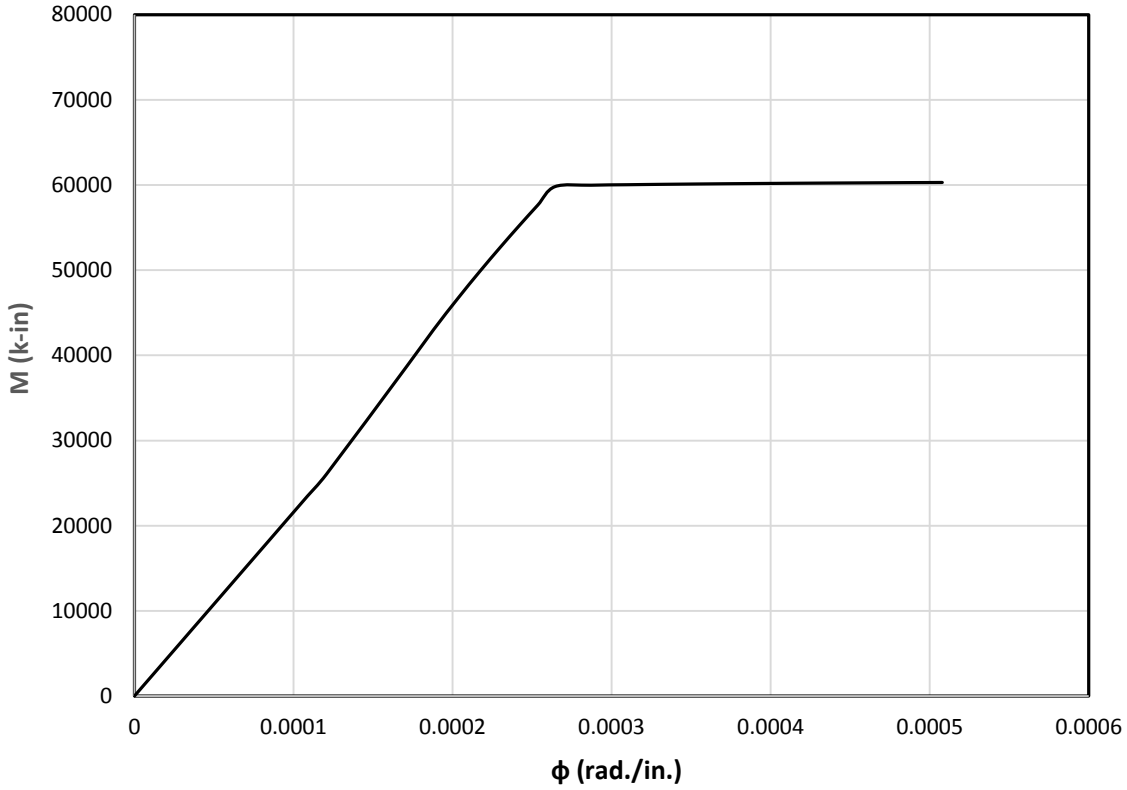

Figure 30. Moment-curvature curve for HCB without concrete arch and FRB box

The load vs deflection values at midspan generated by the finite-difference analysis are given in Table 26 whereas the moment, curvature and deflection values at all nodes for different loads are given in Appendix D. The theoretical and experimental load-deflection relations for the HCB without concrete arch at midspan are shown in Figure 31.

3.3.1 Load-deflection relation and strength for HCB without concrete arch, fin and FRP box

Figure 31 shows theoretical curves given by the elastic theory and nonlinear finite-difference analysis along with the experimental curve [10]. The curves are in very close agreement up to nearly 150 kips where the experimental curves starts deviating from the theoretical one. It can

be seen from the figure that there curves are in close agreement in for small loads. The figure also confirms that that the role of FRP box in shaping deflection response and ultimate strength is more than the concrete arch and fin. The deflections given by this model for HCB are 10 % higher than the deflections given by the analysis for the complete cross section of HCB. The ultimate strength predicted by this model is 13 % lower than that given by the complete cross section of HCB.

Table 28: Load versus midspan deflection given by finite-difference method for HCB without concrete arch and FRP box

Total Load, 2P, (Kips)	Midspan Deflection (in.)
0	0.00
65	3.27
133	6.69
200	9.89
310	14.63
355	17.01
370	27.35

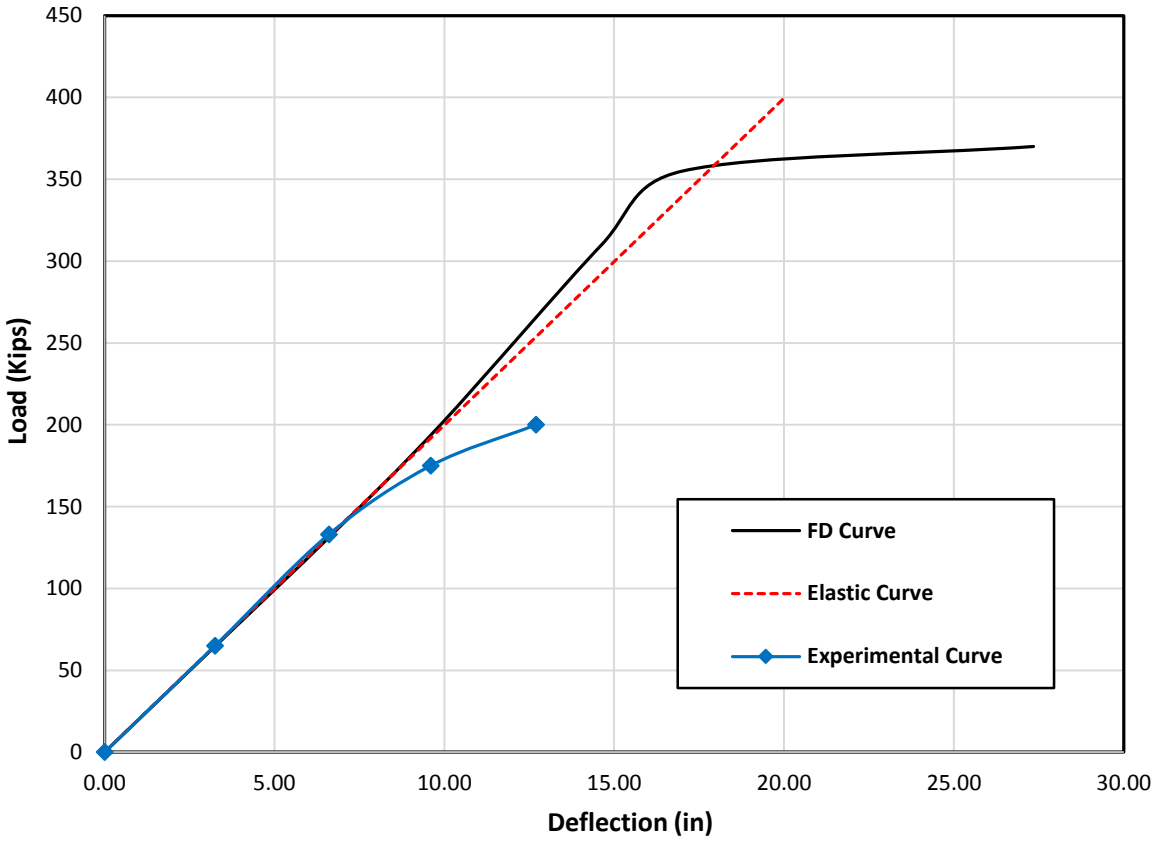

Figure 31. Load-deflection curves for HCB without concrete arch, fin and FRP box

3.4 HCB analyzed as Bernoulli beam using average cross section

This model assumes that instead of a concrete fin of varying depth, HCB has a fin of constant depth equal to the average depth of the fin carved by the parabolic profile of the concrete arch in the actual HCB. The average height of the fin for the cross section is 9.3 inches. The cross section for this HCB model is shown in Figure 32. The elastic equation for deflection of prismatic beam under four point loading condition is applied to calculate the deflection values. The load vs midspan deflection values given by the equation are given in Table 29. The elastic neutral axis distance from the bottom of the cross section and moment of inertia of the beam cross section about the neutral axis are 28.94 in. and 107078.15 in^4, respectively.

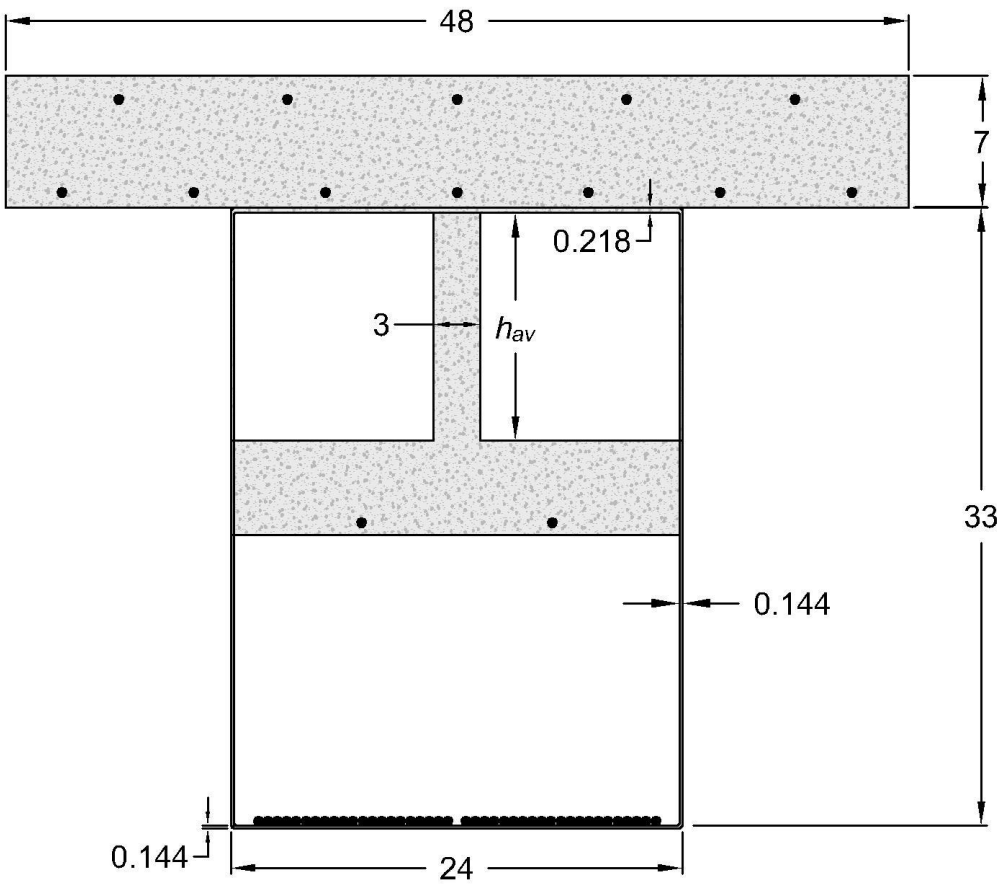

Figure 32. Average cross section of HCB

Table 29: Load versus midspan deflection given by elastic analysis for HCB with average fin depth

Total Load, 2P, (Kips)	Midspan Deflection (in.)
0	0.00
65	2.78
133	5.69
175	7.49
200	8.56
240	10.27
280	11.98
300	12.83
310	13.26
340	14.54
370	15.83
400	17.11
410	17.54
424	18.14

The load-deflection relation for the model using the finite-difference approach is also generated for the model. The moment-curvature curve HCB with hypothetical cross section is shown in Figure 33. The deflections values at the midspan at different loads given by the finite-difference analysis are shown in Table 26.

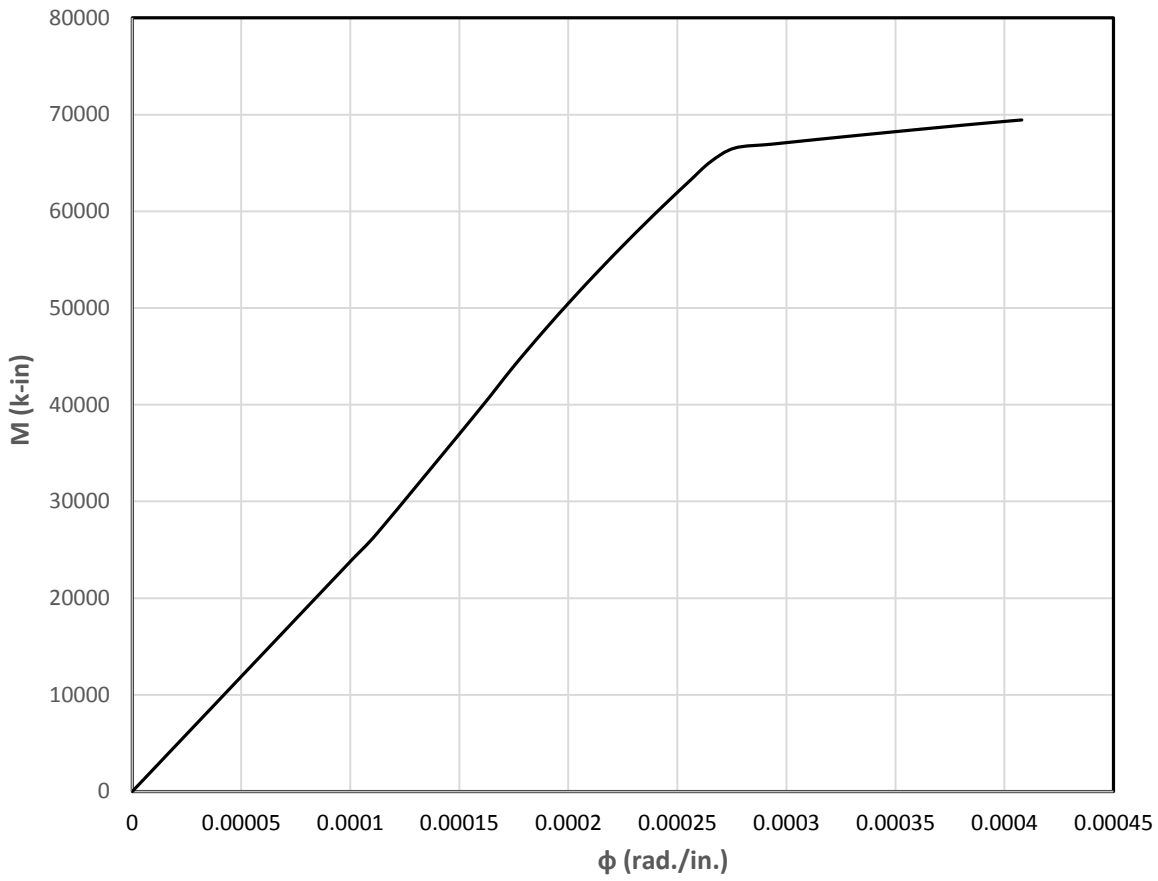

Figure 33. Moment-curvature relation for HCB with average cross section

3.4.1 Load-deflection relation and strength for HCB with average cross section

The deflections values at the midspan at different loads given by the finite-difference analysis are shown in Table 30. Figure 34 shows load-deflection relations for the HCB model given by elastic analysis and nonlinear FD analysis along with the experimental curve [10].

It can be seen from the figure that deflections for the elastic curve only 6 % larger than those for the FD curve and both curves go side by side until the FD curve takes turn near ultimate load.

Table 30: Load vs midspan deflection given by finite-difference method for HCB with average cross section

Total Load, 2P, (Kips)	Midspan Deflection (in.)
0	0
65	2.97
133	6.07
200	9.00
355	15.46
410	18.63
424	22.90

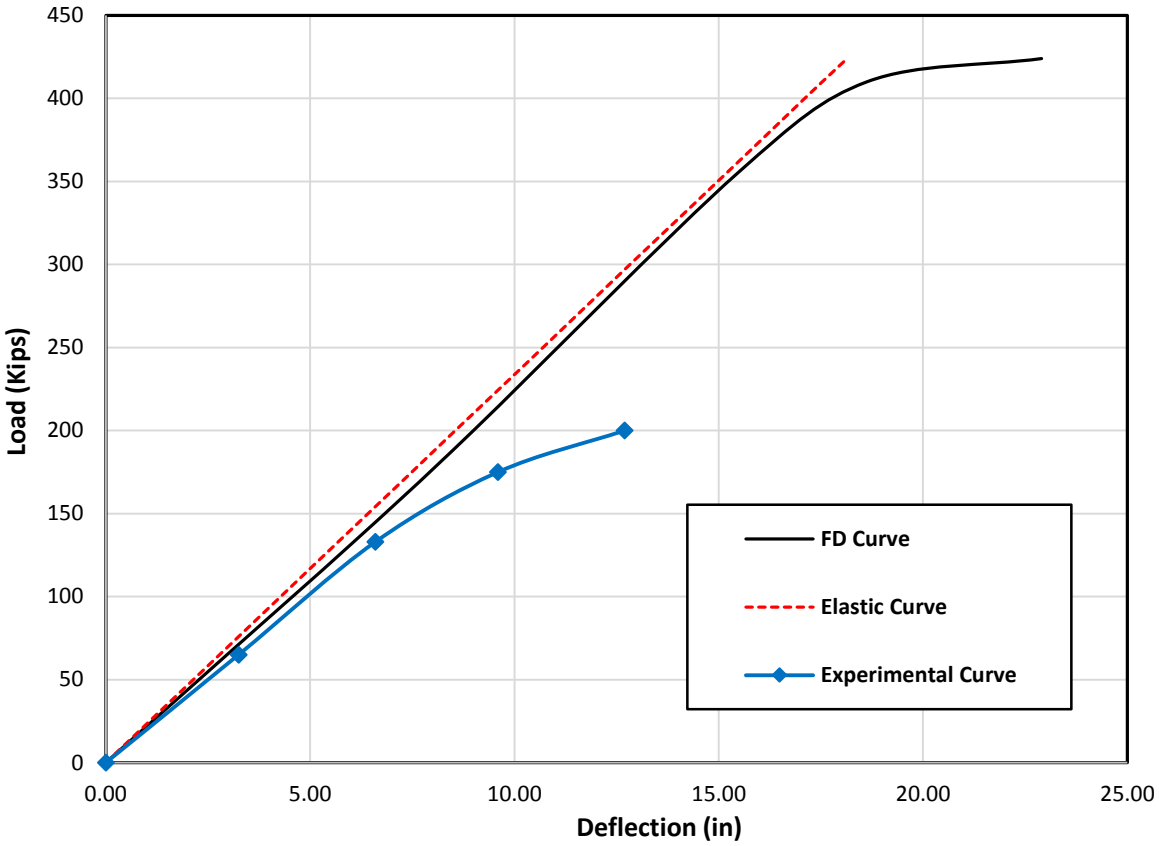

Figure 34. Theoretical load-deflection relations given by elastic and finite-difference analyses for average cross section along with experimental curve [10]

3.5 Comparison of behavior of different HCB models

The load-deflection relations for the four HCB models used discussed above are shown in Figure 35 along with the experimental curve [10]. It can be seen form the figure that ultimate strength of HCB for the actual cross section, cross section without arch and fin and with a hypothetical constant cross section remains same whereas the strength for the cross section without concrete arch, fin and FRP is 13% lesser than the ultimate strength for other three models. This proves that the contribution of concrete arch and fin to the ultimate strength of

HCB when analyzed as Bernoulli's beam remains negligible where the FRP the FRP box adds significantly to the ultimate strength of HCB.

Figure 36 shows the load-deflection relations for four HCB models in the linear range along with the experimental relation. It can be seen form the figure that the three models with FRP box included in the cross section give almost same deflections for a given load whereas the model without box gives 9% higher deflections. When compared with the experimental it turns out that the deflections for the HCB without FRP box and concrete slab and fin are within 1% of the experimental values which is surprising as the three cross-sectional element from analysis cannot give exact values. This could be due to larger deflections of HCB due to local bucking of the very thin HCB webs.

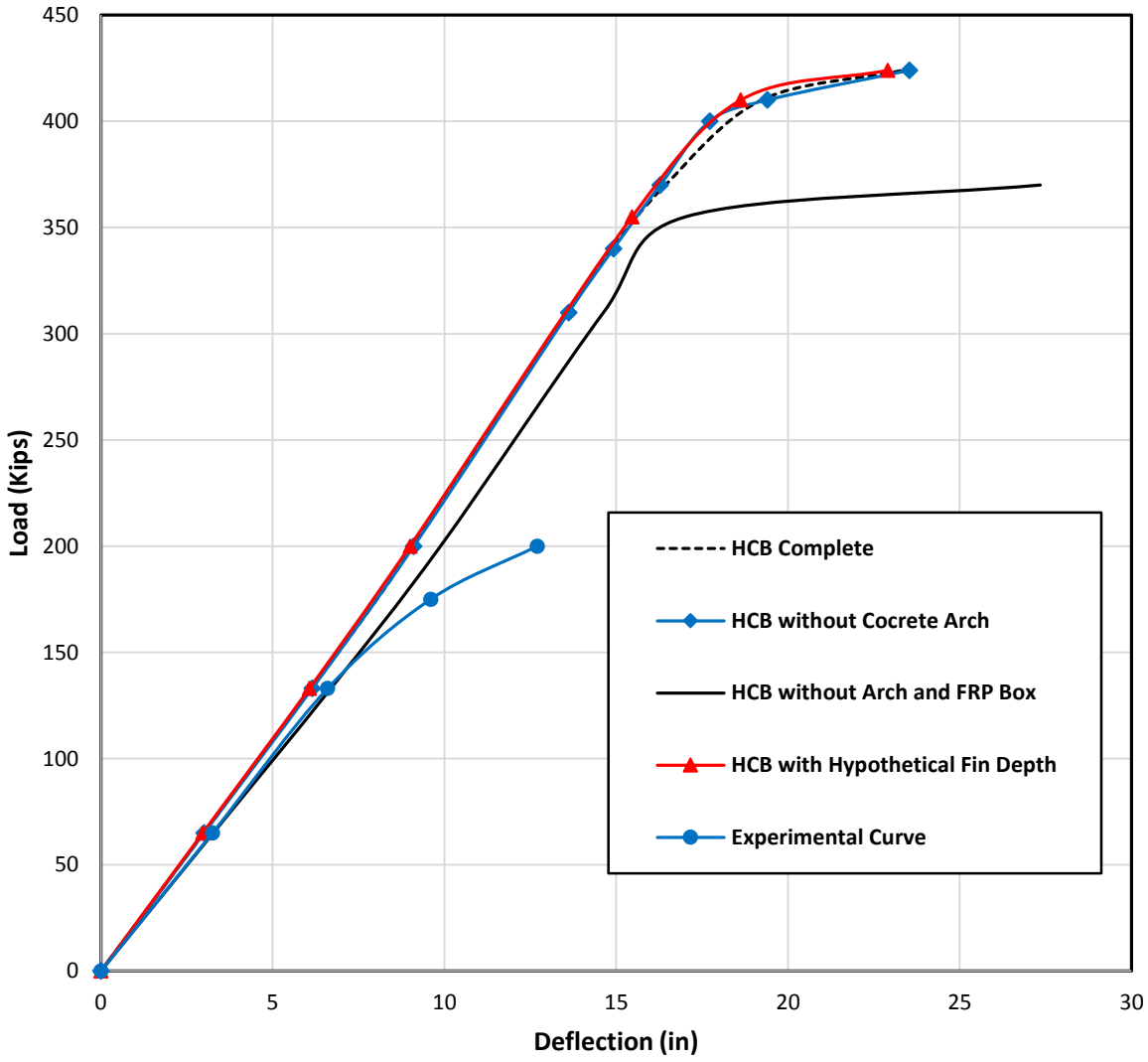

Figure 35. Comparison of the load-deflection curves for the four models with the experimental curve [10].

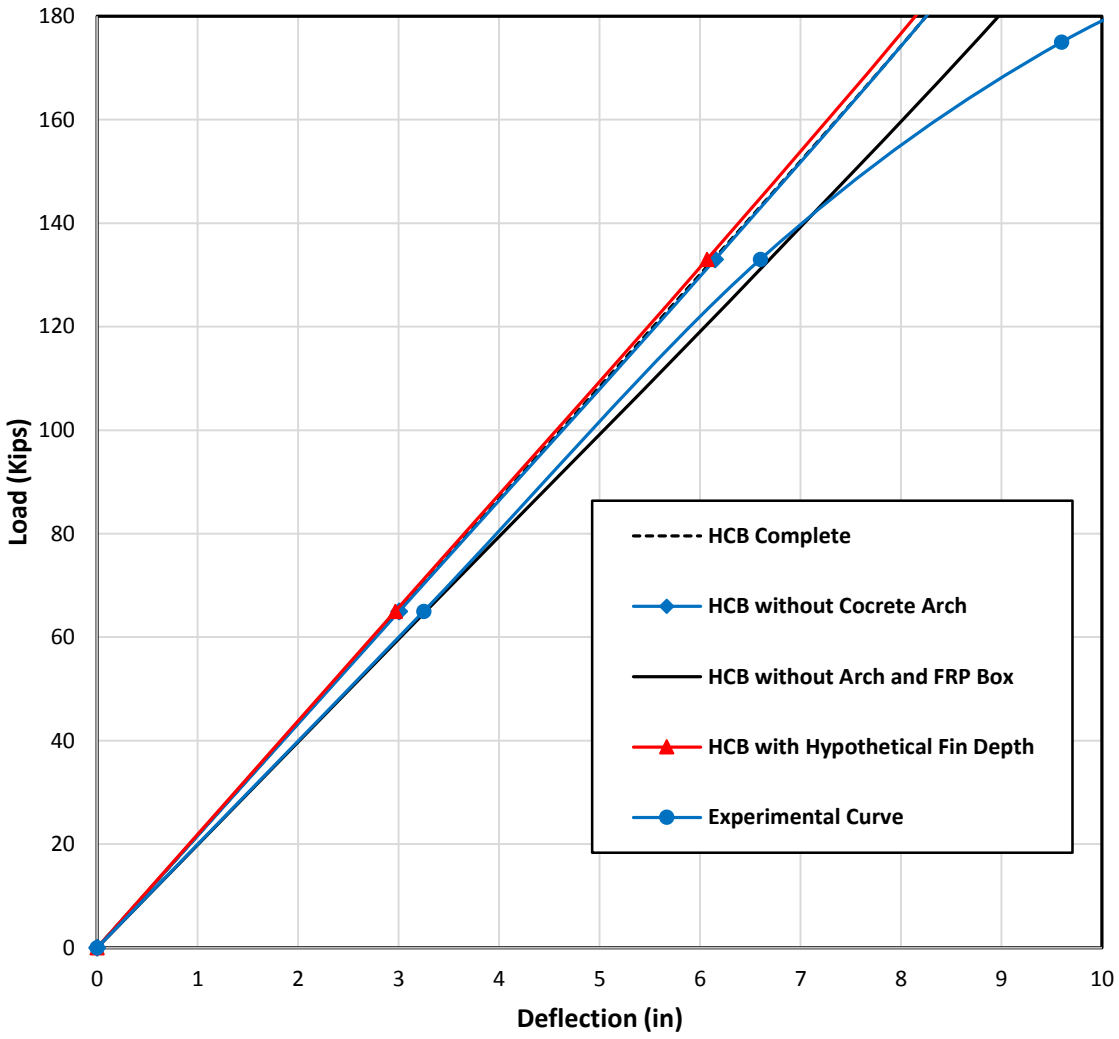

Figure 36. Load-deflection curves for the four models and experimental curve [10] in linear range

3.6 HCB analyzed as arch-and-beam model

The theoretical description of the analysis of HCB as a composite of box beam and concealed arch is presented in chapter 2. The analysis for this model is made for two support conditions of the concealed arch, namely, tied arch and two-hinged arch. The cumulative resistance to the

relative movement of the arch nodes offered by the tie is represented by stiffness k of the spring shown at the roller end of the simply supported arch. Due to being composite with beam, it is not clearly known as to what components of HCB contribute to the stiffness of the spring. Therefore, the behavior of the model is checked for different values of k depending upon the assumptions as to what components of HCB contribute to the stiffness of tie. Likewise, the composition of the box beam that is supposed to resist load in conjunction with the arch is not clearly known. Therefore, the beam properties are also subject to variation as to what component of HCB is assumed to contribute to the beam behavior in resisting the bending load. Depending upon the components of HCB considered as beam part and spring stiffness contributors, the analysis of HCB under beam and arch model is carried out for following cases:

a. Tensions reinforcement acts as tie but does not contribute to the beam action
b. Tension reinforcement acts as tie and contribute to the beam behavior as well
c. All cross section elements except concrete arch and fin contribute to the tie resistance and included in beam as well
d. All cross-sectional elements except concrete arch contribute to the tie resistance and beam action

The analysis will be initially done for the deflection response of HCB under the deck concrete load. Later, the behavior of complete HCB under the external four-point loading will be analyzed.

3.6.1 Load-deflection behavior of HCB without concrete slab

The data provided by the HC Bridge Company[1] for this research includes the midspan deflection measurements for the HCB at different stages of its fabrication process. One such deflection is caused by the deck concrete just after its pouring is measured as 1.44 in. To investigate the validity of arch and beam model for HCB, the deflection at midspan is calculated by using tied arch and beam model and compared with the experimental value. A schematic explanation of the arch and beam model for concrete deck loading is shown in Figure 37.

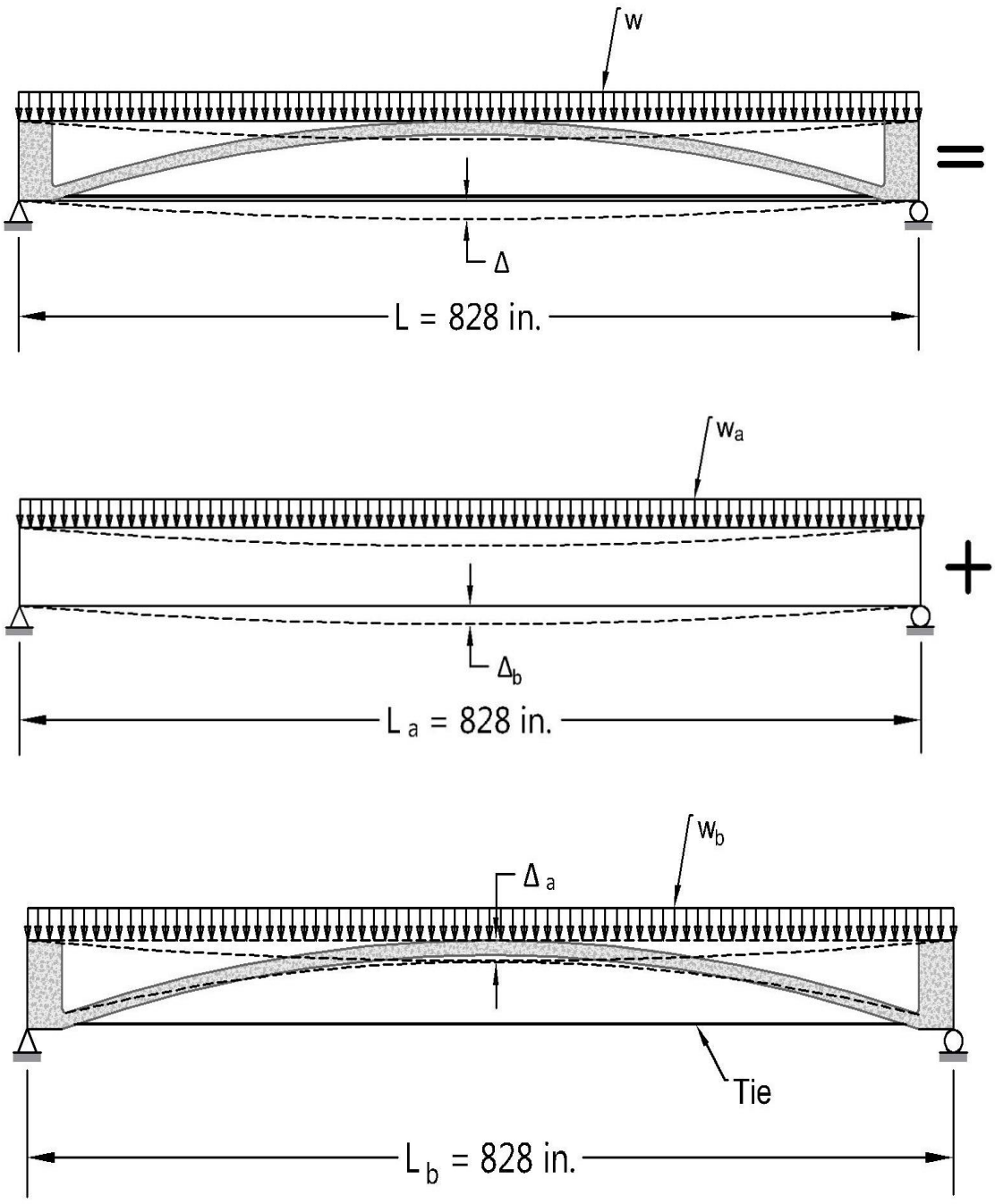

Figure 37. Concrete deck load transfer to tied arch and box beam

The condition of equilibrium gives:

$$w = w_a + w_b \tag{73}$$

Where

$w = Total\ UDL\ on\ the\ HCB$

$w_a = UDL\ \ resisted\ by\ the\ tied\ arch$

$w_b = UDL\ \ resisted\ by\ the\ the\ box\ beam$

The compatibility equation gives:

$$\Delta_A = \Delta_B$$

The condition of concrete arch while jointly resisting load with the box beam can be schematically represented as shown in Figure 38.

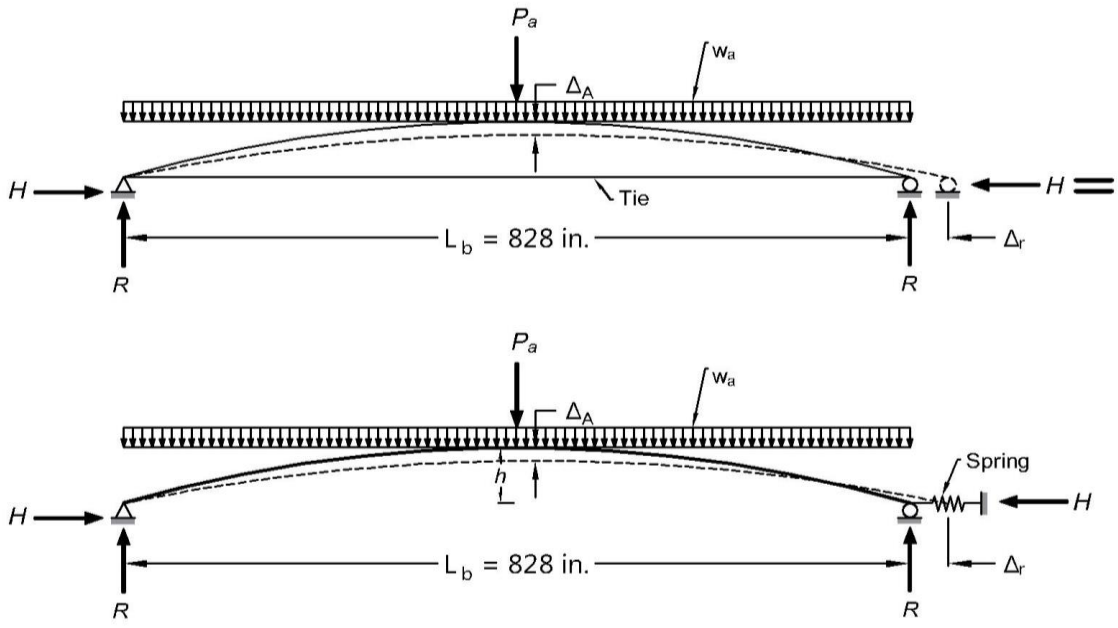

Figure 38. Tied arch modeled as an arch with a spring at one support

As shown in chapter 2, the horizontal reaction H is given by:

$$H = \frac{\int_0^s \frac{M_O y}{EI} ds - \int_0^s \frac{N_O \sin\theta \cos\theta}{EA} ds}{\frac{1}{k} + \int_0^s \frac{y^2}{EI} ds + \int_0^s \frac{\cos^2\theta}{EA} ds}$$

For low arches : ds ≈ dx , $\cos\theta \approx 1$ and $\sin\theta \approx \theta$. So, we get:

$$H = \frac{\int_0^L \frac{M_O y}{EI} dx - \int_0^L \frac{N_O \theta}{EA} dx}{\frac{1}{k} + \int_0^L \frac{y^2}{EI} dx + \int_0^L \frac{1}{EA} dx} \tag{74}$$

For the given case of UDL on the arch span, we get:

$$H = \frac{\int_0^L \frac{(Rx - \frac{w_a x^2}{2}) y}{EI} dx - \int_0^L \frac{(R - w_a x)\theta}{EA} dx}{\frac{1}{k} + \int_0^L \frac{y^2}{EI} dx + \int_0^L \frac{1}{EA} dx} \tag{75}$$

Further simplification, yields:

$$H = \frac{\int_0^L \frac{(Lx - x^2) y}{2EI} dx - \int_0^L \frac{(x - L)\theta}{EA} dx}{\frac{1}{k} + \int_0^L \frac{y^2}{EI} dx + \int_0^L \frac{1}{EA} dx} w_a + \frac{\int_0^L \frac{xy}{2EI} dx - \int_0^L \frac{\theta}{EA} dx}{\frac{1}{k} + \int_0^L \frac{y^2}{EI} dx + \int_0^L \frac{1}{EA} dx} P_a \tag{76}$$

The deflection of arch at the midspan is given by:

$$\Delta_A = \frac{\partial U}{\partial P_a}$$

$$\Delta_A = \frac{\partial}{\partial P_a}\left(\int_0^s \frac{M^2}{2EI} ds + \int_0^s \frac{N^2}{2EA} ds + \frac{H}{2k}^2 \right)$$

The final form of the expression after doing all the mathematics involved is as follows:

$$\Delta_A = \left(\frac{2}{EI}\left(\frac{L}{4}\int_0^{L/2} x^2\,dx - \frac{1}{4}\int_0^{L/2} x^3\,dx - \frac{L}{2}\frac{\partial H}{\partial P_a}\int_0^{L/2} x^3\,dx + \frac{1}{2}\frac{\partial H}{\partial P_a}\int_0^{L/2} x^3 y\,dx\right) + \frac{2}{EA}\left(\frac{L}{2}\frac{\partial H}{\partial P_a}\int_0^{L/2}\theta\,dx - \frac{\partial H}{\partial P_a}\int_0^{L/2} x\theta\,dx + \frac{L}{4}\int_0^{L/2}\theta^2\,dx - \frac{1}{2}\int_0^{L/2} x\theta^2\,dx\right)\right) w_a + \left(\frac{2}{EI}\left(\frac{\partial H}{\partial P_a}\int_0^{L/2} y^3\,dx - \frac{1}{2}\int_0^{L/2} xy\,dx\right) + \frac{2}{EA}\left(\frac{\partial H}{\partial P_a}\int_0^{L/2} dx + \frac{1}{2}\int_0^{L/2}\theta\,dx\right) + \frac{\partial H}{\partial P_a}\right) H$$

(77)

The expression for the deflection of box under its part of UDL i.e., $\boldsymbol{w_b}$ is:

$$\Delta_B = \frac{5 w_b {L_b}^4}{384 E_b I_b} \tag{78}$$

Where

$L_b = Span\ length\ of\ the\ box\ beam$

$E_b = Modulus\ of\ elasticity\ of\ beam$

$I_b = Moment\ \ of\ inertia\ of\ beam$

Using equilibrium and compatibility, the deflection of the HCB at the midspan can be calculated. As clear from the equations involved the value of the deflection also depends cross section of the arch concrete, moment of inertia of the box beam and stiffness of the spring representing tie in the arch. Since, these quantities change depend upon as to what component of the HCB are assumed to contribute to the beam and tie action, therefore, in search for the best theoretical description of the process, following cases of beam cross section and ties resistance will be considered:

a. Case A: Box beam consists of FRP box only; and only tension steel contributes to the spring stiffness
b. Case B: Box beam consists of FRP and tension steel; and tension steel and whole FRP box contribute to the spring stiffness
c. Case C: Box beam consists of FRP, tension steel and inverted T shaped concrete part and the same elements contribute to the stiffness of the spring

The cross section of the concrete arch, shown in Figure 39, remains the same for all cases.

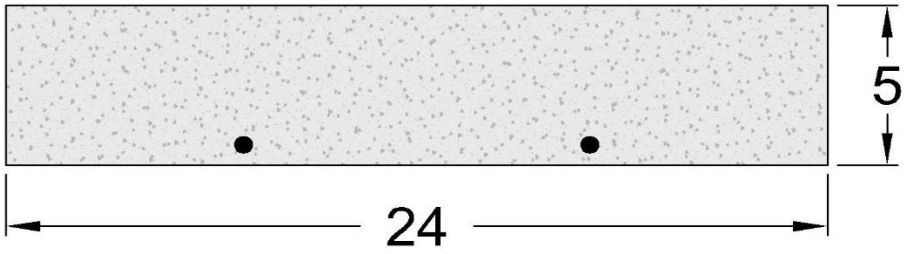

Figure 39. Cross section of concrete arch (Dimensions in inches)

3.6.1.1 Deflection of HCB for case A

The cross section of the beam consisting of the FRP shell only is shown in Figure 40.

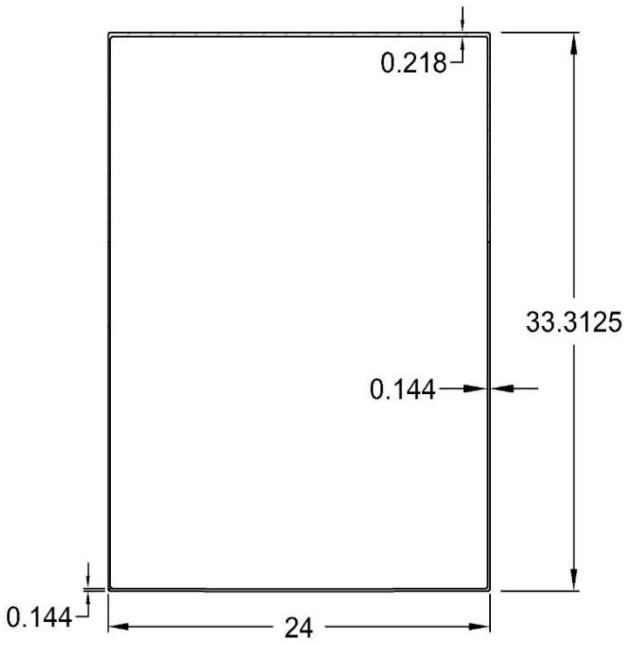

Figure 40. Cross section of the beam used for Case A. (Dimensions in inches)

The properties of the cross section used for calcualitng the deflection of the HCB are:

Moment of inertial about centroidal axis: $I_b = 3004.16\ in^4$

Modulus of elasticity: $E_b = 3240$ ksi

Since, only tension steel (steel strands) is supposed to contribute to the tied action of arch. Therefore, only the properties of steel strands will be used while calculating the stiffness of the spring of the arch. The stiffness k will thus be:

$$k = \frac{E_S A_S}{L} \tag{79}$$

$$k = \frac{28500(6.426)}{828}$$

$$k = 221.19\ k/in$$

The deflection of the HCB at midspan under the load of deck concrete (0.029 k/in) will be 2.79 in and stress at the bottom fibers of concrete arch cross section will be 327.00 psi which is less than the modulus of rupture of the arch concrete i.e. 474 psi; so as per this analysis the concrete arch is not cracked under the deck concrete load.

The deflection of the HCB for the concealed arch to be a two-hinged arch can be calculated by putting the value of spring stiffness to be infinitely large and keeping all the remaining quantities same. Doing so, we get deflection of the HCB at the midspan as 0.97 in. The relationship between the midspan deflection of the HCB under UDL for both tied and two hinged concealed arch assumptions is shown in Figure 41.

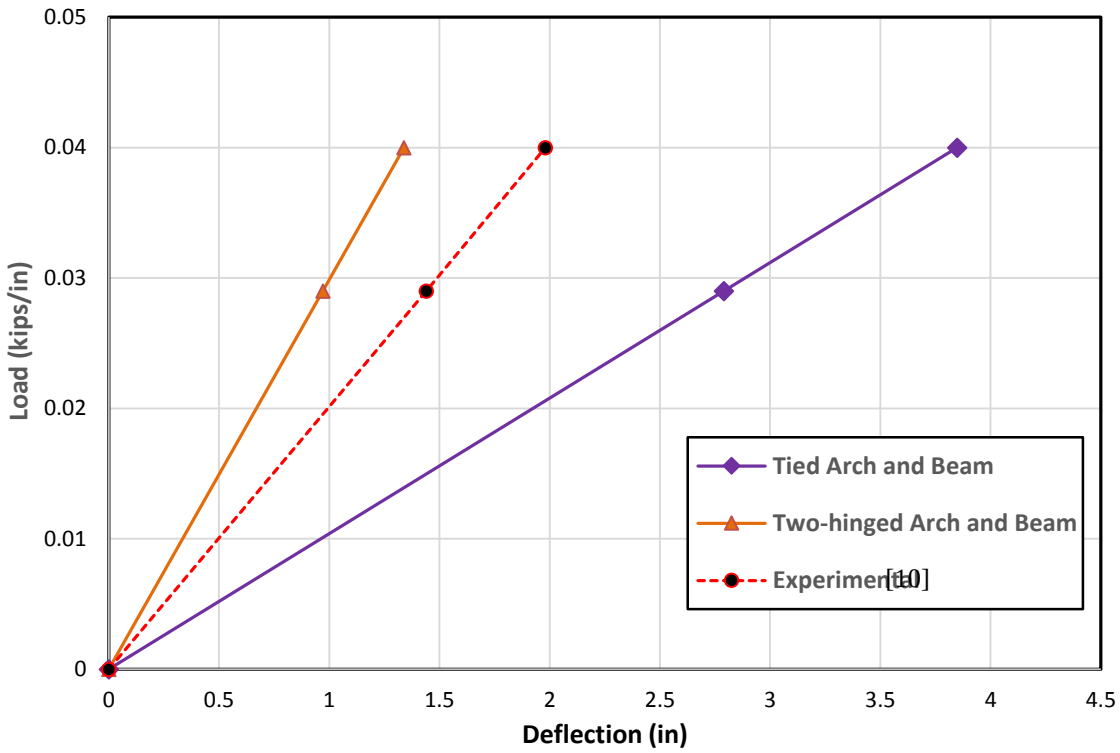

Figure 41. Load vs midspan deflection relations for Case A.

It can be seen from the figure that for Case A the tied arch and beam model gives 93% higher deflections whereas the tow-hinged arch models gives 33% lower values.

3.6.1.2 Deflection of HCB for B

The cross section of the beam for case B consists of the entire FRP part plus tensions steel as shown in Figure 42.

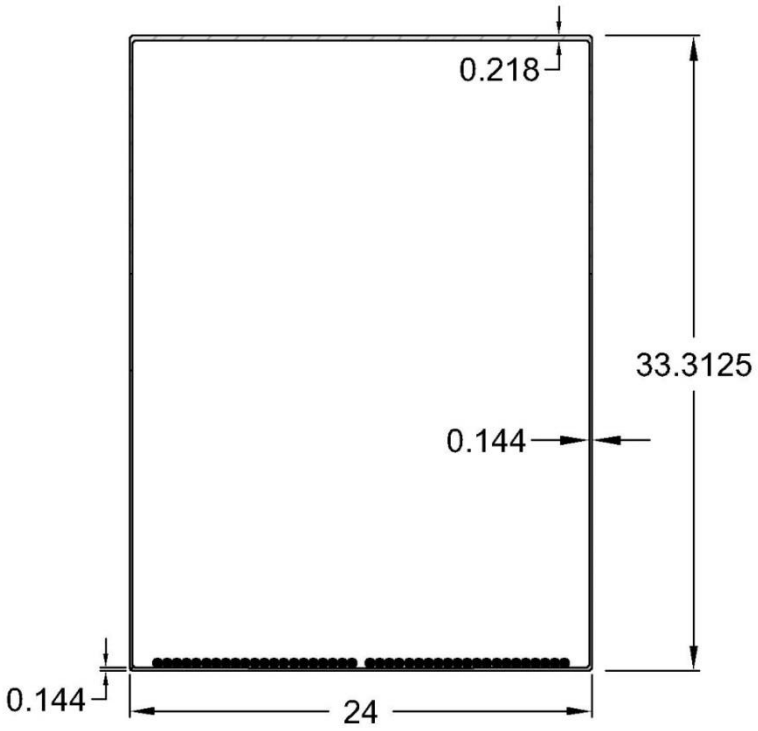

Figure 42. Cross section of the beam used for Case B. (Dimensions in inches)

The properties of the cross section are:

Moment of inertial about centroidal axis: $I_b = 12482.70\ in^4$

Modulus of elasticity: $E_b = 3240$ ksi

The stiffness k of the spring is calculated by using the properties of the transformed area of the cross section:

$$k = \frac{E_t A_t}{L}$$

$$k = \frac{3240(80.63)}{828}$$

$$k = 315.51\ k/in$$

The load-deflection curve for Case B of arch and beam model of HCB is given in Figure 43. It can be seen from the figure that the deflections for Case B for two-hinged arch are 42% lesser than the experimental values whereas the same for tied arch model are 14% higher. The analysis further shows that stresses anywhere in the concrete arch are smaller than the modulus of rupture so concrete has not failed in tension yet.

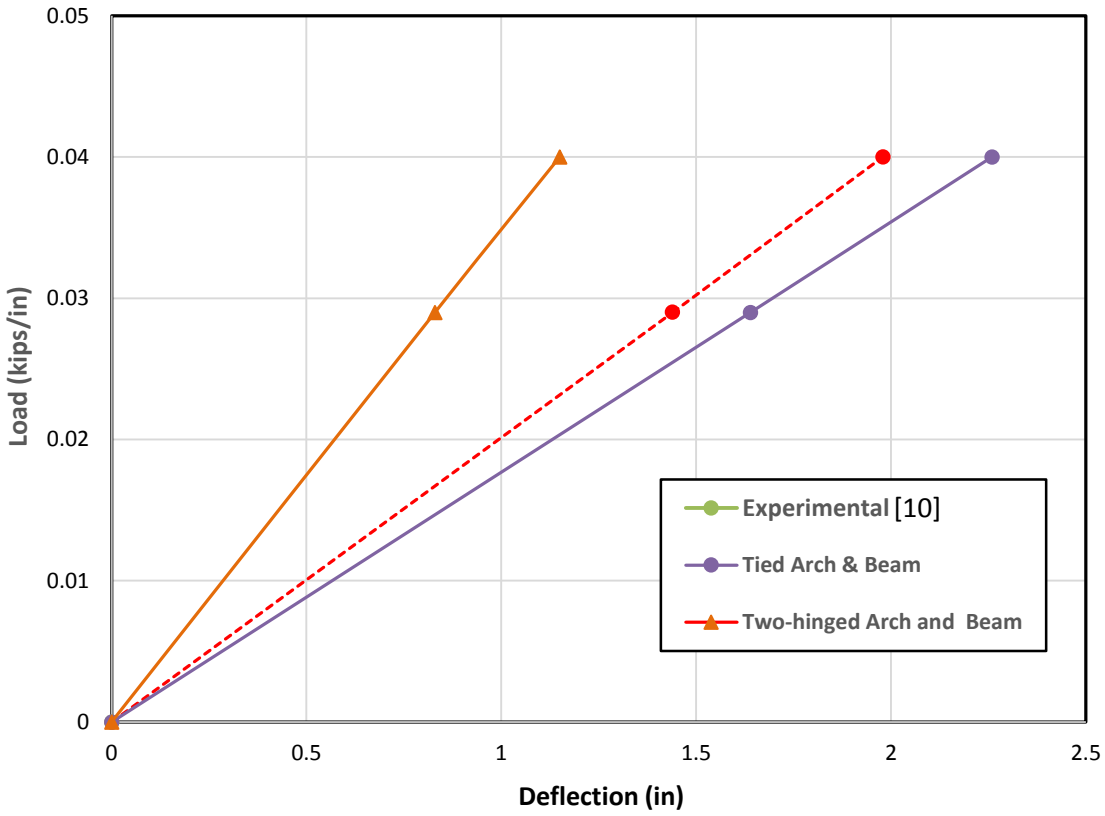

Figure 43. Load vs midspan deflection relations for Case B.

3.6.1.3 Deflection of HCB for Case C

The cross section of the beam for case c consists of the entire FRP box plus a fin of depth equal to the average depth of the fin in the actual arch as shown in Figure 44.

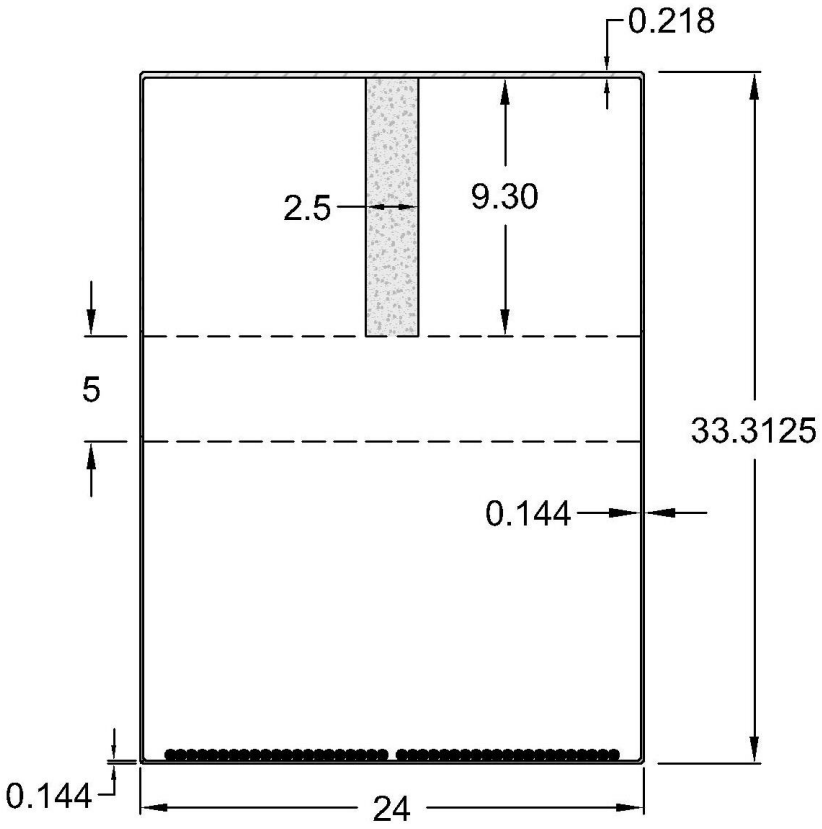

Figure 44. Cross section of the beam used for Case C. (Dimensions in inches)

The properties of the cross section are:

Moment of inertial about centroidal axis: $I_b = 17829.23$ in^4

Modulus of elasticity: $E_b = 3240$ ksi

The stiffness k of the spring is calculated by using the properties of the transformed area of the cross section:

$$k = \frac{E_t A_t}{L}$$

$$k = \frac{3240(97.05)}{828}$$

$$k = 379.76\ k/in$$

The load-deflection curve for the HCB is given in Figure 45. The concrete stress at the extreme bottom fibers of the arch cross section is lesser than the modulus of rupture so concrete has not failed in tension yet.

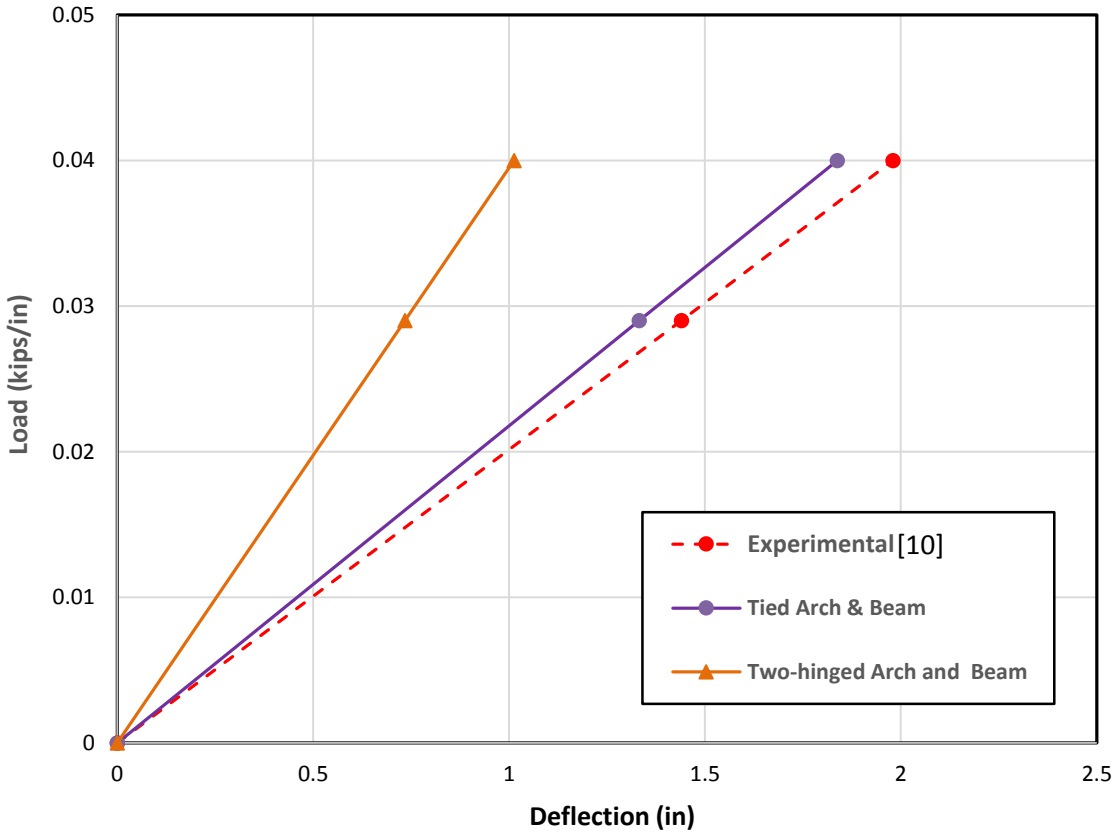

Figure 45. Load vs midspan deflection relations for Case C.

The deflections given by the tied arch-and-beam model are relatively closer to the experimental but smaller by 14% approximately.

3.6.2 Deflection of HCB without slab using Bernoulli beam approach

The deflection of the HCB with under the deck concrete load is also calculated by using the finite-difference method. The process is exactly the same as used for the other cases of the deflection calculation for HCB except that the concrete slab over the FRP box is not president. The moment curvature curves for the HCB cross sections at the nodal points are given in Appendix-E. The nodal interval value is chosen as 82 inches. The nodal deflections given by the method are shown in Table 23.

Table 31: Results for w=0.029 k/in. and h=82 in.

Node	Moment (K-in)	ϕ (radian)	Deflection (in.)
1	0	0	0
3	877.482	0.000013861	0.58
5	1559.968	0.000021497	1.06
7	2047.458	0.000020820	1.40
9	2339.952	0.000019751	1.60
11	2437.45	0.000019739	1.66

Table 32: Results for w=0.040 k/in. and h=82 in.

Node	Moment (K-in)	ϕ (radian)	Deflection (in.)
1	0	0	0
3	877.482	0.000019118	0.80
5	1559.968	0.000029651	1.46
7	2047.458	0.000028717	1.93
9	2339.952	0.000027243	2.20
11	2437.45	0.000027226	2.30

Likewise, the deflections of the HCB at nodes are calculated using Newmark's method to see if the HCB behavior can be precisely predicted by considering it simply a beam with a variable cross section over the span. The nodal deflection given by the Newmark's method are given in Table 24 and Table 25.

Table 33: Nodal Deflections given by Newmark's Method for w=0.029 k/in

Node	Deflection (in.)
1	0
3	0.55
5	1.02
7	1.36
9	1.56
11	1.62

Table 34: Nodal Deflections given by Newmark's Method for w=0.040 k/in

Node	Deflection (in.)
1	0
3	0.76
5	1.41
7	1.87
9	2.15
11	2.24

The laod deflection curves given by the FD and Newmark's methods are shown in Figure 46. The deflections determined from the two methods are almost same but larger than the experimental value of deflection by 12%..

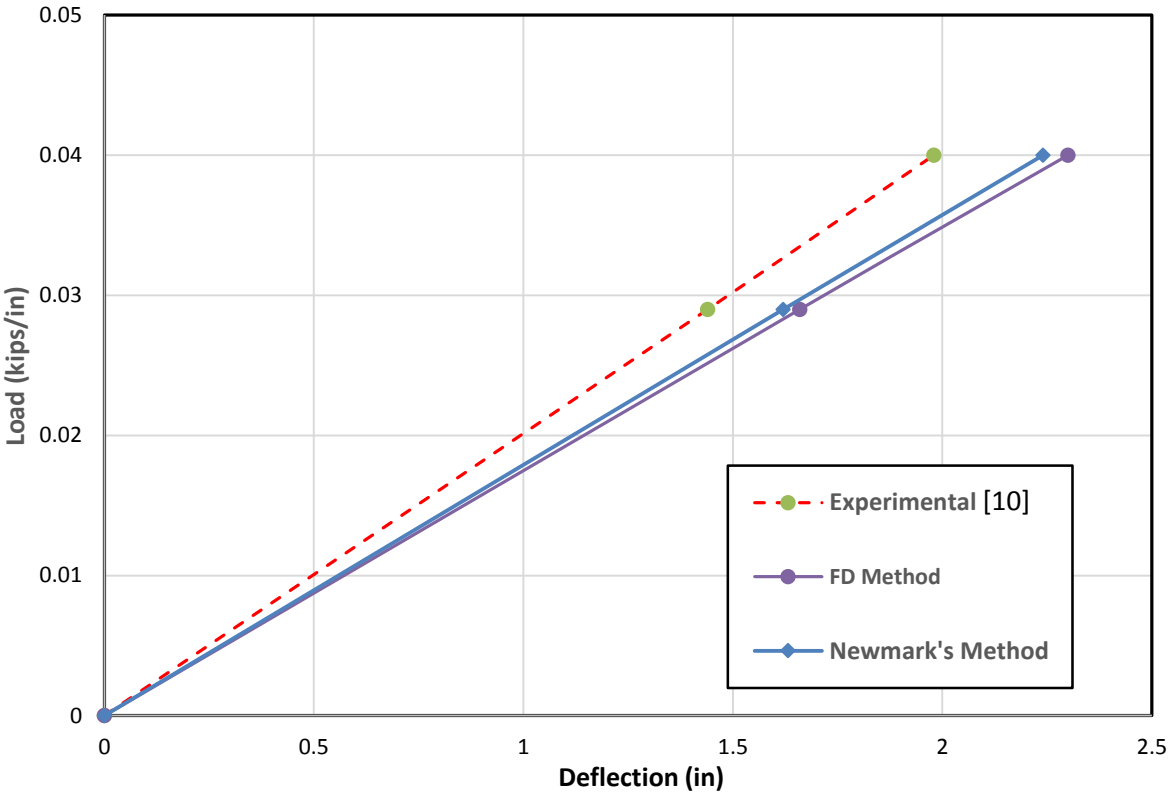

Figure 46. Load-midspan deflection relations HCB without slab given by finite-difference and Newmark's methods

3.6.3 Deflection response of HCB with concrete slab for arch-and-beam model

This section analyses the deflection response of HCB with concrete slab for the arch and beam model. The methodology of analysis is same as done for the HCB without concrete slab in Section 3.2.1. The HCB can be broken down into a box beam and a tied arch each taking its own share of load as shown in Figure 47.

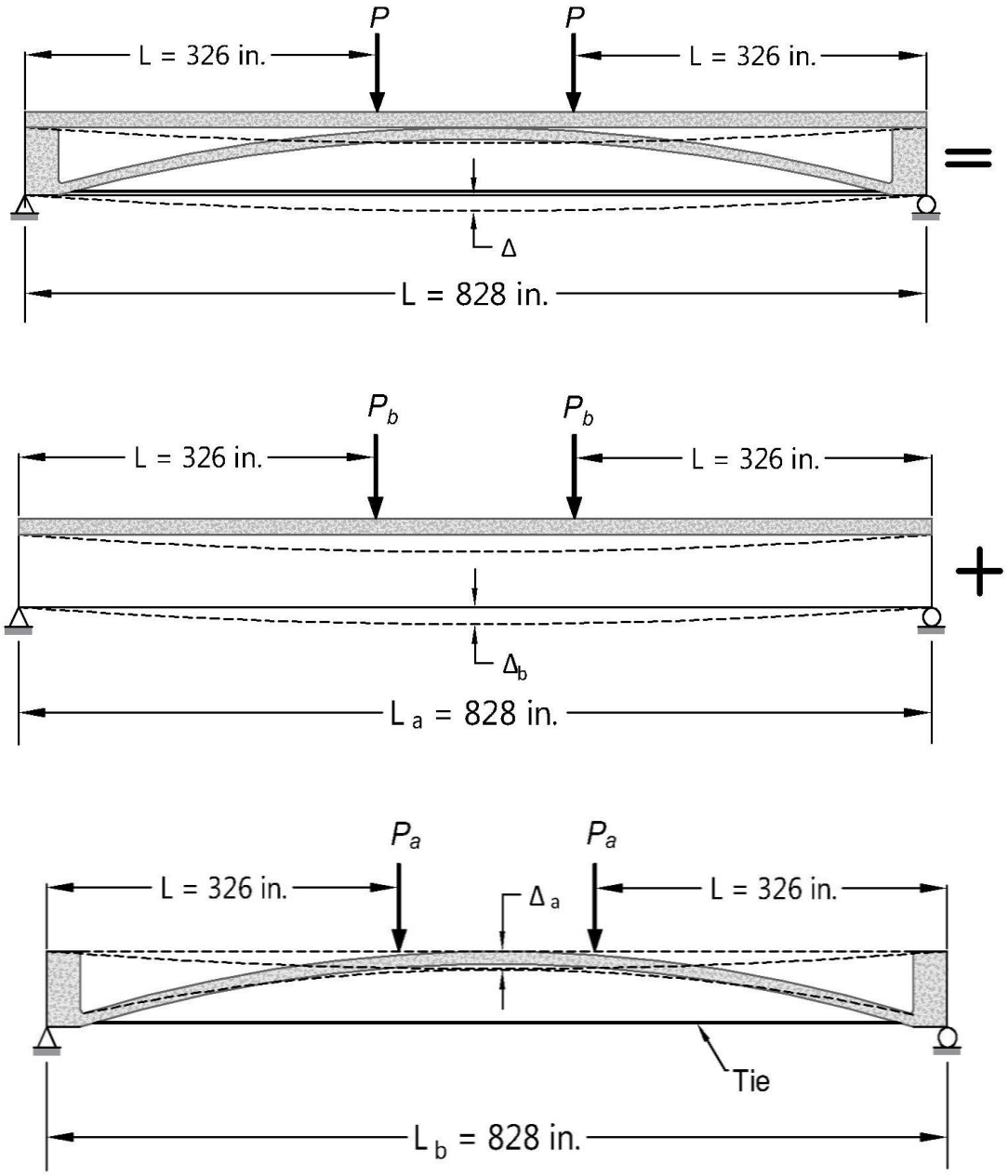

Figure 47. HCB broken down into a box beam and tied arch

The tied arch is represented as a simply supported arch with a spring at the roller end as shown in Figure 48. The stiffness of the spring represents tie action of the arch.

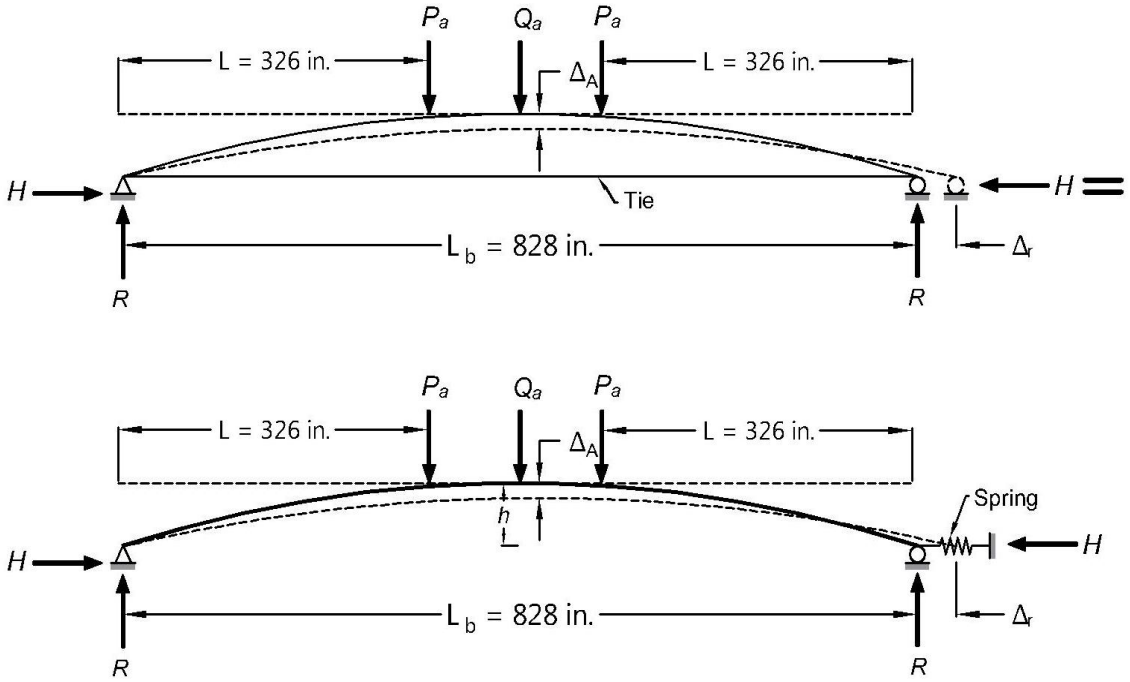

Figure 48. Tied arch modeled as an arch with a spring at one end

The horizontal reaction H can be calculated by using equation 74:

$$H = \frac{\int_0^L \frac{M_o y}{EI} dx - \int_0^L \frac{N_o \theta}{EA} dx}{\frac{1}{k} + \int_0^L \frac{y^2}{EI} dx + \int_0^L \frac{1}{EA} dx}$$

For the given loading condition:

$For \quad 0 \leq x < 326$

$M_o = Rx - Hy$

$r \quad 0 \leq x < 326$

$M_o = Rx - Hy - P_a(x - a)$

$M_o = \left(P_a + {}^{Q_a}/_{2}\right) x + x - Hy - P_a(x - a)$

$$M_o = \frac{Q_a}{2}x - Hy - P_a$$

$$H = \frac{\int_0^{326}\frac{xy}{EI}dx + a\int_{326}^{410}\frac{y}{EI}dx - \int_0^{326}\frac{\theta}{EA}dx}{\frac{1}{2k} + \int_0^{410}\frac{y^2}{EI}dx + \int_0^{410}\frac{1}{EA}dx}P_a + \frac{\int_0^{410}\frac{xy}{2EI}dx - \int_0^{410}\frac{\theta}{2EA}dx}{\frac{1}{2k} + \int_0^{410}\frac{y^2}{EI}dx + \int_0^{410}\frac{1}{EA}dx}Q_a \quad (80)$$

The midspan deflection of the arch will be:

$$\Delta_A = \frac{\partial U}{\partial P_a}$$

Substituting values and simplifying yields following expression:

$$\Delta_A = \left(\frac{2}{EI}\left(\frac{1}{2}\int_0^{330}x^2\,dx - \frac{\partial H}{\partial Q_a}\int_0^{330}xy\,dx + 165\int_{330}^{414}x\,dx - 330\frac{\partial H}{\partial Q_a}\int_{330}^{414}y\,dx\right) + \right.$$
$$\left.\frac{2}{EA}\left(\frac{1}{2}\int_0^{330}\theta^2\,dx - \frac{\partial H}{\partial Q_a}\int_0^{330}\theta\,dx + \frac{L}{4}\int_0^{L/2}\theta^2\,dx - \frac{1}{2}\int_0^{L/2}x\theta^2\,dx\right)\right)P_a + \left(\frac{2}{EI}\left(\frac{\partial H}{\partial Q_a}\int_0^{414}y^2\,dx - \right.\right.$$
$$\left.\left.\frac{1}{2}\int_0^{414}xy\,dx\right) + \frac{2}{EA}\left(\frac{\partial H}{\partial Q_a}\int_0^{414}dx + \frac{1}{2}\int_0^{414}\theta\,dx\right) + \frac{1}{k}\frac{\partial H}{\partial Q_a}\right)H \quad (81)$$

The determination of the stiffness of the tie is a major question in this analysis and, therefore, as done in section 2.1.5 for the UDL different options of box beam cross sections and tie stiffness will be considered for the determination of the correct value of the stiffness.

3.6.3.1 Deflection of HCB for case A

For case A, the cross section of the HCB consist of FRP outer box plus the concrete slab as shown in Figure 49 where only the tension steel contributes toward the stiffness of the spring.

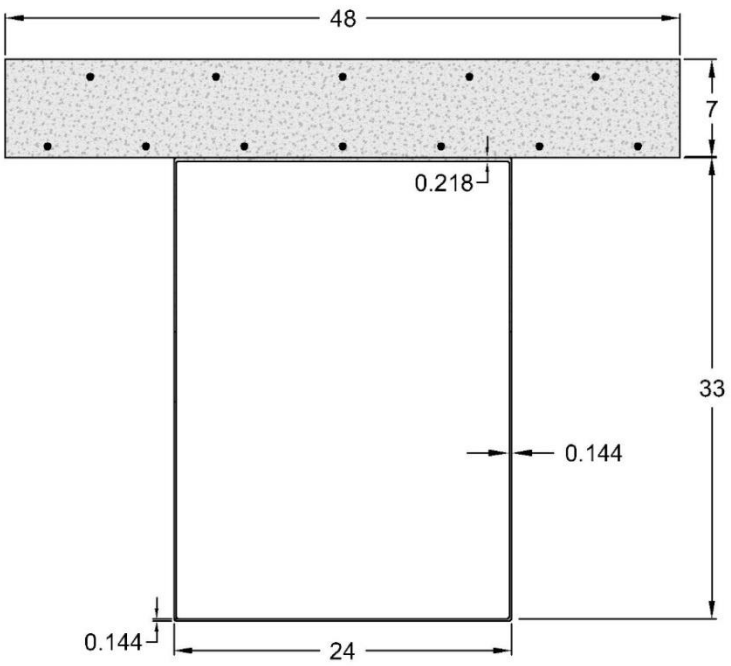

Figure 49. Cross section of box beam for Case A. (Dimensions in inches)

The properties of the cross section are as follows:

Moment of inertial about centroidal axis: $I_b = 12391.54$ in^4

Modulus of elasticity: $E_b = 3240$ ksi

The stiffness of the spring represening the tied arch is achieved from the tension steel only i.e.;

$$k = \frac{28500(6.426)}{828}$$

$$k = 221.19\ k/in$$

The deflections given by the analysis for the tied arch and beam model are shown in Table 25. The same for the two-hinged arch and beam model are shown in Table 26. Figure 50 represents load deflection relations for both conditions as well as the experimental curve. The figure shows that the deflections for the given assumption of load resisting mechanism are far off and, therefore, this model is discarded.

Table 35: load and midspan Deflections for tied arch-and-beam model

Total Load, (Kips)	Deflection (in.)
0	0
4	0.74
7	1.30
80	14.86
175	32.51

Table 36: Deflections for two-hinged arch-and-beam model

Total Load, (Kips)	Deflection (in.)
0	0
4	0.59
7	1.03
80	11.74
175	25.68

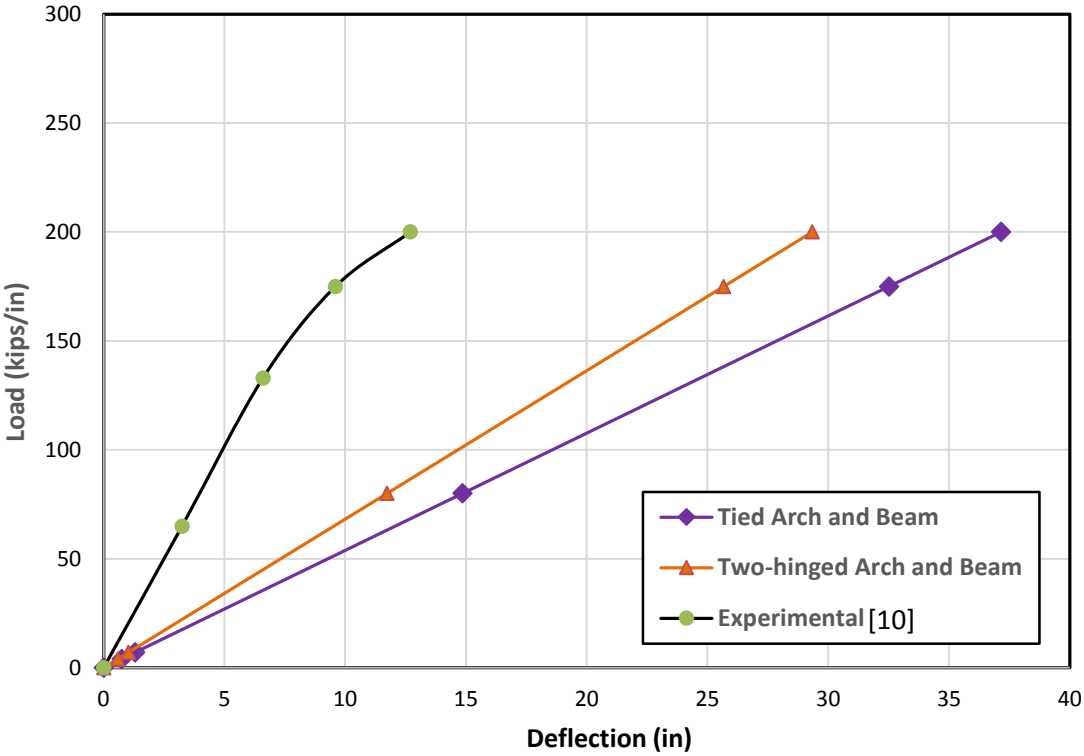

Figure 50. Load vs mid-span deflection relations for Case A

3.6.3.2 Deflection of HCB for case B

The supposed cross section of the box beam for case B is shown in Figure 51 wherein the tension steel is also considered as a part of the box beam. The properties of the beam are as follows:

Moment of inertial about centroidal axis: $I_b = 72697.42$ in^4

Modulus of elasticity: $E_b = 3240$ ksi

The stiffness of the spring representing tied arch come from the complete cross section shown in Figure 51 and is given by:

$$k = \frac{3240(456.2)}{828}$$

$$k = 1785.13\ k/in$$

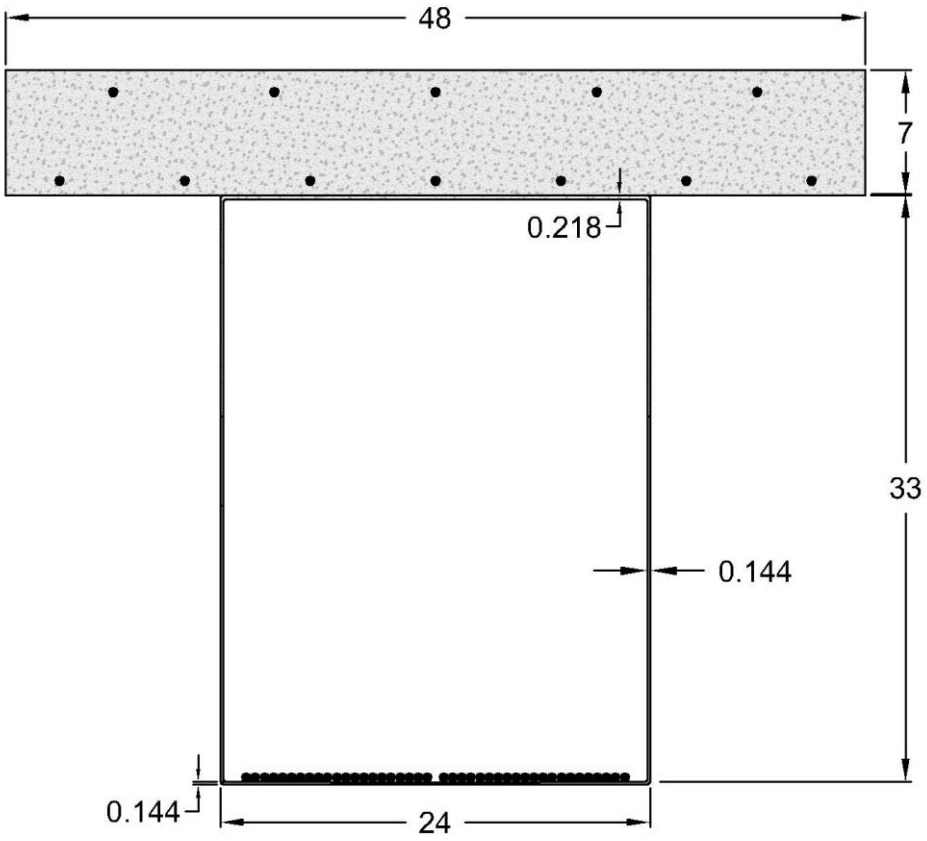

Figure 51. Cross section of box beam for Case A. (Dimensions in inches)

Figure 52 shows load-deflection relations for the model for both cases of arch support. It can be seen from the figure that the deflections given by both models for the supposed beam cross section and stiffness are nearly equal and 20% lesser than those given by the experimental curve.

Table 37: Deflections for tied arch-and-beam model for Case B

Total Load, (Kips)	Deflection (in.)
0	0
4	0.16
7	0.28
80	3.21
175	7.03

Table 38: Deflections for two-hinged arch-and-beam model for Case B

Total Load, (Kips)	Deflection (in.)
0	0
4	0.16
7	0.28
80	3.18
175	6.97

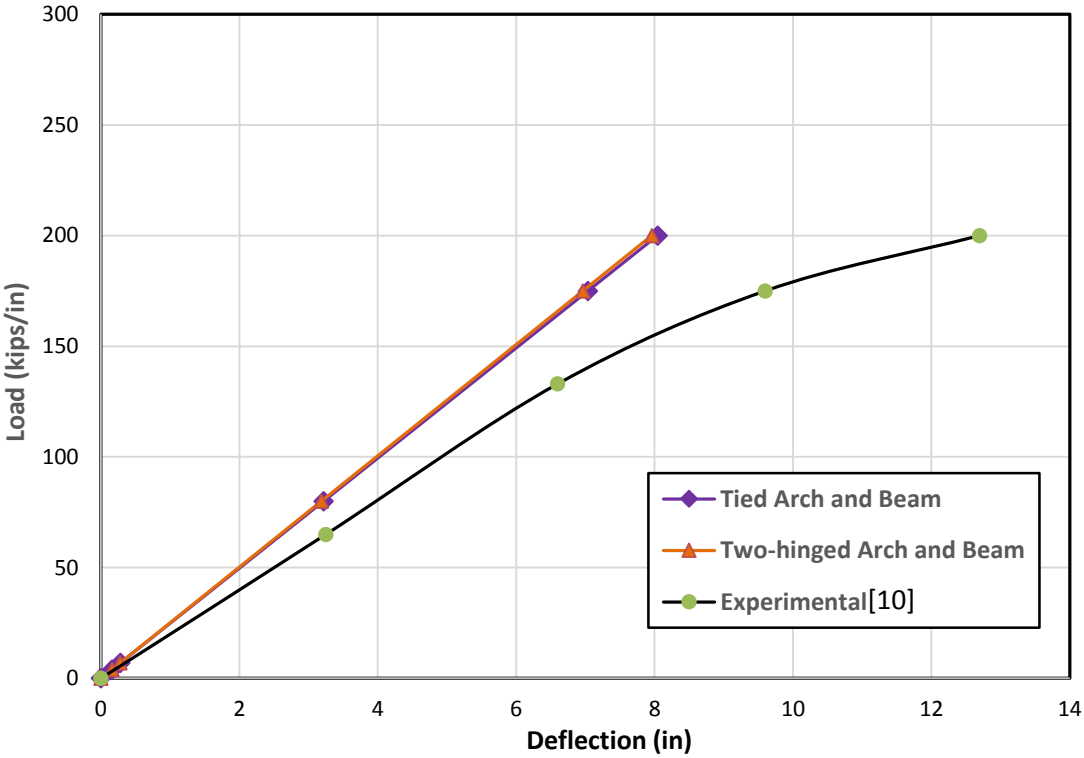

Figure 52. Load vs mid-span deflection relations for Case B

3.6.3.3 Deflection of HCB for case C

The supposed cross section of the box beam for case B is shown in Figure 53. The properties of the beam are as follows:

Moment of inertial about centroidal axis: $I_b = 73091.27\ in^4$

Modulus of elasticity: $E_b = 3240$ ksi

The stiffness of the spring representing tied arch is given by:

$$k = \frac{3240(480.6)}{828}$$

$$k = 1880.60\ k/in$$

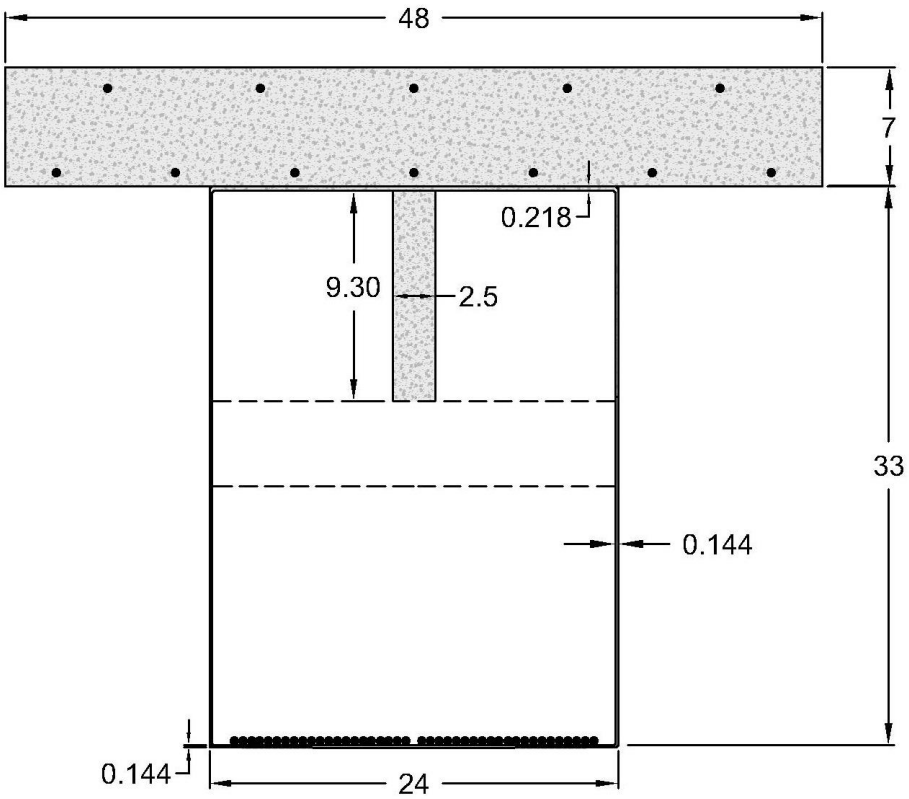

Figure 53. Cross section of box beam for Case C. (Dimensions in inches)

The deflections given by the tied arch and beam and two-hinged arch and beam models for the supposed cross section and stiffness are shown in Figure 54 alongside the experimental curve. The deflection response behavior for both models for Case C is nearly same and resembles the response obtained in the previous case.

Table 39: Deflections for tied arch-and-beam model for Case C

Total Load, (Kips)	Deflection (in.)
0	0
4	0.16
7	0.28
80	3.20
175	7.00

Table 40: Deflections for two-hinged arch-and-beam model for Case C

Total Load, (Kips)	Deflection (in.)
0	0
4	0.16
7	0.28
80	3.17
175	6.93

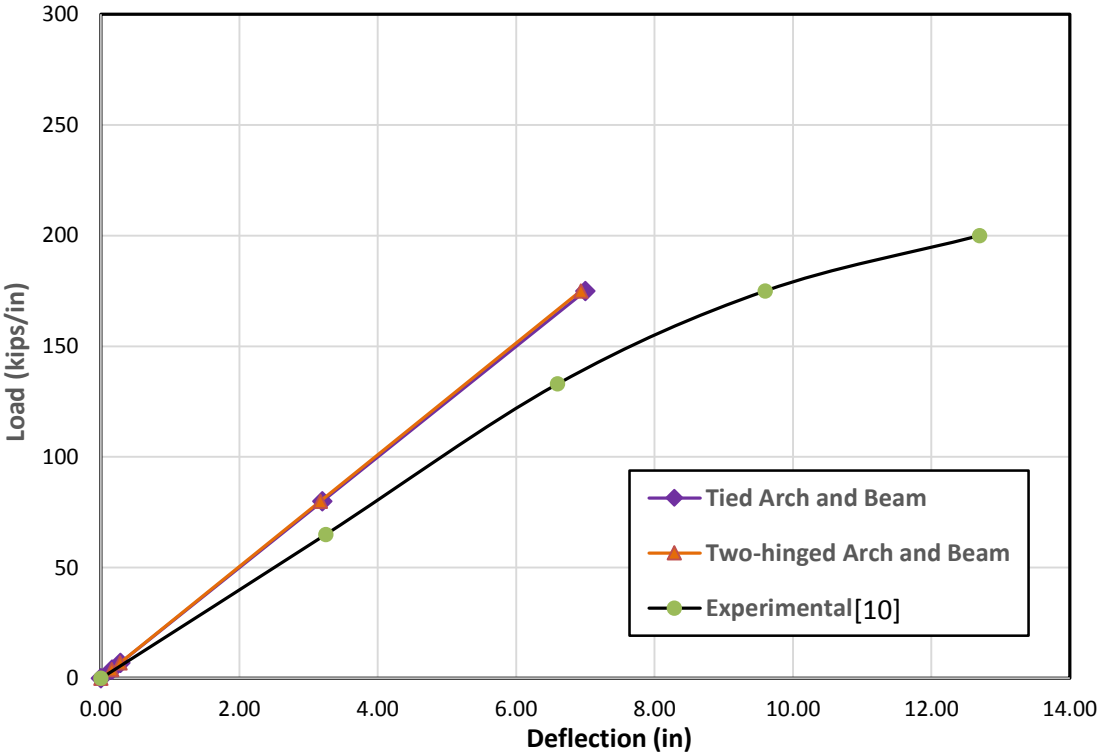

Figure 54. Load vs mid-span deflection relations for Case C

3.7 Discussion on arch and beam model of HCB

The comparison of deflections for HCB without slab given by beam approach are 15% higher than the experimental values[2] which suggest that the beam approach does not give exact values of the deflections. The application of the arch and beam model for various supposed configurations of HCB cross section and spring stiffness values shows that the model that takes average cross section of the HCB for beam and the transformed area of the same cross section for calculating stiffness and using tied arch and box beam approach gives the best results. The application of the model to the externally applied load with slab included in the analysis does not tell anything about the model as the concrete arch fails at very small loads and HCB ceases to act as a combination of arch and beam.

4. LOAD-DEFFECTION BEHAVIOUR OF PRESTRESSED HCB

Since its inception, the HCB has never been practically used as prestressed member in any construction nor is there any published research work available on the behavior of prestressed HCB. This chapter presents the theoretical study of the behavior of prestressed HCB using finite-difference method for analysis up to the collapse load. The behavior of the HCB is investigated for two possible ways of prestressing, namely:

1. Prestressing of HCB without concrete slab
2. Prestressing of HCB with concrete slab included

The first method is easier for the application of prestressing force. The second method, however, allows a large cross-sectional area for prestressing.

4.1 Behavior of prestressed HCB without concrete slab

The cross section of HCB to which prestressing force is applied is shown in Figure 55. The overlaying concrete slab, shown dotted in the figure, is supposed to be constructed later on the top of the already prestressed HCB.

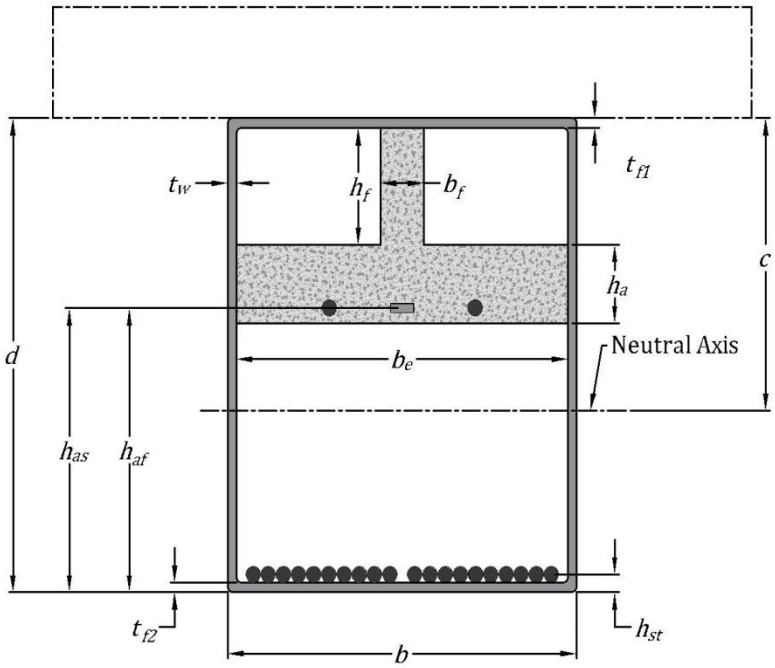

Figure 55. Cross section of prestressed HCB without concrete slab

4.1.1 Maximum prestressing force

The maximum prestressing force applied to the cross section can be limited by the following limit states:

1. Fracture of concrete due to tension at top of concrete fin

$$F \leq \frac{f_r}{\left(\frac{1}{A} + \frac{ec}{I}\right)}$$

where

F = Maximum prestressing force

f_r = Modulus of rupture of concrete = $7.5\sqrt{f_c'}$

E = Eccentricity of the prestressing force

A = Transformed cross-sectional area

I = Moment of inertial of the transformed cross section

2. Failure of FRP top flange in tension

$$F \leq \frac{F_{ft}}{\left(\frac{ec}{I} - \frac{1}{A}\right)}$$

where

F = Maximum prestressing force

F_{ft} = Ultimate tensile strength of flange FRP

e = Eccentricity of the prestressing force

A = Transformed cross-sectional area

I = Moment of inertial of the transformed cross section

3. Failure of FRP web in tension

$$F \leq \frac{F_{wt}}{\left(\frac{e(c - t_{f1)}}{I} - \frac{1}{A}\right)}$$

where

F = Maximum prestressing force

F_{wt} = Ultimate tensile strength of web FRP

4. Failure of FRP web in compression

$$F \leq \frac{F_{wc}}{\left(\frac{e(d - c - t_{f2)}}{I} - \frac{1}{A}\right)}$$

where

F = Maximum prestressing force

F_{wc} = Ultimate compressive strength of web FRP

5. Failure of FRP bottom flange in compression

$$F \leq \frac{F_{fc}}{(\frac{e(d-c)}{I} - \frac{1}{A})}$$

where

F = Maximum prestressing force

F_{fc} =Ultimate compressive strength of flange FRP

The lowest value of the prestressing forces given by the above mentioned limit states for the HCB finite-difference nodal locations is chosen as safe prestressing force. The summary of the prestressing forces for nodes i = 0, 2, 4, … , 10 is shown in Table 41.

Table 41. Summary of prestressing force for applied limit states

Node	Prestressing Force (kips)				
	At Failure (in Compression) of:		At Failure (in Tension) of:		
	Web	Bottom Flange	Web	Top Flange	Concrete
0	10797	11643	25685	27260	215
2	4970	5351	6375	6815	53.76
4	3546	3822	7331	7796	61.5
6	3313	3575	13288	13955	110
8	3286	3548	26455	27083	213.65
10	3285	3547	38340	38382	302.78

The results in the table suggest that safe prestressing force for the beam is 53.76 kips which is given by the tension failure of fin concrete at node 3. Since, tensions cracking at the top of concrete fin does not disturb the structural integrity of HCB during the prestressing process and these cracks are later closed by the dead load of the overlaying concrete. Therefore, the limiting prestressing force of 302.78 kip, given by the tension cracking of concrete arch at the midspan node, is chose as the safe prestressing force.

4.1.2 Moment-curvature relations for prestressed HCB

The moment curvature relations for the prestressed cross sections at the nodes are generated by a computer algorithm written in MATLAB. The script of the program is given in Appendix E whereas the curves generated by the program are shown in Appendix F. The moment-curvature curves at midspan and support cross sections for the prestressed and non-prestressed HCB are also shown in Figure 56 and Figure 57.

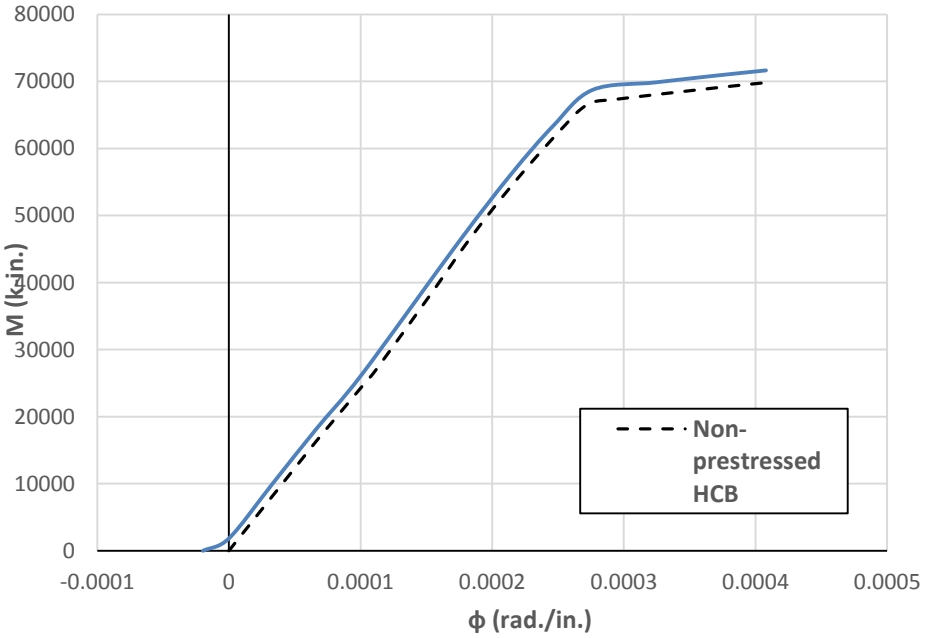

Figure 56. Moment-curvature relation for prestressed and non-prestressed HCB at support

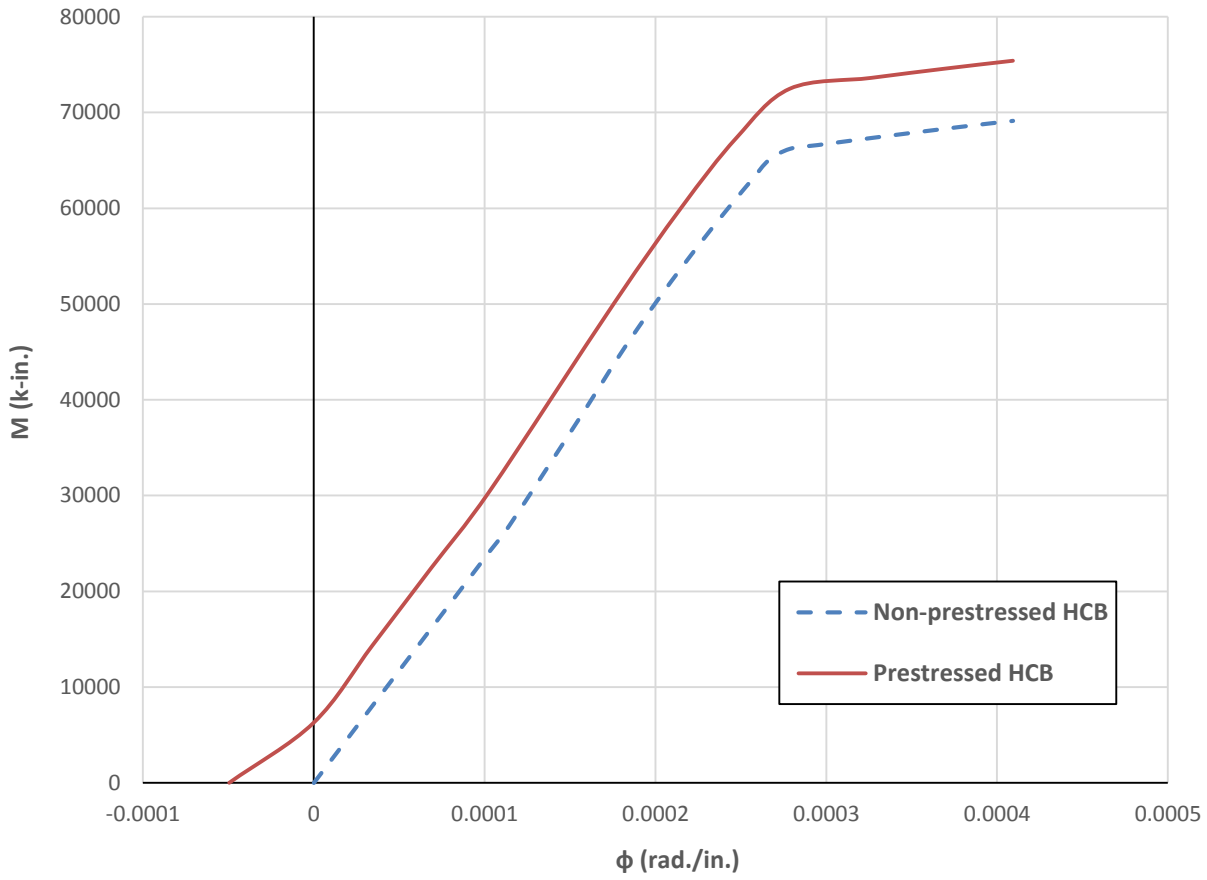

Figure 57. Moment-curvature curves for prestressed and non-prestressed HCB at midspan

4.1.3 Nonlinear finite-difference analysis

The nodal deflection of prestressed HCB are calculated using the finite-difference method and nonlinear moment-curvature analysis as described in Chapter 2. The nodal interval '*h*' is taken as 82 inches. The nodal deflections and corresponding moments and curvature values given by the analysis for different loads are given in Table 42 through 46.

Table 42. Results for prestressed HCB with P = 100 kips.

Node	Moment (K-in.)	ϕ (rad./in.)	Deflection (in.)
0	0	0	0
2	8200.00	0.00001981	1.97
4	16400.00	0.00002473	3.80
6	24600.00	0.00008083	5.46
8	32604.00	0.00011148	6.59
10	32604.00	0.00011092	6.96

Table 43. Results for prestressed HCB with P = 170 kips.

Node	Moment (K-in.)	ϕ (rad./in.)	Deflection (in.)
0	0	0	0
2	13940.00	0.00004372	3.93
4	27880.00	0.00009795	7.57
6	41820.00	0.00014695	10.54
8	55426.80	0.00019746	12.53
10	55426.80	0.00019686	13.20

Table 44. Results for prestressed HCB with P = 212 kips.

Node	Moment (K-in.)	ϕ (rad./in.)	Deflection (in.)
0	0	0	0
2	17384.00	0.00005806	5.08
4	34768.00	0.00012388	9.78
6	52152.00	0.00018625	13.64
8	69120.48	0.00025885	16.25
10	69120.48	0.00025819	17.12

Table 45. Results for prestressed HCB with P = 222 kips.

Node	Moment (K-in.)	ϕ (rad./in.)	Deflection (in.)
0	0	0	0
2	18204.00	0.00006147	5.41
4	36408.00	0.00012994	10.41
6	54612.00	0.00019591	14.53
8	72380.88	0.00028015	17.34
10	72380.88	0.00027431	18.26

Table 46. Results for prestressed HCB with P = 231 kips

Node	Moment (K-in.)	ϕ (rad./in.)	Deflection (in.)
0	0	0	0
2	18942.00	0.00006455	6.84
4	37884.00	0.00013540	13.26
6	56826.00	0.00020460	18.76
8	75315.24	0.00041101	22.88
10	75315.24	0.00040481	24.24

4.1.4 Load-deflections relationship for prestressed HCB

Figure 58 shows load versus midspan deflections relations for the non-prestressed and prestressed HCB (without concrete slab). The prestressed HCB deflections are 10 to 20% less than the corresponding non-prestressed HCB values; the effect of prestressing being more noticeable at the smaller loads. The theoretical ultimate strength of the prestressed HCB for four-point loading is 10 % higher than the non-prestressed HCB.

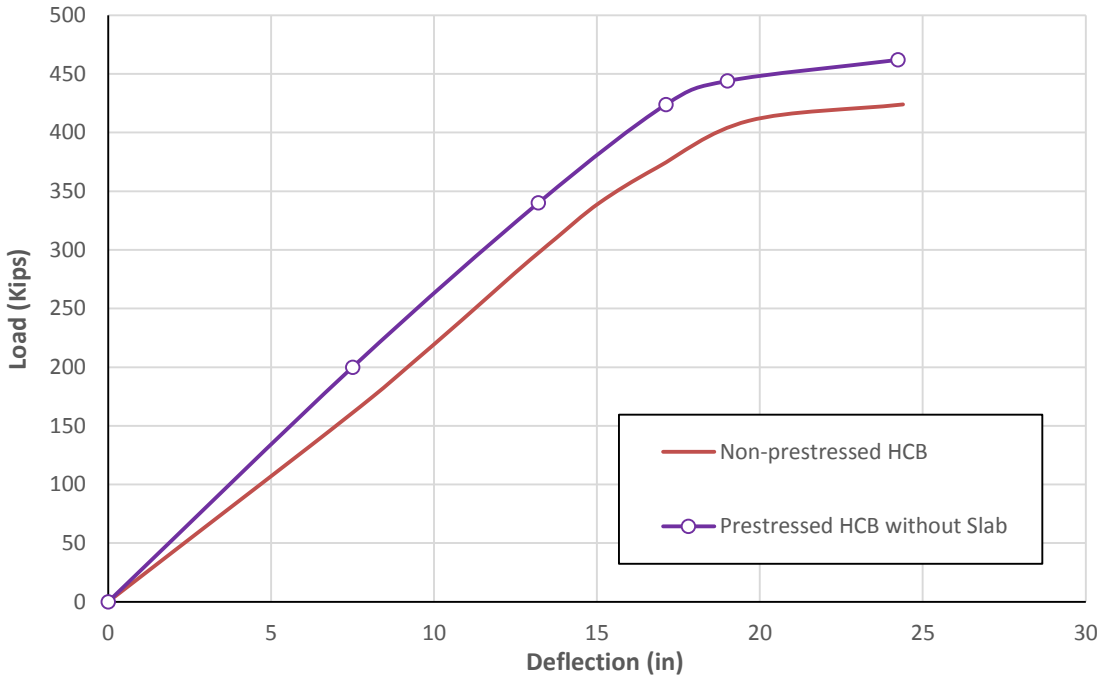

Figure 58. Midspan load-deflection relations for prestressed and non-prestressed HCB

4.2 Behavior of prestressed HCB with concrete slab

The nonlinear analysis procedure for prestressed HCB with concrete slab is same as used for the prestressed HCB without concrete slab except that the entire cross section (including the concrete slab) receives the prestressing force. The cross section used for the analysis is shown in Figure 59.

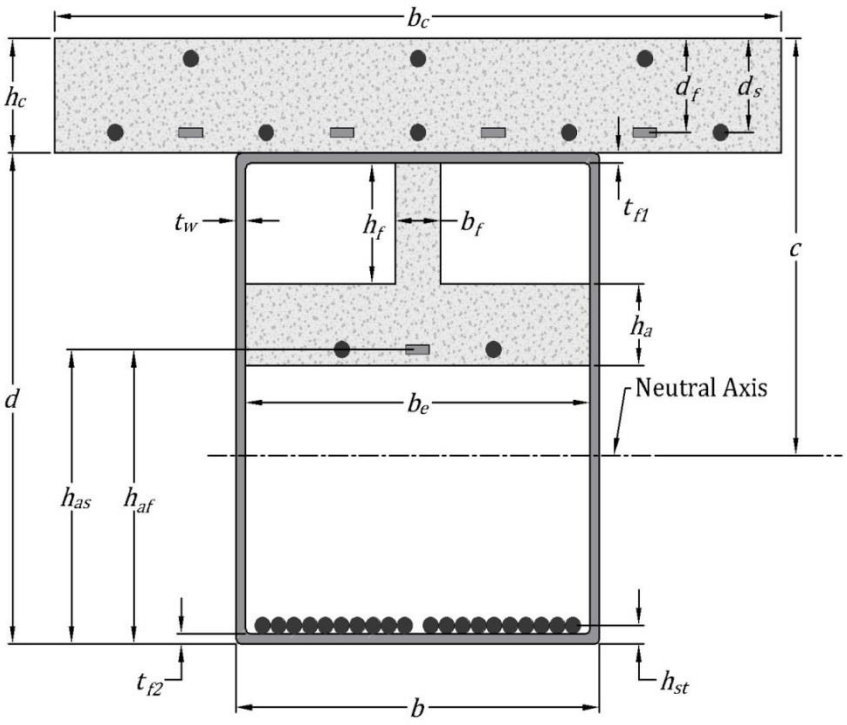

Figure 58. Cross section of the prestressed HCB with concrete slab

4.2.1 Maximum prestressing force

The limit states for the determination of maximum prestressing force for the beam cross section are same as used in the previous case except the values of different variables in the current case are influenced by the presence of the concrete slab. The equations used for determining the limiting values of prestressing force are given below:

1. Fracture of concrete due to tension at top of concrete fin

$$F \leq \frac{f_r}{\left(\frac{1}{A} + \frac{ec}{I}\right)}$$

where

F = Maximum prestressing force

f_r = Modulus of rupture of concrete = $7.5\sqrt{f_c'}$

e = Eccentricity of prestressing force

A = Transformed cross sectional area

I = Moment of inertial of transformed cross section

2. Failure of FRP top flange in tension

$$F \leq \frac{F_{ft}}{\left(\frac{e(c-h_c)}{I} - \frac{1}{A}\right)}$$

where

F = Maximum prestressing force

F_{ft} = Ultimate tensile strength of flange FRP

e = Eccentricity of prestressing force

A = Transformed cross sectional area

I = Moment of inertial of the transformed cross section

3. Failure of FRP web in tension

$$F \leq \frac{F_{wt}}{\left(\frac{e(c-h_c-t_{f1)}}{I} - \frac{1}{A}\right)}$$

where

F = Maximum prestressing force

F_{wt} = Ultimate tensile strength of web FRP

4. Failure of FRP web in compression

$$F \leq \frac{F_{wc}}{\left(\frac{e(d-c-t_{f2)}}{I} - \frac{1}{A}\right)}$$

where

F = Maximum prestressing force

F_{wc} = Ultimate compressive strength of web FRP

5. Failure of FRP flange in compression

$$F \leq \frac{F_{fc}}{(\frac{e(d-c)}{I} - \frac{1}{A})}$$

where

F = Maximum prestressing force

F_{fc} = Ultimate compressive strength of flange FRP

The summary of the prestressing forces given by the above given formulas for the HCB cross sections at nodes is shown in Table 47.

Table 47. Summary of prestressing force given by limiting states

Node	Prestressing Force (kips)				
	At Failure (in Compression) of:		At Failure (in Tension) of:		
	Web	Bottom Flange	Web	Top Flange	Concrete
1	2975	3215	19146	19964	157.5
3	2991	3232	18126	18937	149.39
5	3107	3357	16102	16901	133.33
7	3568	3854	15209	16041	126.55
9	4931	5325	17863	18894	149.05
11	8259	8921	29272	30892	244.5

The prestressing force of 157.5 kips given by the concrete failure in tensions at the midspan is used as the applied prestressing force.

4.2.2 Moment-curvature relations and nodal deflections

The moment-curvature relations for the prestressed HCB with concrete slab included are shown in Appendix G. For comparison purpose, the moment-curvature curves for both cases of prestressed HCB at the midspan and support are shown in Figures 60 and 61. The curvature and nodal deflections for the prestressed HCB with slab included generated by the finite-difference method are given in Tables 48 through 51.

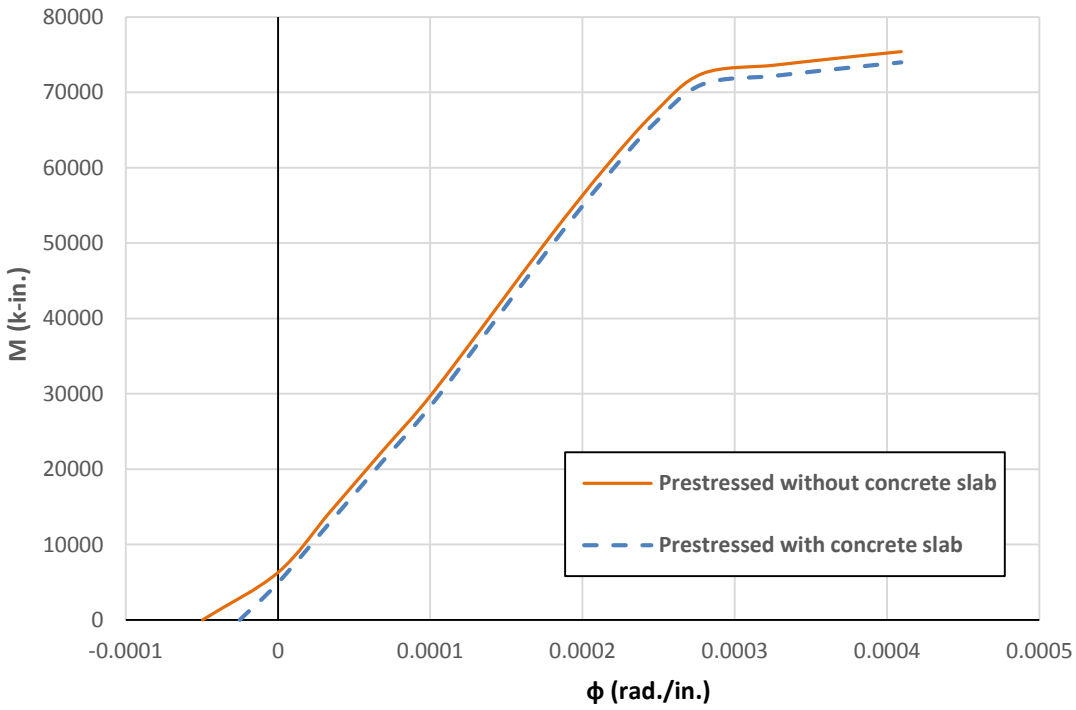

Figure 59. Moment-curvature relations for prestressed HCB with and without concrete slab at midspan

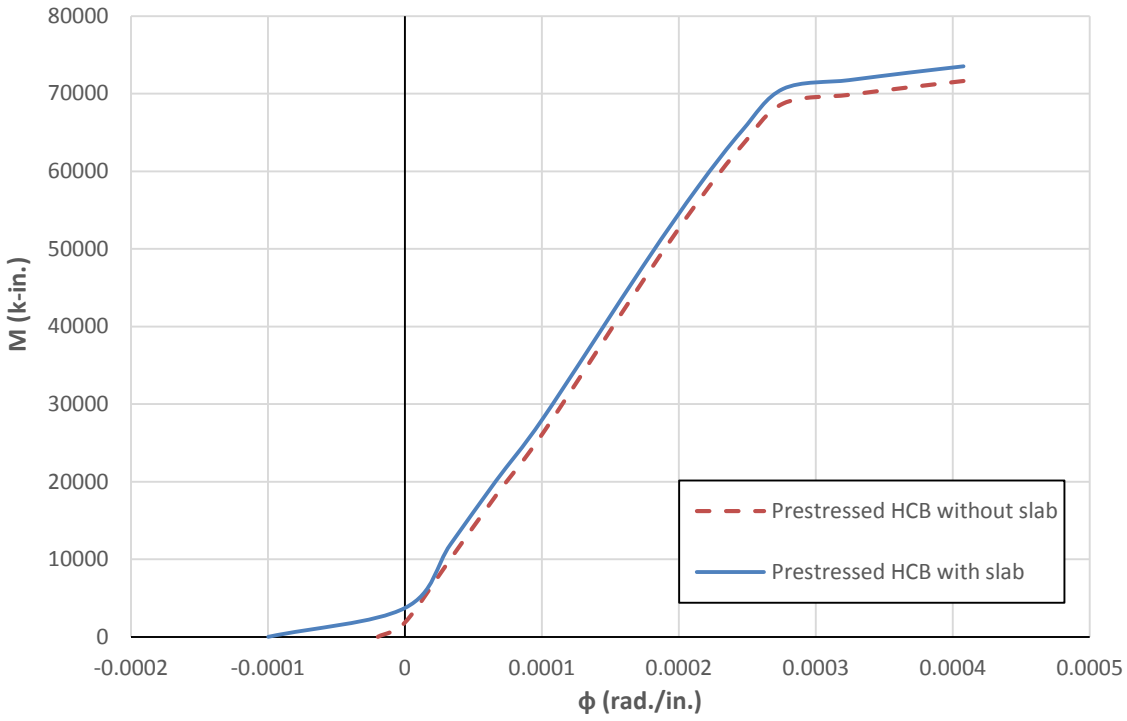

Figure 61. Moment-curvature curves at for prestressed HCB with and without concrete slab at support

Table 48. Results for prestressed HCB with P = 100 kips

Node	Moment (K-in.)	ϕ (rad./in.)	Deflection (in.)
0	0	0	0
2	8200.00	0.00001679	2.19
6	16400.00	0.00005028	4.27
6	24600.00	0.00008449	6.01
8	32604.00	0.00011619	7.18
10	32604.00	0.00011613	7.57

Table 49. Results for prestressed HCB with P = 212 kips

Node	Moment (K-in.)	ϕ (rad./in.)	Deflection (in.)
0	0	0	0
2	17384.00	0.00005504	5.17
6	34768.00	0.00012459	9.97
6	52152.00	0.00018963	13.93
8	69120.48	0.00026632	16.62
10	69120.48	0.00026672	17.52

Table 50. Results for prestressed HCB with P = 222 kips

Node	Moment (K-in.)	ϕ (rad./in.)	Deflection (in.)
0	0	0	0
2	18204.00	0.00005845	5.98
6	36408.00	0.00013066	11.56
6	54612.00	0.00019929	16.27
8	72380.88	0.00033360	19.63
10	72380.88	0.00033370	20.75

Table 51. Results for prestressed HCB with P = 231 kips

Node	Moment (K-in.)	ϕ (rad./in.)	Deflection (in.)
0	0	0	0
2	18942.00	0.00006153	7.49
6	37884.00	0.00013611	14.57
6	56826.00	0.00020798	20.73
8	75315.24	0.00047195	25.49
10	75315.24	0.00047255	27.08

4.3 Comparison of results of prestressed HCB analysis

The load-deflection relations for prestressed HCB without and with concrete slab are shown in Figure 62 along with the experimental curve [10]. It can be seen from the figure that strength and stiffness of the prestressed HCB without slab for a prestressing force of 302.78 kips is comparable with the strength and stiffness of the prestressed HCB with slab for a prestressing force of 157.5 kips. It can be concluded form the results that the prestressing of HCB with slab included though less preferable practically gives same performance for half the prestressing force used when slab not prestressed.

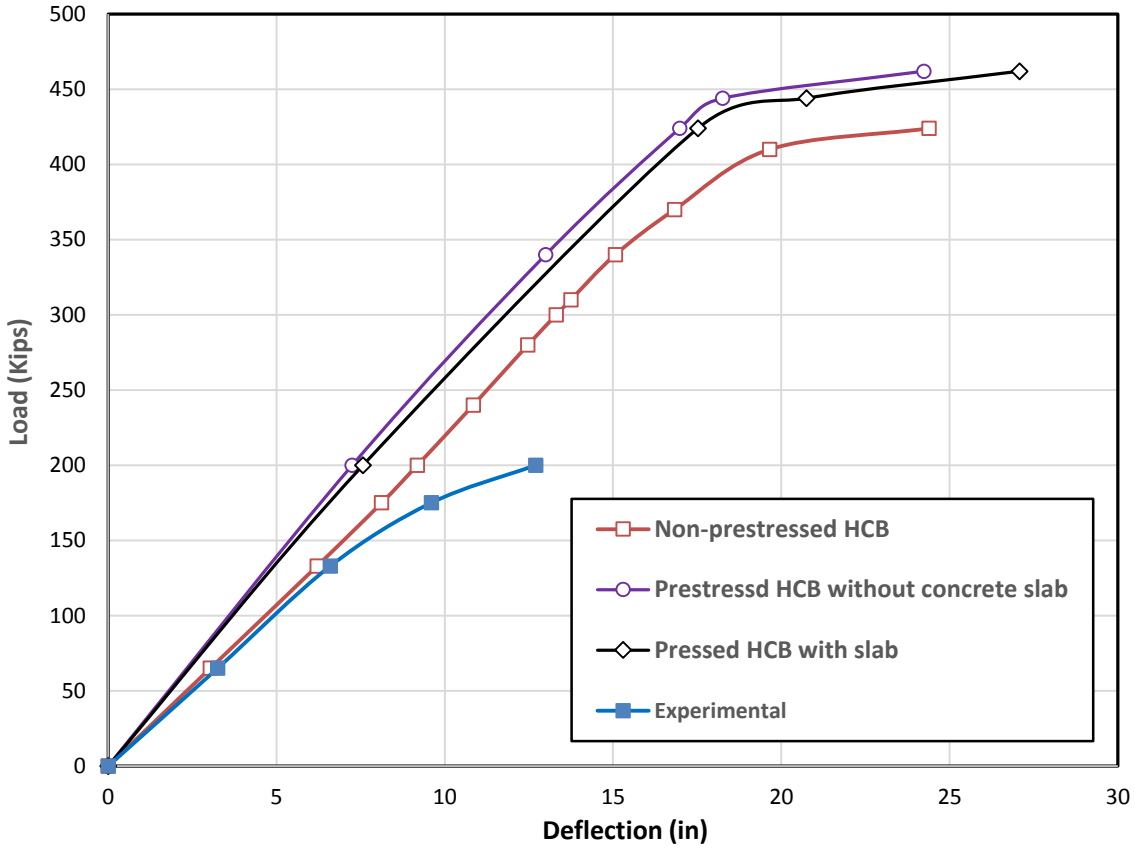

Figure 62: Theoretical load-midspan deflection relations for prestressed, non-prestressed HCB and experimental curve [1]

5. FLEXURAL BEHAVIOR OF CFRP-RETROFITTED HCB

The theoretical study of the behavior of HCB retrofitted with CFRP at different positions across the cross section is presented herein. The retrofitting scheme which shows best results is then studied for the prestressed behavior of HCB. The physical properties of the commonly available CFRP are used in the analysis. Three settings of CFRP retrofitting of HCB without prestressing are studied, namely:

1. Retrofitting at bottom of flange
2. Retrofitting at the top of concrete slab
3. Retrofitting at both top and bottom

The analysis of the nonlinear load-deflection behavior of HCB under bending loading for the above mentioned CFRP use for retrofitting is presented as herein.

5.1 CFRP retrofitting at bottom of HCB

The setting for CFRP sheets is shown in Figure 63. The strength and modulus of elasticity of CFRP used in the analysis are 250 ksi and 20,000 ksi, respectively. The total area of CFRP used is 3.46 in^2.

The finite-difference scheme used for the analysis of non-retrofitted HCB is used here as well. The theoretical moment-curvature curve for the midspan cross section for the retrofitted HCB is shown in Figure 64. The load-deflection relations for the retrofitted and non-retrofitted HCB are shown is Figure 65. It can be seen from the figure that the strength of retrofitted HCB is 19.34 % higher than the non-retrofitted HCB whereas the deflections for the retrofitted HCB in linear range are 18 % less than the corresponding values for non-retrofitted HCB.

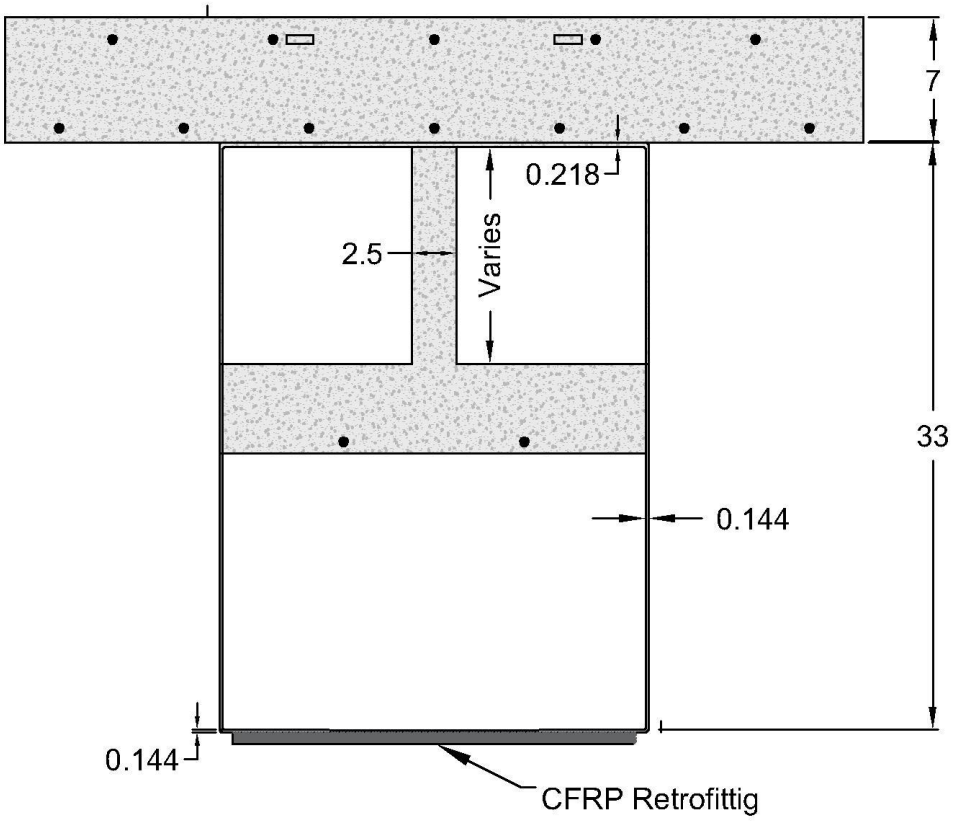

Figure 60. CFRP retrofitting at the bottom of HCB

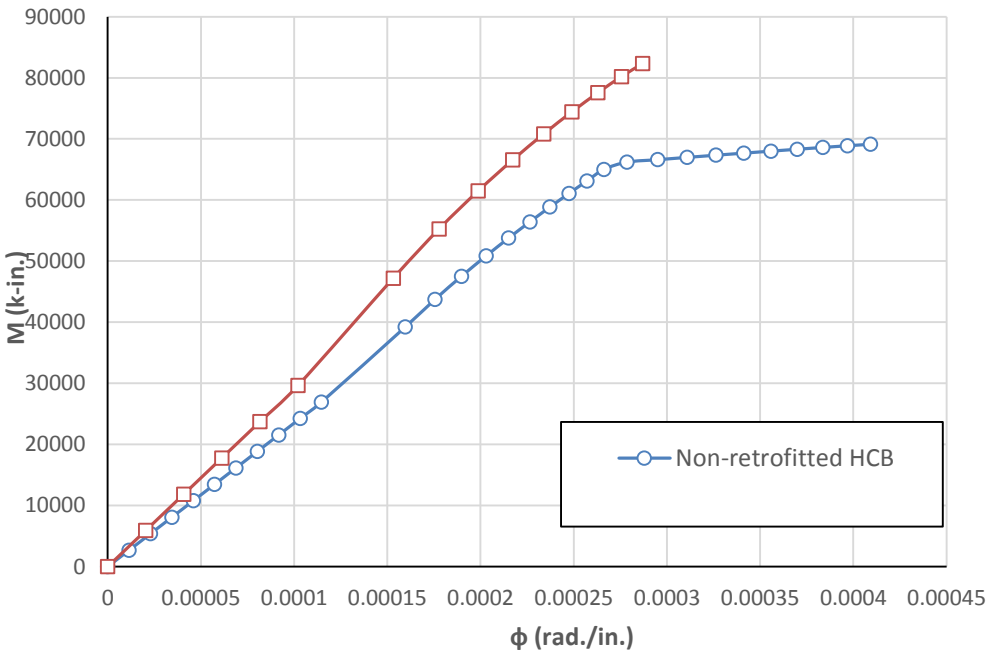

Figure 61. Moment-curvature curve at midspan for CFRP retrofitted HCB at bottom of flange

Table 52. Load versus midspan deflections for HCB with CFRP retrofitting done at bottom flange

Total Load, 2P (Kips)	Deflection (in.)
0	0
200	7.14
472.5	17.45
476	17.58
506	19.04

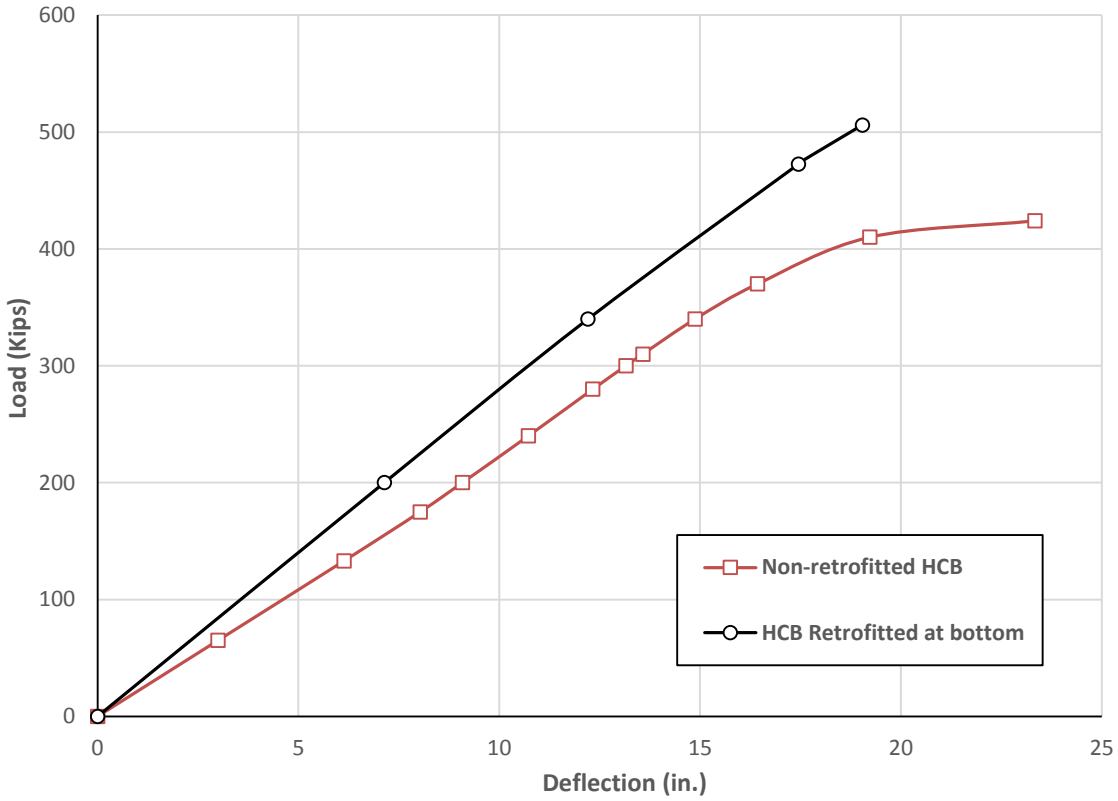

Figure 62. Load-deflection relation for CFRP retrofitted HCB at bottom and non-retrofitted HCB

5.2 CFRP retrofitting at top of concrete slab

In this case the flexural behavior of HCB up to the collapse is analyzed for CFRP plates embedded in the concrete slab as shown in Figure 66. The magnitude of CFRP sued for the previous case i.e., 3.46 in^2 is used here as well. The moment-curvature relation for the midspan cross section for the under discussion HCB retrofitting case is shown in Figure 67 whereas the midspan load-deflection relation is shown in Figures 68. The figure shows that the strength gain for retrofitting at the top of concrete slab is only 3.77% when compared with the non-retrofitted HCB whereas the stiffness remains the same as non-retrofitted HCB.

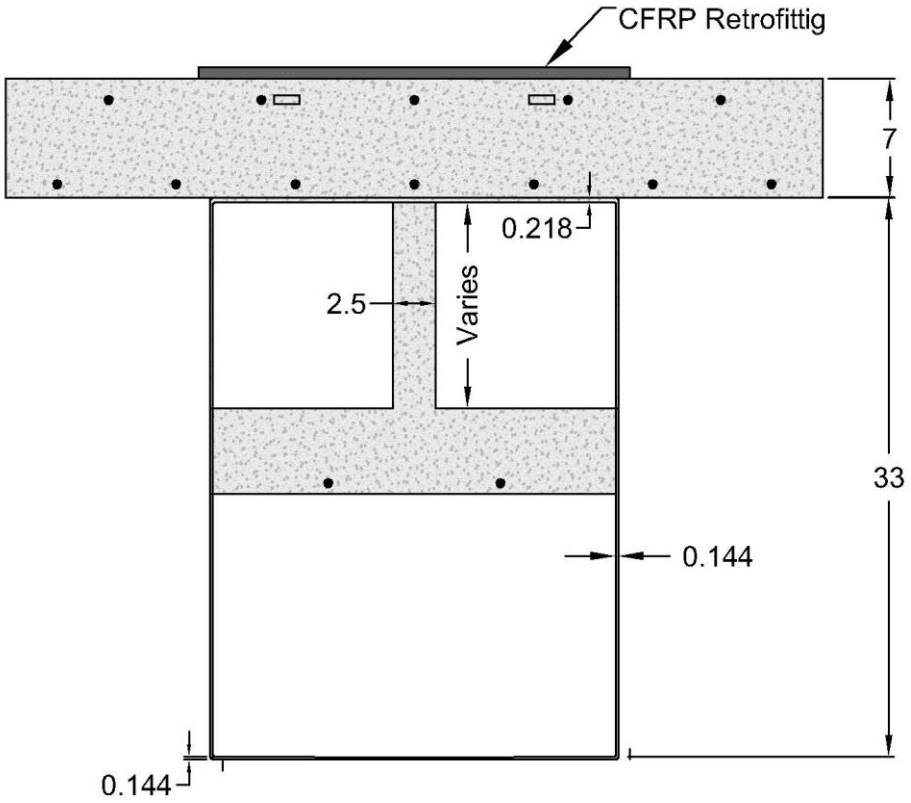

Figure66. CFRP retrofitting at top of concrete slab

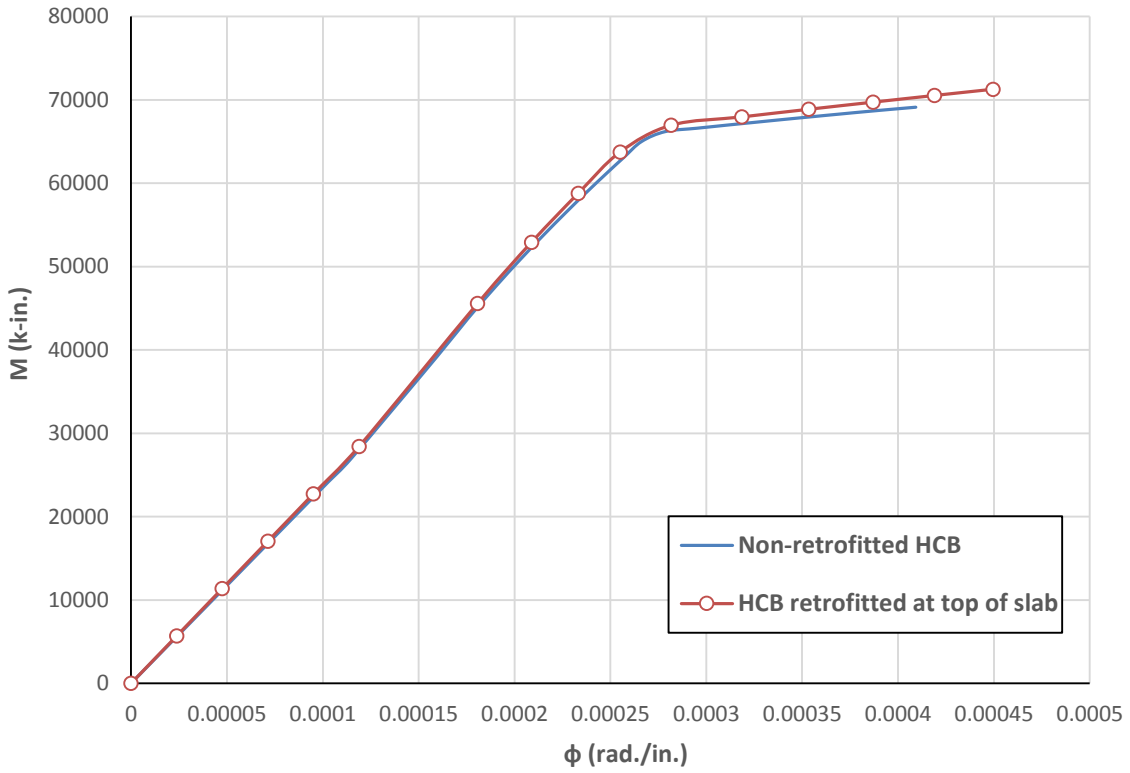

Figure 67. Moment-curvature curve at midspan for CFRP retrofitted HCB at top of concrete slab

Table 53. Load versus midspan deflections of HCB retrofitted at top of slab

Total Load, 2P (Kips)	Deflection (in.)
0	0
65	3.03
200	9.19
370	16.50
440	27.32

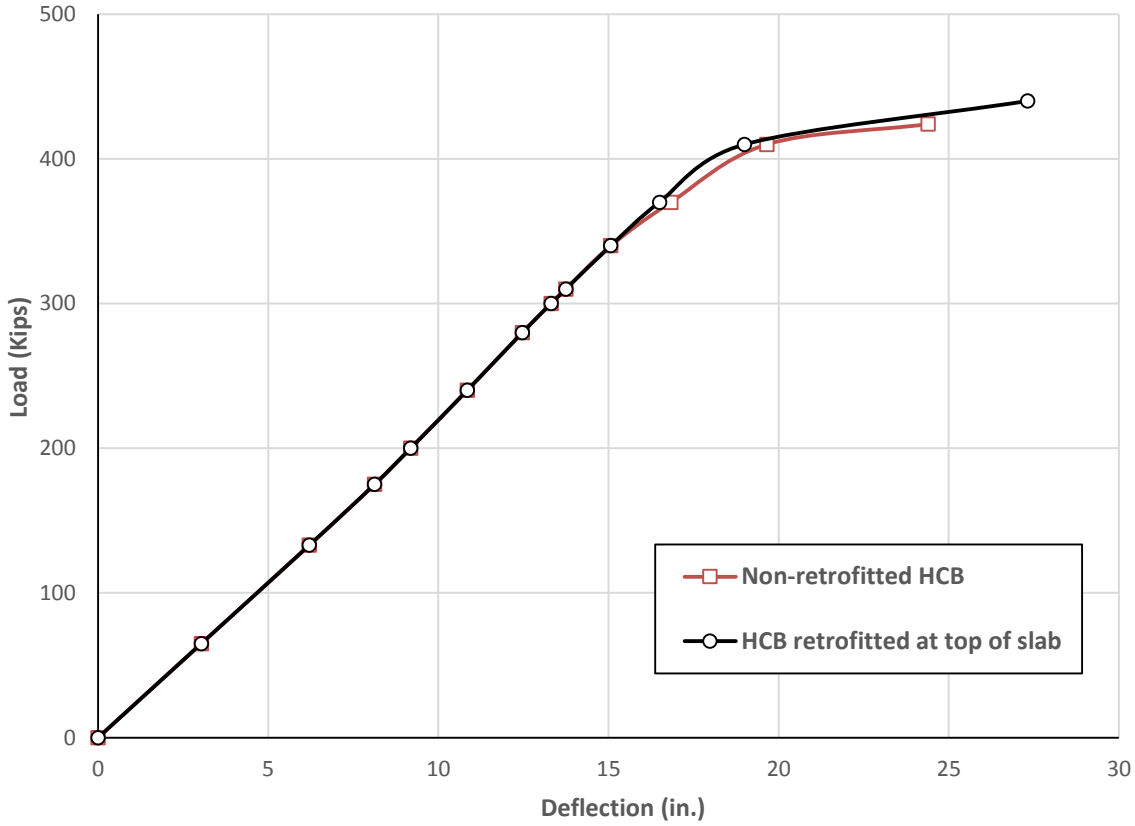

Figure 68. Load-deflection relation for HCB retrofitted at top of slab and non-retrofitted HCB

5.3 CFRP retrofitting at top and bottom of HCB

The CFRP strips setting for this case of HCB retrofitting is shown in Figure 69. The area of CFRP used at the top and bottom is 3.46 in^2. The moment-curvature relation for midspan cross section is shown in Figure 70 whereas the midspan load-deflection relation for the HCB is shown in Figure 71. The comparison of the load-deflection relations with the non-retrofitted HCB shows that strength of the HCB retrofitted at the top and bottom with CFRP is 26% higher than the non-retrofitted HCB whereas deflections for the retrofitted HCB are 21% less as compared with the corresponding values for non-retrofitted HCB.

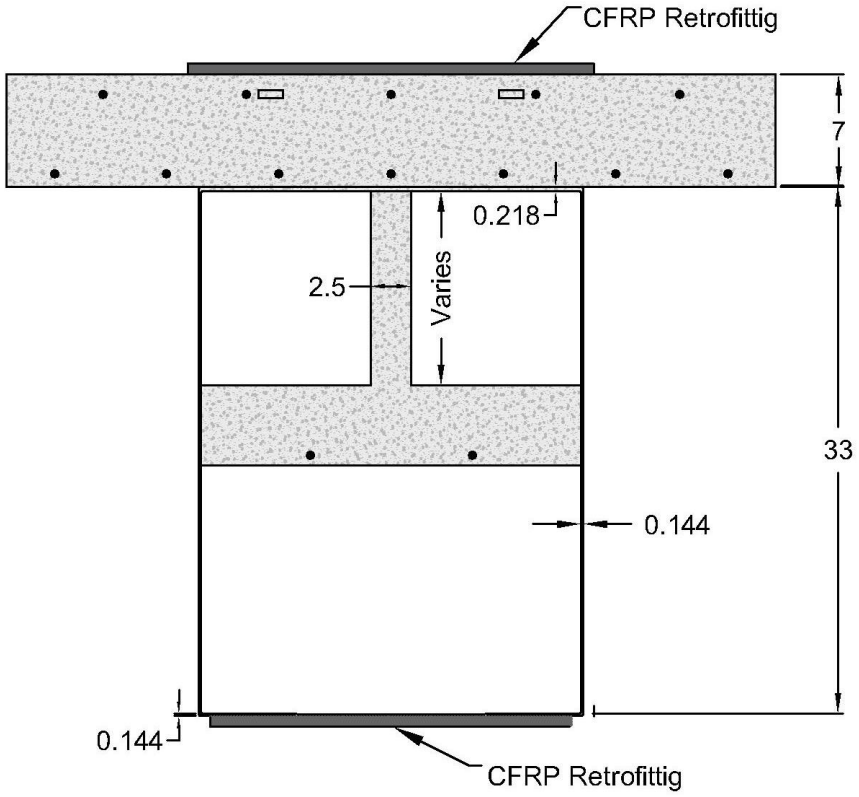

Figure 69. CFRP retrofitting at top and bottom for HCB

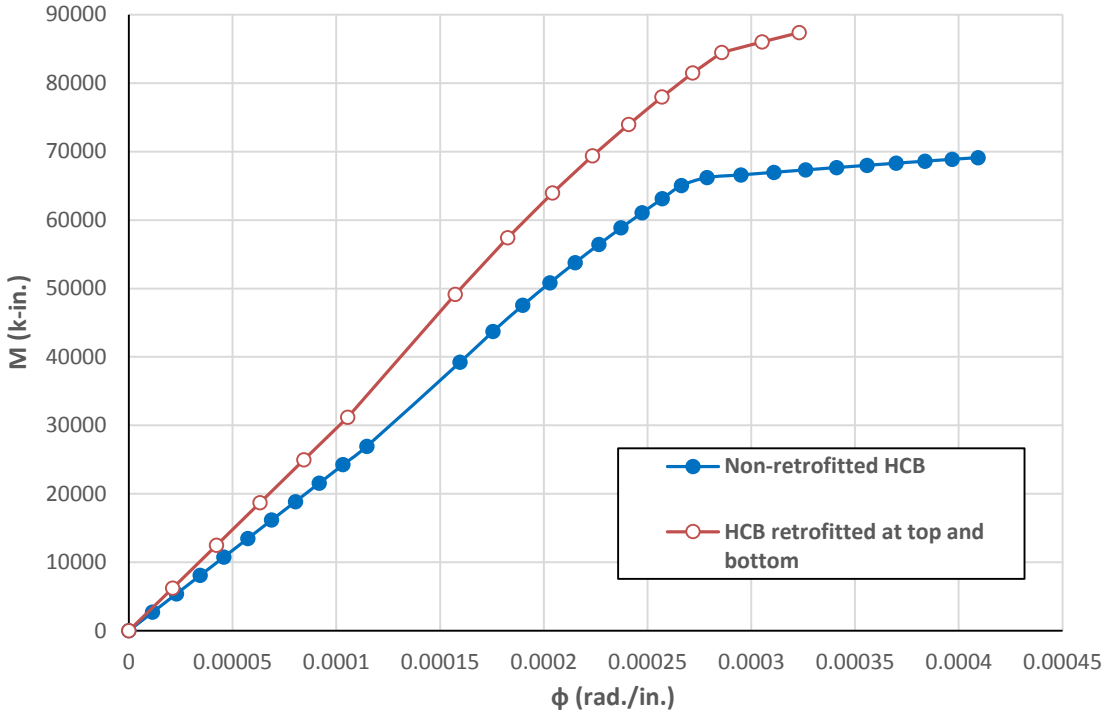

Figure 70. Moment-curvature curve at midspan for CFRP retrofitted HCB at top of concrete slab and bottom of flange

Table 53. Load versus midspan deflections of HCB retrofitted at top of slab and bottom of flange

Total Load, 2P (Kips)	Deflection (in.)
0	0
200	7.14
340	12.21
476	17.38
520	19.04

535	20.76

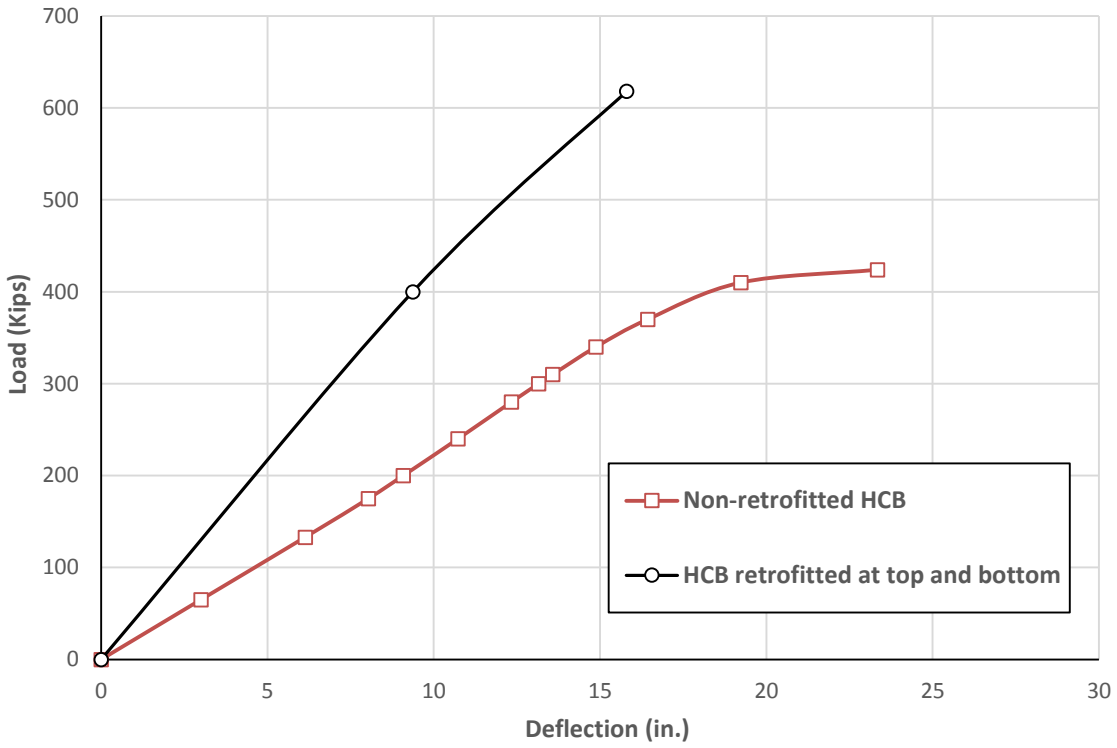

Figure 71. Load-deflection relation for HCB retrofitted at top and bottom and non-retrofitted HCB

5.4 Comparison of load-deflection behavior of CFRP retrofitted HCB cases

The load-deflection relations for the CFRP retrofitted HCB for the three settings of CFRP are shown in Figure 72. It can be seen from the figure that the strength of HCB for CFRP used at the bottom is 15% higher than for the same area of CFRP used at the top. Likewise, the HCB retrofitted at bottom shows 2.23% more stiffness than the same area of CFRP used at the bottom. The comparison of the relation for CFRP at the bottom only with the relation for CFRP at both top and bottom shows that the later offers only 5.7% increase in strength than the former for twice the area of CFRP and no increase in the stiffness at all.

The comparison of the relations for retrofitted HCB cases with the non-retrofitted show that the use of CFRP at the top of slab shows no improvement of HCB at all. The maximum performance of HCB can be achieved by applying retrofitting both at the top and bottom.

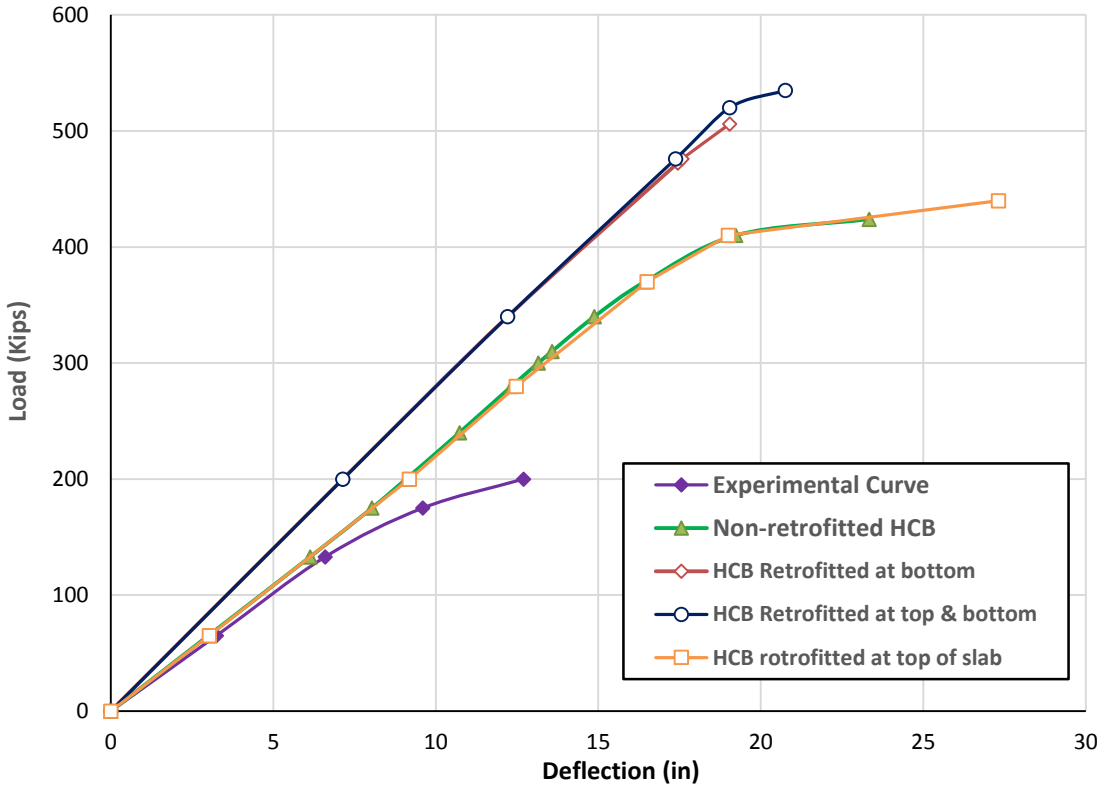

Figure 72. Load-deflection curves for CFRP retrofitted HCBs and non-retrofitted HCB

5.5 HCB retrofitting at top and bottom for greater performance

The behavior of HCB retrofitted with larger area of CFRP and having higher modulus of elasticity used at the top and bottom of HCB is studied in herein. The area of CFRP used is 18 in^2 for top and bottom position each whereas the modulus of elasticity used for analysis is 29,000 ksi. The moment-curvature relation at midspan for such retrofitting of HCB is shown in Figure 73 whereas Figure 74 shows midspan load-deflection relation for the HCB. The figure shows that the strength of the retrofitted HCB is 123% more than the strength of the corresponding non-retrofitted HCB whereas the deflections of the retrofitted HCB in the linear range are 66% lesser than the corresponding deflections of non-retrofitted HCB.

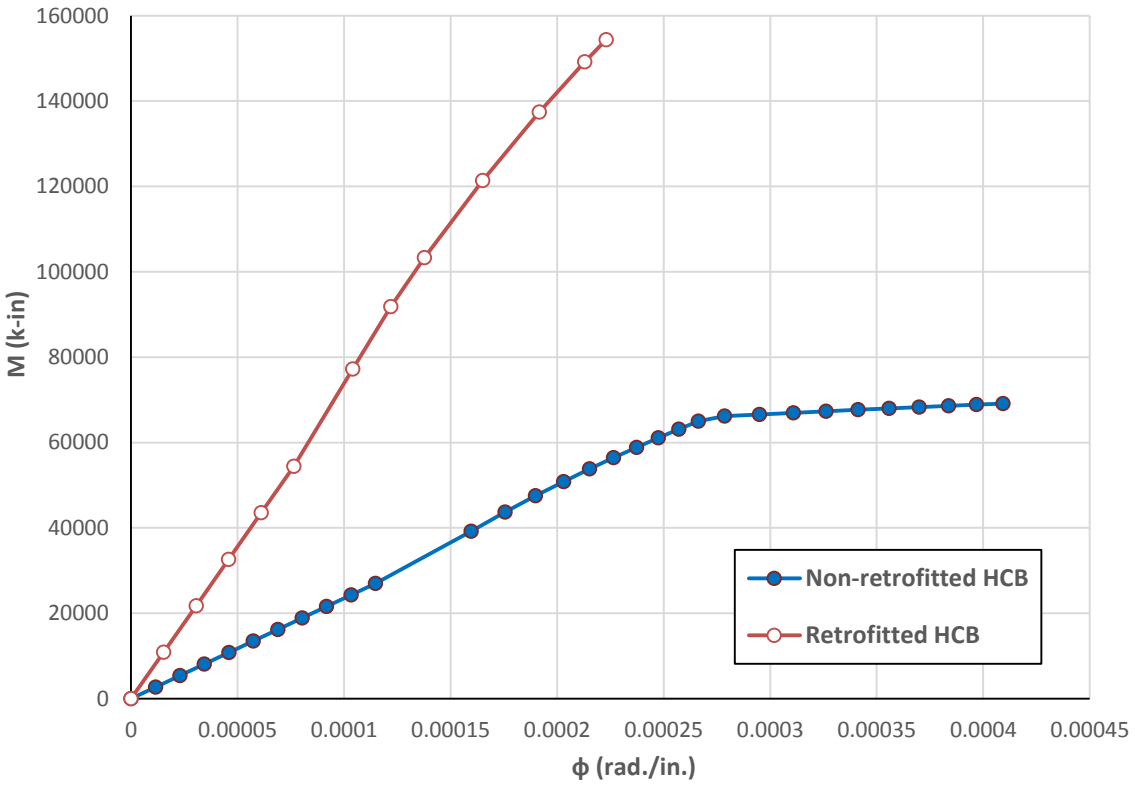

Figure 73. Moment-curvature relation at midspan for HCB retrofitted with CFRP at top and bottom

Table 55. Load versus midspan deflections for high performance CFRP retrofitted HCB at top and bottom

Total Load, 2P (Kips)	Deflection (in.)
0	0
440	6.79
947	14.76

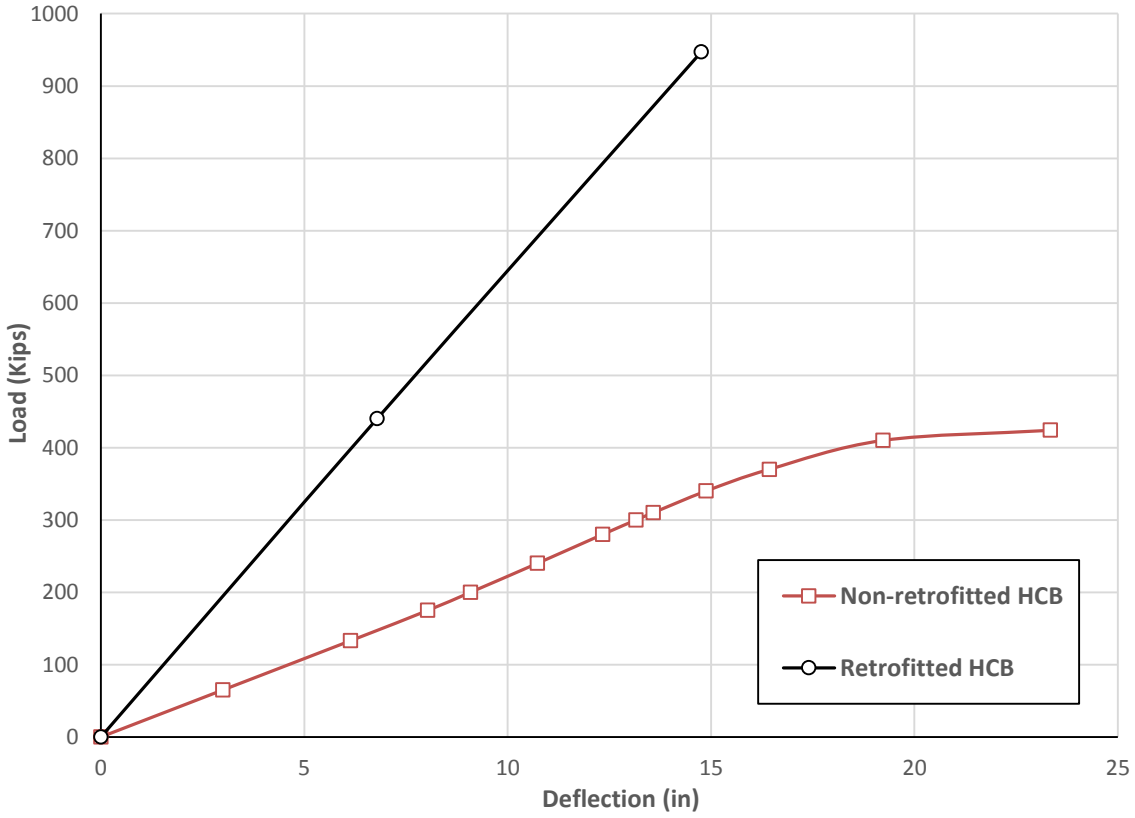

Figure 74. Load-deflection relation for high performance CFRP retrofitted HCB

5.6 HCB retrofitting at top and bottom used with CFRP shell

The behavior of HCB retrofitted at top and bottom with CFRP and FRP box replace with CFRP is presented here. The properties and locations of CFRP used for retrofitting is same as used in the previous section but here the properties of the HCB shell are replaced with the properties of CFRP to investigate its influence on behavior of HCB. The moment-curvature relations for the HCB with above mentioned properties and midspan load-deflection relation generated by the finite-difference analysis are given in Figures 75 and 76, respectively. Figure 76 shows that the strength of HCB retrofitted at top and bottom with CFRP and using CFRP shell is 129 % higher than that of the HCB with no CFRP used at all. Similarly, the deflections of such HCB are 68% less than those of the non-retrofitted HCB in the linear range of loading.

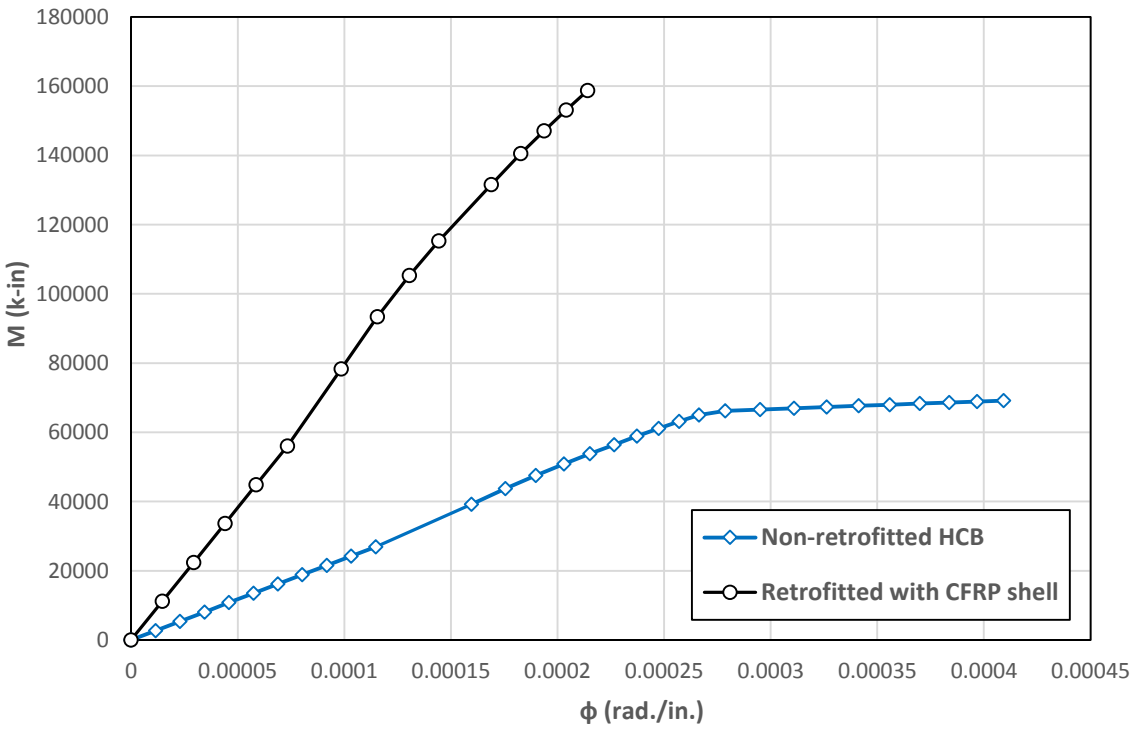

Figure 75. Moment-curvature curve at midspan for HCB having CFRP shell and retrofitted at top and Bottom with CFRP

Table 56. Load versus midspan deflections for high performance CFRP retrofitted HCB with CFRP shell

Total Load, 2P (Kips)	Deflection (in.)
0	0
700	10.07
973.5	13.98

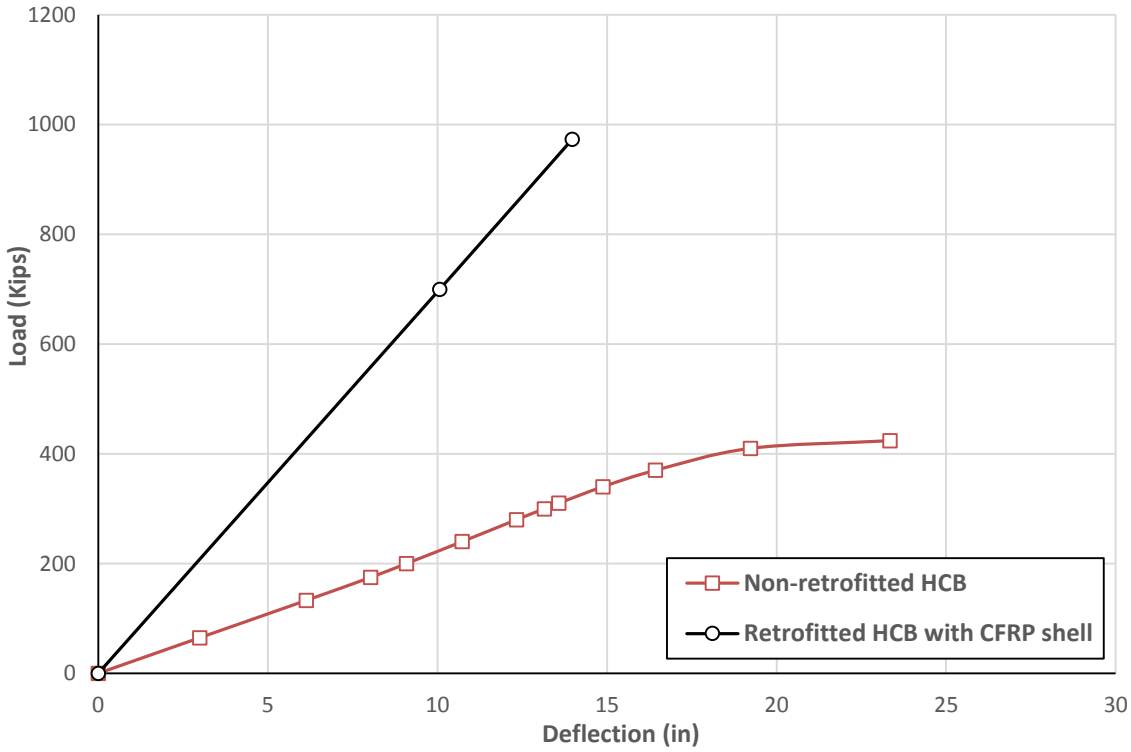

Figure 76. Load-deflection relation for high performance CFRP retrofitted HCB with CFRP shell

5.7 HCB behavior for CFRP shell

The load-deflection behavior of HCB having CFRP under bending load is presented here. The dimensions of the box remain the same as been used throughout the analysis. The moment-curvature relationship for such HCB at midspan cross section is shown in Figure 77 along with the relation for HCB with FRP shell. The load-deflection relationship for the HCB with CFRP shell yielded by the nonlinear finite-difference analysis is shown in Figure 78. The figure shows that the replacement of FRP shell with CFRP one increases the strength of HCB by 45.7% and deflections in the linear range by 48.4%.

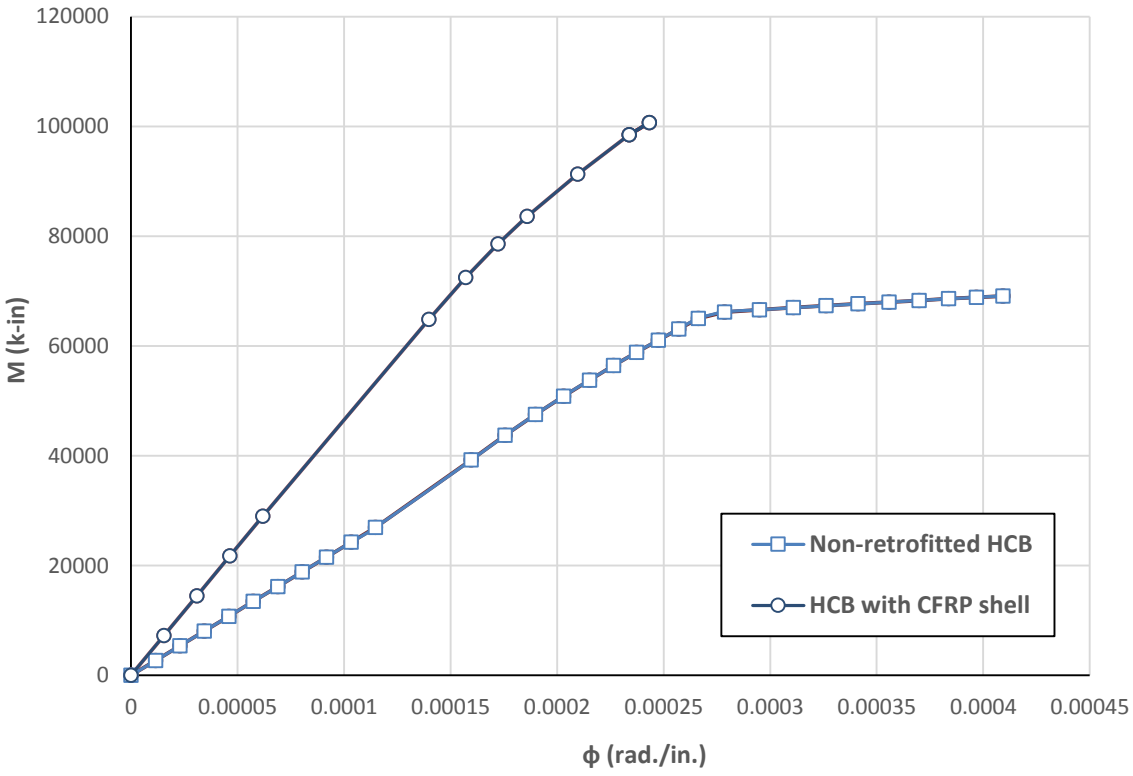

Figure 77. Moment-curvature curve for HCB with CFRP shell

Table 57. Load versus midspan deflections of HCB with CFRP shell

Total Load, 2P (Kips)	Deflection (in.)
0	0
400	9.37
618	15.8

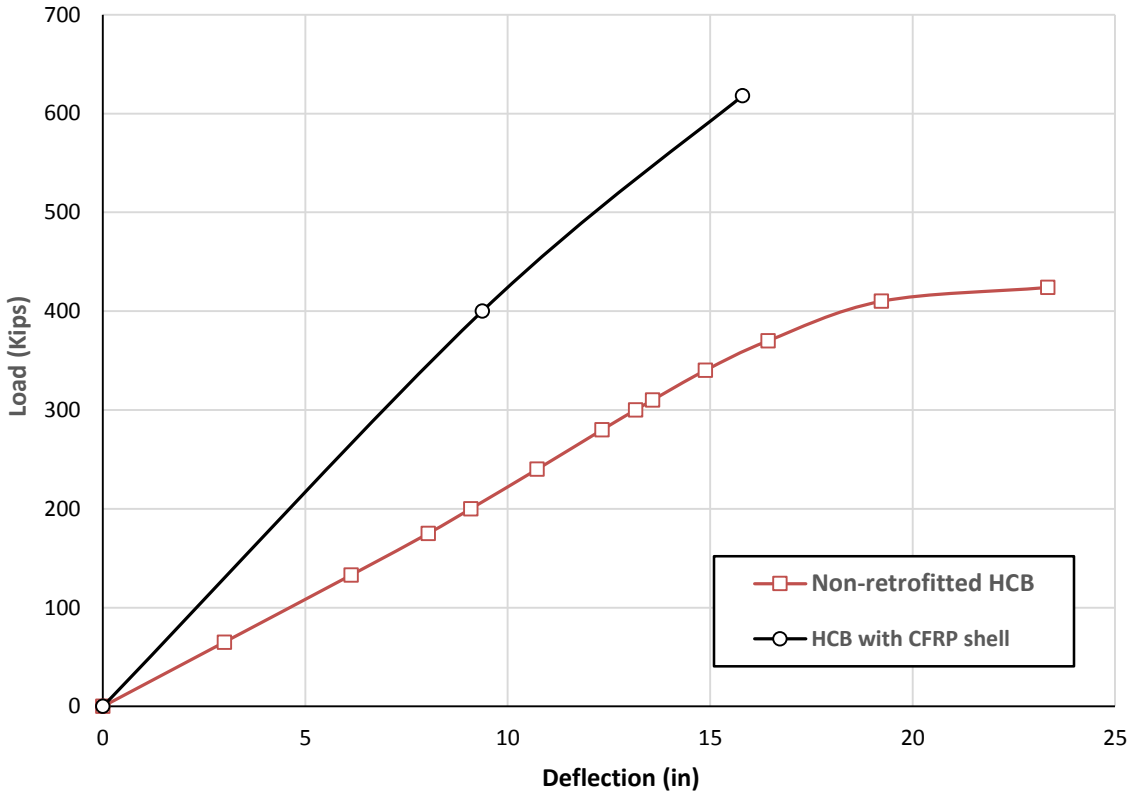

Figure 78. Load-deflection curve for HCB with CFRP shell

5.8 Behavior of prestressed HCB retrofitted at top and bottom and having CFRP shell

The load-deflection behavior of prestressed HCB having CFRP shell and retrofitted at top and bottom with CFRP strips is persistent herein. The beam with CFRP shell and retrofitting at the top and bottom gives best performance without prestressing. This section investigates the performance of the HCB with best retrofitting setting under prestressed conditions. The first step is the determination of the safe prestressing force. The same formulas applied to the non-retrofitted prestressed HCB in chapter 4 are used here. The summary of the prestressing force given by the applied limiting states is given in Table 58.

Table 58. Summary of prestressing force for applied limit states

Node	Prestressing Force (kips)				
	At Failure (in Compression) of:		At Failure (in Tension) of:		
	Web	Bottom Flange	Web	Top Flange	Concrete
0	18777	18526	61695	62487	1011.2
2	15745	15512	74012	75563	12232
4	13831	12789	82610	82546	14256
6	12631	12462	92889	96278	15581
8	12059	12862	95776	99607	16120
10	11889	11693	96376	10033	16236

It can be seen that the prestressing of 1011.2 kips given by the tension failure of concrete at the support is the minimum and same. Therefore, this is used as the safe prestressing force for analysis.

The moment-curvature curve for the prestressed HCB made of CFRP shell and retrofitted with CFRP at top and bottom is shown in Figure 79. The moment-curvature relations for the

non-prestressed HCB with the same shell properties and retrofitting and non-prestressed HCB with GFRP shell and not retrofitted are also shown for comparison.

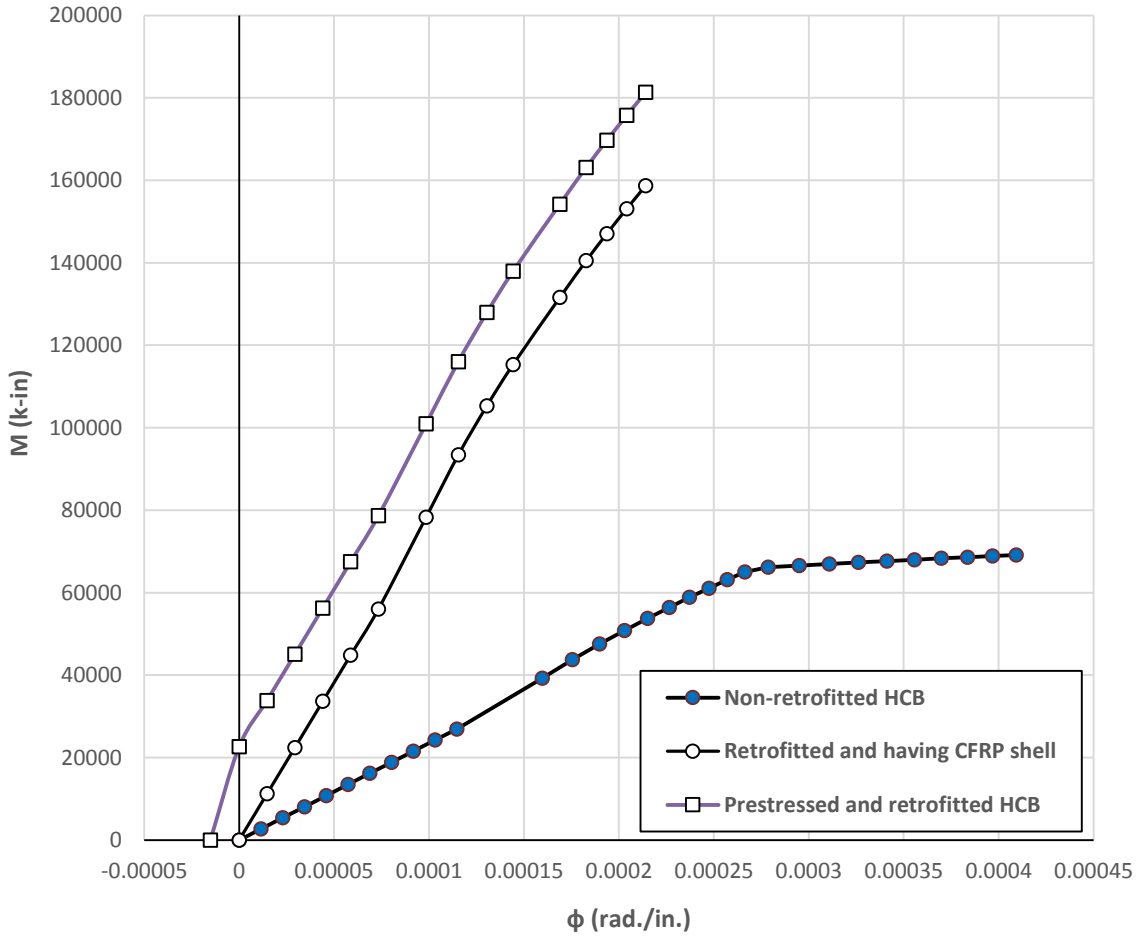

Figure 63. Moment-curvature relations for prestressed and retrofitted, retrofitted only and non-prestressed/non-retrofitted HCB

The midspan deflection for the prestressed HCB having CFRP shell and retrofitted at top and bottom are given in Table 59. The Figure 80 shows load-deflection relation at the midspan for

the same HCB. The curve for non-retrofitted, non-prestressed HCB is also shown for comparison. It can be seen from the figure that ultimate strength for the prestressed HCB made of CFRP shell and retrofitted with 18 in^2 of CFRP retrofitting done at the top and bottom each, is 163% higher that of that of the HCB used by HC Bridge Company in Knickerbocker Bridge [10]. Likewise, the deflection for the HCB are on average 77% less than the HCB used in the Knickerbocker Bridge [10].

Table 59. Load versus midspan deflections of prestressed and retrofitted HCB made of CFRP shell

Total Load, 2P (Kips)	Deflection (in.)
0	-1.27
139	-0.25
650	6.86
1115	13.83

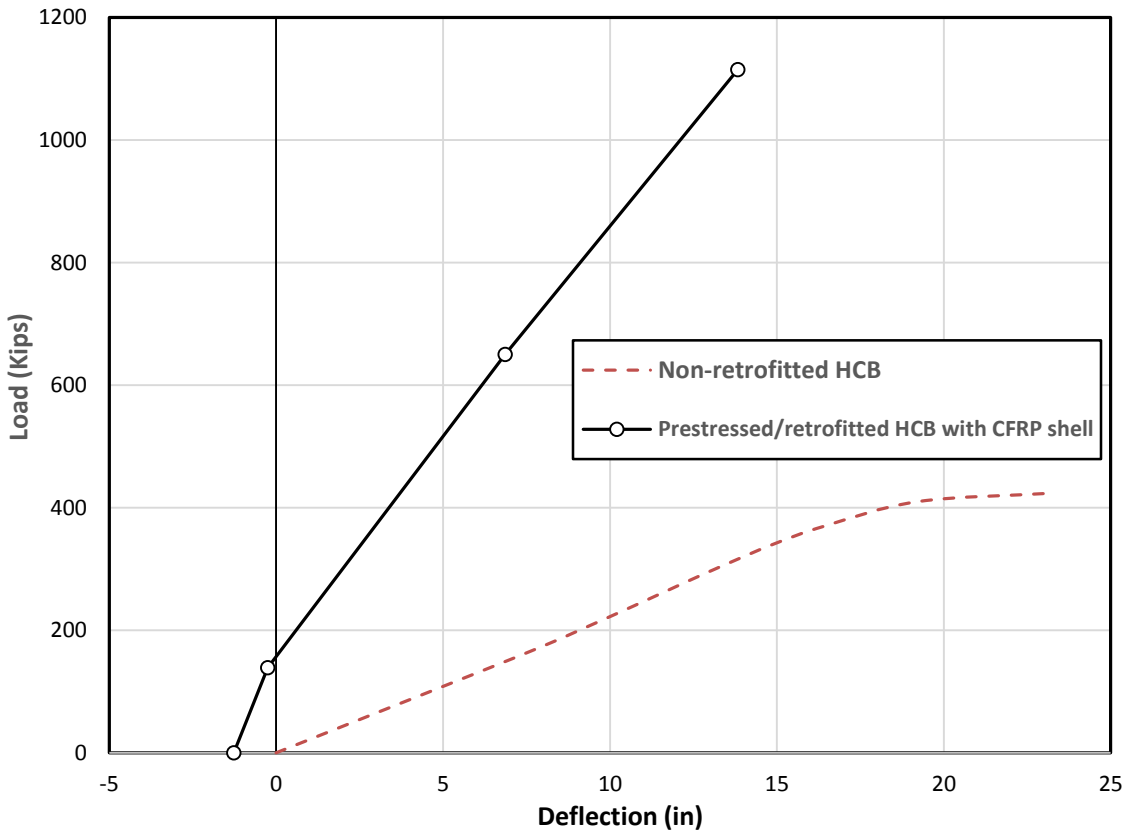

Figure 80. Midspan load-deflection relation for prestressed HCB having CRFP shell and retrofitted with CFRP at top and bottom

6. CONCLUSIONS

The following conclusions can be drawn from the study presented in this dissertation:

1. The materially nonlinear analysis of HCB based on Bernoulli beam approach formulated and programmed in this dissertation is found to be computationally efficient.
2. Retrofitting of HCB with CFRP results in a 123 percent increase in the strength and 66 decrease in the midspan deflections.
3. Replacing FRP shell with that made of CFRP combined with the concrete slab CFRP retrofitting gives a 46 percent increase in strength and 48.4 reduction in the midspan HCB deflection.
4. Retrofitting of HCB with CFRP combined with replacement of FRP with CFRP results in 130 percent increase in the strength and 68 percent decrease in the deflections.
5. Prestressing HCB retrofitted with CFRP and FRP shell replaced with CFRP results in a 163 percent increase in strength and a 77 percent reduction in midspan deflections.
6. When the arch-and-beam model is used with tie stiffness estimation based on the steel tensile reinforcement only, it does not agree with elastic load-deflection curve from HC Bridge Company experiments.
7. When the arch–and-beam elastic model is used with tie stiffness values based on the average fin height, FRP shell and steel reinforcement, it provides a reasonable agreement with the HC Bridge Company experiment.
8. The HCB behavior predicted using Bernoulli beam model indicates that the concrete arch and fin do not contribute much to the overall stiffness and strength.
9. The HCB stiffness and ultimate strength without concrete arch, fin and FRP shell are respectively 13 and 15 percent smaller than those for HCB with complete cross section.
10. The HCB elastic deflection owing to the slab weight predicted by Bernoulli beam approach is 15 percent greater than that form HCB Bridge Company experiment verifying the inherent arch action.
11. The central finite-difference based nonlinear algorithm for predicting HCB behavior and strength based on Bernoulli beam model provided good convergence.

12. In the linear elastic range, the predicted HCB response to external loads based on Bernoulli beam approach shows an excellent agreement with HC Bridge Company experiment indicating the lack of arch action.

APPENDICES

A.

Script of Computer Program in MATLAB for generating M-ϕ Curve for HCB Section

```
% PROGRAM FOR PLOTTING MOMENT-CURVATURE (M-Phi) CURVE FOR HILLMAN-COMPOSITE
BEAM(HCB)
% Description of the program:
% The program takes inputs from user and plots moment-curvature
% (M-Phi)curve for HCB.

clear;
clc;

% User inputs for analysis

% General inputs
% Bc = input('Enter width of concrete slab (in inches); Bc: ');
% hc = input('Enter thickness of concrete slab (in inches); hc: ');
% NoB = input('Enter total number of steel rebars used as top reinforcement
in slab; NoB: ');
% B.Num = input('Enter rebar number used as top reinforcement  in slab;
B.Num: ');
% db = input('Enter depth of top steel reinforcement in slab (in inches); db:
');
% Asb = input('Enter bottom steel reinforcement area in slab (in sq. inches);
Asb: ');
% dbb = input('Enter depth of bottom slab steel reinforcement in slab (in
inches); dbb: ');
% Af = input('Enter area of CFRP reinforcement in slab (in sq. inches); Af:
');
% df = input('Enter depth of CFRP reinforcement in slab (in inches); df: ');
% f = input('Enter thickness of fillet (in inches); f: ');
% b = input('Enter width of HCB (in inches); b: ');
% d  = input('Enter depth of HCB (in inches); d: ');
% tf1 = input('Enter thickness of top flange of HCB (in inches); tf1: ');
% tf2 = input('Enter thickness of bottom flange of HCB (in inches); tf2: ');
% tw = input('Enter thickness of web of HCB (in inches); tw: ');
% bf = input('Enter thickness of fin (in inches); bf: ');
% hf = input('Enter depth of fin (in inches); hf: ');
% ba = input('Enter width of arch (in inches); ba: ');
% ha = input('Enter thickness of arch (in inches); ha: ');
% Aas = input('Enter area of arch steel (in sq. inches); Aas: ');
% has = input('Enter distance of arch steel from bottom of HCB (inches); has:
');
% Aaf = input('Enter area of arch CFRP reinforcement (in sq. inches); Aaf:
');
% haf = input('Enter distance of arch CFRP reinforcement from bottom of HCB
(inches); haf: ');
% Ast = input('Enter area of tension reinforcement (steel strands) (in sq.
inches); Ast: ');
% hs = input('Enter distance of tension reinforcement (steel strands) from
bottom of HCB (in inches); hs: ');
```

```
% Ec = input('Enter modulus of elasticity value for slab concrete (in ksi);
Ec: ');
% Eac = input('Enter modulus of elasticity value for arch concrete (in ksi);
Eac: ');
% Es = input('Enter modulus of elasticity value for steel rebars (in ksi);
Es: ');
% Ef = input('Enter modulus of elasticity value for CFRP reinforcement(in
ksi); Ef: ');
% Ee = input('Enter tension modulus of elasticity value for FRP webs (in
ksi); Ee: ');
% Eec = input('Enter compression modulus of elasticity value for FRP webs(in
ksi); Eec: ');
% Eef = input('Enter tension modulus of elasticity value for FRP flanges (in
ksi); Eef: ');
% Eecf = input('Enter compression modulus of elasticity value for FRP flanges
(in ksi); Eecf: ');
% Est = input('Enter modulus of elasticity value for tension reinforcement
(steel strands) (in ksi); Est: ');
% fc = input('Enter ultimate strength of slab concrete (in ksi); fc: ');
% fac = input('Enter ultimate strength of arch concrete (in ksi); fac: ');
% Fs = input('Enter yield strength of steel rebars (in ksi); Fs: ');
% Ff = input('Enter ultimate strength of CFRP (in ksi); Ff: ');
% Fe = input('Enter ultimate strength of FRP in tension for webs (in ksi);
Fe: ');
% Fec = input('Enter ultimate strength of FRP in compression for webs (in
ksi); Fec: ');
% Fef = input('Enter ultimate strength of FRP in tension for flanges (in
ksi); Fef: ');
% Fecf = input('Enter ultimate strength of FRP in compression for flanges (in
ksi); Fecf: ');
% Fst = input('Enter yield strength of tension reinforcement (steel strands)
(in ksi); Fst: ');


switch B.Num
         case 3
        Ab=0.11;
         case 4
        Ab=0.20;
         case 5
        Ab=0.31;
         case 6
        Ab=0.44;
         case 7
        Ab=0.6;
         case 8
        Ab=0.79;
         case 9
        Ab=1.00;
         case 10
        Ab=1.27;
         case 11
        Ab=1.56;
         case 14
        Ab=2.25;
         case 18
```

```
        Ab=4.00;
         otherwise
        disp('Invalid bar number');
end

% Total area of top steel rebars in slab
As=Ab*NoB;
% Area of concrete in slab
Ac=Bc*hc-As-Af-Asb;
% Equivalent width of concrete slab
bc=Ac/hc;
% Equivalent width of arch
be=(ba*ha-Aas-Aaf)/ha;
% Yield strain of steel rebars
Ts=Fs/Es;
% Yield strain of tension reinforcement (steel strands)
Tst=Fst/Est;
% Rupture strain of CFRP
Tf=Ff/Ef;
% Rupture strain of FRP in tension for webs
Te=Fe/Ee;
% Rupture strain of FRP in compression for webs
Tec=Fec/Eec;
% Rupture strain of FRP in tension for flanges
Tef=Fef/Eef;
% Rupture strain of FRP in compression for flanges
Tecf=Fecf/Eecf;



Ay=2*tw*(d-tf1-tf2)*(hc+f+tf1+(d-tf1-
tf2)/2)+b*tf1*(hc+f+tf1/2)/(Ee/Eef)+b*tf2*(hc+f+d-
tf2/2)/(Ee/Eef)+Ac/(Ee/Ec)*hc/2+As/(Ee/Es)*db+Asb/(Ee/Es)*dbb+Af/(Ee/Ef)*df+b
f*hf/(Ee/Eac)*(hc+f+tf1+hf/2)+be*ha/(Ee/Eac)*(hc+f+tf1+hf+ha/2)+Aas/(Ee/Es)*(
hc+f+d-has)+Aaf/(Ee/Ef)*(hc+f+d-haf)+Ast/(Ee/Est)*(hc+f+d-hs);
A=2*tw*(d-tf1-
tf2)+b*tf1/(Ee/Eef)+b*tf2/(Ee/Eef)+Ac/(Ee/Ec)+As/(Ee/Es)+Asb/(Ee/Es)+Af/(Ee/E
f)+bf*hf/(Ee/Eac)+be*ha/(Ee/Eac)+Aas/(Ee/Es)+Aaf/(Ee/Ef)+Ast/(Ee/Est);
c=Ay/A;
s=c;

for Epc=0.0001:0.0001:0.003;

if c > hc+f+tf1+hf+ha

        % Strain in top slab steel
          Eps=Epc/c*(c-db);
        % Strain in bottom slab steel
          Epsb=Epc/c*(c-dbb);
        % Strain in slab CFRP reinforcement
          Epf=Epc/c*(c-df);
        % Strain in arch steel
          Eas=Epc/c*(c-(hc+f+d-has));
        % Strain in arch CFRP reinforcement
          Eaf=Epc/c*(c-(hc+f+d-haf));
```

```
          Ecc=(0.85*fc-fc)/(0.003-0.002);
          Eacc=(0.85*fac-fac)/(0.003-0.002);

        % Compressive force:

        % Compressive force in slab concrete
        if Epc <= 0.001
            Cc=1/2*(Epc+Epc/c*(c-hc))*Ec*Ac;
        elseif  0.001 < Epc <= 0.002
            if Epc/c*(c-hc) < 0.001
                Cc=fc*bc*c/Epc*(Epc-0.001)+1/2*(0.001+Epc/c*(c-
hc))*Ec*bc*(hc-c/Epc*(Epc-0.001));
            else
                Cc=fc*Ac;
            end
        else
            if Epc/c*(c-hc) < 0.002
                if Epc/c*(c-hc) < 0.001
                    Cc=1/2*(fc+(fc+Ecc*(Epc-0.002)))*bc*c/Epc*(Epc-
0.002)+fc*bc*c/Epc*0.001+1/2*(fc+Epc/c*(c-hc)*Ec)*bc*c/Epc*(0.001-Epc/c*(c-
hc));
                else
                    Cc=1/2*(fc+(fc+Ecc*(Epc-0.002)))*bc*c/Epc*(Epc-
0.002)+fc*bc*c/Epc*(0.002-Epc/c*(c-hc));
                end
            else
                Cc=1/2*((fc+Ecc*(Epc-0.002))+(fc+Ecc*(Epc/c*(c-hc)-
0.002)))*bc*hc;
            end
        end

        % Compressive force in top slab steel
        if Eps < Ts
            Cs=Eps*Es*As;
        else
            Cs=Fs*As;
        end

        % Compressive force in bottom slab steel
        if Epsb < Ts
            Csb=Epsb*Es*Asb;
        else
            Csb=Fs*Asb;
        end

        % Compressive force in slab CFRP reinforcement
        if Epf < Tf
            Cf=Epf*Ef*Af;
        else
            Cf=0;
        end

        % Compressive force in top HCB flange
        if  Epc/c*(c-hc-f) < Tecf
```

```
            Cfl=Epc/c*(c-hc-f-tf1/2)*Eecf*b*tf1;
        else
            Cfl=0;
        end

        % Compressive force in HCB webs
        if  Epc/c*(c-hc-f-tf1) < Tec
            Cw=2*1/2*Epc/c*(c-hc-f-tf1)*Eec*tw*(c-hc-f-tf1);
        else
            Cw=0;
        end

        % Compressive force in fin
        if Epc/c*(c-hc-f-tf1) <= 0.001
            Cfn=Epc/c*(c-hc-f-tf1-hf/2)*Eac*bf*hf;
        elseif  0.001 < Epc/c*(c-hc-f-tf1) <= 0.002
            if Epc/c*(c-hc-f-tf1-hf) < 0.001
                Cfn=fac*bf*(c-hc-f-tf1-c/Epc*0.001)+1/2*(0.001+Epc/c*(c-hc-f-
tf1-hf))*Eac*bf*(hf-(c-hc-f-tf1-c/Epc*0.001));
            else
                Cfn=fac*bf*hf;
            end
        else
            if Epc/c*(c-hc-f-tf1-hf) < 0.001
                Cfn=1/2*(fac+(fac+Eacc*(Epc/c*(c-hc-f-tf1)-
0.002)))*bf*c/Epc*(Epc/c*(c-hc-f-tf1)-
0.002)+fac*bf*c/Epc*0.001+1/2*(fac+Epc/c*(c-hc-f-tf1-
hf)*Eac)*bf*c/Epc*(0.001-Epc/c*(c-hc-f-tf1-hf));
            else
                if Epc/c*(c-hc-f-tf1-hf) < 0.002
                Cfn=1/2*(fac+(fac+Eacc*(Epc/c*(c-hc-f-tf1)-
0.002)))*bf*c/Epc*(Epc/c*(c-hc-f-tf1)-0.002)+fac*bf*(hf-c/Epc*(Epc/c*(c-hc-f-
tf1)-0.002));
                else
                Cfn=1/2*((fac+Eacc*(Epc/c*(c-hc-f-tf1)-
0.002))+(fac+Eacc*(Epc/c*(c-hc-f-tf1-hf)-0.002)))*bf*hf;
                end
            end
        end

        % Compressive force in arch concrete
        if Epc/c*(c-hc-f-tf1-hf) <= 0.001
            Cac=Epc/c*(c-hc-f-tf1-hf-ha/2)*Eac*be*ha;
        elseif 0.001 < Epc/c*(c-hc-f-tf1-hf) <= 0.002
            if Epc/c*(c-hc-f-tf1-hf-ha) < 0.001
                Cac=fac*be*(c-hc-f-tf1-hf-c/Epc*0.001)+1/2*(0.001+Epc/c*(c-
hc-f-tf1-hf-ha))*Eac*be*(ha-(c-hc-f-tf1-hf-c/Epc*0.001));
            else
                Cac=fac*be*ha;
            end
        else
            if Epc/c*(c-hc-f-tf1-hf-ha) < 0.001
                Cac=1/2*(fac+(fac+Eacc*(Epc/c*(c-hc-f-tf1-hf)-
0.002)))*be*c/Epc*(Epc/c*(c-hc-f-tf1-hf)-
0.002)+fac*be*c/Epc*0.001+1/2*(fac+Epc/c*(c-hc-f-tf1-hf-
ha)*Eac)*be*c/Epc*(0.001-Epc/c*(c-hc-f-tf1-hf-ha));
```

```
            else
                if Epc/c*(c-hc-f-tf1-hf-ha) < 0.002
                Cac=1/2*(fac+(fac+Eacc*(Epc/c*(c-hc-f-tf1-hf)-
0.002)))*be*c/Epc*(Epc/c*(c-hc-f-tf1-hf)-0.002)+fac*be*c/Epc*(0.002-Epc/c*(c-
hc-f-tf1-hf-ha));
                else
                Cac=1/2*((fac+Eacc*(Epc/c*(c-hc-f-tf1-hf)-
0.002))+(fac+Eacc*(Epc/c*(c-hc-f-tf1-hf-ha)-0.002)))*be*ha;
                end
            end
        end

        % Compressive force in arch steel
        if Eas < Ts
        Cas = Epc/c*(c-(hc+f+d-has))*Es*Aas;
        else
        Cas = Fs*Aas;
        end

        % Compressive force in arch CFRP
        if Eaf < Tf
        Caf = Epc/c*(c-(hc+f+d-haf))*Ef*Aaf;
        else
        Caf = 0;
        end

        C=Cc+Cs+Csb+Cf+Cfl+Cw+Cfn+Cac+Cas+Caf;

        % Tensile force:

        % Tensile force in tension reinforcement (steel strands)
        if Epc/c*(hc+f+d-c-hs) < Tst
            Tss=Epc/c*(hc+f+d-c-hs)*Est*Ast;
        else
            Tss=Fst*Ast;
        end

        % Tensile force in bottom HCB flange
        if Epc/c*(hc+f+d-c) < Tef
            Tbf=Epc/c*(hc+f+d-c-tf2/2)*Eef*b*tf2;
        else
            Tbf=0;
        end

        % Tensile force in HCB webs
        if Epc/c*(hc+f+d-c-tf2) < Te
            Tw=2*1/2*Epc/c*(hc+f+d-c-tf2)*Ee*tw*(hc+f+d-c-tf2);
        else
            Tw=0;
        end

        T=Tss+Tbf+Tw;

elseif hc < c <= hc+f+tf1+hf+ha
```

```
        % Strain in top slab steel
          Eps=Epc/c*(c-db);
        % Strain in bottom slab steel
          Epsb=Epc/c*(c-dbb);
        % Strain in slab CFRP reinforcement
          Epf=Epc/c*(c-df);
        % Strain in arch steel
          Eas=Epc/c*(c-(hc+f+d-has));
        % Strain in arch CFRP reinforcement
          Eaf=Epc/c*(c-(hc+f+d-haf));

          Ecc=(0.85*fc-fc)/(0.003-0.002);
          Eacc=(0.85*fac-fac)/(0.003-0.002);

        % Compressive force:

        % Compressive force in slab concrete
        if Epc <= 0.001
            Cc=1/2*(Epc+Epc/c*(c-hc))*Ec*Ac;
        elseif  0.001 < Epc <= 0.002
            if Epc/c*(c-hc) < 0.001
                Cc=fc*bc*c/Epc*(Epc-0.001)+1/2*(0.001+Epc/c*(c-
hc))*Ec*bc*(hc-c/Epc*(Epc-0.001));
            else
                Cc=fc*Ac;
            end
        else
            if Epc/c*(c-hc) < 0.002
                if Epc/c*(c-hc) < 0.001
                    Cc=1/2*(fc+(fc+Ecc*(Epc-0.002)))*bc*c/Epc*(Epc-
0.002)+fc*bc*c/Epc*0.001+1/2*(fc+Epc/c*(c-hc)*Ec)*bc*c/Epc*(0.001-Epc/c*(c-
hc));
                else
                    Cc=1/2*(fc+(fc+Ecc*(Epc-0.002)))*bc*c/Epc*(Epc-
0.002)+fc*bc*c/Epc*(0.002-Epc/c*(c-hc));
                end
            else
                Cc=1/2*((fc+Ecc*(Epc-0.002))+(fc+Ecc*(Epc/c*(c-hc)-
0.002)))*bc*hc;
            end
        end

        % Compressive force in top slab steel
        if Eps < Ts
            Cs=Eps*Es*As;
        else
            Cs=Fs*As;
        end

        % Compressive force in bottom slab steel
        if Epsb < Ts
            Csb=Epsb*Es*Asb;
        else
            Csb=Fs*Asb;
```

```
        end

        % Compressive force in slab CFRP reinforcement
        if Epf < Tf
            Cf=Epf*Ef*Af;
        else
            Cf=0;
        end

        % Compressive force in top HCB flange
        if c > hc+f+tf1
           if  Epc/c*(c-hc-f) < Tecf
            Cfl=Epc/c*(c-hc-f-tf1/2)*Eecf*b*tf1;
           else
            Cfl=0;
           end
        else
           if Epc/c*(c-hc-f) < Tecf
           Cfl=1/2*Epc/c*(c-hc-f)*Eecf*b*(c-hc-f);
           else
           Cfl=0;
           end
        end

        % Compressive force in HCB webs
        if c > hc+f+tf1
         if  Epc/c*(c-hc-f-tf1) < Tec
            Cw=2*1/2*Epc/c*(c-hc-f-tf1)*Eec*tw*(c-hc-f-tf1);
         else
            Cw=0;
         end
        else
            Cw=0;
        end

        % Compressive force in fin
        if hc+f+tf1 < c
           if hc+f+tf1+hf < c
            if Epc/c*(c-hc-f-tf1) <= 0.001
             Cfn=Epc/c*(c-hc-f-tf1-hf/2)*Eac*bf*hf;
            elseif  0.001 < Epc/c*(c-hc-f-tf1) <= 0.002
             if Epc/c*(c-hc-f-tf1-hf) < 0.001
                Cfn=fac*bf*(c-hc-f-tf1-c/Epc*0.001)+1/2*(0.001+Epc/c*(c-hc-f-
tf1-hf))*Eac*bf*(hf-(c-hc-f-tf1-c/Epc*0.001));
             else
                Cfn=fac*bf*hf;
             end
            else
             if Epc/c*(c-hc-f-tf1-hf) < 0.001
                Cfn=1/2*(fac+(fac+Eacc*(Epc/c*(c-hc-f-tf1)-
0.002)))*bf*c/Epc*(Epc/c*(c-hc-f-tf1)-
0.002)+fac*bf*c/Epc*0.001+1/2*(fac+Epc/c*(c-hc-f-tf1-
hf)*Eac)*bf*c/Epc*(0.001-Epc/c*(c-hc-f-tf1-hf));
             else
                if Epc/c*(c-hc-f-tf1-hf) < 0.002
```

```
                Cfn=1/2*(fac+(fac+Eacc*(Epc/c*(c-hc-f-tf1)-
0.002)))*bf*c/Epc*(Epc/c*(c-hc-f-tf1)-0.002)+fac*bf*(hf-c/Epc*(Epc/c*(c-hc-f-
tf1)-0.002));
                else
                Cfn=1/2*((fac+Eacc*(Epc/c*(c-hc-f-tf1)-
0.002))+(fac+Eacc*(Epc/c*(c-hc-f-tf1-hf)-0.002)))*bf*hf;
                end
             end
            end
           else
            if Epc/c*(c-hc-f-tf1) <= 0.001
             Cfn=1/2*Epc/c*(c-hc-f-tf1)*Eac*bf*(c-hc-f-tf1);
            elseif  0.001 < Epc/c*(c-hc-f-tf1) <= 0.002
             Cfn=fac*bf*(c-hc-f-tf1-c/Epc*0.001)+1/2*fac*bf*c/Epc*0.001;
            else
             Cfn=1/2*(fac+(fac+Eacc*(Epc/c*(c-hc-f-tf1)-
0.002)))*bf*c/Epc*(Epc/c*(c-hc-f-tf1)-
0.002)+fac*bf*c/Epc*0.001+1/2*fac*bf*c/Epc*0.001;
            end
           end
        else
            Cfn=0;
        end

        % Compressive force in arch concrete
        if  hc+f+tf1+hf < c
            if Epc/c*(c-hc-f-tf1-hf) <= 0.001
             Cac=1/2*Epc/c*(c-hc-f-tf1-hf)*Eac*be*(c-hc-f-tf1-hf);
            elseif  0.001 < Epc/c*(c-hc-f-tf1-hf) <= 0.002
             Cac=fac*be*(c-hc-f-tf1-hf-c/Epc*0.001)+1/2*fac*be*c/Epc*0.001;
            else
             Cac=1/2*(fac+(fac+Eacc*(Epc/c*(c-hc-f-tf1-hf)-
0.002)))*be*c/Epc*(Epc/c*(c-hc-f-tf1-hf)-
0.002)+fac*be*c/Epc*0.001+1/2*fac*be*c/Epc*0.001;
            end
        else
            Cac=0;
        end

        % Compressive force in arch steel
        if hc+f+d-has < c
         if Eas < Ts
          Cas = Eas*Es*Aas;
         else
          Cas = Fs*Aas;
         end
        else
         Cas=0;
        end

        % Compressive force in arch CFRP
        if hc+f+d-haf < c
         if Eaf < Tf
          Caf = Eaf*Ef*Aaf;
         else
          Caf = 0;
```

```
 end
else
 Caf = 0;
end

C=Cc+Cs+Csb+Cf+Cfl+Cw+Cfn+Cac+Cas+Caf;

% Tensile force:

% Tensile force in arch steel
if c < hc+f+d-has
 if Epc/c*(hc+f+d-c-has) < Ts
    Tas=Epc/c*(hc+f+d-c-has)*Es*Aas;
 else
    Tas=Fs*Aas;
 end
else
    Tas=0;
end

% Tensile force in arch CFRP
if c < hc+f+d-haf
 if Epc/c*(hc+f+d-c-haf) < Tf
    Taf=Epc/c*(hc+f+d-c-haf)*Ef*Aaf;
 else
    Taf=0;
 end
else
    Taf=0;
end

% Tensile force in tension reinforcement (steel strands)
if Epc/c*(hc+f+d-c-hs) < Tst
    Tss=Epc/c*(hc+f+d-c-hs)*Est*Ast;
else
    Tss=Fst*Ast;
end

% Tensile force in bottom HCB flange
if Epc/c*(hc+f+d-c) < Tef
    Tbf=Epc/c*(hc+f+d-c-tf2/2)*Eef*b*tf2;
else
    Tbf=0;
end

% Tensile force in HCB webs
if Epc/c*(hc+f+d-c-tf2) < Te
    if c >= hc+f+tf1
    Tw=2*1/2*Epc/c*(hc+f+d-c-tf2)*Ee*tw*(hc+f+d-c-tf2);
    else
    Tw=2*Epc/c*(hc+f+d-c-tf2-1/2*(d-tf1-tf2))*Ee*tw*(d-tf1-tf2);
    end
else
    Tw=0;
end
```

```
        T=Tas+Taf+Tss+Tbf+Tw;

else
        % Strain in top slab steel
          Eps=Epc/c*(c-db);
        % Strain in bottom slab steel
          Epsb=Epc/c*(c-dbb);
        % Strain in slab CFRP reinforcement
          Epf=Epc/c*(c-df);
        % Strain in arch steel
          Eas=Epc/c*(c-(hc+f+d-has));
        % Strain in arch CFRP reinforcement
          Eaf=Epc/c*(c-(hc+f+d-haf));

          Ecc=(0.85*fc-fc)/(0.003-0.002);
          Eacc=(0.85*fac-fac)/(0.003-0.002);


        % Compressive forces:

        % Compressive force in slab concrete
        if Epc <= 0.001
            Cc=1/2*Epc*Ec*bc*c;
        elseif  0.001 < Epc <= 0.002
            Cc=fc*bc*c/Epc*(Epc-0.001)+1/2*fc*bc*c/Epc*0.001;
        else
            Cc=1/2*((fc+Ecc*(Epc-0.002))+fc)*bc*c/Epc*(Epc-
0.002)+fc*bc*c/Epc*0.001+1/2*fc*bc*c/Epc*0.001;
        end

        % Compressive force in top slab steel
        if c > db
         if Eps < Ts
            Cs=Eps*Es*As;
         else
            Cs=Fs*As;
         end
        else
         Cs=0;
        end


        % Compressive force in bottom slab steel
        if c > dbb
         if Epsb < Ts
            Csb=Epsb*Es*Asb;
         else
            Csb=Fs*Asb;
         end
        else
         Csb=0;
        end
```

```
% Compressive force in slab CFRP reinforcement
if c > df
 if Epf < Tf
    Cf=Epf*Ef*Af;
 else
    Cf=0;
 end
else
 Cf=0;
end

C=Cc+Cs+Csb+Cf;

% Tensile forces:

% Tensile force in bottom slab steel
if c < dbb
 if Epc/c*(dbb-c) < Ts
    Tsb=Epc/c*(dbb-c)*Es*Asb;
 else
    Tsb=Fs*Asb;
 end
else
 Tsb=0;
end

% Tensile force in top HCB flange
if Epc/c*(hc+f+d-c-(d-tf1)) < Tef
    Ttf=Epc/c*(hc+f+d-c-(d-tf1/2))*Eef*b*tf1;
else
    Ttf=0;
end

% Tensile force in bottom HCB flange
if Epc/c*(hc+f+d-c) < Tef
    Tbf=Epc/c*(hc+f+d-c-tf2/2)*Eef*b*tf2;
else
    Tbf=0;
end

% Tensile force in arch CFRP
if Epc/c*(hc+f+d-c-haf) < Tf
    Taf=Epc/c*(hc+f+d-c-haf)*Ef*Aaf;
else
    Taf=0;
end

% Tensile force in arch steel
if Epc/c*(hc+f+d-c-has) < Ts
   Tas=Epc/c*(hc+f+d-c-has)*Es*Aas;
else
   Tas=Ts*Aas;
end

% Tensile force in tension reinforcement (steel strands)
```

```
        if Epc/c*(hc+f+d-c-hs) < Tst
            Tss=Epc/c*(hc+f+d-c-hs)*Est*Ast;
        else
            Tss=Fst*Ast;
        end

        % Tensile force in HCB webs
        if Epc/c*(hc+f+d-c-tf2) < Te
            Tw=2*Epc/c*(hc+f+d-c-tf2-1/2*(d-tf1-tf2))*Ee*tw*(d-tf1-tf2);
        else
            Tw=0;
        end

        T=Tsb+Ttf+Tbf+Taf+Tas+Tss+Tw;
end

    C=C*1000;
    T=T*1000;


 while abs(C-T) > 1
     c=c-0.000001;
     if c <= 0
         break
     end

if c > hc+f+tf1+hf+ha

        % Strain in top slab steel
          Eps=Epc/c*(c-db);
        % Strain in bottom slab steel
          Epsb=Epc/c*(c-dbb);
        % Strain in slab CFRP reinforcement
          Epf=Epc/c*(c-df);
        % Strain in arch steel
          Eas=Epc/c*(c-(hc+f+d-has));
        % Strain in arch CFRP reinforcement
          Eaf=Epc/c*(c-(hc+f+d-haf));

          Ecc=(0.85*fc-fc)/(0.003-0.002);
          Eacc=(0.85*fac-fac)/(0.003-0.002);

        % Compressive force:

        % Compressive force in slab concrete
        if Epc <= 0.001
            Cc=1/2*(Epc+Epc/c*(c-hc))*Ec*Ac;
        elseif  0.001 < Epc <= 0.002
            if Epc/c*(c-hc) < 0.001
                Cc=fc*bc*c/Epc*(Epc-0.001)+1/2*(0.001+Epc/c*(c-
hc))*Ec*bc*(hc-c/Epc*(Epc-0.001));
            else
                Cc=fc*Ac;
            end
```

```
        else
            if Epc/c*(c-hc) < 0.002
                if Epc/c*(c-hc) < 0.001
                    Cc=1/2*(fc+(fc+Ecc*(Epc-0.002)))*bc*c/Epc*(Epc-
0.002)+fc*bc*c/Epc*0.001+1/2*(fc+Epc/c*(c-hc)*Ec)*bc*c/Epc*(0.001-Epc/c*(c-
hc));
                else
                    Cc=1/2*(fc+(fc+Ecc*(Epc-0.002)))*bc*c/Epc*(Epc-
0.002)+fc*bc*c/Epc*(0.002-Epc/c*(c-hc));
                end
            else
                Cc=1/2*((fc+Ecc*(Epc-0.002))+(fc+Ecc*(Epc/c*(c-hc)-
0.002)))*bc*hc;
            end
        end

        % Compressive force in top slab steel
        if Eps < Ts
            Cs=Eps*Es*As;
        else
            Cs=Fs*As;
        end

        % Compressive force in bottom slab steel
        if Epsb < Ts
            Csb=Epsb*Es*Asb;
        else
            Csb=Fs*Asb;
        end

        % Compressive force in slab CFRP reinforcement
        if Epf < Tf
            Cf=Epf*Ef*Af;
        else
            Cf=0;
        end

        % Compressive force in top HCB flange
        if  Epc/c*(c-hc-f) < Tecf
            Cfl=Epc/c*(c-hc-f-tf1/2)*Eecf*b*tf1;
        else
            Cfl=0;
        end

        % Compressive force in HCB webs
        if  Epc/c*(c-hc-f-tf1) < Tec
            Cw=2*1/2*Epc/c*(c-hc-f-tf1)*Eec*tw*(c-hc-f-tf1);
        else
            Cw=0;
        end

        % Compressive force in fin
        if Epc/c*(c-hc-f-tf1) <= 0.001
            Cfn=Epc/c*(c-hc-f-tf1-hf/2)*Eac*bf*hf;
        elseif  0.001 < Epc/c*(c-hc-f-tf1) <= 0.002
```

```
            if Epc/c*(c-hc-f-tf1-hf) < 0.001
                Cfn=fac*bf*(c-hc-f-tf1-c/Epc*0.001)+1/2*(0.001+Epc/c*(c-hc-f-
tf1-hf))*Eac*bf*(hf-(c-hc-f-tf1-c/Epc*0.001));
            else
                Cfn=fac*bf*hf;
            end
        else
            if Epc/c*(c-hc-f-tf1-hf) < 0.001
                Cfn=1/2*(fac+(fac+Eacc*(Epc/c*(c-hc-f-tf1)-
0.002)))*bf*c/Epc*(Epc/c*(c-hc-f-tf1)-
0.002)+fac*bf*c/Epc*0.001+1/2*(fac+Epc/c*(c-hc-f-tf1-
hf)*Eac)*bf*c/Epc*(0.001-Epc/c*(c-hc-f-tf1-hf));
            else
                if Epc/c*(c-hc-f-tf1-hf) < 0.002
                Cfn=1/2*(fac+(fac+Eacc*(Epc/c*(c-hc-f-tf1)-
0.002)))*bf*c/Epc*(Epc/c*(c-hc-f-tf1)-0.002)+fac*bf*(hf-c/Epc*(Epc/c*(c-hc-f-
tf1)-0.002));
                else
                Cfn=1/2*((fac+Eacc*(Epc/c*(c-hc-f-tf1)-
0.002))+(fac+Eacc*(Epc/c*(c-hc-f-tf1-hf)-0.002)))*bf*hf;
                end
            end
        end

        % Compressive force in arch concrete
        if Epc/c*(c-hc-f-tf1-hf) <= 0.001
            Cac=Epc/c*(c-hc-f-tf1-hf-ha/2)*Eac*be*ha;
        elseif 0.001 < Epc/c*(c-hc-f-tf1-hf) <= 0.002
            if Epc/c*(c-hc-f-tf1-hf-ha) < 0.001
                Cac=fac*be*(c-hc-f-tf1-hf-c/Epc*0.001)+1/2*(0.001+Epc/c*(c-
hc-f-tf1-hf-ha))*Eac*be*(ha-(c-hc-f-tf1-hf-c/Epc*0.001));
            else
                Cac=fac*be*ha;
            end
        else
            if Epc/c*(c-hc-f-tf1-hf-ha) < 0.001
                Cac=1/2*(fac+(fac+Eacc*(Epc/c*(c-hc-f-tf1-hf)-
0.002)))*be*c/Epc*(Epc/c*(c-hc-f-tf1-hf)-
0.002)+fac*be*c/Epc*0.001+1/2*(fac+Epc/c*(c-hc-f-tf1-hf-
ha)*Eac)*be*c/Epc*(0.001-Epc/c*(c-hc-f-tf1-hf-ha));
            else
                if Epc/c*(c-hc-f-tf1-hf-ha) < 0.002
                Cac=1/2*(fac+(fac+Eacc*(Epc/c*(c-hc-f-tf1-hf)-
0.002)))*be*c/Epc*(Epc/c*(c-hc-f-tf1-hf)-0.002)+fac*be*c/Epc*(0.002-Epc/c*(c-
hc-f-tf1-hf-ha));
                else
                Cac=1/2*((fac+Eacc*(Epc/c*(c-hc-f-tf1-hf)-
0.002))+(fac+Eacc*(Epc/c*(c-hc-f-tf1-hf-ha)-0.002)))*be*ha;
                end
            end
        end

        % Compressive force in arch steel
        if Eas < Ts
        Cas = Epc/c*(c-(hc+f+d-has))*Es*Aas;
        else
```

```
        Cas = Fs*Aas;
        end

        % Compressive force in arch CFRP
        if Eaf < Tf
        Caf = Epc/c*(c-(hc+f+d-haf))*Ef*Aaf;
        else
        Caf = 0;
        end

        C=Cc+Cs+Csb+Cf+Cfl+Cw+Cfn+Cac+Cas+Caf;

        % Tensile force:

        % Tensile force in tension reinforcement (steel strands)
        if Epc/c*(hc+f+d-c-hs) < Tst
            Tss=Epc/c*(hc+f+d-c-hs)*Est*Ast;
        else
            Tss=Fst*Ast;
        end

        % Tensile force in bottom HCB flange
        if Epc/c*(hc+f+d-c) < Tef
            Tbf=Epc/c*(hc+f+d-c-tf2/2)*Eef*b*tf2;
        else
            Tbf=0;
        end

        % Tensile force in HCB webs
        if Epc/c*(hc+f+d-c-tf2) < Te
            Tw=2*1/2*Epc/c*(hc+f+d-c-tf2)*Ee*tw*(hc+f+d-c-tf2);
        else
            Tw=0;
        end

        T=Tss+Tbf+Tw;

elseif hc < c <= hc+f+tf1+hf+ha

        % Strain in top slab steel
          Eps=Epc/c*(c-db);
        % Strain in bottom slab steel
          Epsb=Epc/c*(c-dbb);
        % Strain in slab CFRP reinforcement
          Epf=Epc/c*(c-df);
        % Strain in arch steel
          Eas=Epc/c*(c-(hc+f+d-has));
        % Strain in arch CFRP reinforcement
          Eaf=Epc/c*(c-(hc+f+d-haf));

          Ecc=(0.85*fc-fc)/(0.003-0.002);
          Eacc=(0.85*fac-fac)/(0.003-0.002);

        % Compressive force:
```

```
        % Compressive force in slab concrete
        if Epc <= 0.001
            Cc=1/2*(Epc+Epc/c*(c-hc))*Ec*Ac;
        elseif  0.001 < Epc <= 0.002
            if Epc/c*(c-hc) < 0.001
                Cc=fc*bc*c/Epc*(Epc-0.001)+1/2*(0.001+Epc/c*(c-
hc))*Ec*bc*(hc-c/Epc*(Epc-0.001));
            else
                Cc=fc*Ac;
            end
        else
            if Epc/c*(c-hc) < 0.002
                if Epc/c*(c-hc) < 0.001
                    Cc=1/2*(fc+(fc+Ecc*(Epc-0.002)))*bc*c/Epc*(Epc-
0.002)+fc*bc*c/Epc*0.001+1/2*(fc+Epc/c*(c-hc)*Ec)*bc*c/Epc*(0.001-Epc/c*(c-
hc));
                else
                    Cc=1/2*(fc+(fc+Ecc*(Epc-0.002)))*bc*c/Epc*(Epc-
0.002)+fc*bc*c/Epc*(0.002-Epc/c*(c-hc));
                end
            else
                Cc=1/2*((fc+Ecc*(Epc-0.002))+(fc+Ecc*(Epc/c*(c-hc)-
0.002)))*bc*hc;
            end
        end

        % Compressive force in top slab steel
        if Eps < Ts
            Cs=Eps*Es*As;
        else
            Cs=Fs*As;
        end

        % Compressive force in bottom slab steel
        if Epsb < Ts
            Csb=Epsb*Es*Asb;
        else
            Csb=Fs*Asb;
        end

        % Compressive force in slab CFRP reinforcement
        if Epf < Tf
            Cf=Epf*Ef*Af;
        else
            Cf=0;
        end

        % Compressive force in top HCB flange
        if c > hc+f+tf1
           if  Epc/c*(c-hc-f) < Tecf
            Cfl=Epc/c*(c-hc-f-tf1/2)*Eecf*b*tf1;
           else
            Cfl=0;
           end
```

```
        else
           if Epc/c*(c-hc-f) < Tecf
           Cfl=1/2*Epc/c*(c-hc-f)*Eecf*b*(c-hc-f);
           else
           Cfl=0;
           end
        end

        % Compressive force in HCB webs
        if c > hc+f+tf1
         if  Epc/c*(c-hc-f-tf1) < Tec
            Cw=2*1/2*Epc/c*(c-hc-f-tf1)*Eec*tw*(c-hc-f-tf1);
         else
            Cw=0;
         end
        else
            Cw=0;
        end

        % Compressive force in fin
        if hc+f+tf1 < c
           if hc+f+tf1+hf < c
            if Epc/c*(c-hc-f-tf1) <= 0.001
             Cfn=Epc/c*(c-hc-f-tf1-hf/2)*Eac*bf*hf;
            elseif  0.001 < Epc/c*(c-hc-f-tf1) <= 0.002
             if Epc/c*(c-hc-f-tf1-hf) < 0.001
                Cfn=fac*bf*(c-hc-f-tf1-c/Epc*0.001)+1/2*(0.001+Epc/c*(c-hc-f-
tf1-hf))*Eac*bf*(hf-(c-hc-f-tf1-c/Epc*0.001));
             else
                Cfn=fac*bf*hf;
             end
            else
             if Epc/c*(c-hc-f-tf1-hf) < 0.001
                Cfn=1/2*(fac+(fac+Eacc*(Epc/c*(c-hc-f-tf1)-
0.002)))*bf*c/Epc*(Epc/c*(c-hc-f-tf1)-
0.002)+fac*bf*c/Epc*0.001+1/2*(fac+Epc/c*(c-hc-f-tf1-
hf)*Eac)*bf*c/Epc*(0.001-Epc/c*(c-hc-f-tf1-hf));
             else
                if Epc/c*(c-hc-f-tf1-hf) < 0.002
                Cfn=1/2*(fac+(fac+Eacc*(Epc/c*(c-hc-f-tf1)-
0.002)))*bf*c/Epc*(Epc/c*(c-hc-f-tf1)-0.002)+fac*bf*(hf-c/Epc*(Epc/c*(c-hc-f-
tf1)-0.002));
                else
                Cfn=1/2*((fac+Eacc*(Epc/c*(c-hc-f-tf1)-
0.002))+(fac+Eacc*(Epc/c*(c-hc-f-tf1-hf)-0.002)))*bf*hf;
                end
             end
            end
           else
            if Epc/c*(c-hc-f-tf1) <= 0.001
             Cfn=1/2*Epc/c*(c-hc-f-tf1)*Eac*bf*(c-hc-f-tf1);
            elseif  0.001 < Epc/c*(c-hc-f-tf1) <= 0.002
             Cfn=fac*bf*(c-hc-f-tf1-c/Epc*0.001)+1/2*fac*bf*c/Epc*0.001;
            else
```

```
             Cfn=1/2*(fac+(fac+Eacc*(Epc/c*(c-hc-f-tf1)-
0.002)))*bf*c/Epc*(Epc/c*(c-hc-f-tf1)-
0.002)+fac*bf*c/Epc*0.001+1/2*fac*bf*c/Epc*0.001;
            end
           end
        else
            Cfn=0;
        end

        % Compressive force in arch concrete
        if  hc+f+tf1+hf < c
            if Epc/c*(c-hc-f-tf1-hf) <= 0.001
             Cac=1/2*Epc/c*(c-hc-f-tf1-hf)*Eac*be*(c-hc-f-tf1-hf);
            elseif  0.001 < Epc/c*(c-hc-f-tf1-hf) <= 0.002
             Cac=fac*be*(c-hc-f-tf1-hf-c/Epc*0.001)+1/2*fac*be*c/Epc*0.001;
            else
             Cac=1/2*(fac+(fac+Eacc*(Epc/c*(c-hc-f-tf1-hf)-
0.002)))*be*c/Epc*(Epc/c*(c-hc-f-tf1-hf)-
0.002)+fac*be*c/Epc*0.001+1/2*fac*be*c/Epc*0.001;
            end
        else
            Cac=0;
        end

        % Compressive force in arch steel
        if hc+f+d-has < c
         if Eas < Ts
          Cas = Eas*Es*Aas;
         else
          Cas = Fs*Aas;
         end
        else
         Cas=0;
        end

        % Compressive force in arch CFRP
        if hc+f+d-haf < c
         if Eaf < Tf
          Caf = Eaf*Ef*Aaf;
         else
          Caf = 0;
         end
        else
         Caf = 0;
        end

        C=Cc+Cs+Csb+Cf+Cfl+Cw+Cfn+Cac+Cas+Caf;

        % Tensile force:

        % Tensile force in arch steel
        if c < hc+f+d-has
         if Epc/c*(hc+f+d-c-has) < Ts
            Tas=Epc/c*(hc+f+d-c-has)*Es*Aas;
         else
```

```
            Tas=Fs*Aas;
         end
        else
            Tas=0;
        end

        % Tensile force in arch CFRP
        if c < hc+f+d-haf
         if Epc/c*(hc+f+d-c-haf) < Tf
            Taf=Epc/c*(hc+f+d-c-haf)*Ef*Aaf;
         else
            Taf=0;
         end
        else
            Taf=0;
        end

        % Tensile force in tension reinforcement (steel strands)
        if Epc/c*(hc+f+d-c-hs) < Tst
            Tss=Epc/c*(hc+f+d-c-hs)*Est*Ast;
        else
            Tss=Fst*Ast;
        end

        % Tensile force in bottom HCB flange
        if Epc/c*(hc+f+d-c) < Tef
            Tbf=Epc/c*(hc+f+d-c-tf2/2)*Eef*b*tf2;
        else
            Tbf=0;
        end

        % Tensile force in HCB webs
        if Epc/c*(hc+f+d-c-tf2) < Te
            if c >= hc+f+tf1
            Tw=2*1/2*Epc/c*(hc+f+d-c-tf2)*Ee*tw*(hc+f+d-c-tf2);
            else
            Tw=2*Epc/c*(hc+f+d-c-tf2-1/2*(d-tf1-tf2))*Ee*tw*(d-tf1-tf2);
            end
        else
            Tw=0;
        end

        T=Tas+Taf+Tss+Tbf+Tw;

else
        % Strain in top slab steel
          Eps=Epc/c*(c-db);
        % Strain in bottom slab steel
          Epsb=Epc/c*(c-dbb);
        % Strain in slab CFRP reinforcement
          Epf=Epc/c*(c-df);
        % Strain in arch steel
          Eas=Epc/c*(c-(hc+f+d-has));
        % Strain in arch CFRP reinforcement
          Eaf=Epc/c*(c-(hc+f+d-haf));
```

```
          Ecc=(0.85*fc-fc)/(0.003-0.002);
          Eacc=(0.85*fac-fac)/(0.003-0.002);


        % Compressive forces:

        % Compressive force in slab concrete
        if Epc <= 0.001
            Cc=1/2*Epc*Ec*bc*c;
        elseif  0.001 < Epc <= 0.002
            Cc=fc*bc*c/Epc*(Epc-0.001)+1/2*fc*bc*c/Epc*0.001;
        else
            Cc=1/2*((fc+Ecc*(Epc-0.002))+fc)*bc*c/Epc*(Epc-
0.002)+fc*bc*c/Epc*0.001+1/2*fc*bc*c/Epc*0.001;
        end

        % Compressive force in top slab steel
        if c > db
         if Eps < Ts
            Cs=Eps*Es*As;
         else
            Cs=Fs*As;
         end
        else
         Cs=0;
        end


        % Compressive force in bottom slab steel
        if c > dbb
         if Epsb < Ts
            Csb=Epsb*Es*Asb;
         else
            Csb=Fs*Asb;
         end
        else
         Csb=0;
        end

        % Compressive force in slab CFRP reinforcement
        if c > df
         if Epf < Tf
            Cf=Epf*Ef*Af;
         else
            Cf=0;
         end
        else
         Cf=0;
        end

        C=Cc+Cs+Csb+Cf;

        % Tensile forces:
```

```
% Tensile force in bottom slab steel
if c < dbb
 if Epc/c*(dbb-c) < Ts
    Tsb=Epc/c*(dbb-c)*Es*Asb;
 else
    Tsb=Fs*Asb;
 end
else
 Tsb=0;
end

% Tensile force in top HCB flange
if Epc/c*(hc+f+d-c-(d-tf1)) < Tef
    Ttf=Epc/c*(hc+f+d-c-(d-tf1/2))*Eef*b*tf1;
else
    Ttf=0;
end

% Tensile force in bottom HCB flange
if Epc/c*(hc+f+d-c) < Tef
    Tbf=Epc/c*(hc+f+d-c-tf2/2)*Eef*b*tf2;
else
    Tbf=0;
end

% Tensile force in arch CFRP
if Epc/c*(hc+f+d-c-haf) < Tf
    Taf=Epc/c*(hc+f+d-c-haf)*Ef*Aaf;
else
    Taf=0;
end

% Tensile force in arch steel
if Epc/c*(hc+f+d-c-has) < Ts
   Tas=Epc/c*(hc+f+d-c-has)*Es*Aas;
else
   Tas=Ts*Aas;
end

% Tensile force in tension reinforcement (steel strands)
if Epc/c*(hc+f+d-c-hs) < Tst
    Tss=Epc/c*(hc+f+d-c-hs)*Est*Ast;
else
    Tss=Fst*Ast;
end

% Tensile force in HCB webs
if Epc/c*(hc+f+d-c-tf2) < Te
    Tw=2*Epc/c*(hc+f+d-c-tf2-1/2*(d-tf1-tf2))*Ee*tw*(d-tf1-tf2);
else
    Tw=0;
end

T=Tsb+Ttf+Tbf+Taf+Tas+Tss+Tw;
```

```
end

    C=C*1000;
    T=T*1000;

 end

while abs(C-T) > 1
     c=c+0.000001;

if c > hc+f+tf1+hf+ha

        % Strain in top slab steel
          Eps=Epc/c*(c-db);
        % Strain in bottom slab steel
          Epsb=Epc/c*(c-dbb);
        % Strain in slab CFRP reinforcement
          Epf=Epc/c*(c-df);
        % Strain in arch steel
          Eas=Epc/c*(c-(hc+f+d-has));
        % Strain in arch CFRP reinforcement
          Eaf=Epc/c*(c-(hc+f+d-haf));

          Ecc=(0.85*fc-fc)/(0.003-0.002);
          Eacc=(0.85*fac-fac)/(0.003-0.002);

        % Compressive force:

        % Compressive force in slab concrete
        if Epc <= 0.001
            Cc=1/2*(Epc+Epc/c*(c-hc))*Ec*Ac;
        elseif  0.001 < Epc <= 0.002
            if Epc/c*(c-hc) < 0.001
                Cc=fc*bc*c/Epc*(Epc-0.001)+1/2*(0.001+Epc/c*(c-
hc))*Ec*bc*(hc-c/Epc*(Epc-0.001));
            else
                Cc=fc*Ac;
            end
        else
            if Epc/c*(c-hc) < 0.002
                if Epc/c*(c-hc) < 0.001
                    Cc=1/2*(fc+(fc+Ecc*(Epc-0.002)))*bc*c/Epc*(Epc-
0.002)+fc*bc*c/Epc*0.001+1/2*(fc+Epc/c*(c-hc)*Ec)*bc*c/Epc*(0.001-Epc/c*(c-
hc));
                else
                    Cc=1/2*(fc+(fc+Ecc*(Epc-0.002)))*bc*c/Epc*(Epc-
0.002)+fc*bc*c/Epc*(0.002-Epc/c*(c-hc));
                end
            else
                Cc=1/2*((fc+Ecc*(Epc-0.002))+(fc+Ecc*(Epc/c*(c-hc)-
0.002)))*bc*hc;
            end
        end
```

```
        % Compressive force in top slab steel
        if Eps < Ts
            Cs=Eps*Es*As;
        else
            Cs=Fs*As;
        end

        % Compressive force in bottom slab steel
        if Epsb < Ts
            Csb=Epsb*Es*Asb;
        else
            Csb=Fs*Asb;
        end

        % Compressive force in slab CFRP reinforcement
        if Epf < Tf
            Cf=Epf*Ef*Af;
        else
            Cf=0;
        end

        % Compressive force in top HCB flange
        if  Epc/c*(c-hc-f) < Tecf
            Cfl=Epc/c*(c-hc-f-tf1/2)*Eecf*b*tf1;
        else
            Cfl=0;
        end

        % Compressive force in HCB webs
        if  Epc/c*(c-hc-f-tf1) < Tec
            Cw=2*1/2*Epc/c*(c-hc-f-tf1)*Eec*tw*(c-hc-f-tf1);
        else
            Cw=0;
        end

        % Compressive force in fin
        if Epc/c*(c-hc-f-tf1) <= 0.001
            Cfn=Epc/c*(c-hc-f-tf1-hf/2)*Eac*bf*hf;
        elseif  0.001 < Epc/c*(c-hc-f-tf1) <= 0.002
            if Epc/c*(c-hc-f-tf1-hf) < 0.001
                Cfn=fac*bf*(c-hc-f-tf1-c/Epc*0.001)+1/2*(0.001+Epc/c*(c-hc-f-
tf1-hf))*Eac*bf*(hf-(c-hc-f-tf1-c/Epc*0.001));
            else
                Cfn=fac*bf*hf;
            end
        else
            if Epc/c*(c-hc-f-tf1-hf) < 0.001
                Cfn=1/2*(fac+(fac+Eacc*(Epc/c*(c-hc-f-tf1)-
0.002)))*bf*c/Epc*(Epc/c*(c-hc-f-tf1)-
0.002)+fac*bf*c/Epc*0.001+1/2*(fac+Epc/c*(c-hc-f-tf1-
hf)*Eac)*bf*c/Epc*(0.001-Epc/c*(c-hc-f-tf1-hf));
            else
                if Epc/c*(c-hc-f-tf1-hf) < 0.002
```

```
                Cfn=1/2*(fac+(fac+Eacc*(Epc/c*(c-hc-f-tf1)-
0.002)))*bf*c/Epc*(Epc/c*(c-hc-f-tf1)-0.002)+fac*bf*(hf-c/Epc*(Epc/c*(c-hc-f-
tf1)-0.002));
                else
                Cfn=1/2*((fac+Eacc*(Epc/c*(c-hc-f-tf1)-
0.002))+(fac+Eacc*(Epc/c*(c-hc-f-tf1-hf)-0.002)))*bf*hf;
                end
            end
        end

        % Compressive force in arch concrete
        if Epc/c*(c-hc-f-tf1-hf) <= 0.001
            Cac=Epc/c*(c-hc-f-tf1-hf-ha/2)*Eac*be*ha;
        elseif 0.001 < Epc/c*(c-hc-f-tf1-hf) <= 0.002
            if Epc/c*(c-hc-f-tf1-hf-ha) < 0.001
                Cac=fac*be*(c-hc-f-tf1-hf-c/Epc*0.001)+1/2*(0.001+Epc/c*(c-
hc-f-tf1-hf-ha))*Eac*be*(ha-(c-hc-f-tf1-hf-c/Epc*0.001));
            else
                Cac=fac*be*ha;
            end
        else
            if Epc/c*(c-hc-f-tf1-hf-ha) < 0.001
                Cac=1/2*(fac+(fac+Eacc*(Epc/c*(c-hc-f-tf1-hf)-
0.002)))*be*c/Epc*(Epc/c*(c-hc-f-tf1-hf)-
0.002)+fac*be*c/Epc*0.001+1/2*(fac+Epc/c*(c-hc-f-tf1-hf-
ha)*Eac)*be*c/Epc*(0.001-Epc/c*(c-hc-f-tf1-hf-ha));
            else
                if Epc/c*(c-hc-f-tf1-hf-ha) < 0.002
                Cac=1/2*(fac+(fac+Eacc*(Epc/c*(c-hc-f-tf1-hf)-
0.002)))*be*c/Epc*(Epc/c*(c-hc-f-tf1-hf)-0.002)+fac*be*c/Epc*(0.002-Epc/c*(c-
hc-f-tf1-hf-ha));
                else
                Cac=1/2*((fac+Eacc*(Epc/c*(c-hc-f-tf1-hf)-
0.002))+(fac+Eacc*(Epc/c*(c-hc-f-tf1-hf-ha)-0.002)))*be*ha;
                end
            end
        end

        % Compressive force in arch steel
        if Eas < Ts
        Cas = Epc/c*(c-(hc+f+d-has))*Es*Aas;
        else
        Cas = Fs*Aas;
        end

        % Compressive force in arch CFRP
        if Eaf < Tf
        Caf = Epc/c*(c-(hc+f+d-haf))*Ef*Aaf;
        else
        Caf = 0;
        end

        C=Cc+Cs+Csb+Cf+Cfl+Cw+Cfn+Cac+Cas+Caf;

        % Tensile force:
```

```
        % Tensile force in tension reinforcement (steel strands)
        if Epc/c*(hc+f+d-c-hs) < Tst
            Tss=Epc/c*(hc+f+d-c-hs)*Est*Ast;
        else
            Tss=Fst*Ast;
        end

        % Tensile force in bottom HCB flange
        if Epc/c*(hc+f+d-c) < Tef
            Tbf=Epc/c*(hc+f+d-c-tf2/2)*Eef*b*tf2;
        else
            Tbf=0;
        end

        % Tensile force in HCB webs
        if Epc/c*(hc+f+d-c-tf2) < Te
            Tw=2*1/2*Epc/c*(hc+f+d-c-tf2)*Ee*tw*(hc+f+d-c-tf2);
        else
            Tw=0;
        end

        T=Tss+Tbf+Tw;

elseif hc < c <= hc+f+tf1+hf+ha

        % Strain in top slab steel
          Eps=Epc/c*(c-db);
        % Strain in bottom slab steel
          Epsb=Epc/c*(c-dbb);
        % Strain in slab CFRP reinforcement
          Epf=Epc/c*(c-df);
        % Strain in arch steel
          Eas=Epc/c*(c-(hc+f+d-has));
        % Strain in arch CFRP reinforcement
          Eaf=Epc/c*(c-(hc+f+d-haf));

          Ecc=(0.85*fc-fc)/(0.003-0.002);
          Eacc=(0.85*fac-fac)/(0.003-0.002);

        % Compressive force:

        % Compressive force in slab concrete
        if Epc <= 0.001
            Cc=1/2*(Epc+Epc/c*(c-hc))*Ec*Ac;
        elseif  0.001 < Epc <= 0.002
            if Epc/c*(c-hc) < 0.001
                Cc=fc*bc*c/Epc*(Epc-0.001)+1/2*(0.001+Epc/c*(c-
hc))*Ec*bc*(hc-c/Epc*(Epc-0.001));
            else
                Cc=fc*Ac;
            end
        else
            if Epc/c*(c-hc) < 0.002
```

```
                if Epc/c*(c-hc) < 0.001
                    Cc=1/2*(fc+(fc+Ecc*(Epc-0.002)))*bc*c/Epc*(Epc-
0.002)+fc*bc*c/Epc*0.001+1/2*(fc+Epc/c*(c-hc)*Ec)*bc*c/Epc*(0.001-Epc/c*(c-
hc));
                else
                    Cc=1/2*(fc+(fc+Ecc*(Epc-0.002)))*bc*c/Epc*(Epc-
0.002)+fc*bc*c/Epc*(0.002-Epc/c*(c-hc));
                end
            else
                Cc=1/2*((fc+Ecc*(Epc-0.002))+(fc+Ecc*(Epc/c*(c-hc)-
0.002)))*bc*hc;
            end
        end

        % Compressive force in top slab steel
        if Eps < Ts
            Cs=Eps*Es*As;
        else
            Cs=Fs*As;
        end

        % Compressive force in bottom slab steel
        if Epsb < Ts
            Csb=Epsb*Es*Asb;
        else
            Csb=Fs*Asb;
        end

        % Compressive force in slab CFRP reinforcement
        if Epf < Tf
            Cf=Epf*Ef*Af;
        else
            Cf=0;
        end

        % Compressive force in top HCB flange
        if c > hc+f+tf1
           if  Epc/c*(c-hc-f) < Tecf
            Cfl=Epc/c*(c-hc-f-tf1/2)*Eecf*b*tf1;
           else
            Cfl=0;
           end
        else
           if Epc/c*(c-hc-f) < Tecf
           Cfl=1/2*Epc/c*(c-hc-f)*Eecf*b*(c-hc-f);
           else
           Cfl=0;
           end
        end

        % Compressive force in HCB webs
        if c > hc+f+tf1
         if  Epc/c*(c-hc-f-tf1) < Tec
            Cw=2*1/2*Epc/c*(c-hc-f-tf1)*Eec*tw*(c-hc-f-tf1);
         else
```

```
            Cw=0;
         end
        else
            Cw=0;
        end

        % Compressive force in fin
        if hc+f+tf1 < c
           if hc+f+tf1+hf < c
            if Epc/c*(c-hc-f-tf1) <= 0.001
             Cfn=Epc/c*(c-hc-f-tf1-hf/2)*Eac*bf*hf;
            elseif  0.001 < Epc/c*(c-hc-f-tf1) <= 0.002
             if Epc/c*(c-hc-f-tf1-hf) < 0.001
                Cfn=fac*bf*(c-hc-f-tf1-c/Epc*0.001)+1/2*(0.001+Epc/c*(c-hc-f-
tf1-hf))*Eac*bf*(hf-(c-hc-f-tf1-c/Epc*0.001));
             else
                Cfn=fac*bf*hf;
             end
            else
             if Epc/c*(c-hc-f-tf1-hf) < 0.001
                Cfn=1/2*(fac+(fac+Eacc*(Epc/c*(c-hc-f-tf1)-
0.002)))*bf*c/Epc*(Epc/c*(c-hc-f-tf1)-
0.002)+fac*bf*c/Epc*0.001+1/2*(fac+Epc/c*(c-hc-f-tf1-
hf)*Eac)*bf*c/Epc*(0.001-Epc/c*(c-hc-f-tf1-hf));
             else
                if Epc/c*(c-hc-f-tf1-hf) < 0.002
                Cfn=1/2*(fac+(fac+Eacc*(Epc/c*(c-hc-f-tf1)-
0.002)))*bf*c/Epc*(Epc/c*(c-hc-f-tf1)-0.002)+fac*bf*(hf-c/Epc*(Epc/c*(c-hc-f-
tf1)-0.002));
                else
                Cfn=1/2*((fac+Eacc*(Epc/c*(c-hc-f-tf1)-
0.002))+(fac+Eacc*(Epc/c*(c-hc-f-tf1-hf)-0.002)))*bf*hf;
                end
             end
            end
           else
            if Epc/c*(c-hc-f-tf1) <= 0.001
             Cfn=1/2*Epc/c*(c-hc-f-tf1)*Eac*bf*(c-hc-f-tf1);
            elseif  0.001 < Epc/c*(c-hc-f-tf1) <= 0.002
             Cfn=fac*bf*(c-hc-f-tf1-c/Epc*0.001)+1/2*fac*bf*c/Epc*0.001;
            else
             Cfn=1/2*(fac+(fac+Eacc*(Epc/c*(c-hc-f-tf1)-
0.002)))*bf*c/Epc*(Epc/c*(c-hc-f-tf1)-
0.002)+fac*bf*c/Epc*0.001+1/2*fac*bf*c/Epc*0.001;
            end
           end
        else
            Cfn=0;
        end

        % Compressive force in arch concrete
        if  hc+f+tf1+hf < c
            if Epc/c*(c-hc-f-tf1-hf) <= 0.001
             Cac=1/2*Epc/c*(c-hc-f-tf1-hf)*Eac*be*(c-hc-f-tf1-hf);
            elseif  0.001 < Epc/c*(c-hc-f-tf1-hf) <= 0.002
             Cac=fac*be*(c-hc-f-tf1-hf-c/Epc*0.001)+1/2*fac*be*c/Epc*0.001;
```

```
            else
             Cac=1/2*(fac+(fac+Eacc*(Epc/c*(c-hc-f-tf1-hf)-
0.002)))*be*c/Epc*(Epc/c*(c-hc-f-tf1-hf)-
0.002)+fac*be*c/Epc*0.001+1/2*fac*be*c/Epc*0.001;
            end
        else
            Cac=0;
        end

        % Compressive force in arch steel
        if hc+f+d-has < c
         if Eas < Ts
          Cas = Eas*Es*Aas;
         else
          Cas = Fs*Aas;
         end
        else
         Cas=0;
        end

        % Compressive force in arch CFRP
        if hc+f+d-haf < c
         if Eaf < Tf
          Caf = Eaf*Ef*Aaf;
         else
          Caf = 0;
         end
        else
         Caf = 0;
        end

        C=Cc+Cs+Csb+Cf+Cfl+Cw+Cfn+Cac+Cas+Caf;

        % Tensile force:

        % Tensile force in arch steel
        if c < hc+f+d-has
         if Epc/c*(hc+f+d-c-has) < Ts
            Tas=Epc/c*(hc+f+d-c-has)*Es*Aas;
         else
            Tas=Fs*Aas;
         end
        else
            Tas=0;
        end

        % Tensile force in arch CFRP
        if c < hc+f+d-haf
         if Epc/c*(hc+f+d-c-haf) < Tf
            Taf=Epc/c*(hc+f+d-c-haf)*Ef*Aaf;
         else
            Taf=0;
         end
        else
            Taf=0;
```

```
        end

        % Tensile force in tension reinforcement (steel strands)
        if Epc/c*(hc+f+d-c-hs) < Tst
            Tss=Epc/c*(hc+f+d-c-hs)*Est*Ast;
        else
            Tss=Fst*Ast;
        end

        % Tensile force in bottom HCB flange
        if Epc/c*(hc+f+d-c) < Tef
            Tbf=Epc/c*(hc+f+d-c-tf2/2)*Eef*b*tf2;
        else
            Tbf=0;
        end

        % Tensile force in HCB webs
        if Epc/c*(hc+f+d-c-tf2) < Te
            if c >= hc+f+tf1
            Tw=2*1/2*Epc/c*(hc+f+d-c-tf2)*Ee*tw*(hc+f+d-c-tf2);
            else
            Tw=2*Epc/c*(hc+f+d-c-tf2-1/2*(d-tf1-tf2))*Ee*tw*(d-tf1-tf2);
            end
        else
            Tw=0;
        end

        T=Tas+Taf+Tss+Tbf+Tw;

else
        % Strain in top slab steel
          Eps=Epc/c*(c-db);
        % Strain in bottom slab steel
          Epsb=Epc/c*(c-dbb);
        % Strain in slab CFRP reinforcement
          Epf=Epc/c*(c-df);
        % Strain in arch steel
          Eas=Epc/c*(c-(hc+f+d-has));
        % Strain in arch CFRP reinforcement
          Eaf=Epc/c*(c-(hc+f+d-haf));

          Ecc=(0.85*fc-fc)/(0.003-0.002);
          Eacc=(0.85*fac-fac)/(0.003-0.002);



        % Compressive forces:

        % Compressive force in slab concrete
        if Epc <= 0.001
            Cc=1/2*Epc*Ec*bc*c;
        elseif  0.001 < Epc <= 0.002
            Cc=fc*bc*c/Epc*(Epc-0.001)+1/2*fc*bc*c/Epc*0.001;
        else
```

```
            Cc=1/2*((fc+Ecc*(Epc-0.002))+fc)*bc*c/Epc*(Epc-
0.002)+fc*bc*c/Epc*0.001+1/2*fc*bc*c/Epc*0.001;
        end

        % Compressive force in top slab steel
        if c > db
         if Eps < Ts
            Cs=Eps*Es*As;
         else
            Cs=Fs*As;
         end
        else
         Cs=0;
        end


        % Compressive force in bottom slab steel
        if c > dbb
         if Epsb < Ts
            Csb=Epsb*Es*Asb;
         else
            Csb=Fs*Asb;
         end
        else
         Csb=0;
        end

        % Compressive force in slab CFRP reinforcement
        if c > df
         if Epf < Tf
            Cf=Epf*Ef*Af;
         else
            Cf=0;
         end
        else
         Cf=0;
        end

        C=Cc+Cs+Csb+Cf;

        % Tensile forces:

        % Tensile force in bottom slab steel
        if c < dbb
         if Epc/c*(dbb-c) < Ts
            Tsb=Epc/c*(dbb-c)*Es*Asb;
         else
            Tsb=Fs*Asb;
         end
        else
         Tsb=0;
        end

        % Tensile force in top HCB flange
        if Epc/c*(hc+f+d-c-(d-tf1)) < Tef
```

```
            Ttf=Epc/c*(hc+f+d-c-(d-tf1/2))*Eef*b*tf1;
        else
            Ttf=0;
        end

        % Tensile force in bottom HCB flange
        if Epc/c*(hc+f+d-c) < Tef
            Tbf=Epc/c*(hc+f+d-c-tf2/2)*Eef*b*tf2;
        else
            Tbf=0;
        end

        % Tensile force in arch CFRP
        if Epc/c*(hc+f+d-c-haf) < Tf
            Taf=Epc/c*(hc+f+d-c-haf)*Ef*Aaf;
        else
            Taf=0;
        end

        % Tensile force in arch steel
        if Epc/c*(hc+f+d-c-has) < Ts
           Tas=Epc/c*(hc+f+d-c-has)*Es*Aas;
        else
           Tas=Ts*Aas;
        end

        % Tensile force in tension reinforcement (steel strands)
        if Epc/c*(hc+f+d-c-hs) < Tst
            Tss=Epc/c*(hc+f+d-c-hs)*Est*Ast;
        else
            Tss=Fst*Ast;
        end

        % Tensile force in HCB webs
        if Epc/c*(hc+f+d-c-tf2) < Te
            Tw=2*Epc/c*(hc+f+d-c-tf2-1/2*(d-tf1-tf2))*Ee*tw*(d-tf1-tf2);
        else
            Tw=0;
        end

        T=Tsb+Ttf+Tbf+Taf+Tas+Tss+Tw;
end

    C=C*1000;
    T=T*1000;

end

%  end

 fprintf('Epc = %10.5f\n', Epc)
 fprintf('c = %10.6f in\n', c)
 fprintf('C = %10.4f lb\n', C)
 fprintf('T = %10.4f lb\n', T)
```

```
% Moments:

 if c > hc+f+tf1+hf+ha

        % Strain in top slab steel
          Eps=Epc/c*(c-db);
        % Strain in bottom slab steel
          Epsb=Epc/c*(c-dbb);
        % Strain in slab CFRP reinforcement
          Epf=Epc/c*(c-df);
        % Strain in arch steel
          Eas=Epc/c*(c-(hc+f+d-has));
        % Strain in arch CFRP reinforcement
          Eaf=Epc/c*(c-(hc+f+d-haf));

          Ecc=(0.85*fc-fc)/(0.003-0.002);
          Eacc=(0.85*fac-fac)/(0.003-0.002);

        % Moment due to compressive force in slab concrete
        if Epc <= 0.001
            Mc=1/2*(Epc+Epc/c*(c-hc))*Ec*Ac*(c-hc/3*(Epc+2*Epc/c*(c-
hc))/(Epc+Epc/c*(c-hc)));
        elseif  0.001 < Epc <= 0.002
            if c/Epc*(Epc-0.001) < hc
                Mc=fc*bc*c/Epc*(Epc-0.001)*(c-1/2*c/Epc*(Epc-
0.001))+1/2*(0.001+Epc/c*(c-hc))*Ec*bc*(hc-c/Epc*(Epc-0.001))*(c-c/Epc*(Epc-
0.001)-(hc-c/Epc*(Epc-0.001))/3*(0.001+2*Epc/c*(c-hc))/(0.001+Epc/c*(c-hc)));
            else
                Mc=fc*Ac*(c-hc/2);
            end
        else
            if Epc/c*(c-hc) < 0.002
                if Epc/c*(c-hc) < 0.001
                    Mc=1/2*(fc+(fc+Ecc*(Epc-0.002)))*bc*c/Epc*(Epc-0.002)*(c-
1/3*c/Epc*(Epc-0.002)*(Epc+2*0.002)/(Epc+0.002))+fc*bc*c/Epc*0.001*(c-
c/Epc*(Epc-0.002)-1/2*c/Epc*0.001)+1/2*(fc+Epc/c*(c-hc)*Ec)*bc*c/Epc*(0.001-
Epc/c*(c-hc))*(c-c/Epc*(Epc-0.001)-1/3*(hc-c/Epc*(Epc-
0.001))*(0.001+2*Epc/c*(c-hc))/(0.001+Epc/c*(c-hc)));
                else
                    Mc=1/2*(fc+(fc+Ecc*(Epc-0.002)))*bc*c/Epc*(Epc-0.002)*(c-
1/3*c/Epc*(Epc-0.002)*(Epc+2*0.002)/(Epc+0.002))+fc*bc*c/Epc*(0.002-Epc/c*(c-
hc))*(c-hc+1/2*c/Epc*(0.002-Epc/c*(c-hc)));
                end
            else
                Mc=1/2*((fc+Ecc*(Epc-0.002))+(fc+Ecc*(Epc/c*(c-hc)-
0.002)))*bc*hc*(c-1/3*hc*(Epc+2*Epc/c*(c-hc))/(Epc+Epc/c*(c-hc)));
            end
        end

        % Moment due to compressive force in top slab steel
        if Eps < Ts
            Ms=Eps*Es*As*(c-db);
        else
            Ms=Fs*As*(c-db);
```

```
        end

        % Moment due to compressive force in bottom slab steel
        if Epsb < Ts
            Msb=Epsb*Es*Asb*(c-dbb);
        else
            Msb=Fs*Asb*(c-dbb);
        end

        % Moment due to compressive force in slab CFRP reinforcement
        if Epf < Tf
            Mf=Epf*Ef*Af*(c-df);
        else
            Mf=0;
        end

        % Moment due to compressive force in top HCB flange
        if  Epc/c*(c-hc-f) < Tecf
            Mfl=Epc/c*(c-hc-f-tf1/2)*Eecf*b*tf1*(c-hc-f-tf1/2);
        else
            Mfl=0;
        end

        % Moment due to compressive force in HCB webs
        if  Epc/c*(c-hc-f-tf1) < Tec
            Mw=2*1/2*Epc/c*(c-hc-f-tf1)*Eec*tw*(c-hc-f-tf1)*(2/3*(c-hc-f-
tf1));
        else
            Mw=0;
        end

        % Moment due to compressive force in fin
        if Epc/c*(c-hc-f-tf1) <= 0.001
            Mfn=Epc/c*(c-hc-f-tf1-hf/2)*Eac*bf*hf*(c-hc-f-tf1-
1/3*hf*(Epc/c*(c-hc-f-tf1)+2*Epc/c*(c-hc-f-tf1-hf))/(Epc/c*(c-hc-f-
tf1)+Epc/c*(c-hc-f-tf1-hf)));
        elseif  0.001 < Epc/c*(c-hc-f-tf1) <= 0.002
            if Epc/c*(c-hc-f-tf1-hf) < 0.001
                Mfn=fac*bf*(c-hc-f-tf1-c/Epc*0.001)*(c-hc-f-tf1-1/2*(c-hc-f-
tf1-c/Epc*0.001))+1/2*(0.001+Epc/c*(c-hc-f-tf1-hf))*Eac*bf*(hf-(c-hc-f-tf1-
c/Epc*0.001))*(c-hc-f-tf1-(c-hc-f-tf1-c/Epc*0.001)-1/3*(hf-(c-hc-f-tf1-
c/Epc*0.001))*(0.001+2*Epc/c*(c-hc-f-tf1-hf))/(0.001+Epc/c*(c-hc-f-tf1-hf)));
            else
                Mfn=fac*bf*hf*(c-hc-f-tf1-hf/2);
            end
        else
            if Epc/c*(c-hc-f-tf1-hf) < 0.001
                Mfn=1/2*(fac+(fac+Eacc*(Epc/c*(c-hc-f-tf1)-
0.002)))*bf*c/Epc*(Epc/c*(c-hc-f-tf1)-0.002)*(c-hc-f-tf1-1/3*c/Epc*(Epc/c*(c-
hc-f-tf1)-0.002)*(Epc/c*(c-hc-f-tf1)+2*0.002)/(Epc/c*(c-hc-f-
tf1)+0.002))+fac*bf*c/Epc*0.001*(c-hc-f-tf1-c/Epc*(Epc/c*(c-hc-f-tf1)-0.002)-
1/2*c/Epc*0.001)+1/2*(fac+Epc/c*(c-hc-f-tf1-hf)*Eac)*bf*c/Epc*(0.001-
Epc/c*(c-hc-f-tf1-hf))*(c-hc-f-tf1-hf+1/3*(hf-(c-hc-f-tf1-
c/Epc*0.001))*(2*0.001+Epc/c*(c-hc-f-tf1-hf))/(0.001+Epc/c*(c-hc-f-tf1-hf)));
            else
```

```
                if Epc/c*(c-hc-f-tf1-hf) < 0.002
                Mfn=1/2*(fac+(fac+Eacc*(Epc/c*(c-hc-f-tf1)-
0.002)))*bf*c/Epc*(Epc/c*(c-hc-f-tf1)-0.002)*(c-hc-f-tf1-1/3*c/Epc*(Epc/c*(c-
hc-f-tf1)-0.002)*(Epc/c*(c-hc-f-tf1)+2*0.002)/(Epc/c*(c-hc-f-
tf1)+0.002))+fac*bf*(hf-c/Epc*(Epc/c*(c-hc-f-tf1)-0.002))*(c-hc-f-tf1-
hf+1/2*(hf-c/Epc*(Epc/c*(c-hc-f-tf1)-0.002)));
                else
                Mfn=1/2*((fac+Eacc*(Epc/c*(c-hc-f-tf1)-
0.002))+(fac+Eacc*(Epc/c*(c-hc-f-tf1-hf)-0.002)))*be*ha*(c-hc-f-tf1-
hf/3*(Epc/c*(c-hc-f-tf1)+2*Epc/c*(c-hc-f-tf1-hf))/(Epc/c*(c-hc-f-
tf1)+Epc/c*(c-hc-f-tf1-hf)));
                end
            end
        end

        % Moment due to compressive force in arch concrete
        if Epc/c*(c-hc-f-tf1-hf) <= 0.001
            Mac=Epc/c*(c-hc-f-tf1-hf-ha/2)*Eac*be*ha*(c-hc-f-tf1-hf-
1/3*ha*(Epc/c*(c-hc-f-tf1-hf)+2*Epc/c*(c-hc-f-tf1-hf-ha))/(Epc/c*(c-hc-f-tf1-
hf)+Epc/c*(c-hc-f-tf1-hf-ha)));
        elseif 0.001 < Epc/c*(c-hc-f-tf1-hf) <= 0.002
            if Epc/c*(c-hc-f-tf1-hf-ha) < 0.001
                Mac=fac*be*(c-hc-f-tf1-hf-c/Epc*0.001)*(c-hc-f-tf1-hf-1/2*(c-
hc-f-tf1-hf-c/Epc*0.001))+1/2*(0.001+Epc/c*(c-hc-f-tf1-hf-ha))*Eac*be*(ha-(c-
hc-f-tf1-hf-c/Epc*0.001))*(c-hc-f-tf1-hf-(c-hc-f-tf1-hf-c/Epc*0.001)-1/3*(ha-
(c-hc-f-tf1-hf-c/Epc*0.001))*(0.001+2*Epc/c*(c-hc-f-tf1-hf-
ha))/(0.001+Epc/c*(c-hc-f-tf1-hf-ha)));
            else
                Mac=fac*be*ha*(c-hc-f-tf1-hf-ha/2);
            end
        else
            if Epc/c*(c-hc-f-tf1-hf-ha) < 0.001
                Mac=1/2*(fac+(fac+Eacc*(Epc/c*(c-hc-f-tf1-hf)-
0.002)))*be*c/Epc*(Epc/c*(c-hc-f-tf1-hf)-0.002)*(c-hc-f-tf1-hf-
1/3*c/Epc*(Epc/c*(c-hc-f-tf1-hf)-0.002)*(Epc/c*(c-hc-f-tf1-
hf)+2*0.002)/(Epc/c*(c-hc-f-tf1-hf)+0.002))+fac*be*c/Epc*0.001*(c-hc-f-tf1-
hf-c/Epc*(Epc/c*(c-hc-f-tf1-hf)-0.002)-1/2*c/Epc*0.001)+1/2*(fac+Epc/c*(c-hc-
f-tf1-hf-ha)*Eac)*be*c/Epc*(0.001-Epc/c*(c-hc-f-tf1-hf-ha))*(c-hc-f-tf1-hf-
ha+1/3*(ha-(c-hc-f-tf1-hf-c/Epc*0.001))*(2*0.001+Epc/c*(c-hc-f-tf1-hf-
ha))/(0.001+Epc/c*(c-hc-f-tf1-hf-ha)));
            else
                if Epc/c*(c-hc-f-tf1-hf-ha) < 0.002
                Mac=1/2*(fac+(fac+Eacc*(Epc/c*(c-hc-f-tf1-hf)-
0.002)))*be*c/Epc*(Epc/c*(c-hc-f-tf1-hf)-0.002)*(c-hc-f-tf1-hf-
1/3*c/Epc*(Epc/c*(c-hc-f-tf1-hf)-0.002)*(Epc/c*(c-hc-f-tf1-
hf)+2*0.002)/(Epc/c*(c-hc-f-tf1-hf)+0.002))+fac*be*c/Epc*(0.002-Epc/c*(c-hc-
f-tf1-hf-ha))*(c-hc-f-tf1-hf-c/Epc*(Epc/c*(c-hc-f-tf1-hf)-0.002)-
1/2*c/Epc*(0.002-Epc/c*(c-hc-f-tf1-hf-ha)));
                else
                Mac=1/2*((fac+Eacc*(Epc/c*(c-hc-f-tf1-hf)-
0.002))+(fac+Eacc*(Epc/c*(c-hc-f-tf1-hf-ha)-0.002)))*be*ha*(c-hc-f-tf1-hf-
ha/3*(Epc/c*(c-hc-f-tf1-hf)+2*Epc/c*(c-hc-f-tf1-hf-ha))/(Epc/c*(c-hc-f-tf1-
hf)+Epc/c*(c-hc-f-tf1-hf-ha)));
                end
            end
        end
```

```
        % Moment due to compressive force in arch steel
        if Eas < Ts
        Mas=Epc/c*(c-(hc+f+d-has))*Es*Aas*(c-(hc+f+d-has));
        else
        Mas=Fs*Aas*(c-(hc+f+d-has));
        end

        % Moment due to compressive force in arch CFRP
        if Eaf < Tf
        Maf=Epc/c*(c-(hc+f+d-haf))*Ef*Aaf*(c-(hc+f+d-haf));
        else
        Maf=0;
        end

        MC=Mc+Ms+Msb+Mf+Mfl+Mw+Mfn+Mac+Mas+Maf;

        % Moment due to tensile forces:

        % Moment due to tensile force in tension reinforcement (steel
strands)
        if Epc/c*(hc+f+d-c-hs) < Tst
            MTss=Epc/c*(hc+f+d-c-hs)*Est*Ast*(hc+f+d-c-hs);
        else
            MTss=Fst*Ast*(hc+f+d-c-hs);
        end

        % Moment due to tensile force in bottom HCB flange
        if Epc/c*(hc+f+d-c) < Tef
            MTbf=Epc/c*(hc+f+d-c-tf2/2)*Eef*b*tf2*(hc+f+d-c-tf2/2);
        else
            MTbf=0;
        end

        % Moment due to tensile force in HCB webs
        if Epc/c*(hc+f+d-c-tf2) < Te
            MTw=2*1/2*Epc/c*(hc+f+d-c-tf2)*Ee*tw*(hc+f+d-c-tf2)*2/3*(hc+f+d-
c-tf2);
        else
            MTw=0;
        end

        MT=MTss+MTbf+MTw;

 elseif hc <= c < hc+f+tf1+hf+ha

        % Moment due to compressive forces:

        % Strain in top slab steel
          Eps=Epc/c*(c-db);
        % Strain in bottom slab steel
          Epsb=Epc/c*(c-dbb);
        % Strain in slab CFRP reinforcement
          Epf=Epc/c*(c-df);
```

```
        % Strain in arch steel
          Eas=Epc/c*(c-(hc+f+d-has));
        % Strain in arch CFRP reinforcement
          Eaf=Epc/c*(c-(hc+f+d-haf));

          Ecc=(0.85*fc-fc)/(0.003-0.002);
          Eacc=(0.85*fac-fac)/(0.003-0.002);

        % Moment due to compressive force in slab concrete
        if Epc <= 0.001
            Mc=1/2*(Epc+Epc/c*(c-hc))*Ec*Ac*(c-hc/3*(Epc+2*Epc/c*(c-
hc))/(Epc+Epc/c*(c-hc)));
        elseif  0.001 < Epc <= 0.002
            if c/Epc*(Epc-0.001) < hc
                Mc=fc*bc*c/Epc*(Epc-0.001)*(c-1/2*c/Epc*(Epc-
0.001))+1/2*(0.001+Epc/c*(c-hc))*Ec*bc*(hc-c/Epc*(Epc-0.001))*(c-c/Epc*(Epc-
0.001)-(hc-c/Epc*(Epc-0.001))/3*(0.001+2*Epc/c*(c-hc))/(0.001+Epc/c*(c-hc)));
            else
                Mc=fc*Ac*(c-hc/2);
            end
        else
            if Epc/c*(c-hc) < 0.002
                if Epc/c*(c-hc) < 0.001
                    Mc=1/2*(fc+(fc+Ecc*(Epc-0.002)))*bc*c/Epc*(Epc-0.002)*(c-
1/3*c/Epc*(Epc-0.002)*(Epc+2*0.002)/(Epc+0.002))+fc*bc*c/Epc*0.001*(c-
c/Epc*(Epc-0.002)-1/2*c/Epc*0.001)+1/2*(fc+Epc/c*(c-hc)*Ec)*bc*c/Epc*(0.001-
Epc/c*(c-hc))*(c-c/Epc*(Epc-0.001)-1/3*(hc-c/Epc*(Epc-
0.001))*(0.001+2*Epc/c*(c-hc))/(0.001+Epc/c*(c-hc)));
                else
                    Mc=1/2*(fc+(fc+Ecc*(Epc-0.002)))*bc*c/Epc*(Epc-0.002)*(c-
1/3*c/Epc*(Epc-0.002)*(Epc+2*0.002)/(Epc+0.002))+fc*bc*c/Epc*(0.002-Epc/c*(c-
hc))*(c-hc+1/2*c/Epc*(0.002-Epc/c*(c-hc)));
                end
            else
                Mc=1/2*((fc+Ecc*(Epc-0.002))+(fc+Ecc*(Epc/c*(c-hc)-
0.002)))*bc*hc*(c-1/3*hc*(Epc+2*Epc/c*(c-hc))/(Epc+Epc/c*(c-hc)));
            end
        end

        % Moment due to compressive force in slab steel
        if Eps < Ts
            Ms=Eps*Es*As*(c-db);
        else
            Ms=Fs*As*(c-db);
        end

        % Moment due to compressive force in bottom slab steel
        if Epsb < Ts
            Msb=Epsb*Es*Asb*(c-dbb);
        else
            Msb=Fs*Asb*(c-dbb);
        end

        % Moment due to compressive force in slab CFRP reinforcement
        if Epf < Tf
```

```
            Mf=Epf*Ef*Af*(c-df);
        else
            Mf=0;
        end

        % Moment due to compressive force in top HCB flange
        if c > hc+f+tf1
           if  Epc/c*(c-hc-f) < Tecf
            Mfl=Epc/c*(c-hc-f-tf1/2)*Eecf*b*tf1*(c-hc-f-tf1/2);
           else
            Mfl=0;
           end
        else
           if Epc/c*(c-hc-f) < Tecf
           Mfl=1/2*Epc/c*(c-hc-f)*Eecf*b*(c-hc-f)*2/3*(c-hc-f);
           else
           Mfl=0;
           end
        end

        % Moment due to compressive force in HCB webs
        if c > hc+f+tf1
         if  Epc/c*(c-hc-f-tf1) < Tec
            Mw=2*1/2*Epc/c*(c-hc-f-tf1)*Eec*tw*(c-hc-f-tf1)*2/3*(c-hc-f-tf1);
         else
            Mw=0;
         end
        else
            Mw=0;
        end

        % Moment due to compressive force in fin
        if hc+f+tf1 < c
          if hc+f+tf1+hf < c
            if Epc/c*(c-hc-f-tf1) <= 0.001
             Mfn=Epc/c*(c-hc-f-tf1-hf/2)*Eac*bf*hf*(c-hc-f-tf1-
1/3*hf*(Epc/c*(c-hc-f-tf1)+2*Epc/c*(c-hc-f-tf1-hf))/(Epc/c*(c-hc-f-
tf1)+Epc/c*(c-hc-f-tf1-hf)));
            elseif  0.001 < Epc/c*(c-hc-f-tf1) <= 0.002
             if Epc/c*(c-hc-f-tf1-hf) < 0.001
                Mfn=fac*bf*(c-hc-f-tf1-c/Epc*0.001)*(c-hc-f-tf1-1/2*(c-hc-f-
tf1-c/Epc*0.001))+1/2*(0.001+Epc/c*(c-hc-f-tf1-hf))*Eac*bf*(hf-(c-hc-f-tf1-
c/Epc*0.001))*(c-hc-f-tf1-(c-hc-f-tf1-c/Epc*0.001)-1/3*(hf-(c-hc-f-tf1-
c/Epc*0.001))*(0.001+2*Epc/c*(c-hc-f-tf1-hf))/(0.001+Epc/c*(c-hc-f-tf1-hf)));
             else
                Mfn=fac*bf*hf*(c-hc-f-tf1-hf/2);
             end
            else
             if Epc/c*(c-hc-f-tf1-hf) < 0.001
                Mfn=1/2*(fac+(fac+Eacc*(Epc/c*(c-hc-f-tf1)-
0.002)))*bf*c/Epc*(Epc/c*(c-hc-f-tf1)-0.002)*(c-hc-f-tf1-1/3*c/Epc*(Epc/c*(c-
hc-f-tf1)-0.002)*(Epc/c*(c-hc-f-tf1)+2*0.002)/(Epc/c*(c-hc-f-
tf1)+0.002))+fac*bf*c/Epc*0.001*(c-hc-f-tf1-c/Epc*(Epc/c*(c-hc-f-tf1)-0.002)-
1/2*c/Epc*0.001)+1/2*(fac+Epc/c*(c-hc-f-tf1-hf)*Eac)*bf*c/Epc*(0.001-
Epc/c*(c-hc-f-tf1-hf))*(c-hc-f-tf1-hf+1/3*(hf-(c-hc-f-tf1-
c/Epc*0.001))*(2*0.001+Epc/c*(c-hc-f-tf1-hf))/(0.001+Epc/c*(c-hc-f-tf1-hf)));
```

```
             else
                if Epc/c*(c-hc-f-tf1-hf) < 0.002
                Mfn=1/2*(fac+(fac+Eacc*(Epc/c*(c-hc-f-tf1)-
0.002)))*bf*c/Epc*(Epc/c*(c-hc-f-tf1)-0.002)*(c-hc-f-tf1-1/3*c/Epc*(Epc/c*(c-
hc-f-tf1)-0.002)*(Epc/c*(c-hc-f-tf1)+2*0.002)/(Epc/c*(c-hc-f-
tf1)+0.002))+fac*bf*(hf-c/Epc*(Epc/c*(c-hc-f-tf1)-0.002))*(c-hc-f-tf1-
hf+1/2*(hf-c/Epc*(Epc/c*(c-hc-f-tf1)-0.002)));
                else
                Mfn=1/2*((fac+Eacc*(Epc/c*(c-hc-f-tf1)-
0.002))+(fac+Eacc*(Epc/c*(c-hc-f-tf1-hf)-0.002)))*be*ha*(c-hc-f-tf1-
hf/3*(Epc/c*(c-hc-f-tf1)+2*Epc/c*(c-hc-f-tf1-hf))/(Epc/c*(c-hc-f-
tf1)+Epc/c*(c-hc-f-tf1-hf)));
                end
             end
            end
          else
            if Epc/c*(c-hc-f-tf1) <= 0.001
             Mfn=1/2*Epc/c*(c-hc-f-tf1)*Eac*bf*(c-hc-f-tf1)*2/3*(c-hc-f-tf1);
            elseif  0.001 < Epc/c*(c-hc-f-tf1) <= 0.002
             Mfn=fac*bf*(c-hc-f-tf1-c/Epc*0.001)*(c-hc-f-tf1-1/2*(c-hc-f-tf1-
c/Epc*0.001))+1/2*fac*bf*c/Epc*0.001*2/3*c/Epc*0.001;
            else
             Mfn=1/2*(fac+(fac+Eacc*(Epc/c*(c-hc-f-tf1)-
0.002)))*bf*c/Epc*(Epc/c*(c-hc-f-tf1)-0.002)*(c-hc-f-tf1-1/3*c/Epc*(Epc/c*(c-
hc-f-tf1)-0.002)*(Epc/c*(c-hc-f-tf1)+2*0.002)/(Epc/c*(c-hc-f-
tf1)+0.002))+fac*bf*c/Epc*0.001*(c-hc-f-tf1-c/Epc*(Epc/c*(c-hc-f-tf1)-0.002)-
1/2*c/Epc*0.001)+1/2*fac*bf*c/Epc*0.001*2/3*c/Epc*0.001;
            end
          end
        else
            Mfn=0;
        end

        % Moment due to compressive force in arch concrete
        if  hc+f+tf1+hf < c
            if Epc/c*(c-hc-f-tf1-hf) <= 0.001
            Mac=1/2*Epc/c*(c-hc-f-tf1-hf)*Eac*be*(c-hc-f-tf1-hf)*2/3*(c-hc-f-
tf1-hf);
            elseif  0.001 < Epc/c*(c-hc-f-tf1-hf) <= 0.002
            Mac=fac*be*(c-hc-f-tf1-hf-c/Epc*0.001)*(c-hc-f-tf1-hf-
1/2*c/Epc*(Epc/c*(c-hc-f-tf1-hf)-
0.001))+1/2*fac*be*c/Epc*0.001*2/3*c/Epc*0.001;
            else
            Mac=1/2*(fac+(fac+Eacc*(Epc/c*(c-hc-f-tf1-hf)-
0.002)))*be*c/Epc*(Epc/c*(c-hc-f-tf1-hf)-0.002)*(c-hc-f-tf1-hf-
1/3*c/Epc*(Epc/c*(c-hc-f-tf1-hf)-0.002)*(Epc/c*(c-hc-f-tf1-
hf)+2*0.002)/(Epc/c*(c-hc-f-tf1-hf)+0.002))+fac*be*c/Epc*0.001*(c-hc-f-tf1-
hf-c/Epc*(Epc/c*(c-hc-f-tf1-hf)-0.002)-
1/2*c/Epc*0.001)+1/2*fac*be*c/Epc*0.001*2/3*c/Epc*0.001;
            end
        else
            Mac=0;
        end

        % Moment due to compressive force in arch steel
        if hc+f+d-has < c
```

```
   if Epc/c*(c-(hc+f+d-has)) < Ts
     Mas=Epc/c*(c-(hc+f+d-has))*Es*Aas*(c-(hc+f+d-has));
   else
     Mas=Fs*Aas*(c-(hc+f+d-has));
   end
else
Mas=0;
end

% Moment due to compressive force in arch CFRP
if hc+f+d-haf < c
   if Epc/c*(c-(hc+f+d-haf)) < Tf
     Maf=Epc/c*(c-(hc+f+d-haf))*Ef*Aaf*(c-(hc+f+d-haf));
   else
     Maf=Ff*Aaf*(c-(hc+f+d-haf));
   end
else
 Maf=0;
end

MC=Mc+Ms+Msb+Mf+Mfl+Mw+Mfn+Mac+Mas+Maf;

% Moment due to tensile forces:

% Moment due to tensile force in arch steel
if c < hc+f+d-has
 if Epc/c*(hc+f+d-c-has) < Ts
    MTas=Epc/c*(hc+f+d-c-has)*Es*Aas*(hc+f+d-c-has);
 else
    MTas=Fs*Aas*(hc+f+d-c-has);
 end
else
    MTas=0;
end

% Moment due to tensile force in arch CFRP
if c < hc+f+d-haf
 if Epc/c*(hc+f+d-c-haf) < Tf
    MTaf=Epc/c*(hc+f+d-c-haf)*Ef*Aaf*(hc+f+d-c-haf);
 else
    MTaf=0;
 end
else
    MTaf=0;
end

% Moment due to tensile force in tension reinforcement (steel
strands)
if Epc/c*(hc+f+d-c-hs) < Tst
    MTss=Epc/c*(hc+f+d-c-hs)*Est*Ast*(hc+f+d-c-hs);
else
    MTss=Fst*Ast*(hc+f+d-c-hs);
end

% Moment due to tensile force in bottom HCB flange
```

```
        if Epc/c*(hc+f+d-c) < Tef
            MTbf=Epc/c*(hc+f+d-c-tf2/2)*Eef*b*tf2*(hc+f+d-c-tf2/2);
        else
            MTbf=0;
        end

        % Moment due to tensile force in HCB webs
        if Epc/c*(hc+f+d-c-tf2) < Te
            if c >= hc+f+tf1
             MTw=2*1/2*Epc/c*(hc+f+d-c-tf2)*Ee*tw*(hc+f+d-c-tf2)*2/3*(hc+f+d-
c-tf2);
            else
             MTw=2*Epc/c*(hc+f+d-c-tf2-1/2*(d-tf1-tf2))*Ee*tw*(d-tf1-
tf2)*(hc+f+d-c-tf2-1/3*(d-tf1-tf2)*(Epc/c*(hc+f+d-c-tf2)+2*Epc/c*(hc+f+d-c-
tf2-(d-tf1-tf2)))/(Epc/c*(hc+f+d-c-tf2)+Epc/c*(hc+f+d-c-tf2-(d-tf1-tf2))));
            end
        else
            MTw=0;
        end

        MT=MTas+MTaf+MTss+MTbf+MTw;

 else

        % Moment due to compressive forces:

        % Strain in top slab steel
          Eps=Epc/c*(c-db);
        % Strain in bottom slab steel
          Epsb=Epc/c*(c-dbb);
        % Strain in slab CFRP reinforcement
          Epf=Epc/c*(c-df);
        % Strain in arch steel
          Eas=Epc/c*(c-(hc+f+d-has));
        % Strain in arch CFRP reinforcement
          Eaf=Epc/c*(c-(hc+f+d-haf));

          Ecc=(0.85*fc-fc)/(0.003-0.002);
          Eacc=(0.85*fac-fac)/(0.003-0.002);

        % Moment due to compressive force in slab concrete
        if Epc <= 0.001
            Mc=1/2*Epc*Ec*bc*c*2/3*c;
        elseif  0.001 < Epc <= 0.002
            Mc=fc*bc*c/Epc*(Epc-0.001)*(c-1/2*c/Epc*(Epc-
0.001))+1/2*fc*bc*c/Epc*0.001*2/3*c/Epc*0.001;
        else
            Mc=1/2*((fc+Ecc*(Epc-0.002))+fc)*bc*c/Epc*(Epc-0.002)*(c-
1/3*c/Epc*(Epc-
0.002)*(Epc+2*0.002)/(Epc+0.002))+fc*bc*c/Epc*0.001*(1/2*c/Epc*0.001+c/Epc*0.
001)+1/2*fc*bc*c/Epc*0.001*2/3*c/Epc*0.001;
        end

        % Moment due to compressive force in top slab steel
        if c > db
```

```
 if Eps < Ts
    Ms=Eps*Es*As*(c-db);
 else
    Ms=Fs*As*(c-db);
 end
else
 Ms=0;
end

% Moment due to compressive force in bottom slab steel
if c > dbb
 if Epsb < Ts
    Msb=Epsb*Es*Asb*(c-dbb);
 else
    Msb=Fs*Asb*(c-dbb);
 end
else
 Msb=0;
end

% Moment due to compressive force in slab CFRP reinforcement
if c > df
 if Epf < Tf
    Mf=Epf*Ef*Af*(c-df);
 else
    Mf=0;
 end
else
 Mf=0;
end

MC=Mc+Ms+Msb+Mf;

% Moment due to tensile forces:

% Moment due to tensile force in bottom slab steel
if c < dbb
 if Epc/c*(dbb-c) < Ts
    MTsb=Epc/c*(dbb-c)*Es*Asb*(dbb-c);
 else
    MTsb=Fs*Asb*(dbb-c);
 end
else
 MTsb=0;
end

% Moment due to tensile force in top HCB flange
if Epc/c*(hc+f+d-c-(d-tf1)) < Tef
    MTtf=Epc/c*(hc+f+d-c-(d-tf1/2))*Eef*b*tf1*(hc+f+tf1/2-c);
else
    MTtf=0;
end

% Moment due to tensile force in bottom HCB flange
if Epc/c*(hc+f+d-c) < Tef
```

```
            MTbf=Epc/c*(hc+f+d-c-tf2/2)*Eef*b*tf2*(hc+f+d-c-tf2/2);
        else
            MTbf=0;
        end

        % Moment due to tensile force in arch CFRP
        if Epc/c*(hc+f+d-c-haf) < Tf
            MTaf=Epc/c*(hc+f+d-c-haf)*Ef*Aaf*(hc+f+d-c-haf);
        else
            MTaf=0;
        end

        % Moment due to tensile force in arch steel
        if Epc/c*(hc+f+d-c-has) < Ts
           MTas=Epc/c*(hc+f+d-c-has)*Es*Aas*(hc+f+d-c-has);
        else
           MTas=Ts*Aas*(hc+f+d-c-has);
        end

        % Moment due to tensile force in tension reinforcement (steel
strands)
        if Epc/c*(hc+f+d-c-hs) < Tst
            MTss=Epc/c*(hc+f+d-c-hs)*Est*Ast*(hc+f+d-c-hs);
        else
            MTss=Fst*Ast*(hc+f+d-c-hs);
        end

        % Moment due to tensile force in HCB webs
        if Epc/c*(hc+f+d-c-tf2) < Te
            MTw=2*Epc/c*(hc+f+d-c-tf2-(d-tf1-tf2)/2)*Ee*tw*(d-tf1-
tf2)*(hc+f+d-c-tf2-1/3*(d-tf1-tf2)*(Epc/c*(hc+f+d-c-tf2)+2*Epc/c*(hc+f+d-c-
d+tf1))/(Epc/c*(hc+f+d-c-tf2)+Epc/c*(hc+f+d-c-d+tf1)));
        else
            MTw=0;
        end

        MT=MTsb+MTtf+MTbf+MTaf+MTas+MTss+MTw;
  end

 Cy(1)=s;
 CF(1)=0;
 TF(1)=0;
 M(1)=0;
 Phi(1)=0;
 i=1+Epc/0.0001;
 i=round(i)

 Cy(i)=c
 CF(i)=C
 TF(i)=T
 M(i)=MC+MT
 Phi(i)=atan(Epc/c)

end
plot(Phi,M)
```

B.

The complete form of square matrix C used in Equations 28 & 29 is:

$$[C_{nn}] = \begin{bmatrix} -2 & 1 & 0 & 0 & 0 & \dots & \dots & 0 & 0 & 0 \\ 1 & -2 & 1 & 0 & 0 & \dots & \dots & 0 & 0 & 0 \\ 0 & 1 & -2 & 1 & 0 & \dots & \dots & 0 & 0 & 0 \\ 0 & 0 & 1 & -2 & 1 & \dots & \dots & 0 & 0 & 0 \\ 0 & 0 & 0 & 1 & -2 & \dots & \dots & 0 & 0 & 0 \\ \dots & \dots & \dots & \dots & \dots & \dots & \dots & \dots & \dots & \dots \\ \dots & \dots & \dots & \dots & \dots & \dots & \dots & \dots & \dots & \dots \\ 0 & 0 & 0 & 0 & 0 & \dots & \dots & -2 & 1 & 0 \\ 0 & 0 & 0 & 0 & 0 & \dots & \dots & 1 & -2 & 1 \\ 0 & 0 & 0 & 0 & 0 & \dots & \dots & 0 & 2 & -2 \end{bmatrix}$$

C.

Theoretical M-ϕ Curves for HCB Cross sections at Nodes

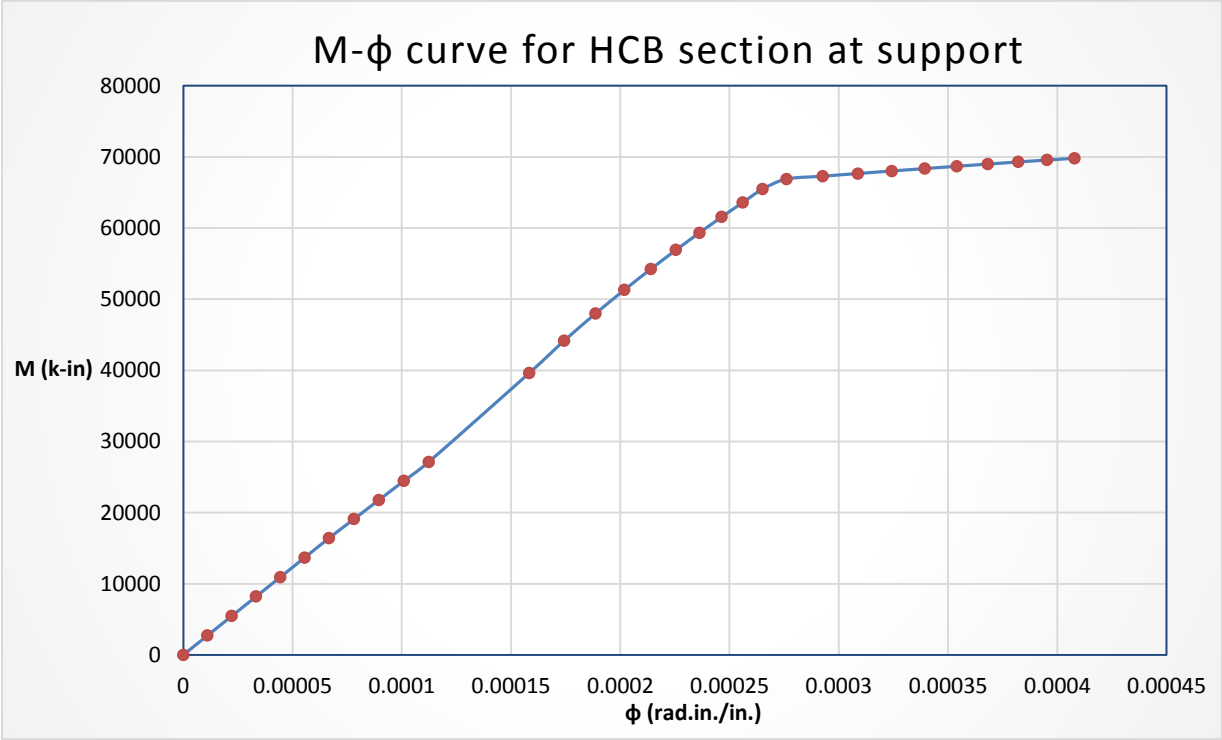

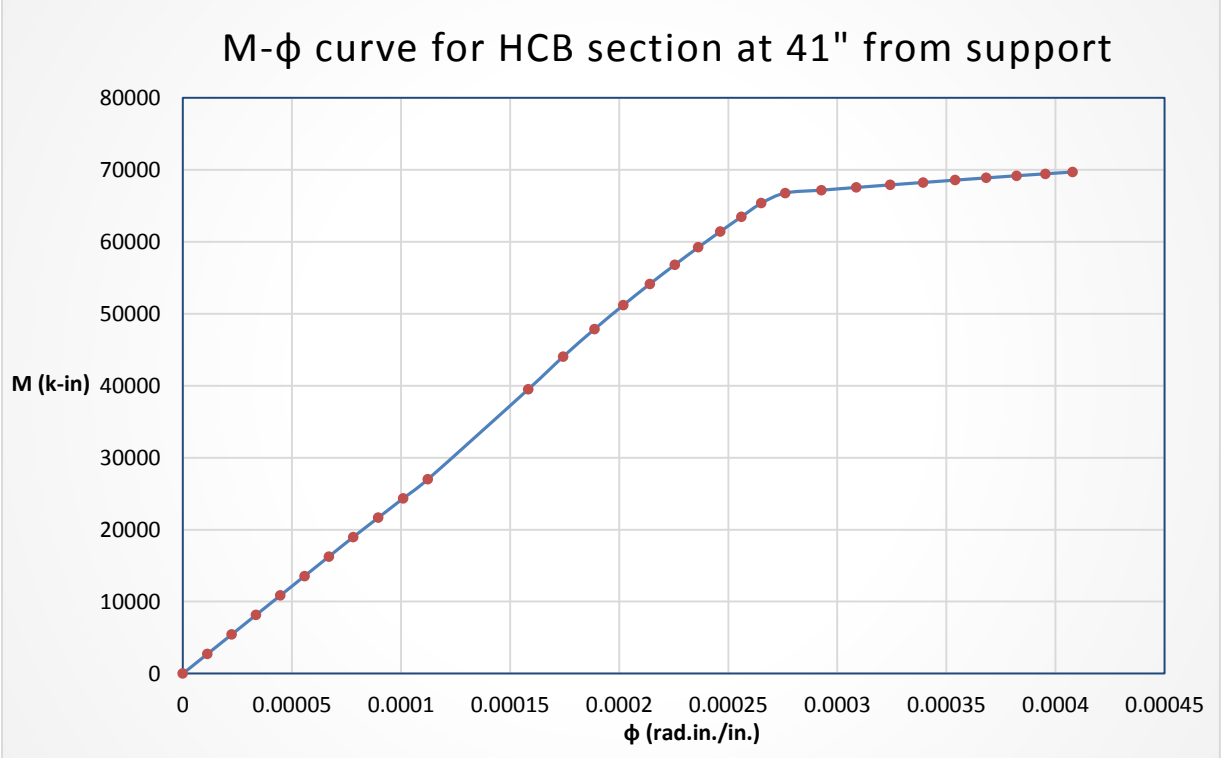

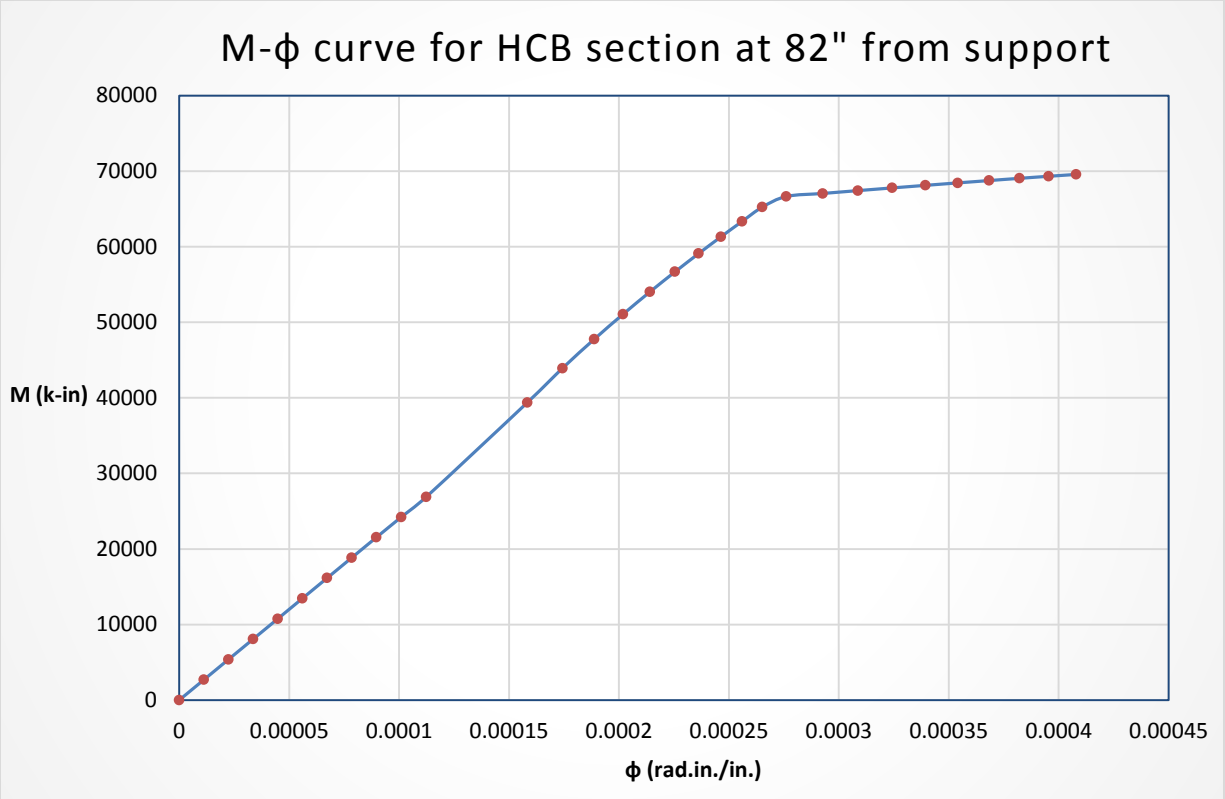
M-ϕ curve for HCB section at 82" from support
M (k-in)
80000
70000
60000
50000
40000
30000
20000
10000
0
0
0.00005
0.0001
0.00015
0.0002
0.00025
0.0003
0.00035
0.0004
0.00045
ϕ (rad.in./in.)

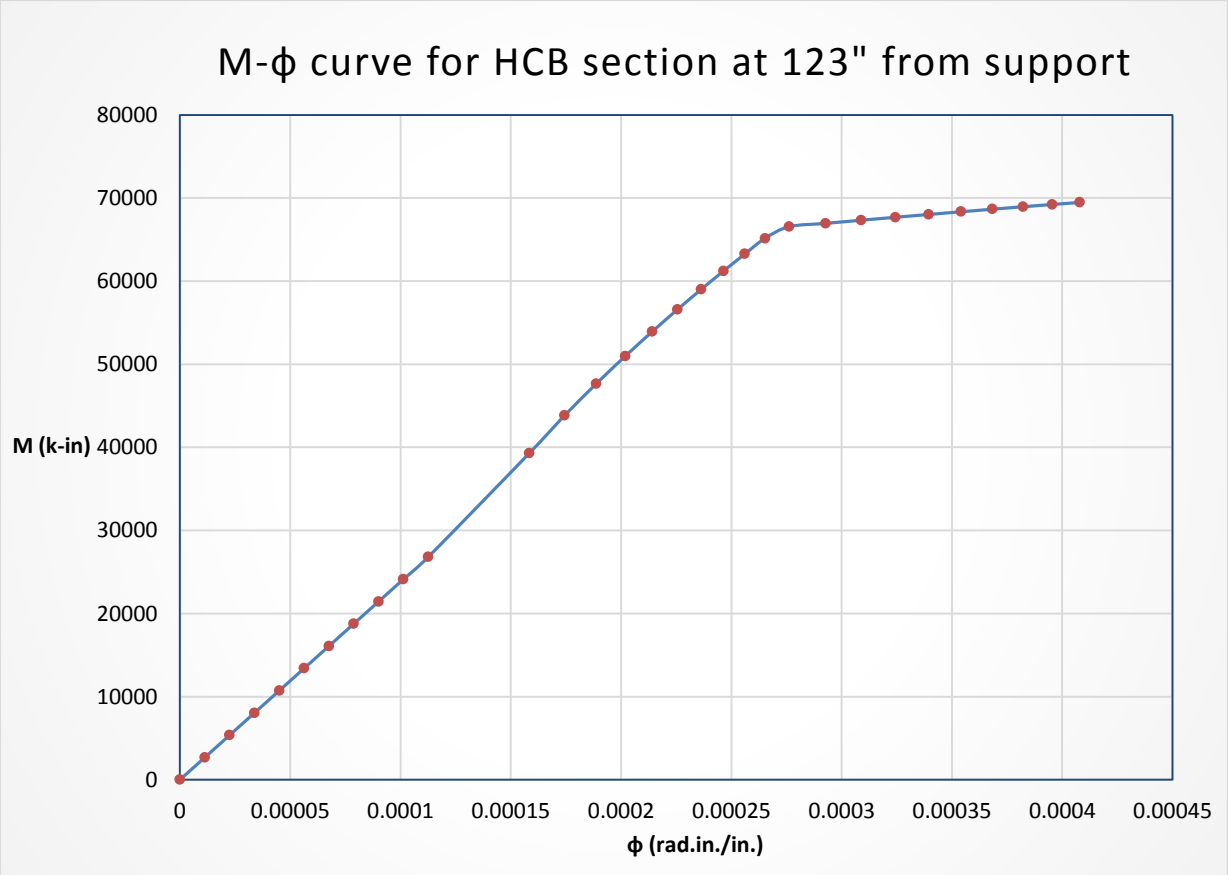
M-ϕ curve for HCB section at 123" from support
M (k-in)
80000
70000
60000
50000
40000
30000
20000
10000
0
0
0.00005
0.0001
0.00015
0.0002
0.00025
0.0003
0.00035
0.0004
0.00045
ϕ (rad.in./in.)

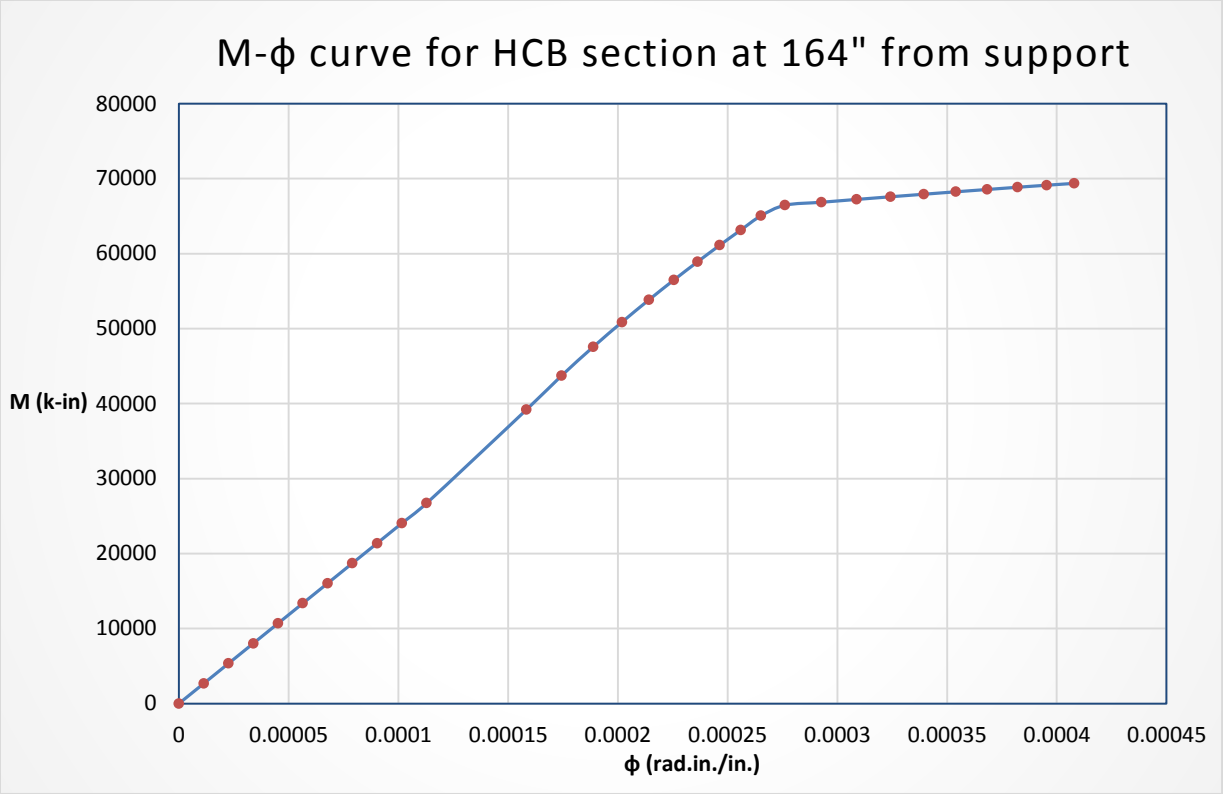
M-ϕ curve for HCB section at 164" from support
M (k-in)
80000
70000
60000
50000
40000
30000
20000
10000
0
0
0.00005
0.0001
0.00015
0.0002
0.00025
0.0003
0.00035
0.0004
0.00045
ϕ (rad.in./in.)

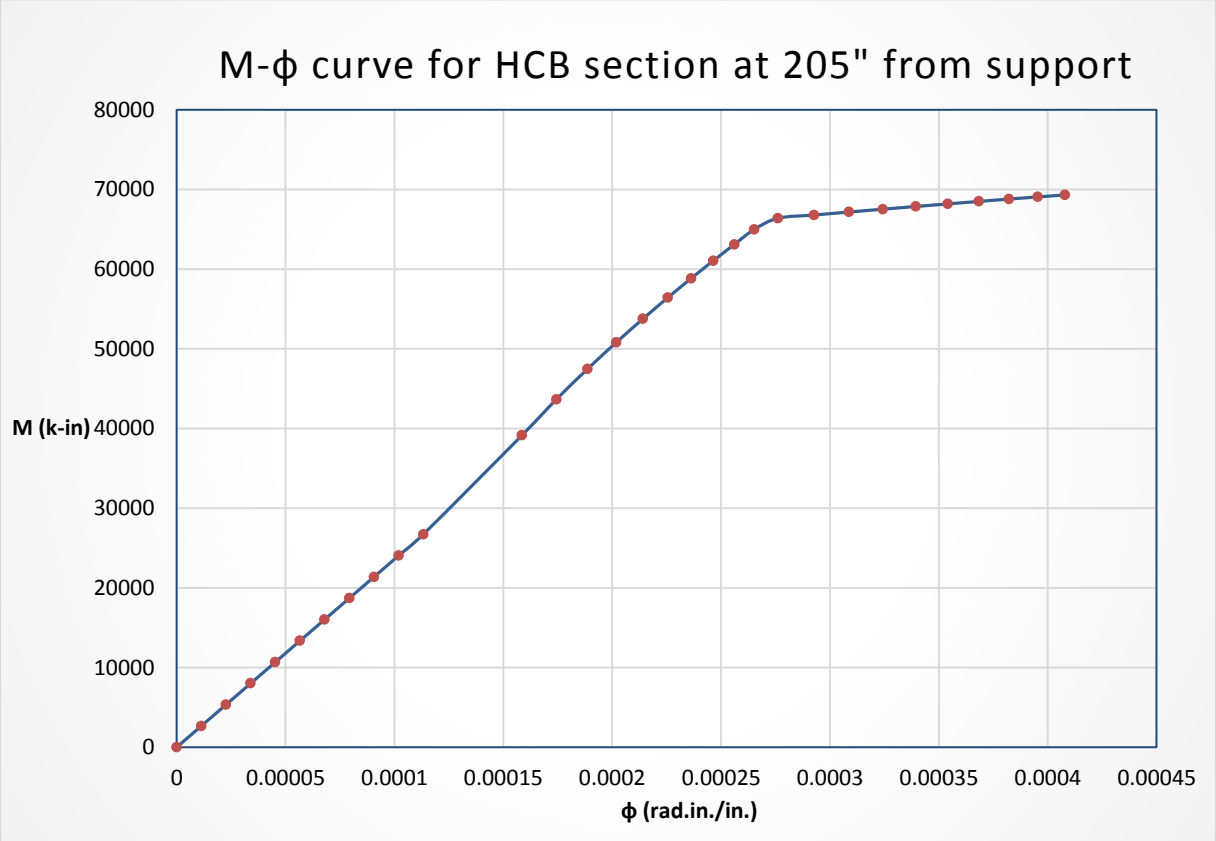
M-ϕ curve for HCB section at 205" from support
M (k-in)
80000
70000
60000
50000
40000
30000
20000
10000
0
0
0.00005
0.0001
0.00015
0.0002
0.00025
0.0003
0.00035
0.0004
0.00045
ϕ (rad.in./in.)

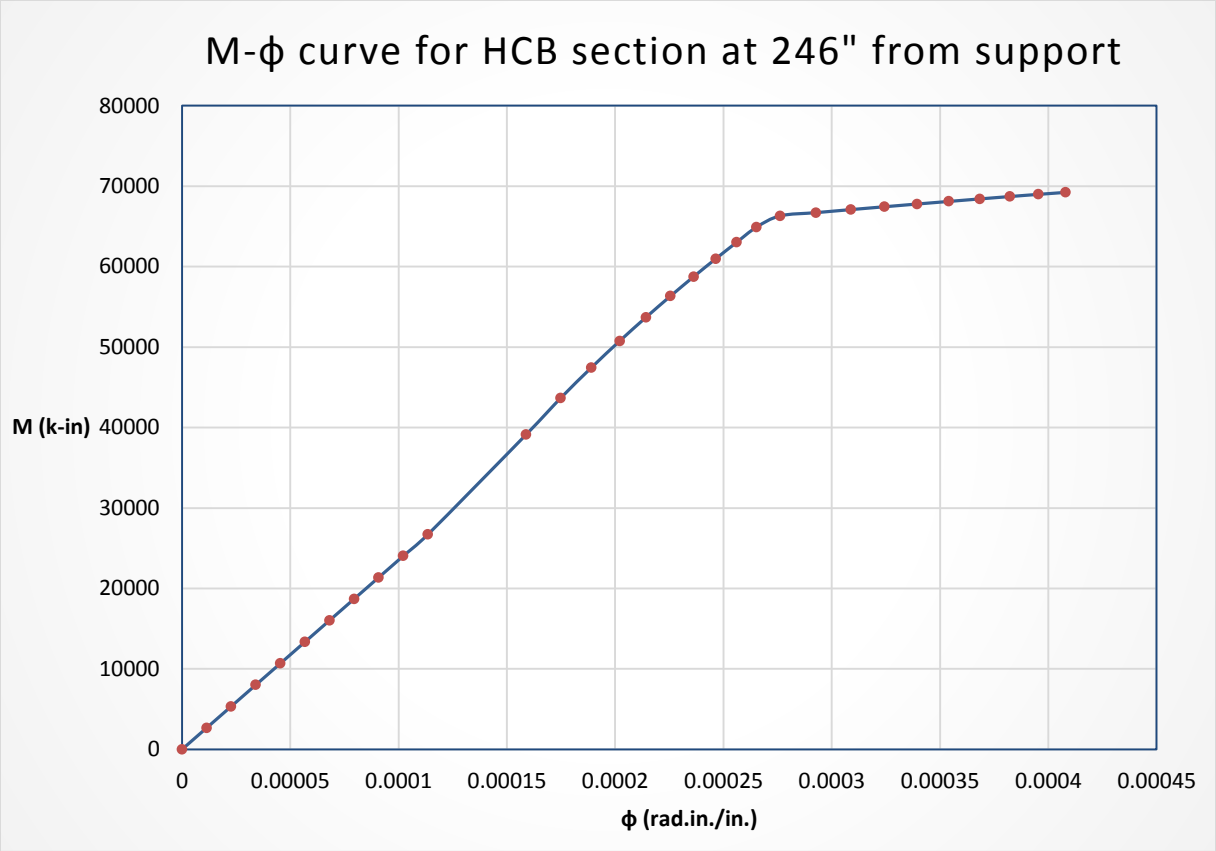
M-ϕ curve for HCB section at 246" from support
80000
70000
60000
50000
40000
30000
20000
10000
0
M (k-in)
0
0.00005
0.0001
0.00015
0.0002
0.00025
0.0003
0.00035
0.0004
0.00045
ϕ (rad.in./in.)

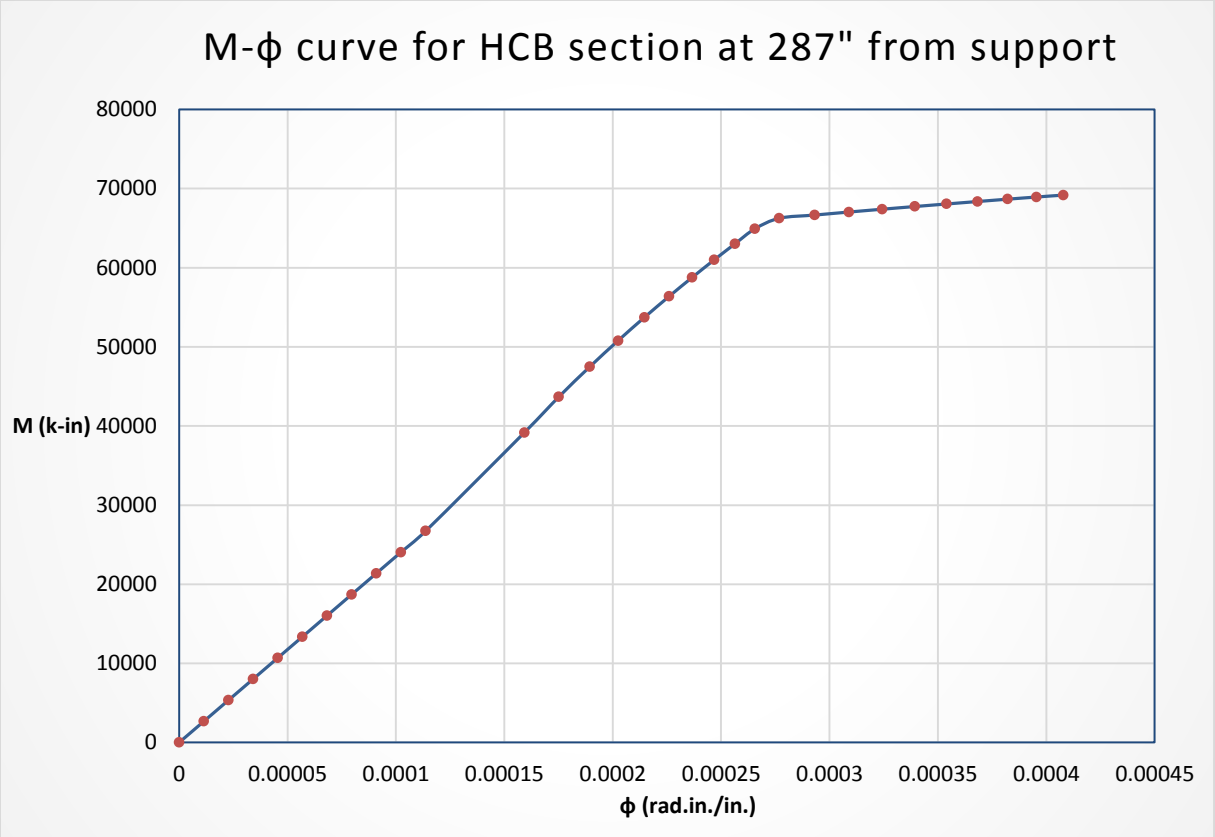
M-ϕ curve for HCB section at 287" from support
80000
70000
60000
50000
M (k-in) 40000
30000
20000
10000
0
0
0.00005
0.0001
0.00015
0.0002
0.00025
0.0003
0.00035
0.0004
0.00045
ϕ (rad.in./in.)

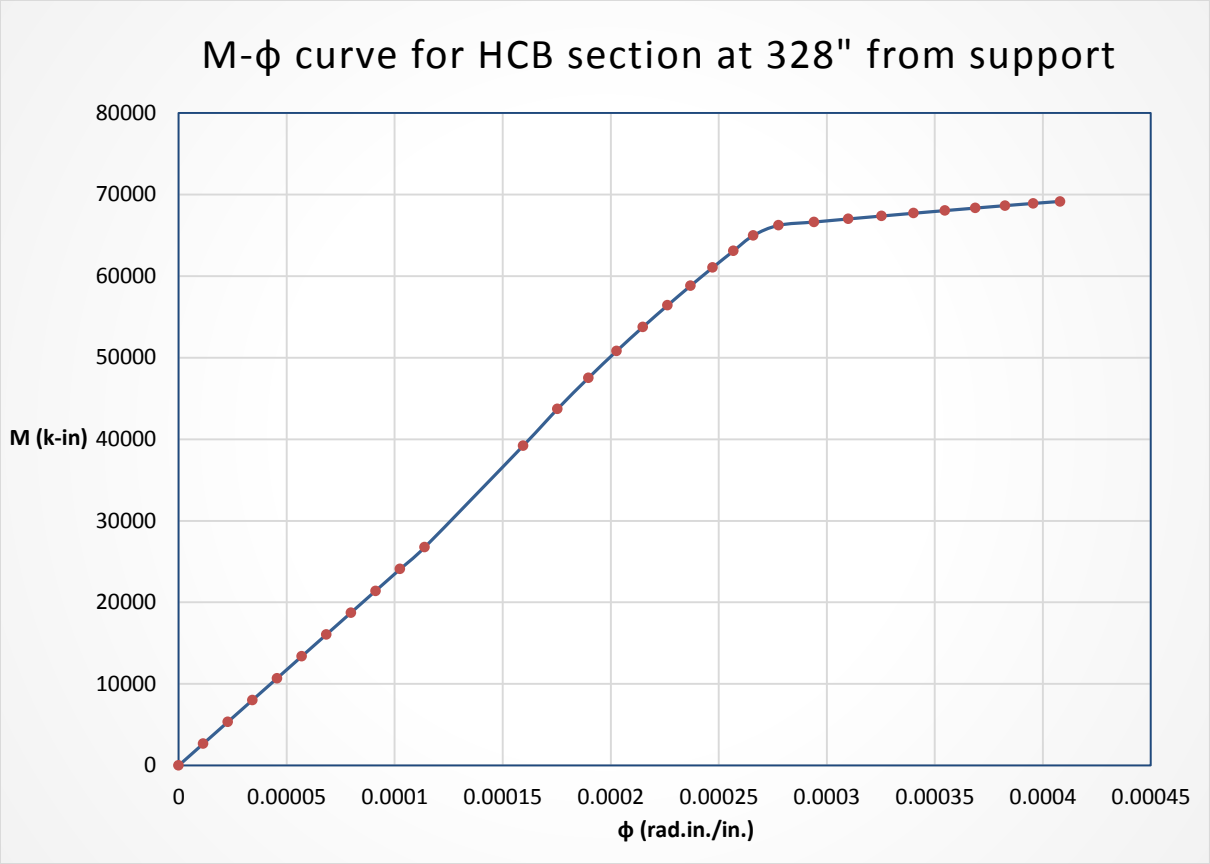
M-ϕ curve for HCB section at 328" from support
M (k-in)
80000
70000
60000
50000
40000
30000
20000
10000
0
0
0.00005
0.0001
0.00015
0.0002
0.00025
0.0003
0.00035
0.0004
0.00045
ϕ (rad.in./in.)

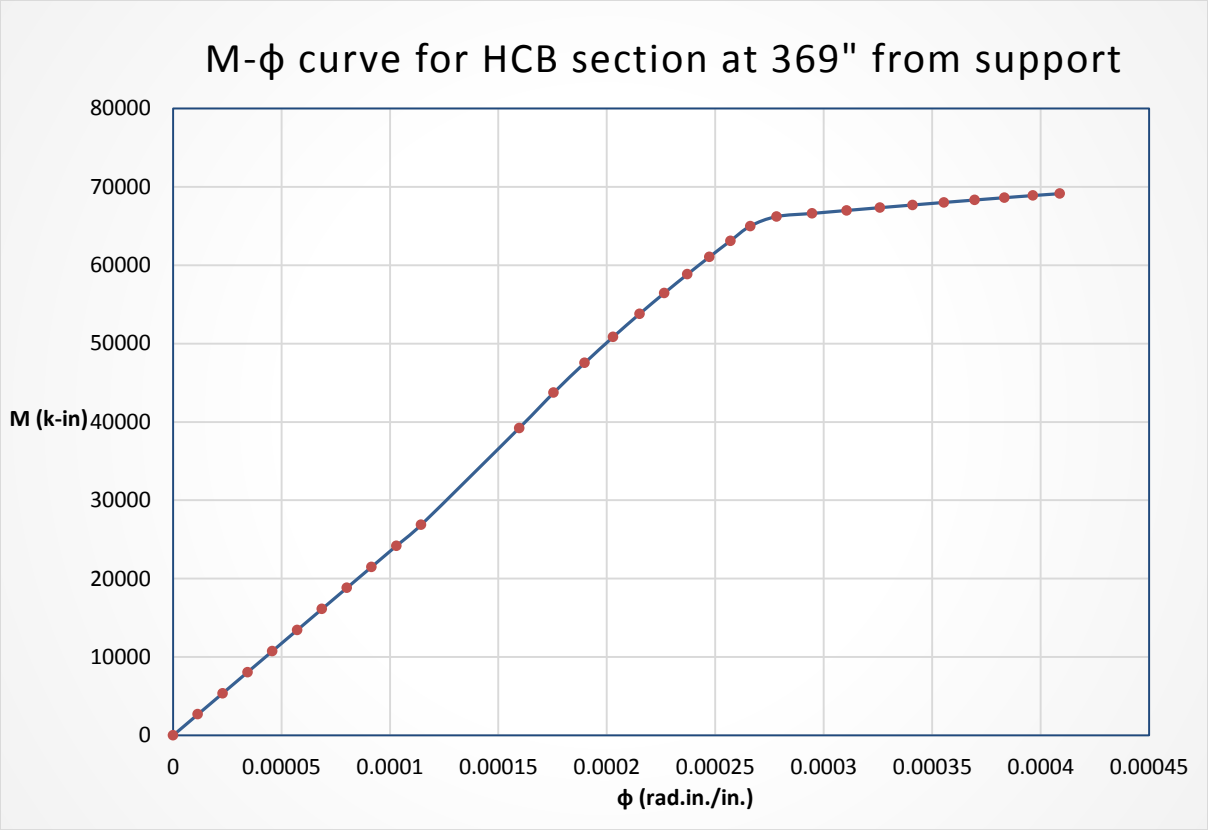
M-ϕ curve for HCB section at 369" from support
M (k-in)
80000
70000
60000
50000
40000
30000
20000
10000
0
0
0.00005
0.0001
0.00015
0.0002
0.00025
0.0003
0.00035
0.0004
0.00045
ϕ (rad.in./in.)

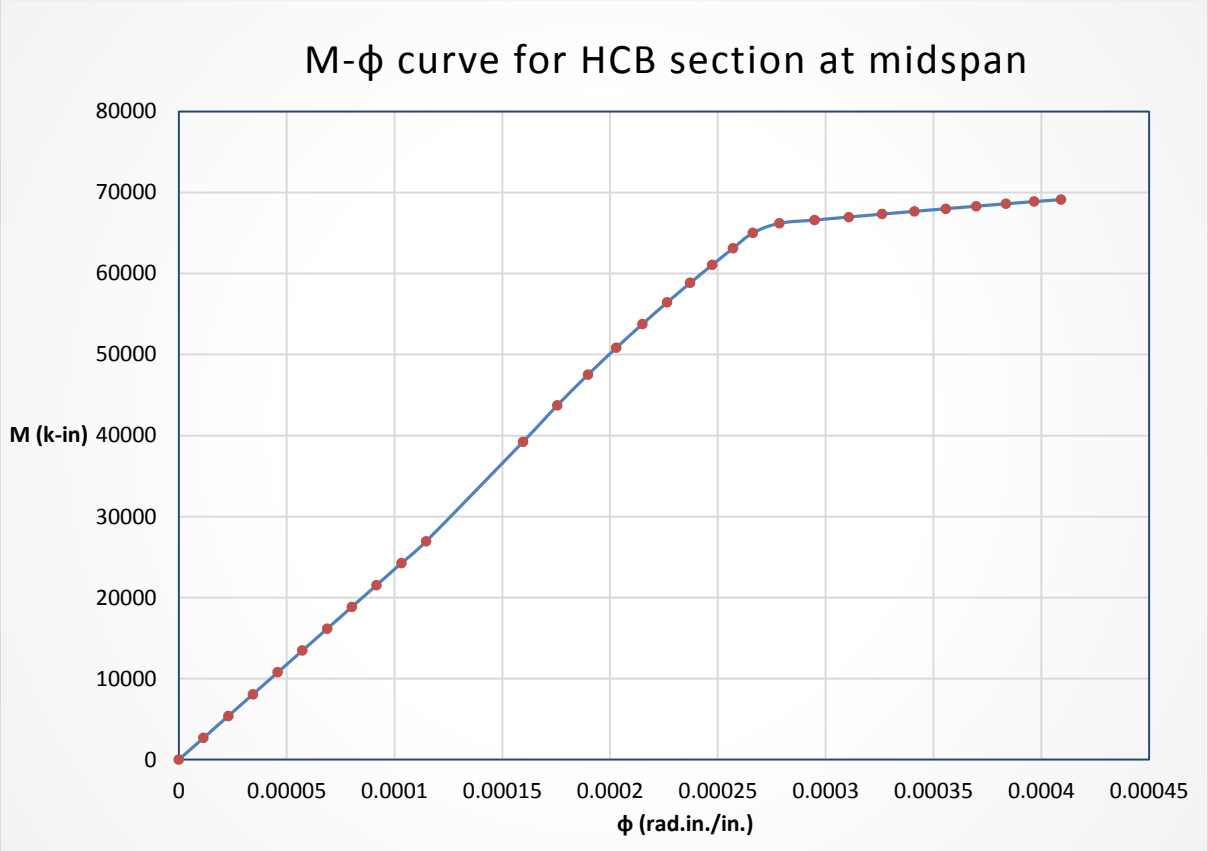
M-ϕ curve for HCB section at midspan
M (k-in)
80000
70000
60000
50000
40000
30000
20000
10000
0
0
0.00005
0.0001
0.00015
0.0002
0.00025
0.0003
0.00035
0.0004
0.00045
ϕ (rad.in./in.)

D.

a. Finite-difference Formulation of Curvature Equation for n = 10

The central difference equation for the finite-difference formulation of the curvature equation is:

$$\frac{d^2v_i}{dx^2} = \frac{v_{i-1} - 2v_i + v_{i+1}}{h^2}$$

$$\phi_i h^2 = v_{i-1} - 2v_i + v_{i+1}$$

Where $i = 1, 2, 3, \ldots, n$

For $n = 10$, we get following set of linear equations:

$$\phi_2 h^2 = v_1 - 2v_2 + v_3$$

$$\phi_3 h^2 = v_2 - 2v_3 + v_4$$

$$\phi_4 h^2 = v_3 - 2v_4 + v_5$$

$$\phi_5 h^2 = v_4 - 2v_5 + v_6$$

$$\phi_6 h^2 = v_5 - 2v_6 + v_7$$

$$\phi_7 h^2 = v_6 - 2v_7 + v_8$$

$$\phi_8 h^2 = v_7 - 2v_8 + v_9$$

$$\phi_9 h^2 = v_8 - 2v_9 + v_{10}$$

$$\phi_{10} h^2 = v_9 - 2v_{10} + v_{11}$$

The boundary condition and symmetry of loads gives:

$$v_1 = 0$$

$$v_9 = v_{11}$$

The first and the last equations in the above set would change to the following:

$\phi_2 h^2 = -2v_2 + v_3$

$\phi_{10} h^2 = 2v_9 - 2v_{10}$

The set of equations in matrix form will be:

$$h^2 \begin{Bmatrix} \phi_1 \\ \phi_2 \\ \phi_3 \\ \phi_4 \\ \phi_5 \\ \phi_6 \\ \phi_7 \\ \phi_8 \\ \phi_9 \\ \phi_{10} \end{Bmatrix} = \begin{bmatrix} -2 & 1 & 0 & 0 & 0 & 0 & 0 & 0 & 0 & 0 \\ 1 & -2 & 1 & 0 & 0 & 0 & 0 & 0 & 0 & 0 \\ 0 & 1 & -2 & 1 & 0 & 0 & 0 & 0 & 0 & 0 \\ 0 & 0 & 1 & -2 & 1 & 0 & 0 & 0 & 0 & 0 \\ 0 & 0 & 0 & 1 & -2 & 1 & 0 & 0 & 0 & 0 \\ 0 & 0 & 0 & 0 & 1 & -2 & 1 & 0 & 0 & 0 \\ 0 & 0 & 0 & 0 & 0 & 1 & -2 & 1 & 0 & 0 \\ 0 & 0 & 0 & 0 & 0 & 0 & 1 & -2 & 1 & 0 \\ 0 & 0 & 0 & 0 & 0 & 0 & 0 & 1 & -2 & 1 \\ 0 & 0 & 0 & 0 & 0 & 0 & 0 & 0 & 2 & -2 \end{bmatrix} \begin{Bmatrix} v_1 \\ v_2 \\ v_3 \\ v_4 \\ v_5 \\ v_6 \\ v_7 \\ v_8 \\ v_9 \\ v_{10} \end{Bmatrix}$$

The nodal deflections are given by the following matrix equation:

$$\begin{Bmatrix} v_1 \\ v_2 \\ v_3 \\ v_4 \\ v_5 \\ v_6 \\ v_7 \\ v_8 \\ v_9 \\ v_{10} \end{Bmatrix} = h^2 \begin{bmatrix} -2 & 1 & 0 & 0 & 0 & 0 & 0 & 0 & 0 & 0 \\ 1 & -2 & 1 & 0 & 0 & 0 & 0 & 0 & 0 & 0 \\ 0 & 1 & -2 & 1 & 0 & 0 & 0 & 0 & 0 & 0 \\ 0 & 0 & 1 & -2 & 1 & 0 & 0 & 0 & 0 & 0 \\ 0 & 0 & 0 & 1 & -2 & 1 & 0 & 0 & 0 & 0 \\ 0 & 0 & 0 & 0 & 1 & -2 & 1 & 0 & 0 & 0 \\ 0 & 0 & 0 & 0 & 0 & 1 & -2 & 1 & 0 & 0 \\ 0 & 0 & 0 & 0 & 0 & 0 & 1 & -2 & 1 & 0 \\ 0 & 0 & 0 & 0 & 0 & 0 & 0 & 1 & -2 & 1 \\ 0 & 0 & 0 & 0 & 0 & 0 & 0 & 0 & 2 & -2 \end{bmatrix}^{-1} \begin{Bmatrix} \phi_1 \\ \phi_2 \\ \phi_3 \\ \phi_4 \\ \phi_5 \\ \phi_6 \\ \phi_7 \\ \phi_8 \\ \phi_9 \\ \phi_{10} \end{Bmatrix}$$

Where *h = 41 in.*

b. Finite-difference Formulation of Curvature Equation for n = 10

The nodal deflections for *n=5,* are given by the following equation:

$$\begin{Bmatrix} v_2 \\ v_4 \\ v_6 \\ v_8 \\ v_{10} \end{Bmatrix} = h^2 \begin{bmatrix} -2 & 1 & 0 & 0 & 0 \\ 1 & -2 & 1 & 0 & 0 \\ 0 & 1 & -2 & 1 & 0 \\ 0 & 0 & 1 & -2 & 1 \\ 0 & 0 & 0 & 2 & -2 \end{bmatrix}^{-1} \begin{Bmatrix} \phi_2 \\ \phi_4 \\ \phi_6 \\ \phi_8 \\ \phi_{10} \end{Bmatrix}$$

Where *h = 82 in*.

E.

Theoretical M-ϕ Curves for HCB Cross sections without Concrete Slab

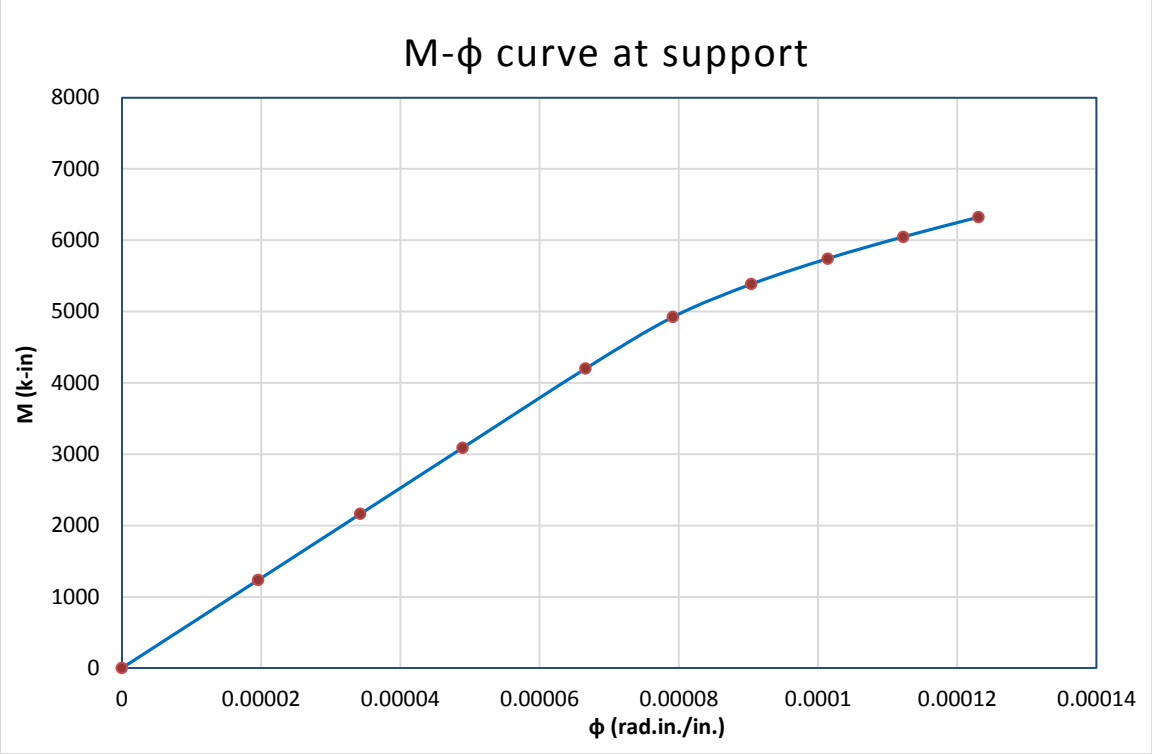

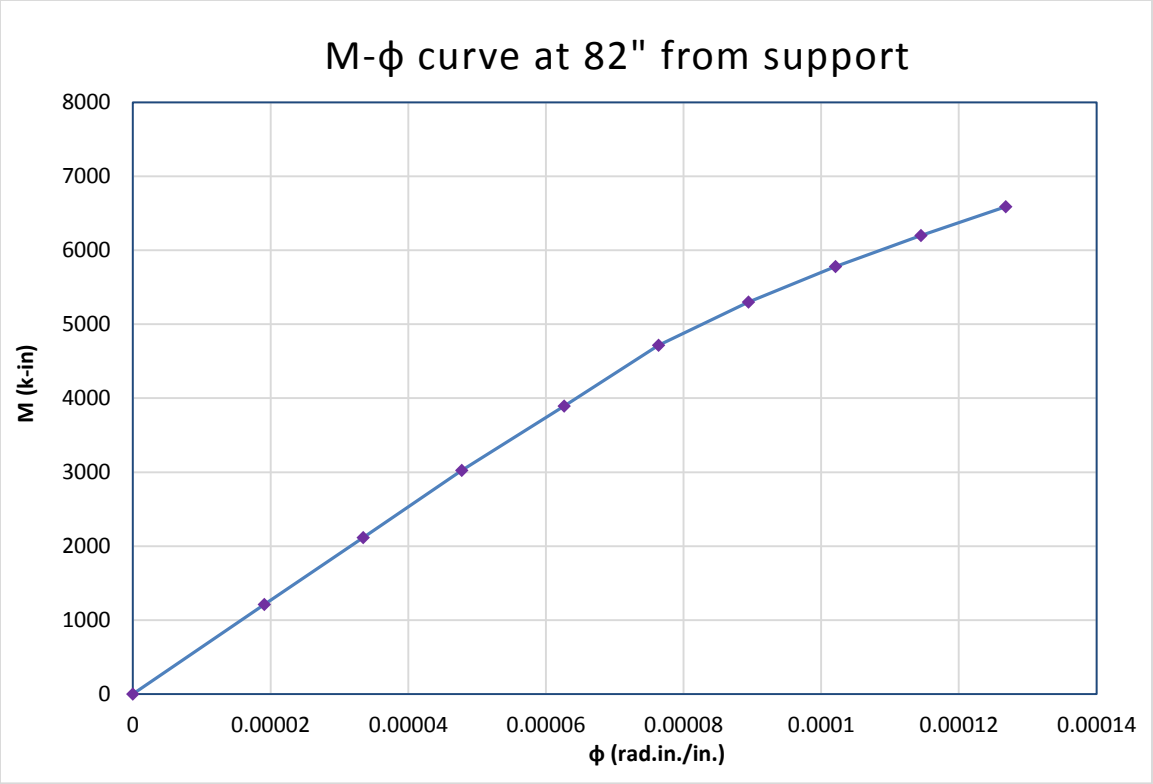
M-ϕ curve at 82" from support
8000
7000
6000
5000
4000
3000
2000
1000
0
M (k-in)
0
0.00002
0.00004
0.00006
0.00008
0.0001
0.00012
0.00014
ϕ (rad.in./in.)

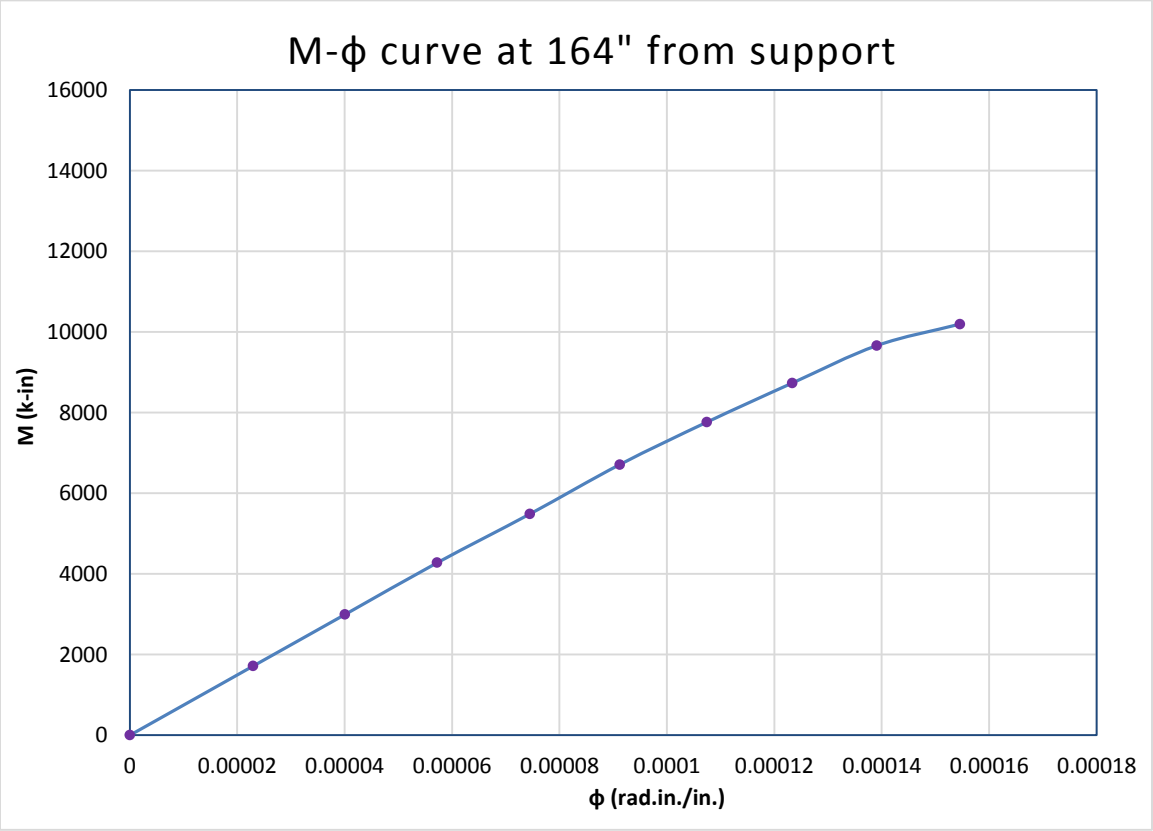
M-ϕ curve at 164" from support
16000
14000
12000
10000
8000
6000
4000
2000
0
M (k-in)
0
0.00002
0.00004
0.00006
0.00008
0.0001
0.00012
0.00014
0.00016
0.00018
ϕ (rad.in./in.)

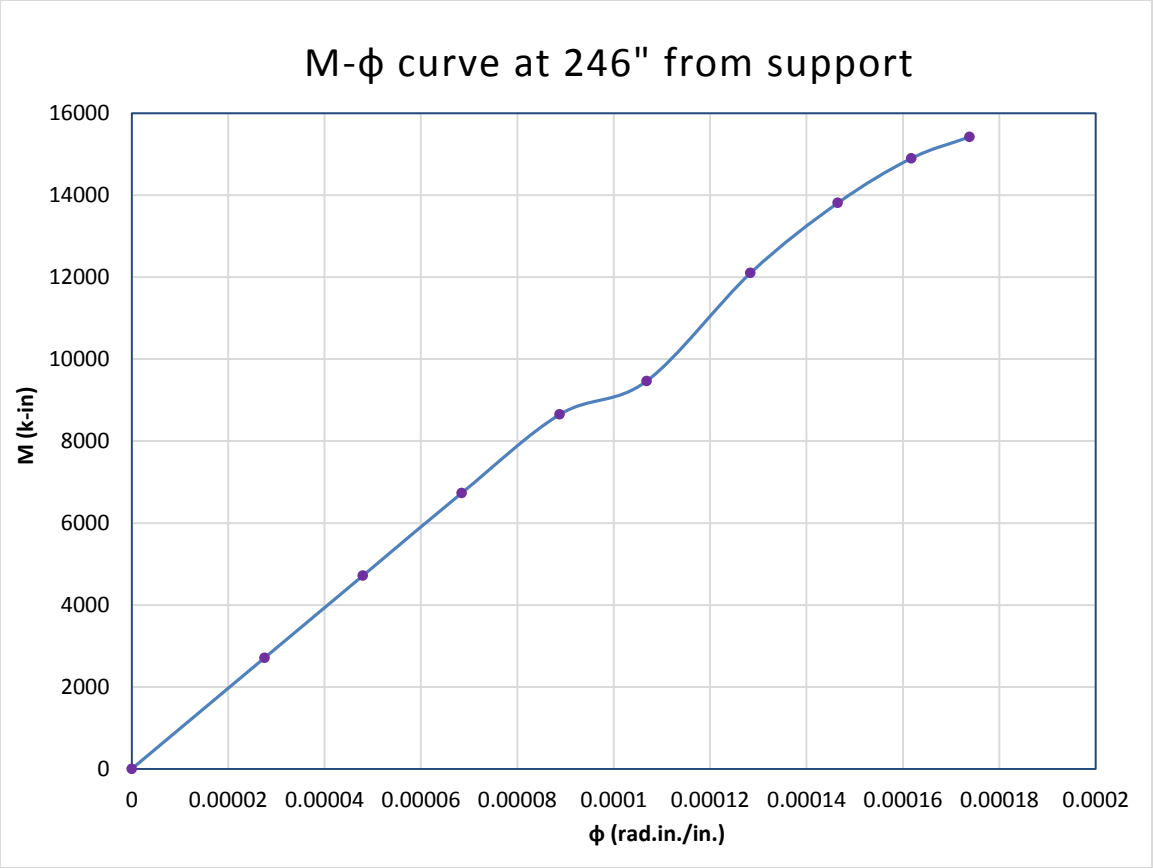
M-ϕ curve at 246" from support
16000
14000
12000
10000
8000
6000
4000
2000
0
M (k-in)
0
0.00002
0.00004
0.00006
0.00008
0.0001
0.00012
0.00014
0.00016
0.00018
0.0002
ϕ (rad.in./in.)

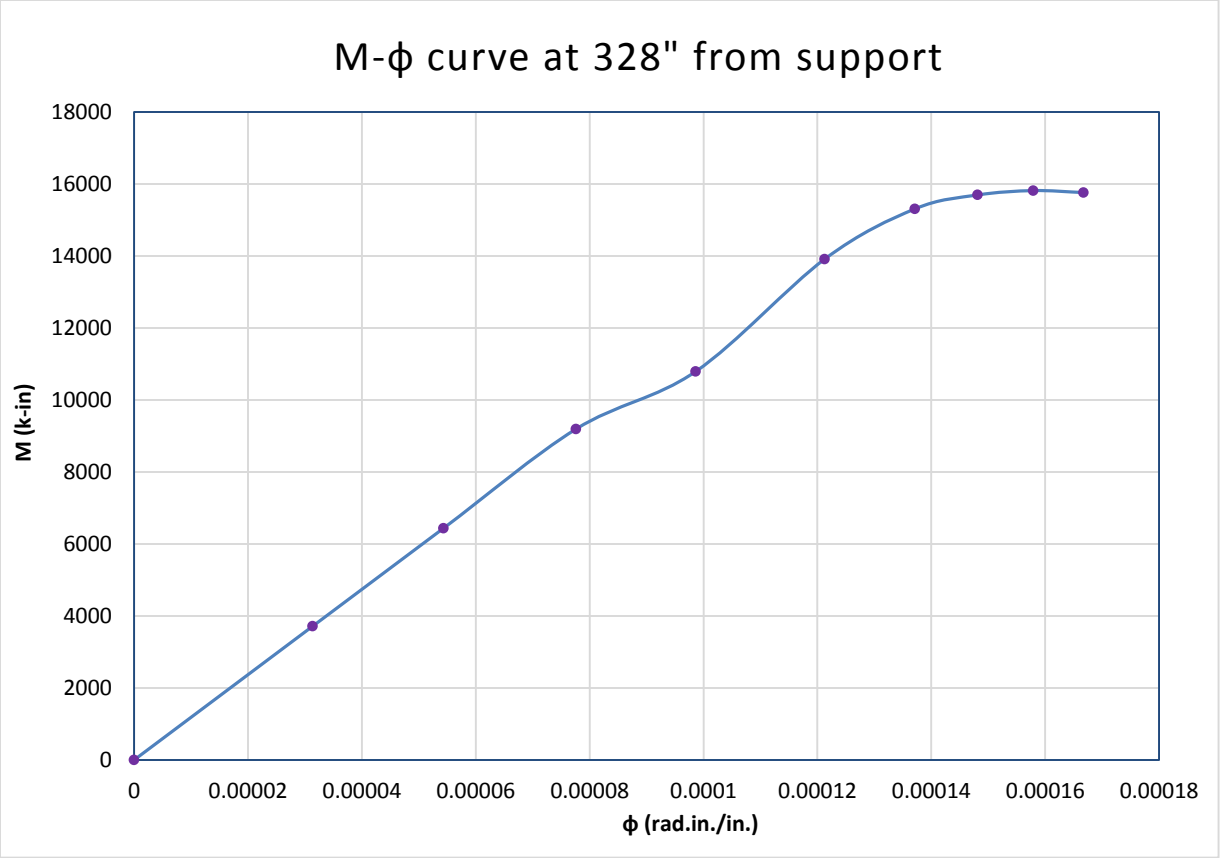
M-ϕ curve at 328" from support
18000
16000
14000
12000
10000
8000
6000
4000
2000
0
M (k-in)
0
0.00002
0.00004
0.00006
0.00008
0.0001
0.00012
0.00014
0.00016
0.00018
ϕ (rad.in./in.)

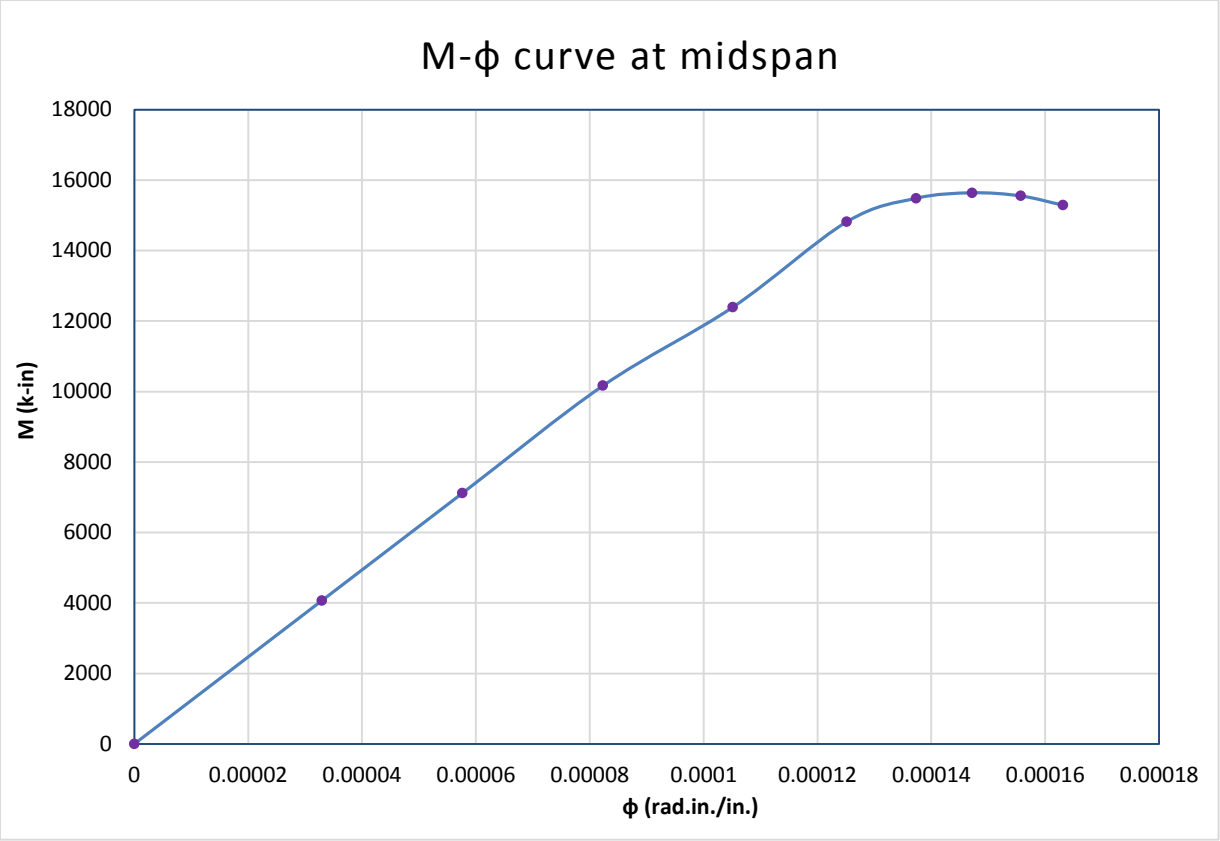
M-ϕ curve at midspan
M (k-in)
18000
16000
14000
12000
10000
8000
6000
4000
2000
0
0
0.00002
0.00004
0.00006
0.00008
0.0001
0.00012
0.00014
0.00016
0.00018
ϕ (rad.in./in.)

F.

Theoretical M-ϕ Curves for Prestressed HCB Cross sections without Concrete Slab

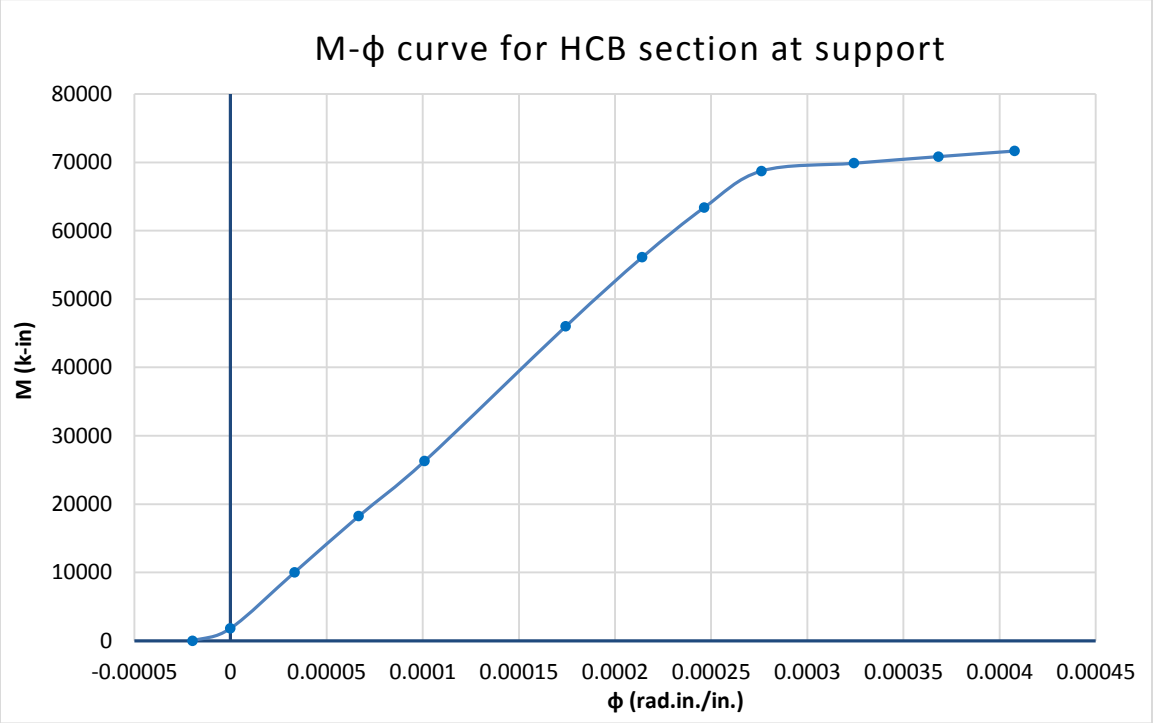

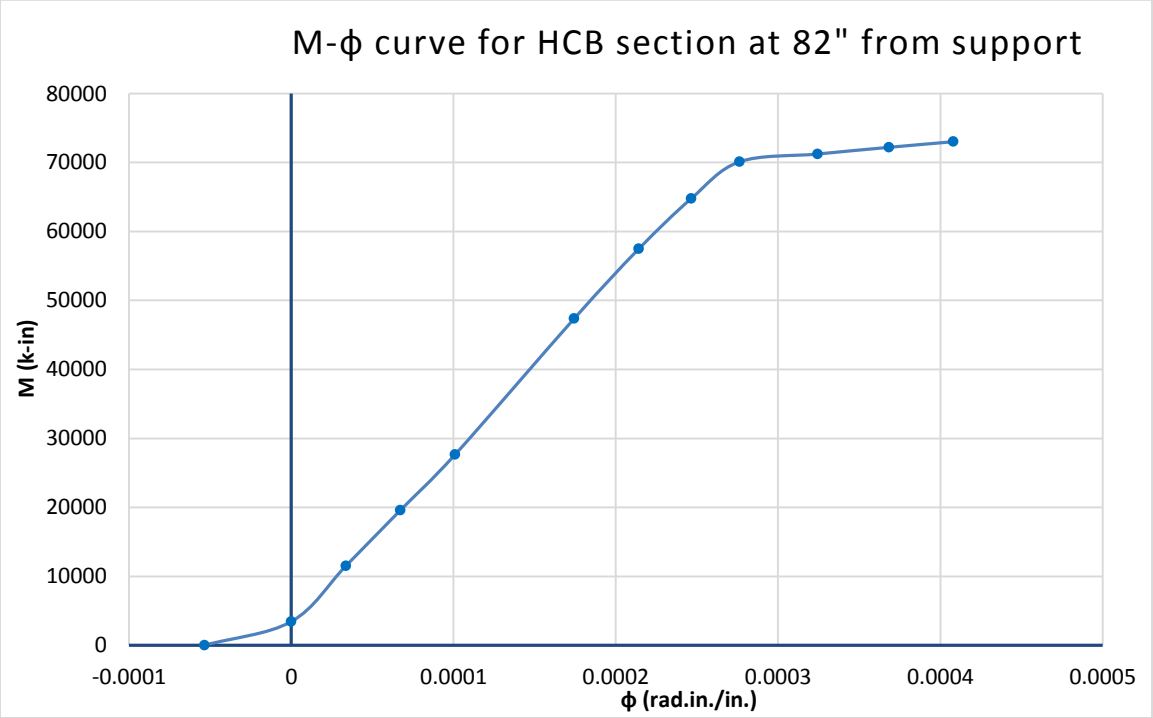

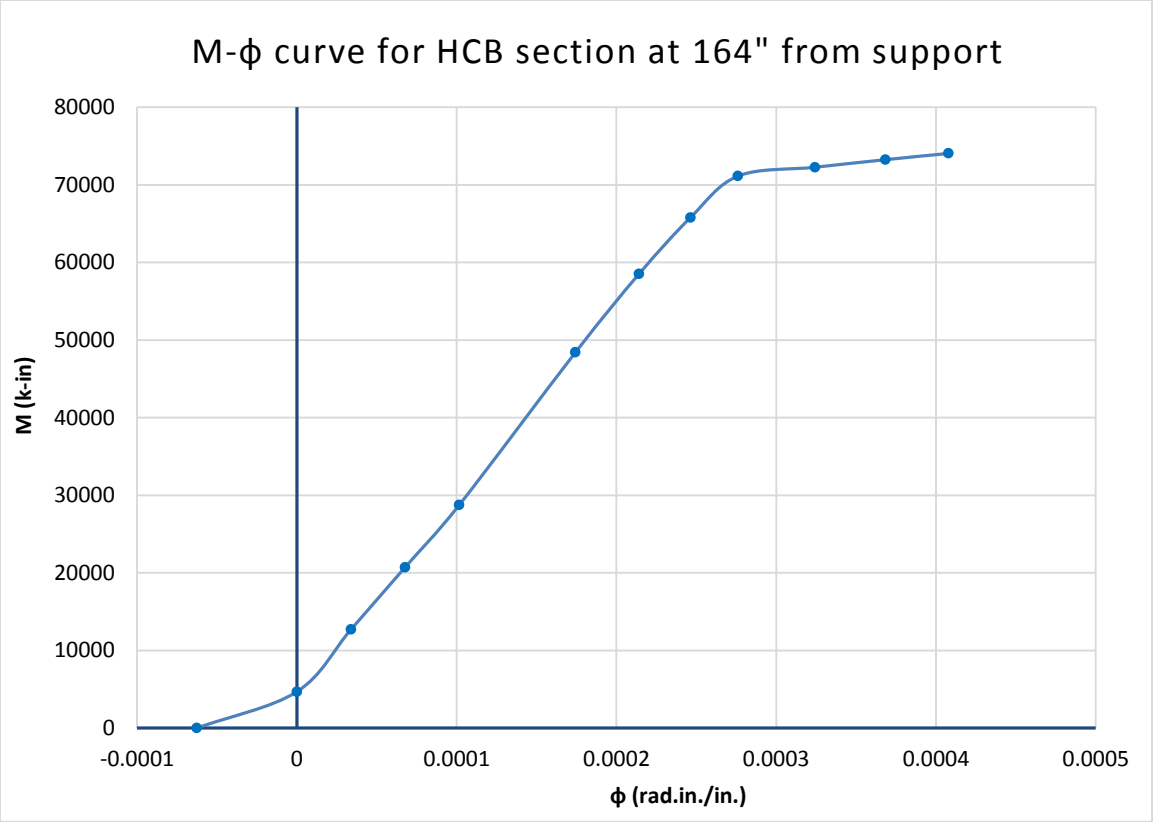
M-ϕ curve for HCB section at 164" from support
80000
70000
60000
50000
40000
30000
20000
10000
0
M (k-in)
-0.0001
0
0.0001
0.0002
0.0003
0.0004
0.0005
ϕ (rad.in./in.)

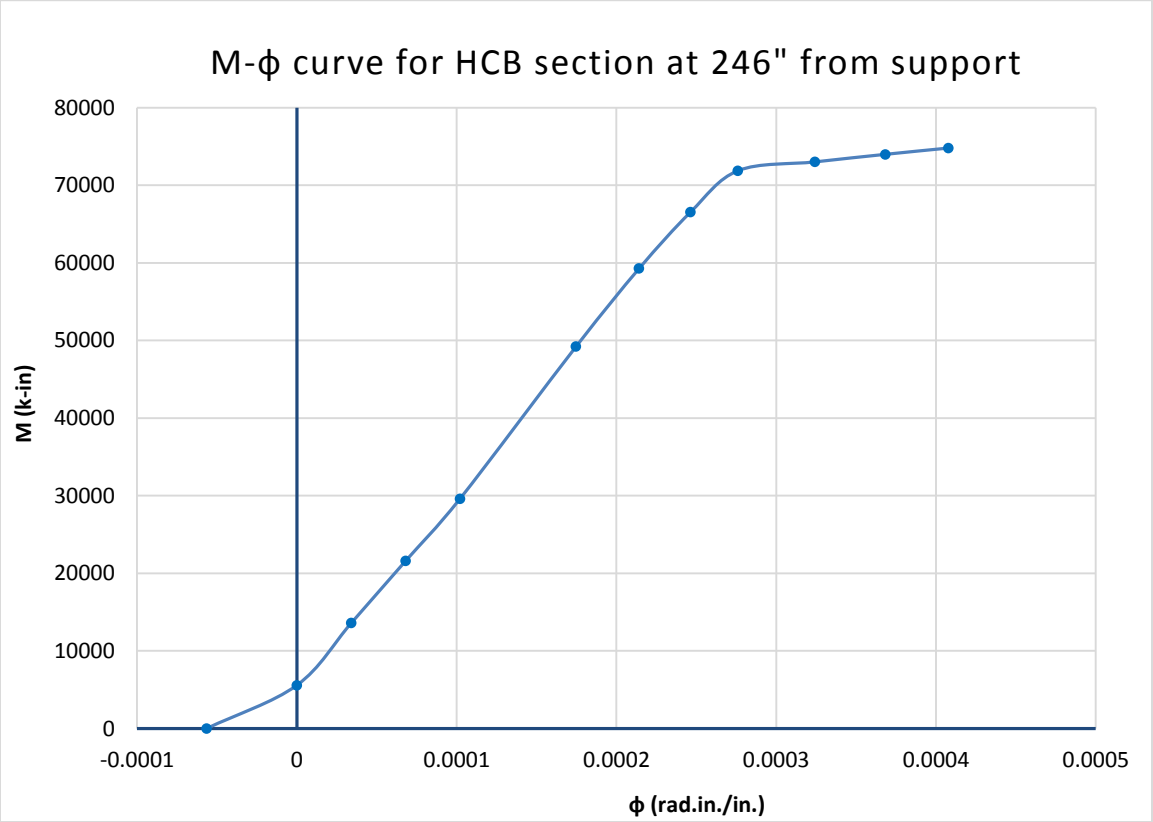
M-ϕ curve for HCB section at 246" from support
80000
70000
60000
50000
40000
30000
20000
10000
0
M (k-in)
-0.0001
0
0.0001
0.0002
0.0003
0.0004
0.0005
ϕ (rad.in./in.)

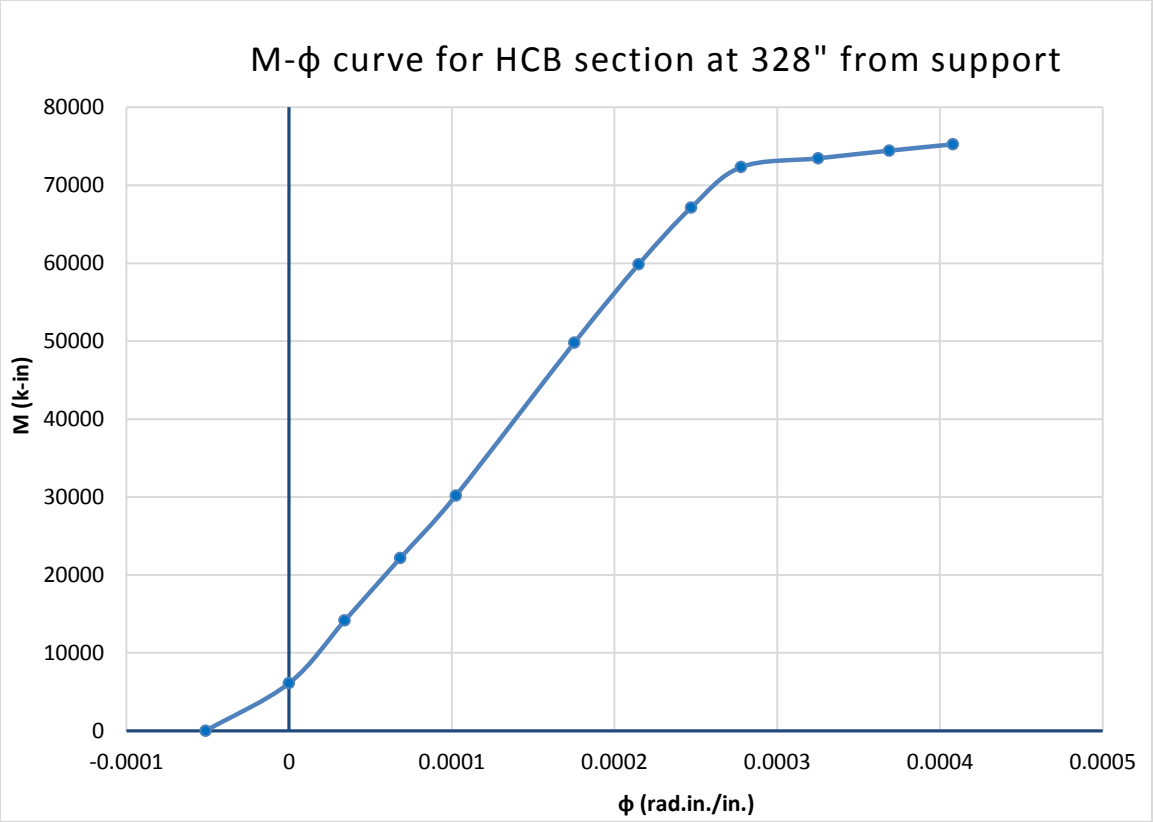
M-ϕ curve for HCB section at 328" from support
80000
70000
60000
50000
40000
30000
20000
10000
0
M (k-in)
-0.0001
0
0.0001
0.0002
0.0003
0.0004
0.0005
ϕ (rad.in./in.)

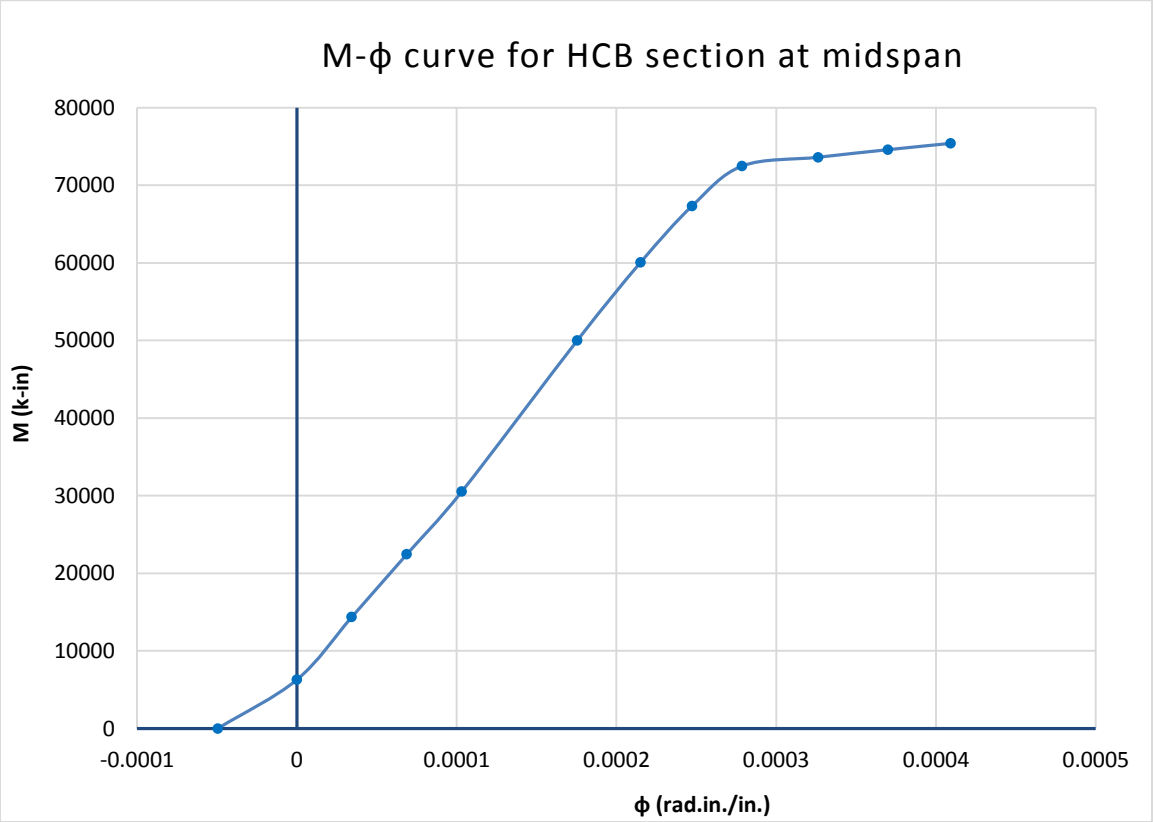
M-ϕ curve for HCB section at midspan
80000
70000
60000
50000
40000
30000
20000
10000
0
M (k-in)
-0.0001
0
0.0001
0.0002
0.0003
0.0004
0.0005
ϕ (rad.in./in.)

G.

Theoretical M-ϕ Curves for Prestressed HCB Cross sections with Concrete Slab

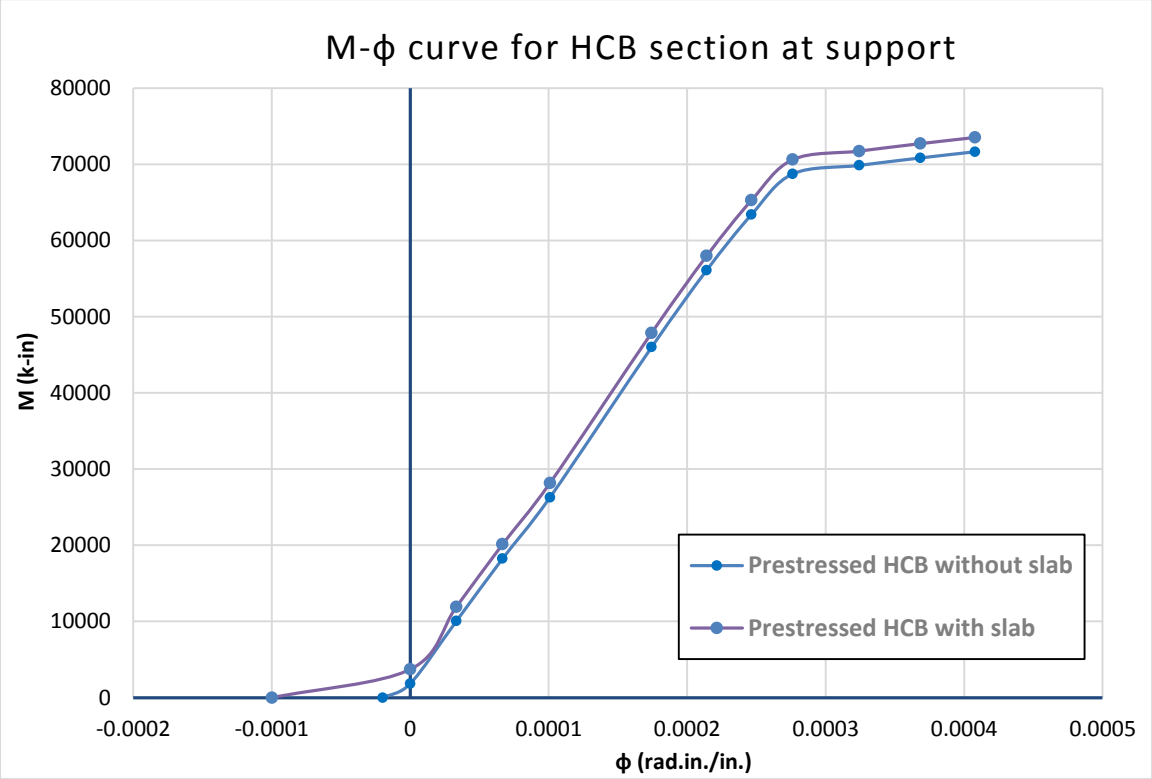

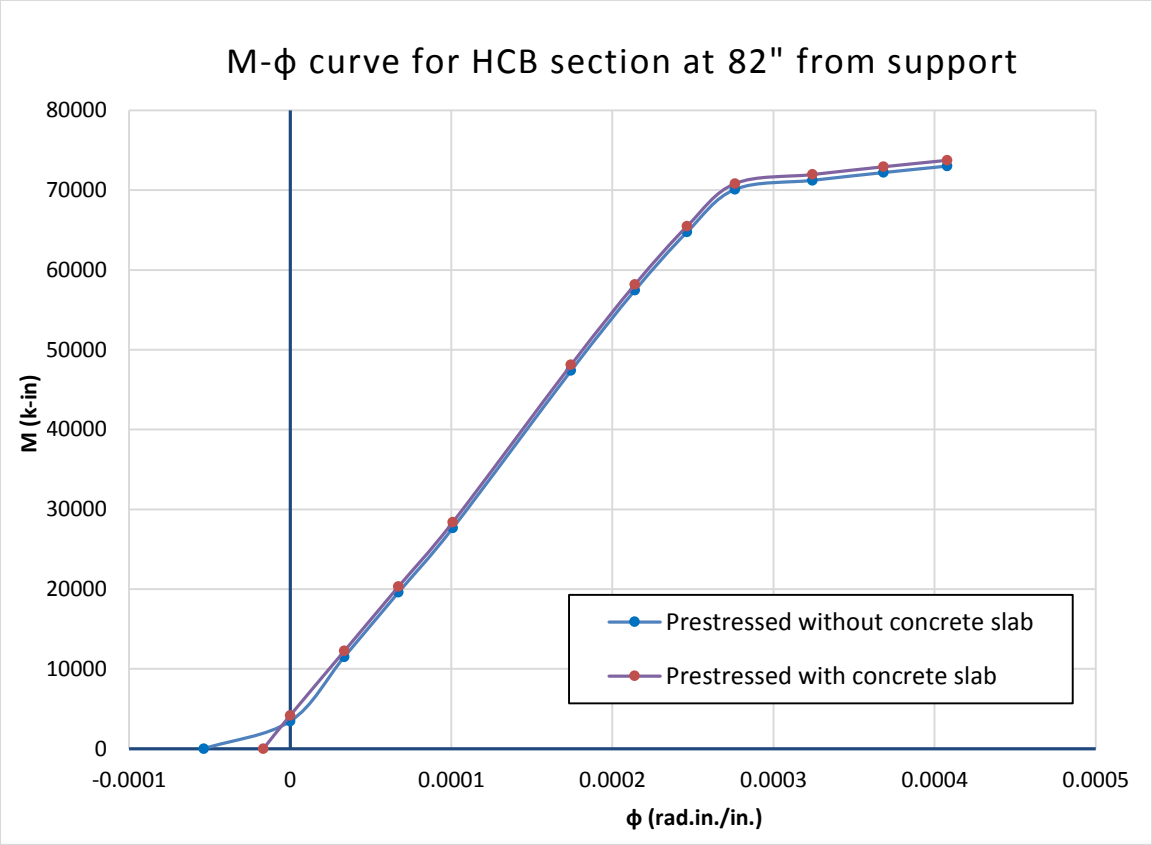
M-ϕ curve for HCB section at 82" from support
80000
70000
60000
50000
40000
30000
20000
10000
0
M (k-in)
-0.0001
0
0.0001
0.0002
0.0003
0.0004
0.0005
ϕ (rad.in./in.)
Prestressed without concrete slab
Prestressed with concrete slab

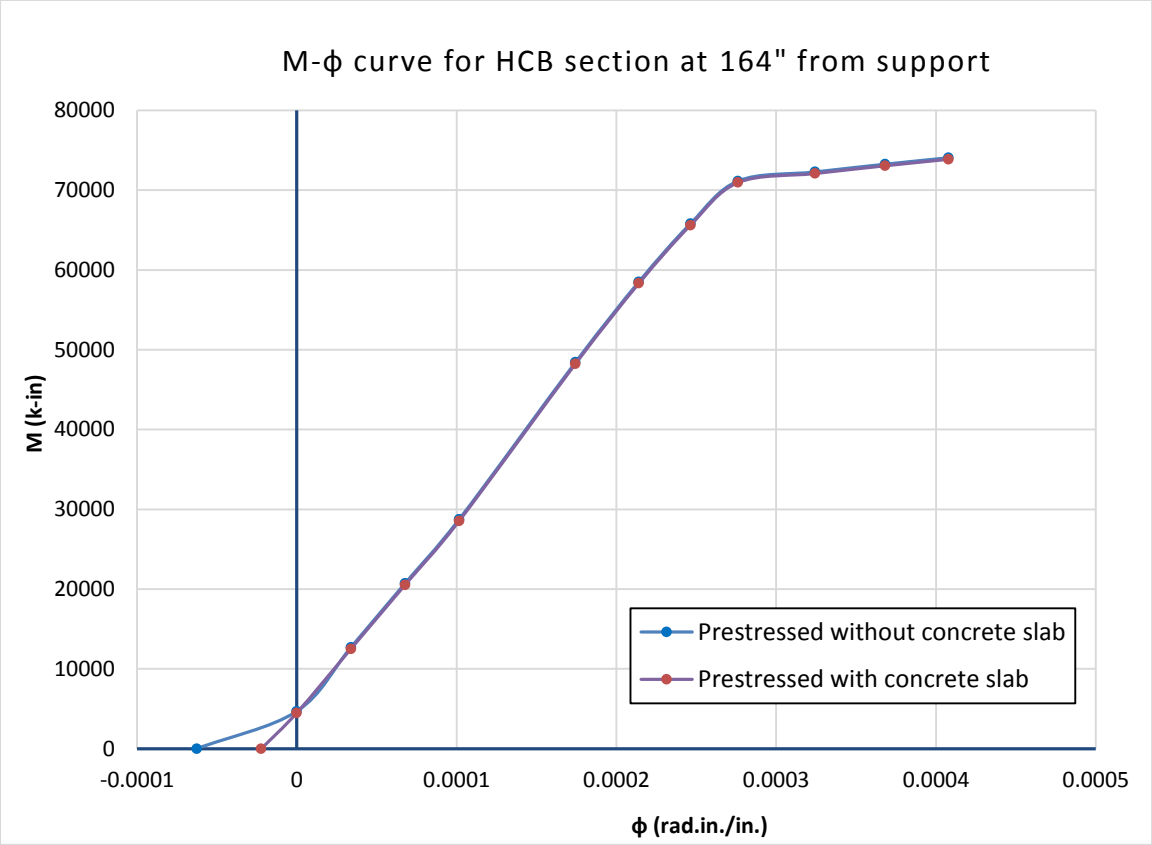
M-ϕ curve for HCB section at 164" from support
80000
70000
60000
50000
40000
30000
20000
10000
0
M (k-in)
-0.0001
0
0.0001
0.0002
0.0003
0.0004
0.0005
ϕ (rad.in./in.)
Prestressed without concrete slab
Prestressed with concrete slab

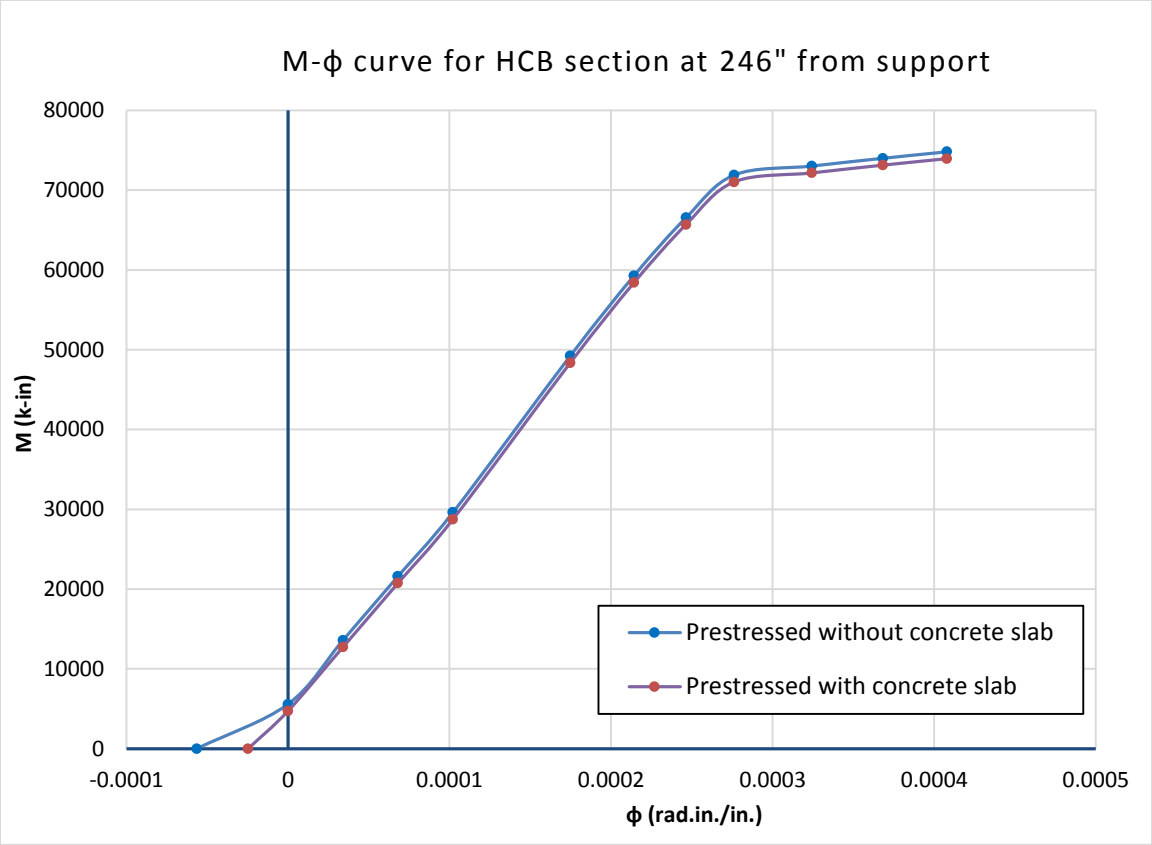
M-ϕ curve for HCB section at 246" from support
80000
70000
60000
50000
40000
30000
20000
10000
0
M (k-in)
-0.0001
0
0.0001
0.0002
0.0003
0.0004
0.0005
ϕ (rad.in./in.)
Prestressed without concrete slab
Prestressed with concrete slab

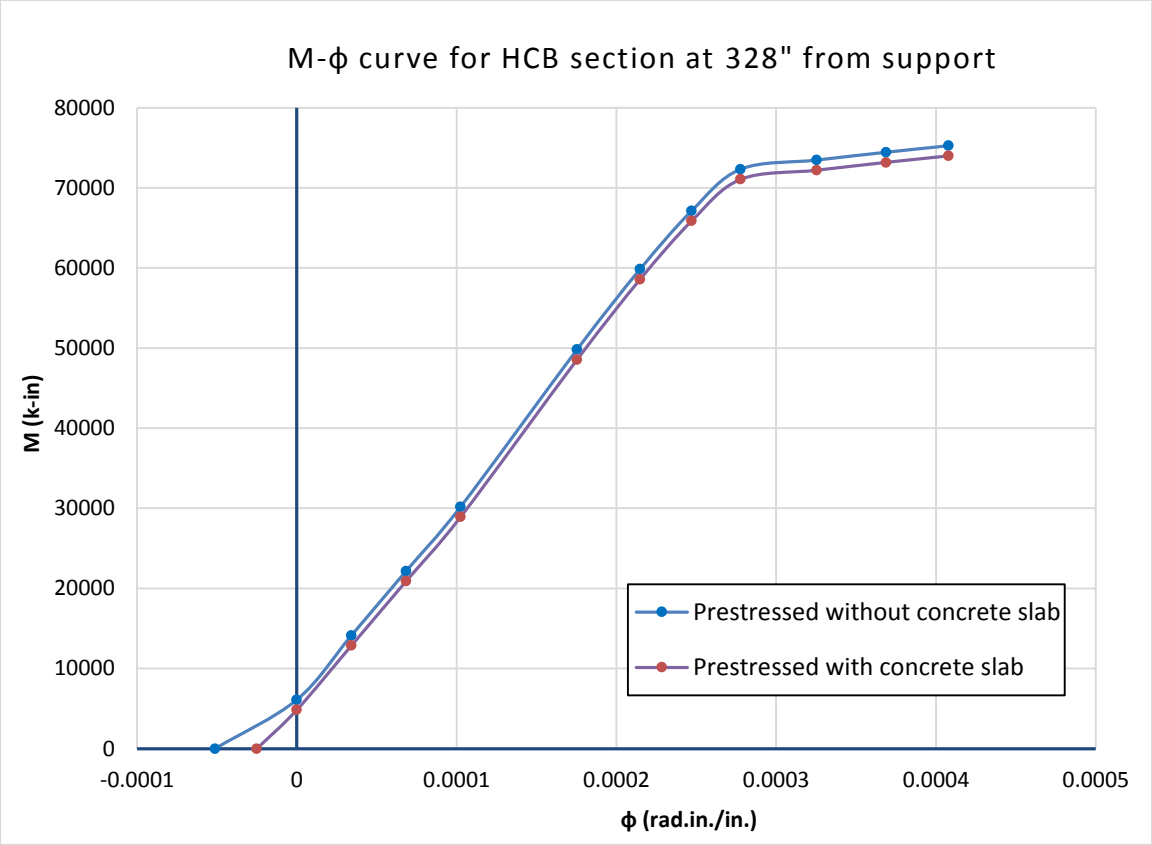
M-ϕ curve for HCB section at 328" from support
M (k-in)
80000
70000
60000
50000
40000
30000
20000
10000
0
-0.0001
0
0.0001
0.0002
0.0003
0.0004
0.0005
ϕ (rad.in./in.)
Prestressed without concrete slab
Prestressed with concrete slab

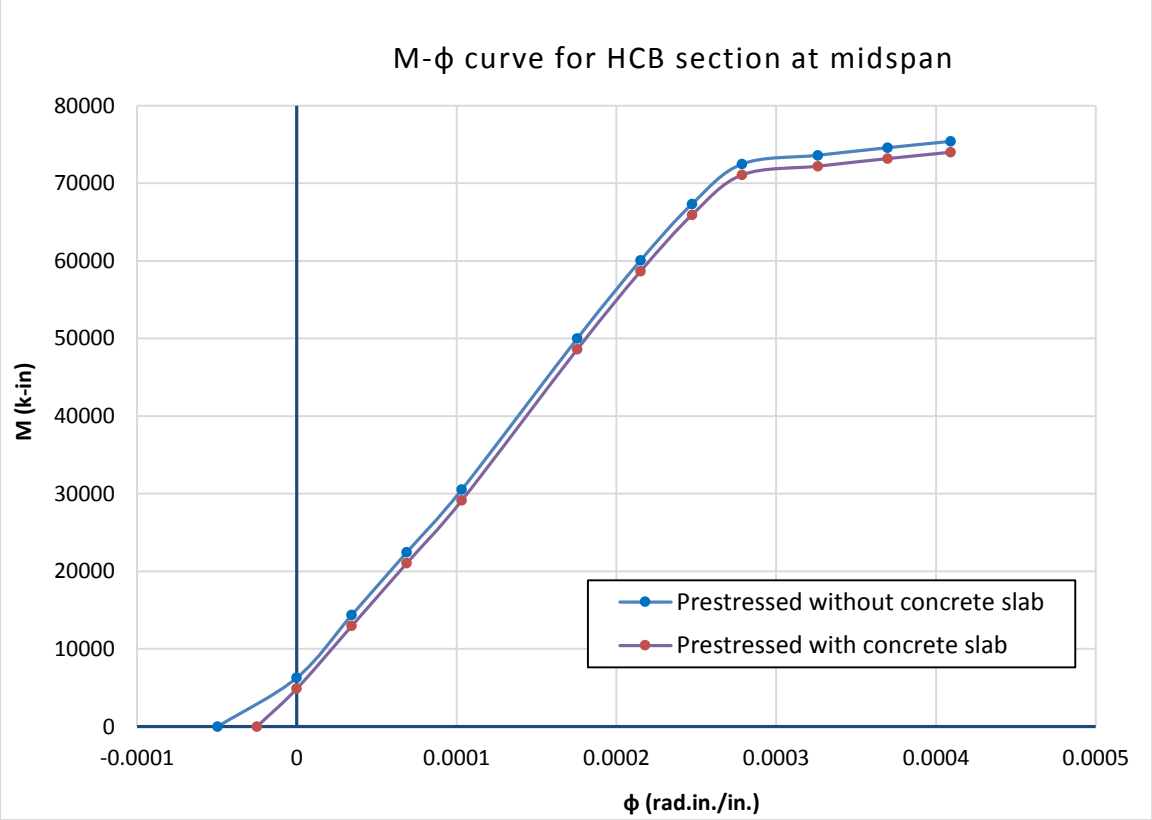
M-ϕ curve for HCB section at midspan
M (k-in)
80000
70000
60000
50000
40000
30000
20000
10000
0
-0.0001
0
0.0001
0.0002
0.0003
0.0004
0.0005
ϕ (rad.in./in.)
Prestressed without concrete slab
Prestressed with concrete slab

REFERENCES

[1] https://en.wikipedia.org/wiki/John_R._Hillman,

[2] John R. Hillman, *Investigation of a Hybrid-Composite Beam System,* Final Report for High- Speed Rail IDEA Project 23

[3] https://worldwide.espacenet.com

[4] http://hcbridge.com/about/hcb-history

[5] John R. Hillman, *Product Application of a Hybrid-Composite Beam System,* IDEA Program Final Report For the Period

[6] Stephen Van Nosdall, Christopher D Moen, Thomas E Cousins and Carin L Roberts-Wollmann, *Experiments on a Hybrid-Composite Beam for Bridge Application*

[7] Mohamed A Aboelseound and John J Myers, F. ASCE, *Finite Element Modeling of Hybrid-Composite Beam Bridges in Missouri*

[8] Harris, D.K., Civitillo, J. M., and Gheitasi, A. (2015 – accepted). "*Performance and Behavior of Hybrid Composite Beam Bridge in Virginia – Live Load Testing."* ASCE Journal of Bridge Engineering.

[9] www.hcbridge.com

[10]…Thomas Snape Robert Lindyberg, Ph.D., P.E., *Test Results: HC Beam for the Knickerbocker Bridge, AEWC Report 10-15, Project 671 September 2009*

[11] James J Gere, *Mechanics of Materials* 6th Edition

[12] Singer Pytel, *Strength of Materials* 4th Edition

[13] Paolo Brandimarte, *Finite Difference Methods for Partial Differential Equations*

[14] Egor P. Popov, *Engineering Mechanics of Solids, 2nd Edition*

[15] J M Gere & S P Timoshenko, *Mechanics of Materials*

[16] Chu Kia Wang, *Intermediate Structural Analysis*

[17] R C Hibbler, Statics and Mechanics of Materials